

**ADVERTIMENT.** La consulta d'aquesta tesi queda condicionada a l'acceptació de les següents condicions d'ús: La difusió d'aquesta tesi per mitjà del servei TDX ([www.tesisenxarxa.net](http://www.tesisenxarxa.net)) ha estat autoritzada pels titulars dels drets de propietat intel·lectual únicament per a usos privats emmarcats en activitats d'investigació i docència. No s'autoritza la seva reproducció amb finalitats de lucre ni la seva difusió i posada a disposició des d'un lloc aliè al servei TDX. No s'autoritza la presentació del seu contingut en una finestra o marc aliè a TDX (framing). Aquesta reserva de drets afecta tant al resum de presentació de la tesi com als seus continguts. En la utilització o cita de parts de la tesi és obligat indicar el nom de la persona autora.

**ADVERTENCIA.** La consulta de esta tesis queda condicionada a la aceptación de las siguientes condiciones de uso: La difusión de esta tesis por medio del servicio TDR ([www.tesisenred.net](http://www.tesisenred.net)) ha sido autorizada por los titulares de los derechos de propiedad intelectual únicamente para usos privados enmarcados en actividades de investigación y docencia. No se autoriza su reproducción con finalidades de lucro ni su difusión y puesta a disposición desde un sitio ajeno al servicio TDR. No se autoriza la presentación de su contenido en una ventana o marco ajeno a TDR (framing). Esta reserva de derechos afecta tanto al resumen de presentación de la tesis como a sus contenidos. En la utilización o cita de partes de la tesis es obligado indicar el nombre de la persona autora.

**WARNING.** On having consulted this thesis you're accepting the following use conditions: Spreading this thesis by the TDX ([www.tesisenxarxa.net](http://www.tesisenxarxa.net)) service has been authorized by the titular of the intellectual property rights only for private uses placed in investigation and teaching activities. Reproduction with lucrative aims is not authorized neither its spreading and availability from a site foreign to the TDX service. Introducing its content in a window or frame foreign to the TDX service is not authorized (framing). This rights affect to the presentation summary of the thesis as well as to its contents. In the using or citation of parts of the thesis it's obliged to indicate the name of the author

# Tracing the dynamics of dissolved organic matter in marine systems exposed to natural and experimental perturbations

Francisco Luis Aparicio-Bernat

Tracing the dynamics of dissolved organic matter in marine systems exposed to natural and experimental perturbations

Francisco Luis Aparicio-Bernat 2016



Instituto de Ciencias del Mar

ICM



CSIC

IIM  
Instituto de Investigaciones Marinas de Vigo

# Tracing the dynamics of dissolved organic matter in marine systems exposed to natural and experimental perturbations

Francisco Luis Aparicio Bernat

Academic advisors:

Dr. Cèlia Marrasé Peña

Dr. María del Mar Nieto Cid

En Barcelona, a

de

de

Tesis doctoral presentada para obtener el título de Doctor en Ciencias del Mar por la Universitat Politècnica de Catalunya (UPC).



UNIVERSITAT POLITÈCNICA  
DE CATALUNYA  
BARCELONATECH

“Tracing the dynamics of dissolved organic matter in marine systems exposed to natural and experimental perturbations”

Esta tesis ha sido realizada gracias a la financiación de una beca pre-doctoral JAE-Pre (JAEPRE\_2011\_00923) de la Agencia Estatal Consejo Superior de Investigaciones Científicas (CSIC).

Los trabajos de investigación presentados en esta tesis fueron financiados por los proyectos del Ministerio de Economía y Competitividad: *STORM* (CTM2009-09352), *ADEPT* (CTM2011-23458), *DOREMI* (CTM2012-342949) y *SUAVE* (CTM2014/23456/1) llevados a cabo en las instalaciones de los siguientes centros de investigación: Instituto de Ciencias del Mar (ICM-CSIC; Barcelona, España), Instituto de Investigaciones Marinas (IIM-CSIC; Vigo, España) y National Institute of Aquatic Resources de la Technical University of Denmark (DTU-Aqua; Copenhagen, Dinamarca). Las estancias de investigación en los centros IIM-CSIC y DTU-Aqua fueron financiadas por una beca de movilidad asociada a la beca principal JAE-Pre.

*A mis padres, mis hermanos  
y mi abuela*



*“Ha sido durante mucho tiempo mi axioma que las  
pequeñas cosas son infinitamente lo más importante”*

Sir Arthur Conan Doyle

*“It has long been an axiom of mine that the little things are  
infinitely the most important”*

Sir Arthur Conan Doyle

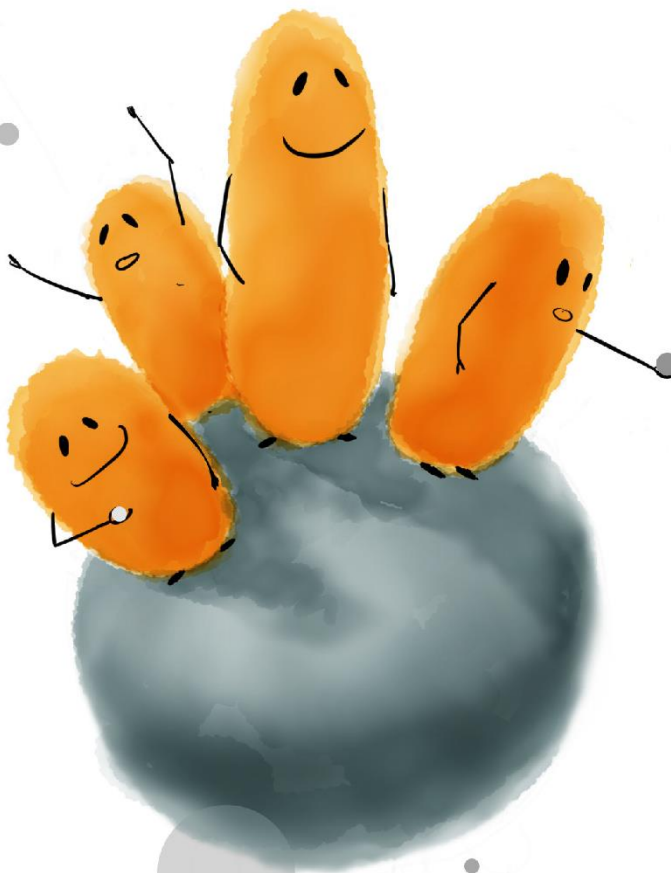


## TABLE OF CONTENTS

ACKNOWLEDGEMENTS / AGRADECIMIENTOS	<b>p. 1</b>
ABSTRACT / RESUMEN / RESUM / RESUMO	<b>p. 15</b>
GLOSSARY OF TERMS	<b>p. 25</b>
CHAPTER 1. Introduction	<b>p. 27</b>
LIST OF SPECTROSCOPIC INDICES	<b>p. 47</b>
CHAPTER 2. Microbially-mediated FDOM transformations in the deep ocean	<b>p. 49</b>
CHAPTER 3. Eutrophication & acidification. Implications in the FDOM transformations	<b>p. 72</b>
CHAPTER 4. Eutrophication & acidification. Implications in the microbial food web	<b>p. 91</b>
CHAPTER 5. Wind-induced transformations in the FDOM dynamics in a coastal system	<b>p. 109</b>
CHAPTER 6. General Discussion	<b>p. 136</b>
CHAPTER 7. Conclusions	<b>p. 150</b>
LITERATURE CITED	<b>p. 154</b>



Acknowledgements /  
Agradecimientos /  
Agraïments





Conseguir una beca de doctorado siempre se antojó un reto difícil. Sin embargo, la oportunidad de poder trabajar en un laboratorio, investigar y ser doctor en Oceanografía, eran unas metas por las que merecía la pena luchar. Cinco años más tarde, llegado este momento y echando la vista atrás, me doy cuenta que no cambiaría nada de lo que he vivido por cumplir este sueño.

La experiencia que he adquirido trabajando, los momentos que he compartido y, en definitiva, el hecho de ser la persona que soy hoy en día os lo debo a todos y cada uno de vosotros. El periodista americano George Matthew Adams escribió una vez «*La frase "la persona se hizo sola" carece de veracidad. Todos estamos hechos por otros miles de personas. Cada ser que hizo algo por nosotros, influyó en nuestra personalidad y nuestras vivencias. Es por eso que se vuelven parte de cualquier éxito nuestro*». Con estas líneas, me gustaría haceros llegar mi más sincero agradecimiento por todo lo que hemos compartido a lo largo de estos años.

Mis inicios en la andadura por la investigación en las Ciencias del Mar se los debo principalmente a dos personas que han ayudado a encauzar mis primeros pasos como científico:

- A ti, Cèlia Marrasé. Gracias por transmitirme, con ese entusiasmo que te caracteriza, todo lo que he aprendido de tu mano. A pesar de que al comenzar me costó comprender la importancia de la DOM en el contexto del ciclo del carbono, tu tesón e infinita paciencia consiguieron hacerme ver la envergadura del mundo de la fluorescencia por el que nos movíamos. Siempre recordaré tus esquemas improvisados en una hoja de papel, junto a una taza de café. Gracias por darme la oportunidad de embarcarme, muestrear, ver y visitar lugares que de otra forma solo habrían seguido en mi imaginación. Gracias por animarme a seguir adelante en todo momento. Gracias por ser mi directora y guiarme hasta ser doctor.
- A ti, Mar Nieto-Cid. Aunque te incorporaste un poco más adelante a este proyecto, tus ideas, tu tenacidad, tu paciencia, tu profesionalidad y tu capacidad de transmitir la meticulosidad por el trabajo bien hecho, proveyeron a esta tesis de las renovadas energías que precisaba en el momento oportuno. Gracias por enseñarme los entresijos del análisis del TOC, por tu disponibilidad en cualquier momento (sobre todo en la recta final), por tu empatía hacia mí y por enseñarme rincones de Vigo y Baiona. Gracias por haber accedido a ser mi co-directora. Gracias por ayudarme a crecer como científico.

Una vez incorporado al ICM, esa palabra de cinco letras, aquello desconocido y que se vislumbraba borroso en el horizonte – la tesis – iba poco a poco tomando forma. Ha sido un viaje de cinco años, un viaje que me permitió independizarme y establecerme en Barcelona. Siempre que nombro Barcelona viene a mi mente el refrán que dice «*Barcelona és bona si la bossa sona. I tant si sona com si no sona, Barcelona sempre és bona*». Y vaya si tiene razón. Dejando de lado cuánto ruido hizo la bolsa al sonar, lo que está claro es que la riqueza la he medido en el número de personas con las que he podido compartir mi vida aquí.

- Tu vas ser de les primeres persones amb qui em vaig topar per aquí, Mireia Mestre. Tot i que jo no estava acostumat a parlar en valencià, ara resulta que amb tu no puc deixar de parlar-lo. Mireia, aquestos anys has sigut més que una amiga per a mi, m'has ajudat a entendre conceptes, m'has ensenyat la ciutat, hem anat a ballar, a la platja, al gym, de barbacoes, a congressos, museus, a sopar l'un a casa de l'altre, he aconseguit fins i tot que vages a El Corte Inglés. Trobaré molt a faltar els nostres passejos per Montjuïc les vesprades d'estiu. Has estat al meu costat des de que vaig arribar, que afortunat sóc de poder tenir-te!.
- Empezar casi a la par que tú hizo que el aterrizaje en el ICM fuera más fácil al contar con otro espíritu libre y novatillo en esto de la tesis. Desde que comenzamos, tuvieron que pasar unos meses hasta que tu jefe te dejó instalarte por fin en el despacho que nos habían asignado para los que, en aquel momento, fuimos la nueva generación de doctorandos. Definitivamente Caterina R. Giner, no cambiaría por nada nuestros ratos de risas en el despacho y fuera de él, los momentos en la campaña (tanto en mar como en tierra), las meriendas, las anécdotas de cosas extrañas que solo te pueden ocurrir a ti, las notas que me dejabas en la mesa cuando me iba al despacho de la jefa, las salidas al teatro, al cine y todo lo que me has enseñado de Barcelona y Cataluña. Cuánto te voy a echar de menos.
- Tronca, ¿qué puedo decirte que no sepas ya? Llegaste al ICM un par de años después que yo, pero enseguida me percaté de qué pie cojeabas y que a ti con un par de birras se te ganaba pronto (las birras te las bebías tú mientras yo miraba). Me he divertido mucho contigo estos años. Gracias por todos los momentos de risas, las idas y venidas a la playa, a la montaña, al parque acuático, a los guateques, a las fiestas de Gràcia; por esos mails larguísimos cuando estábamos de estancia pero que aun así nos hacían estar al tanto de las novedades; por esas expresiones que solo con mirarnos ya sabemos que no nos hemos coscao de lo que nos están explicando 0\_o ('¿Qué dise usted?'). Aunque te me resistes a entrar en El Corte Inglés, gracias por estar ahí, Isabel Marín.
- A brasileira mais bonita do mundo, você roubou meu coração. Ya sabes que mi portugués es limitado, y si me sacas de 'Cereais com irresistível sabor a chocolate' o 'Cabelo limpo sem complicações' no puedo comunicarme contigo. Definitivamente, tengo que leer más botes de champú y paquetes de cereales para incorporar nuevas palabras a mi vocabulario. De ti he aprendido mucho, Sdena Nunes. Me has enseñado a ver las cosas desde diferentes puntos de vista, a reírme y quitar importancia a los problemas. Aun cuando tú no estabas al 100%, siempre has demostrado fortaleza y dulzura hacia nosotros con esa sonrisa que te caracteriza. Gracias por compartir conmigo meriendas, momentos de cotilleos, la pasión por comprar en Mercadona, viajes a congresos, a

Valencia, dar vueltas por Barcelona, estrategias para escaquearte de la Tronca. Me alegra saber que puedo contar contigo siempre que lo necesite.

- ¿Qué sería de mi paso por Barcelona si tú no hubieses llegado a hacer tu postdoc en el ICM, Daffne López-Sandoval? Gracias por venir cada día con esa risa que se contagiaba y que irradiaba alegría, por esos abrazos que te recargan de energía y por ese perfume que le hace saber a uno que habías pasado por el pasillo segundos antes. Gracias por haberte mostrado siempre dispuesta a escuchar y ayudarme sin condición cuando necesité apoyo u opinión. Que bien saber que te tengo ahí para lo que sea, ya estés en México, Arabia Saudí o Vigo.
- Carmen Herrero-Navarro, o más conocida en las altas esferas como la Sra. Dra. Dña. ¿Has visto?, voy a tener los mismos títulos nobiliarios que tú. Me alegro mucho de haberme cruzado contigo por estos lares. Nunca se me habría ocurrido pensar que aquí conocería a alguien relacionada con Macastre. Gracias por haber compartido conmigo momentos importantes como el banquete de tu boda, comidas en la playa y en la Crêperie, cotilleos, consejos, chistes, risas, charlas en las que defendías a capa y espada iPhone frente a BlackBerry, aun a sabiendas de que no tenías argumentos convincentes... Gracias por transmitir siempre esa energía positiva que te caracteriza.
- Una mañana, llegó un mail de una chica que estaba haciendo el doctorado en Banyuls-sur-mer y a la que posteriormente conocí en unas jornadas Interlab. En aquel momento no me imaginaba que compartiríamos tantas experiencias juntos, Denisse Sánchez-Pérez. Gracias por enseñarme los alrededores de Banyuls, por viajar conmigo a Andorra, Granada, Foix, Girona, por venir a visitarme a Valencia y a Copenhague, por compartir conmigo ratos de risas y confianzas. Tenías razón, paso a paso, se llega al final.
- Estela Romero, gracias porque en cada conversación en la playa cuando comemos, en el despacho o cuando hemos estado embarcados, me has enseñado cómo defender opiniones con argumentos convincentes y bien argumentados, también que varios idiomas se pueden hablar con perfecta pronunciación y que los pequeños detalles en el Illustrator marcan la diferencia. Gracias por ser un espejo en el que querer mirarse. Gracias a ti y a Jorge Sandua por acogerme en vuestro piso cuando lo necesité.
- La chica con la que comparto día de cumpleaños, Rosana Arizmendi. Recuerdo que, con esa tonalidad musical al hablar, me dejabas embobado al principio de conocerte. Gracias colombiana de mi corazón por escucharme siempre y aconsejarme, por compartir cotilleos, risas, preocupaciones, caminatas a pie por la montaña y porque hemos estado a punto de casarnos. Sé que tengo un viaje pendiente a Medellín, así que prepárame una habitación, que pronto iré.

- Dorleta Orúe-Echevarría, la primera amiga que tengo del País Vasco, que sepas que nos queda pendiente ir de pintxos por el norte. Gracias por estar dispuesta siempre a escuchar y dar consejos. Aunque tú has sido de las últimas incorporaciones al grupo, gracias por compartir conmigo salidas por Barcelona, barbacoas y comidas y meriendas del ICM.
- Yaiza M. Castillo. Un momento, ¿qué quiere decir esa eme mayúscula entre tu nombre y apellidos? Aaaahhh es que eres Yaiza Mercedes, así mucho mejor. Hablando con propiedad se entiende la gente. Tú también fuiste de las últimas incorporaciones al grupo, pero las comidas, las visitas por la ciudad, las calçotadas, los ratos de birras y las cenas no habrían sido lo mismo sin ti, tus risas y tus fotos indiscretas. Sigue así con tus virus marinos y expande infecciones por doquier.
- Encarna Borrull y Rachele Gallisai fuisteis de las primeras personas que conocí cuando me incorporé al ICM. Gracias Encarna por enseñarme las macros de Excel, las técnicas de filtración, el espectrofluorómetro y por compartir conmigo tus opiniones, risas y mareos en las campañas. Rachele, gracias por enseñarme tantos lugares de Barcelona durante mi primer año aquí y por acogerme en tu piso antes de que me fuera de campaña.
- A María de la Fuente (Zanguanga), Elisa Fernández-Guallart, Norma Zoe Neszi y Edgar Casas porque también fuisteis parte importante durante mi aterrizaje en el ICM. Gracias María por tus abrazos y risas. Gracias Elisa por enseñarme Vilanova i la Geltrú y por las risas compartidas con las frases de la Angelines. Norma, thank you for your help and for offering me a place to stay when I came back from the cruise. Edgar, gràcies per compartir converses i estones quan m'avorria i baixava al vostre despatx.
- A Teresa Morganti y Maria Pascual, quienes han sido componentes clave del despacho P39 durante estos años. Morganti, ho imparato un po italiano te al mio fianco, ragazza. Se me va a hacer raro no estar a tu lado para preguntarte cosas de estadística o discutir las variaciones del DOC en l'Estartit. Gracias por el apoyo moral y las conversaciones de cualquier tema a cualquier hora de la jornada laboral. Maria, creo que no encontraré compañera trasera mejor que tú. ¿Con quién me voy a reír ahora de 'La Competència' y 'La Segona Hora'? Que sepas, que nos queda pendiente ir a verlos en directo. Gracias por tu ayuda en los temas de estadística, en el Illustrator y porque nunca te ha importado cuando te interrumpía mientras estabas tratando datos. ¡Lo hemos conseguido a la vez, chicas!
- Ramiro Logares y Xavi Leal siempre habéis sido los espíritus jóvenes que nos habéis encendido la chispa para ir al Friday Beer, alargarlo hasta las tantas, ir de barbacoa... Cualquier excusa siempre fue buena para juntarnos. Gracias chicos.

- Me gustaría también agradecer a todos los compañeros becarios, no sólo del departamento de Biología Marina y Oceanografía del ICM, sino de cualquier otro departamento y también del Instituto de Biología Evolutiva (IBE), por cuyas becas o contratos han sido coetáneos a mí. Gracias Stefano Ambroso, Jordi Grinyó, Elena Guerrero, Eli Alacid, Carlos Domínguez, Pau Cortés, Marta Royo, Pablo Rodríguez, Marina Zamanillo, Lucía Quirós, Anna Arias, Isabel Sanz, Marta Masdeu, Marc Catllá, Marc Farré, Ricardo Santos, Ana Fernández, Oriol Sánchez, Raúl Bardají, Carine Simon, Paola Castellanos... por las comidas al sol, las charlas improvisadas en el pasillo o un simple 'Hola' al cruzarnos que siempre saca una sonrisa.
  
- Gran parte de todo el trabajo que hay escrito en esta tesis no habría sido posible sin la ayuda de los/as técnicos/as que han ayudado con la toma y el tratamiento de datos estos años. Sin Berta de la Vega, Carolina Antequera, Laura Fernández, Raquel Gutiérrez, Idaira Santos, Vanessa Balagué, Clara Cardelús y Àngel López-Sanz esta tesis seguro que no habría llegado a buen puerto. Me gustaría hacer una mención especial al trabajo de Mara Abad. Su tesón, profesionalidad y minuciosidad con cada una de las muestras que ha analizado han ayudado mucho a darle coherencia al resto del trabajo. Voldria agrair la feina feta per Josep Pascual, els seus mostrejos diaris a l'Estartit han proveït aquesta tesi de dades molt valuoses i de segur que gràcies a ell vindran molts més treballs posteriorment. De todo corazón, muchas gracias por vuestra ayuda (y por dejarme cambiar la emisora de la radio... ya sabes por quién digo esto :p).
  
- Cuando empecé, ya había otros doctorandos y postdocs en el departamento: Cristina Romera-Castillo, Eva Ortega-Retuerta, Gonzalo Luis Pérez, Fran Cornejo, AnaMari Cabello, Guillem Salazar, Clara Ruíz, Juancho Movilla, Massimo Pernice, Martí Galí, Sarah-Jeanne Royer, Elena Lara, Raquel Rodríguez, Cristina Díez, Beatriz Fernández, Ana Gomes, Pedro Llanillo, Patricia de la Fuente, Suso Peña, Isabel Ferrera, Marta Sebastián, Pedro Cermeño (gracias por las aportaciones que tu proyecto, SUAVE ha hecho a la tesis), Sergio Vallina. A todos/as, muchas gracias por vuestros consejos, charlas por los pasillos, risas y barbacoas que hemos compartido. Gonzalo, gracias por haber accedido a ser revisor externo de este trabajo y compartir conmigo tus opiniones. Eva, te agradezco que siempre te hayas ofrecido a ayudar con una sonrisa. Con tu acento granadino, los problemas no parecen tan serios y con tu apoyo los espectros de absorbancia no tienen misterios. Gracias por transmitir fortaleza y alegría día a día. Cristina, me gustaría agradecerte especialmente todo el apoyo y ayuda que me has brindado, primero desde el otro lado del charco y últimamente ya desde un poco más cerca. Gracias por tus extensos mails relativizando los problemas, tus consejos, tu disponibilidad para ayudar y por haber dicho 'sí' a ser revisora externa y miembro del tribunal evaluador de esta tesis.

- Aunque una gran parte de los días los pasaba en el ICM, un poco de tiempo también estaba por mi casa de Barcelona. A Fran Olivas me gustaría agradecerle haber venido al piso y terminar por demostrarme que el compañero perfecto para compartir piso sí que existía... a pesar de que tardó cuatro años en llegar. A mi casera Lola Martínez me gustaría agradecerle toda la ayuda y amabilidad que me ha brindado en estos años.

Parte de mi tesis se desarrolló estando embarcado y en dos centros de investigación diferentes al ICM. Durante estas estancias tuve la gran suerte de encontrarme con grandes profesionales y magníficas personas.

- Me gustaría agradecer a Xosé Antón Álvarez-Salgado (Pepe) y M<sup>a</sup> José Pazó su calurosa acogida en el Instituto de Investigaciones Marinas (IIM-CSIC) así como su profesionalidad a la hora de explicar la metodología para el análisis de muestras de carbono orgánico en agua de mar. También me gustaría mucho agradecer a Pepe la cena en Copenhague, los consejos a lo largo de estos años y el haber podido formar parte del tribunal evaluador de esta tesis.
- A Fiz Pérez, Aida Ríos, Antón Velo, Toni Padín, Maribel García, Fernando Alonso, Trini Rellán, Alba Martínez y Vanesa Vietez que os conocí, bien en mi estancia en el IIM, bien en la campaña FICARAM, muchas gracias por vuestra ayuda y vuestros ánimos. Con estas líneas me gustaría recordar con especial cariño a Aida, que con su alegría siempre consiguió hacerme reír en los momentos más duros de la campaña.
- I would sincerely like to acknowledge Colin A. Stedmon for his patience while explaining concepts that for me were new and the time he dedicated in teaching me the application of the PARAFAC modelisation. To Rafael Gonçalves-Araujo, Heather Reather, Evandro Malanski, Kasia Kenitz, Nis Sand Jacobsen, Jan Heuschele, Mette Dalgaard Agersted, Hans Van Someren Greve, Laurène Pécuchet, Karin Olsson, Phillip Georg Brun, Maria Lund Paulsen for their friendship that made my stay in Copenhagen very comfortable and a very happy moment of my life. Specially, I would like to acknowledge Jan for his help and his wonderful work in designing this thesis' cover and chapter's separations. Thank you for letting 'The Hopfs' finishing shaping this work.
- También quisiera agradecer a las tripulaciones de los B/O 'García del Cid' y 'Hespérides' su ayuda y su profesionalidad con la que nos facilitaron y permitieron que la toma de muestras en alta mar fuera de lo más divertida. Por supuesto, también dar las gracias al personal de la UTM que estuvo de apoyo para echar una mano cuando nos cargábamos algo: Quim Llinàs, Gustavo Agudo, Alberto Hernández, Gustavo Agudo, Alberto Arias, Dulce Afonso y Antonio Sandoval.

També voldria agrair a tot el grup de científics que formen el departament de Biologia Marina i Oceanografia de l'ICM:

- Especialment, Montse Sala, Pep Gasol, Carles Pelejero i Eva Calvo perquè he treballat més a prop de vosaltres últimament. Montse, gràcies per solucionar els dubtes que al llarg d'aquests anys he anat tenint i per oferir sempre que calia la teua ajuda. Pep, sense el teu punt de vista, la teua sinceritat alhora d'avaluar correccions i la teua experiència, estic segur que part dels treballs encara no estarien publicats. A en Carles, gràcies per haver demostrat disposició a resoldre dubtes, ajudar i corregir treballs, sempre amb un somriure. A l'Eva, gràcies per les converses i els ànims que em donaves quan, de tant en tant, ens hem creuat als passadissos i parlàvem de cómo anava la tesi o jo et posava al dia dels avenços amb les dades de l'Estartit.
- A Cesc Peters, perquè mentre la Cèlia estava embarcada a la 'Malaspina', tu vas donar-me l'oportunitat d'una entrevista telefònica com a possible candidat per a la beca. Gràcies per la teua actitud tan diligent com a cap de departament, pels teus consells durant aquests anys i per mostrar-te sempre disposat a ajudar en qualsevol tasca en la que he necessitat ajut.
- Als altres jefes que són uns professionals com la copa d'un pi: Dolors Vaqué (ha sigut un plaer trobar-te als passadissos mentre practicaves els teus càntics per la coral), Rafel Simó (un pou de saviesa, que sap treure l'art continguda a la ciència; moltes gràcies per acceptar formar part del tribunal de tesi), Elisa Berdalet, Marta Estrada, Ramón Massana, Albert Calbet, Enric Saiz, Esther Garcés (ets l'últim bastió de resistència per BlackBerry), Laura Arín, Silvia Acinas, Josep M<sup>a</sup> Gili, Marta Ribes, Lluïsa Cros...
- Quería hacer constar la disposición y profesionalidad que siempre mostraron Genoveva Comas, desde el Departamento de Ingeniería Hidráulica, Marítima y Ambiental de la Universidad Politécnica de Cataluña (UPC), y Nuria Angosto, Eva M. López y Conchita Borrueal desde el ICM. Sin lugar a dudas, gracias a su ayuda, los trámites para presentar documentos y hacer matrículas cada año se agilizaron considerablemente.

Las fases que componen un doctorado son muchas y variadas, sin embargo, considero que pueden diferenciarse en dos principales: picos de éxtasis y alegría cuando ves que las cosas cuadran y momentos de lenta angustia cuando a los datos les da por torcerse y la hipótesis que intentabas demostrar se va al traste. Tanto en los momentos en los que estuve animado, como en los que no, ir a casa siempre me ayudó a tomar un poco de aire fresco, ver desde otra perspectiva los problemas y recargar las pilas.

- Las comidas, meriendas o cenas del 'Consejo de Sabios' (Kata, Laura, Cris, Diana, Maca y Poli) son ya una tradición que no debemos perder. Gracias chicas por hacer, siempre un hueco para verme y ponernos al día. Poli, 'amicga', gracias por tu apoyo incondicional, por los ratos de risas a 'troche y moche' que pasamos juntos, por las tardes de compras y paseos por ECI y porque espero que todo siga 'acsolutamente' genial en nuestras vidas. Diana, gracias por buscarle el lado positivo siempre a todo y animarme a luchar por mis sueños (igual que tú estás haciendo ahora en Vancouver). Cris, por darme 'trato especial' en tu bar y por apoyarme para seguir hasta el final. Lau, ya sabes que cuando quieras voy a recogerte a la salida de la tienda y nos vamos al Mercado de Colón a por una horchata. Gracias por las palabras de ánimo y por los ratos de risas. Kata, gracias por esos abrazos tan fuertes cuando nos vemos y por mantenerme al día de todos los cotilleos. Maca, gracias porque aún desde Australia te has ido poniendo al día de cómo avanzaba todo por aquí, gracias por tus palabras de ánimo.

Toda la gente que desde la Universidad Católica de Valencia siempre me ha ayudado, se ha interesado por mis avances y me han alentado también tiene gran parte de culpa de que haya llegado hasta donde lo he hecho.

- A mis profesores de la carrera, todo un gran grupo de profesionales, pero especialmente a José Tena, Lola Cejalvo, Javi Torres y Carolina Padrón. Gracias por transmitirme vuestra pasión por el medioambiente marino y por enseñarme que, a pesar de que Valencia 'siempre había vivido de espaldas al mar', Barcelona era siempre el objetivo al que mirar si quería seguir creciendo como oceanógrafo.
- A Amanda Sancho y a Ana Hernández. Amanda, gracias porque fuiste tú la que me informó de la posibilidad de pedir la beca en el ICM. Gracias por enseñarme la ciudad durante mi primer año de beca. Ana, gracias por ser mi mentora en el laboratorio de la universidad, por los momentos de charlas y por tus palabras de ánimo.
- A María Lapido (mi Maruxiña), me gustaría agradecerle que me recibiera con los brazos abiertos cuando fui, por fin, a conocer Boiro. Gracias por tus risas, por escucharme y por nuestras llamadas telefónicas en las que nos ponemos al día de todo.

A veces ir a casa, no representaba estrictamente ir a Valencia, ya que 'casa' está en cualquier lugar que estén parte de los tuyos. Por eso, Oslo en estos años, se ha convertido en un destino que me ha encantado visitar.

- Y aquí es donde entra Sandra Gran Stadniczeñko (o Sanders). Sabes que eres como una hermana para mí y que te 'I love you a lot'. Contigo he aprendido que da igual lo lejos que puedan estar dos amigos cuando tienen a mano WhatsApp, Hangouts o Skype.

Gracias por todos los momentos de risas y más risas, de comilonas, por los ratos en el laboratorio limpiando con 'Jocabel al limón', por los rascas de la 'ONCE' que comprábamos juntos, por enseñarme Oslo y por poner tu casa a mi disposición, por los viajes a Banyuls-sur-mer, Montpellier, Narbonne, por aparecer por sorpresa en Barcelona cuando volví de campaña, por escucharme y aconsejarme a toda hora, por no parar quieta, por las mañanas de tortitas con Nocilla y mantequilla de cacahuete, por las pizzas con piña, por todos los moomuuuts que nos hemos comido juntos, por ver conmigo la saga 'Sharknado'... Sabes que podría hacer esta lista inacabable, pero sobre todo gracias por darme la oportunidad de estar cerca de Julia para verla crecer y comérmela a bocados cada vez que la veo. De todo corazón mi Sanders, muchas gracias por estar siempre a mi lado. Muchas gracias a Johann también por acogerme en vuestra casa todas las veces que he ido y por ofrecermelo de todo para que esté a gusto. Gracias a tus padres, Ewa Stadniczeńko y Federico Gran por tratarme como un hijo más cada vez que voy a verlos.

Y por si todos los agradecimientos anteriores no fueran pocos, todavía no he empezado a agradecer al pilar que en mi vida siempre ha sido clave, mi familia.

- A mis padres, Mado y Paco que les debo la persona que soy hoy en día. Os quiero muchísimo. Gracias por haber hecho siempre todo lo que ha estado a vuestro alcance y mucho más para que nunca me faltase de nada. Muchas gracias porque vosotros me llevasteis aquel día a 'Formaemple@' en Feria Valencia y allí fue donde empezó mi andadura real en la Oceanografía. Gracias por estar siempre al pie del cañón, ya sea al otro lado del teléfono, del monitor del ordenador o en casa. Mamá, muchas gracias por esos abrazos fuertes que me das cuando bajo del tren y que me recargan de energía. Gracias por tu paciencia, por escucharme siempre que lo he necesitado, por hacer siempre que voy a casa, mis platos preferidos, por los paseos junto a papá por el centro de Valencia y por animarme siempre con el último empujón para terminar de escribir un buen trabajo. Papá, la persona más fuerte que conozco. Gracias por transmitirme tu pasión por el mar y el mundo de la náutica desde bien pequeño. Aunque no te gusta que me maree cuando estoy embarcado, eso no lo puedo evitar. Gracias por comprarme el primer acuario a los 7 años con esos guppies de colores. Gracias por escuchar y escuchar largos ratos de contarte por qué los datos no cuadran, por cuidar de la tropa cuando no estoy en casa y por organizar viajes para venir a visitarme allá donde el doctorado y esta carrera como científico me lleve. Papá, mamá, gracias por quererme tanto y, en definitiva, por ser los mejores.
- A mis hermanos, Fernando y Patricia. Brother, gracias porque un '¿qué pasa gordo?' no sería lo mismo si no viene de ti. Gracias por dejar de hacer planes con tus amigos los fines de semana que yo bajo a Valencia para pasar tiempo conmigo. Gracias por

enseñarme las últimas novedades de juegos y vídeos de las que te enteras. Gracias por tener siempre esas ganas de jugar conmigo a la Play, a la Wii y por ser mi asesor de moda. Chu, por mucho que crezcas, siempre serás para mí la enana de la casa. Gracias por esa alegría con la que vienes corriendo a darme un abrazo en cuanto me ves llegar. Gracias por transmitir toda esa energía que tienes y por querer hacer que todos nos sintamos a gusto cuando estamos juntos. Gracias a los dos por hacerme sentir cuando llego a casa como si el tiempo no hubiera pasado, por ver los Simpsons juntos a la hora de la comida, por tratar siempre de cenar pizzas de Telepizza y por todos los ratos de risas cuando decimos tonterías. A mi 'brother in law', Jose, gracias por ser un compañero de vida perfecto para mi hermana, por estar pendiente de cómo me va, por preguntar y por interesarte de este mundo de la biología marina y por animarme cuando lo veía todo negro.

- A mi abuela Remedios. Muchas gracias por estar siempre pendiente de ver salir algo relacionado con el mar por la tele para llamarme corriendo y contármelo. Gracias por enseñarme a amar Valencia desde bien pequeño, por enseñarme a ser humilde y la importancia que tiene saber de dónde viene uno. Gracias por preocuparte por mí y llamarme todas las semanas, por escucharme siempre con esa mirada tan atenta cuando te explico las cosas, por comentar conmigo los episodios de 'Isabel' y, sobre todo, gracias por tus consejos y la filosofía matutina en la hora del desayuno. Te quiero mucho Yaya.
- A mis tíos y primos. Porque este doctorado ha sido un largo viaje que me ha hecho darme cuenta de lo importante que es para mí contar con todos vosotros unidos. Sé que desde la distancia he contado, de una forma u otra, con el apoyo de todos. A mis tíos Luís y Lene gracias por recibirme con los brazos abiertos en Dinamarca todas las veces que he ido a veros, por vuestros consejos, las cenas y comidas 'a la danesa' y por vuestra ayuda incondicional. A mis primas Michelle y Kristina, gracias por todos los buenos momentos que pasamos en Copenhague, eso incluye las cenas con tortilla de patatas y macarrones. ¡Tengo muchas ganas de conocer a Valentina! A Luca por enseñarme Copenhague cuando apenas la conocía. A mi primo Sebastian, desde hace poco, ciudadano barcelonés, gracias por todas las noches que hemos pasado juntos jugando a la Play y viendo pelis. Gracias por transmitirme tu pasión por Star Wars. Tenemos que pensar en cuál va a ser nuestra siguiente saga para ver. A mis tíos Boro y M<sup>a</sup> Reme y mis primos Ismael y Alejandro. He crecido con vosotros y siempre habéis sido una parte muy importante de mi vida. Gracias por preocuparos por mí, por todas las noches que hemos pasado cenando todos juntos, por los veranos en Tavernes y por quererme tanto. A Ismael especialmente, gracias por esas llamadas para ponernos al día y por compartir conmigo opiniones y anécdotas. A mis tíos Abelardo y Mariví y mis primos Alberto y Guillermo. Sois una parte importante en que esto haya salido bien. Muchas gracias por preguntar siempre qué tal me iba, por las cenas compartidas, por los veranos en

Macastre, por las recetas de comida y por estar ahí para hablar en cualquier momento. A mis tíos M<sup>a</sup> Carmen y Emilio y mis primos Sergio, Sandro, Raúl, Sandra y las enanas Lydia y Azahara. Gracias por preocuparos por cómo me iba todo durante los años de la tesis.

- A mi Nilo, gracias por hacer que los ratos que compartí contigo fueran siempre tan felices. Porque tú me enseñaste que amor es una palabra de cuatro patas. Aunque no has llegado hasta el final conmigo, me gustaría que sepas que te quiero mucho y te echo de menos, pequeña.

Y con este párrafo cierro este capítulo. Pero no solo el capítulo 'Agradecimientos' de este libro, sino también un capítulo de mi vida. Esta etapa ya se acaba y es el momento de comenzar una nueva. Espero poder seguir compartiendo con muchos de vosotros/as todo lo bueno que está por venir.

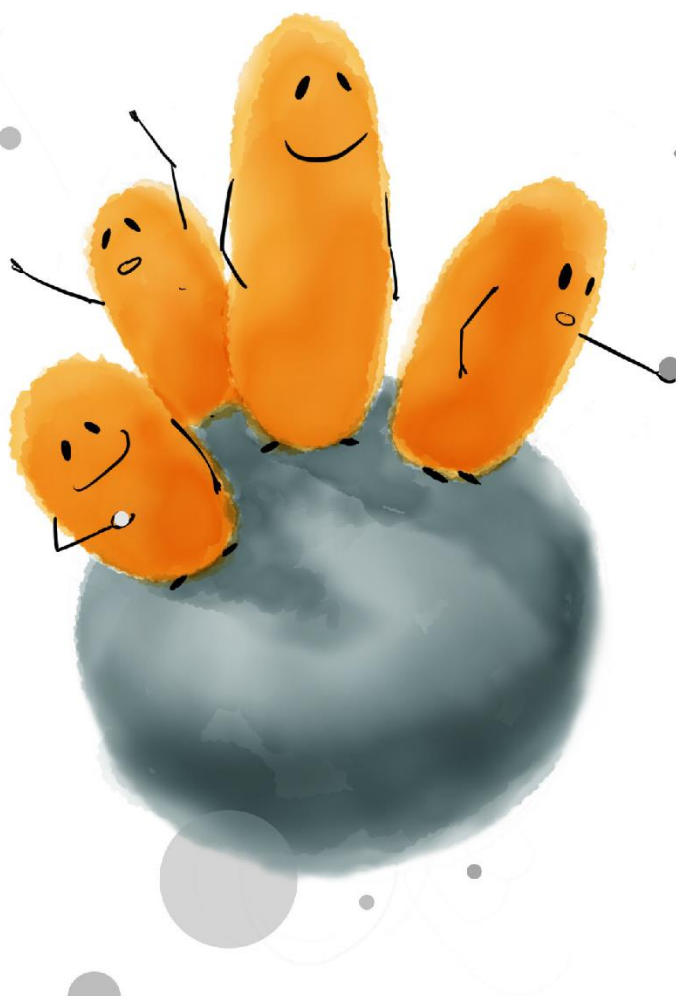
Aunque he intentado mencionar a todas las personas que, de una u otra forma me ha ayudado a alcanzar esta meta, si me he dejado a alguien en el tintero, ruego me disculpe.

Fran

P.D.: Si has llegado hasta aquí, gracias por tragarte todo este tostón



Abstract / Resumen /  
Resum / Resumo





## Abstract

In the coming decades, global warming will affect the biogeochemical cycles evolution, particularly the carbon cycle. In this context, it is necessary to gain knowledge on the Earth natural mechanisms to relieve the atmosphere of the greenhouse gases excess. The 'biological pump' is one of the main mechanisms employed by the oceans to "sequester" the CO<sub>2</sub> accumulated in the atmosphere. Thereby, the organic carbon produced by the biological activity is transferred from surface to deep waters where part of this pool is accumulated in the seafloor. Another mechanism involving the accumulation of carbon in the ocean, called the 'microbial carbon pump' (MCP), has been described recently. It is composed by an intricate set of microbial processes that enable the formation of highly recalcitrant dissolved material and therefore facilitate the accumulation of carbon in the deep waters. The oceans store about 660 Pg C in the form of dissolved organic matter (DOM), a quantity comparable to the atmospheric CO<sub>2</sub>. Understanding the processes that control the dynamics, recycling and exportation of the DOM is crucial to evaluate the oceans capability to gather the excess of atmospheric CO<sub>2</sub>.

On its course down throughout the water column, microorganisms degraded the DOM produced at the surface layers. Concentrations decrease from ~90 μmol C L<sup>-1</sup> down to 40-50 μmol C L<sup>-1</sup>, values homogeneously distributed in the deep oceans throughout the planet. The fact that below 1000 m and deeper the DOM is degraded at lower speed is still unknown, and the processes that can affect this DOM degradation have been studied in this thesis.

In this regard, we performed experiments with deep Atlantic Ocean microbial communities. These communities were exposed to DOM of different quality. The results revealed that the presence of humic-like allochthonous compounds favored the generation of new humic-like compounds *in situ*. Consequently, we proved that the composition of the DOM that reach the deep ocean conditions its ease-to-degrade nature. In this thesis we also evaluated the effect of global change (acidification and eutrophication) on the quality of the DOM. With this purpose in mind, we developed mesocosms experiments in tanks of 200 L in which we enclosed coastal planktonic communities from the NW Mediterranean Sea. The planktonic populations were exposed to different treatments of pH and eutrophication (addition of inorganic nutrients). The results of these experiments demonstrated that low pH levels favored the increase of the planktonic organisms' growth rates, while the input of nutrients promoted the transformation to complex DOM. Finally, a monthly monitoring sampling of several biogeochemical variables was carried out at the Estartit Oceanographic Station (EOS). One of the principal aims consisted in identify the DOM sources and its inter-annual variability. The results revealed the importance of the winds in transporting oceanic DOM inputs to the system, which contrasted with previous results observed in nearby sampling stations (e.g. Blanes Bay, Bay of Banyuls-sur-mer), where the major DOM contributions were terrestrial inputs.



## Resumen

En las próximas décadas el cambio climático afectará globalmente a la evolución de los ciclos biogeoquímicos en general, y al ciclo del carbono en particular. En este contexto, es necesario adquirir conocimiento sobre los mecanismos naturales de los que dispone el planeta para eliminar de la atmósfera el exceso de gases de efecto invernadero. La 'bomba biológica' es uno de los principales mecanismos que presentan los océanos para "secuestrar" el CO<sub>2</sub> acumulado en la atmósfera. De este modo, el carbono orgánico producido por la acción biológica es transferido desde la superficie a las capas profundas del océano hasta su parcial almacenamiento en los fondos marinos. Recientemente se ha descrito otro mecanismo que facilita la acumulación de carbono, la "bomba microbiana de carbono" (MCP). Está compuesta por un conjunto de complejos mecanismos microbianos que posibilitan la formación de material disuelto altamente recalcitrante y por tanto conllevan a la acumulación de carbono en las aguas profundas. Los océanos albergan alrededor de 660 Pg C en forma de materia orgánica disuelta (DOM), cantidad equiparable al CO<sub>2</sub> atmosférico. Entender los procesos que controlan la dinámica, el reciclado y la exportación de la DOM es crucial para evaluar la capacidad de los océanos en acumular el exceso de carbono atmosférico.

A su paso a través de la columna de agua, la DOM generada en superficie es degradada por los microorganismos. Su concentración disminuye desde ~90  $\mu\text{mol C L}^{-1}$  en las aguas superficiales hasta 40-50  $\mu\text{mol C L}^{-1}$ , rango uniforme de valores presentes en las aguas profundas de los océanos de todo el planeta. A partir de 1000 m de profundidad, la DOM se descompone a una tasa mucho más lenta y aparentemente imperceptible. Las causas de esta dilación en la descomposición a día de hoy son todavía inciertas y han sido objeto de estudio en esta tesis.

En este sentido, se realizaron experimentos con comunidades microbianas del Océano Atlántico profundo, las cuales fueron sometidas a varios tratamientos de enriquecimiento con compuestos orgánicos. Los resultados revelaron que la presencia de precursores húmicos alóctonos favorecía la generación de nuevos compuestos húmicos dentro del sistema. Consecuentemente, la composición de la DOM que llega al océano profundo condiciona su facilidad para ser degradada. Por otro lado, en esta tesis también se ha examinado experimentalmente el efecto del cambio global (acidificación y eutrofización) sobre la calidad de la DOM. En este caso los experimentos se realizaron con comunidades planctónicas costeras del Mediterráneo noroccidental incubadas en mesocosmos de 200 litros. Las comunidades se sometieron a distintas condiciones de pH y eutrofización. El seguimiento de la respuesta de los microorganismos y la dinámica de la DOM demostraron por un lado que las tasas de reproducción de los organismos planctónicos se aceleraron con la disminución de los niveles de pH, y, por otro lado, que el aumento de nutrientes inorgánicos favoreció la generación de compuestos orgánicos de estructura compleja. Por último, se realizó un seguimiento mensual de medición de diferentes variables biogeoquímicas en el punto de muestreo de l'Estartit (EOS) con el objetivo de identificar la variabilidad interanual de la DOM así como identificar la procedencia

de los aportes. Los resultados obtenidos muestran la importancia de factores ambientales como el viento, que en este caso acentúa la presencia de inputs de origen oceánico, contrastando con lo descrito previamente en otros puntos de muestreo cercanos (Bahía de Blanes, Bahía de Banyuls-sur-mer), donde el principal origen de los aportes orgánicos fue atribuido a una influencia terrestre.

## Resum

En les properes dècades el canvi climàtic afectarà globalment a l'evolució dels cicles biogeoquímics en general, i al cicle del carboni en particular. En aquest context, és necessari adquirir coneixement sobre els mecanismes naturals dels quals disposa el planeta per eliminar de l'atmosfera l'excés de gasos d'efecte hivernacle. La 'bomba biològica' és un dels principals mecanismes que presenten els oceans per "segrestar" el CO<sub>2</sub> acumulat en l'atmosfera. D'aquesta manera, el carboni orgànic produït per l'acció biològica és transferit des de la superfície a les capes profundes de l'oceà fins al seu parcial emmagatzematge en els fons marins. Recentment s'ha descrit un altre mecanisme que facilita l'acumulació de carboni, la "bomba microbiana de carboni" (MCP). Està composta per un conjunt de complexos mecanismes microbians que possibiliten la formació de material dissolt altament recalcitrant i, per tant, comporten a l'acumulació de carboni en les aigües profundes. Els oceans alberguen al voltant de 660 Pg C en forma de matèria orgànica dissolta (DOM), quantitat equiparable al CO<sub>2</sub> atmosfèric. Entendre els processos que controlen la dinàmica, el reciclat i l'exportació de la DOM és crucial per avaluar la capacitat dels oceans a acumular l'excés de carboni atmosfèric.

Al seu pas a través de la columna d'aigua, la DOM generada en superfície és degradada pels microorganismes. La seva concentració disminueix des de ~90 µmol C L<sup>-1</sup> en les aigües superficials fins a 40-50 µmol C L<sup>-1</sup>, rang uniforme de valors presents en les aigües profundes dels oceans de tot el planeta. A partir de 1000 m de profunditat, la DOM es descompon a una taxa molt més lenta i aparentment imperceptible. Les causes d'aquesta dilació en la descomposició a dia d'avui són encara incertes i han estat objecte d'estudi en aquesta tesi.

En aquest sentit, es van realitzar experiments amb comunitats microbianes de l'Oceà Atlàntic profund, les quals van ser sotmeses a diversos tractaments d'enriquiment amb compostos orgànics. Els resultats van revelar que la presència de precursors húmics al·lòctons afavoria la generació de nous compostos húmics dins del sistema. Conseqüentment, la composició de la DOM que arriba a l'oceà profund condiona la seva facilitat per ser degradada. D'altra banda, en aquesta tesi també s'ha examinat experimentalment l'efecte del canvi global (acidificació i eutrofització) sobre la qualitat de la DOM. En aquest cas els experiments es van realitzar amb comunitats planctòniques costaneres del Mediterrani nord-occidental incubades en mesocosmos de 200 litres. Les comunitats es van sotmetre a diferents condicions de pH i eutrofització. El seguiment de la resposta dels microorganismes i la dinàmica de la DOM van demostrar d'una banda que les taxes de reproducció dels organismes planctònics es van accelerar amb la disminució dels nivells de pH, i d'altra banda, que l'augment de nutrients inorgànics va afavorir la generació de compostos orgànics d'estructura complexa. Finalment, es va realitzar un seguiment mensual de mesurament de diferents variables biogeoquímiques en el punt de mostreig de l'Estartit (EOS) amb l'objectiu d'identificar la variabilitat interanual de la DOM així com identificar la procedència de les aportacions. Els resultats obtinguts mostren la importància de factors ambientals com el vent que, en aquest cas, accentua la presència d'aportacions d'origen oceànic, contrastant amb el descrit prèviament en altres punts de mostreig propers (Badia de Blanes,

Badia de Banyuls-sud-mer), on el principal origen de les aportacions orgàniques va ser atribuït a una influència terrestre.

## Resumo

Nas próximas décadas o cambio climático afectará globalmente á evolución dos ciclos bioxeoquímicos en xeral, e ó ciclo do carbono en particular. Neste contexto, é necesario adquirir coñecemento sobre os mecanismos naturais dos que dispón o planeta para eliminar da atmósfera o exceso de gases de efecto invernadeiro. A "bomba biolóxica" é un dos principais mecanismos que presentan os océanos para "secuestrar" o CO<sub>2</sub> acumulado na atmósfera. Desta forma, o carbono orgánico producido pola acción biolóxica é transferido dende a superficie das capas profundas do océano hasta o seu parcial almacenamento nos fondos mariños. Recentemente describiuse outro mecanismo que facilita a acumulación de carbono, a "bomba microbiana de carbono" (MCP). Está composta por un conxunto de complexos mecanismos microbianos que posibilitan a formación de material disolto altamente recalcitrante e por tanto levan á acumulación de carbono nas augas profundas. Os océanos albergan ó redor de 660 Pg C na forma de materia orgánica disolta (DOM), cantidade equiparable ó CO<sub>2</sub> atmosférico. Entender os procesos que controlan a dinámica, o reciclado e a exportación da DOM é crucial para avaliar a capacidade dos océanos en acumular o exceso de carbono atmosférico.

Ó seu paso a través da columna de auga, a DOM producida na superficie é degradada polos microorganismos. A súa concentración diminúe dende ~90  $\mu\text{mol C L}^{-1}$  nas augas superficiais ate 40-50  $\mu\text{mol C L}^{-1}$ , rango uniforme de valores presentes nas augas profundas dos océanos de todo o planeta. A partir dos 1000 m de profundidade, a DOM descomponse a unha taxa moito máis lenta e aparentemente imperceptible. As causas desta dilación na descomposición son todavía incertas na actualidade e foron obxecto de estudio nesta tesis.

Neste sentido realizáronse experimentos con comunidades microbianas do Océano Atlántico profundo, as cales foron sometidas a varios tratamentos de enriquecemento con compostos orgánicos. Os resultados revelaron ca presenza de precursores húmicos alóctonos favorecía a produción de novos compostos húmicos dentro do sistema. Consecuentemente, a composición da DOM que chega ó océano profundo condiciona a súa facilidade de ser degradada. Por outro lado, nesta tesis tamén se examinou experimentalmente o efecto do cambio global (acidificación e eutrofización) sobre a calidade da DOM. Neste caso os experimentos realizáronse con comunidades planctónicas costeiras do Mediterráneo noroccidental, incubadas en mesocosmos de 200 litros. As comunidades someteronse a distintas condicións de pH e eutrofización. O seguemento da resposta dos microorganismos e a dinámica da DOM demostraron que as taxas de reprodución dos organismos planctónicos aceleráronse coa diminución dos niveis de pH, e tamén que o aumento de nutrientes inorgánicos favoreceu a produción de compostos orgánicos de estrutura complexa. Ademais realizouse un seguemento mensual de varias variables bioxeoquímicas no punto na estación oceanográfica de l'Estartit (EOS) co obxectivo de identificar a variabilidade interanual da DOM, ademais de identificar a procedencia dos aportes. Os resultados obtidos mostran a importancia de factores ambientais como o vento, que neste caso acentúa a presenza de inputs de orixe oceánica, contrastando co descrito previamente noutras

estacións oceanográficas cercanas (Bahía de Blanes, Bahía de Banyuls-sur-mer), onde a principal orixe dos aportes orgánicos foi atribuído a unha influencia terrestre.

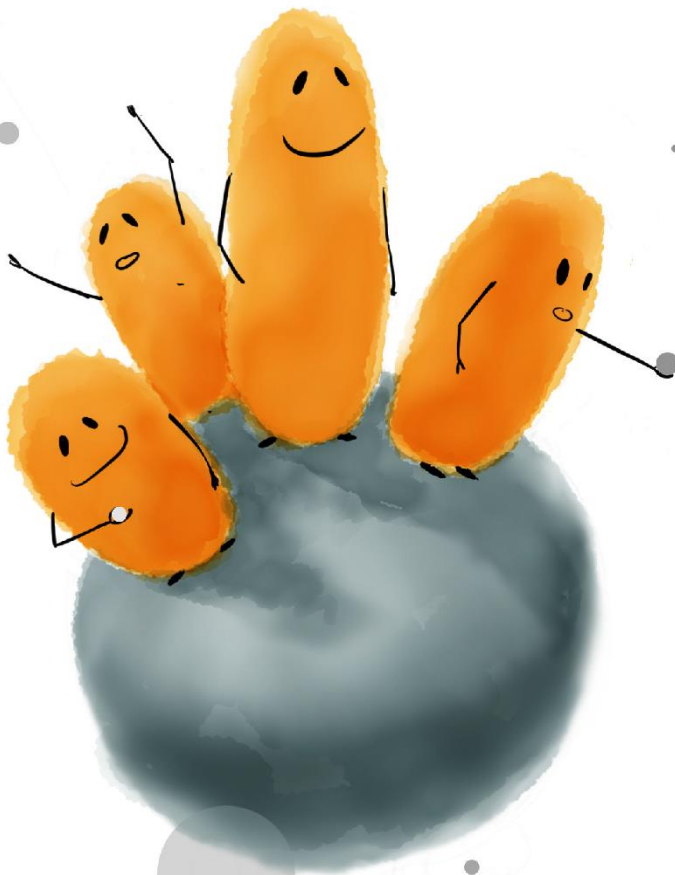
## Glossary of relevant terms used in this thesis

Acronym	Description
$a_\lambda$	Absorption coefficient at wavelength $\lambda$
AABW	AntArctic Bottom Water
ANOVA	ANalysis Of VAriance
AOU	Apparent Oxygen Utilization
BB	Bacterial Biomass
BBMO	Blanes Bay Microbial Observatory
BIX	Biological IndeX
CDOM	Chromophoric Dissolved Organic Matter
CDW	Circumpolar Deep Water
Chl <i>a</i>	Chlorophyll pigment 'a'
DIC	Dissolved Inorganic Carbon
DOC	Dissolved Organic Carbon
DOM	Dissolved Organic Matter
EEM	Excitation-Emission Matrix
EOS	Estartit Oceanographic Station
FDOM	Fluorescent Dissolved Organic Matter
FT ICR MS	Fourier Transform Ion Cyclotron Mass Spectrometry
HIX	Humification IndeX
MCP	Microbial Carbon Pump
NO <sub>3</sub>	Nitrate
OA	Ocean Acidification
PARAFAC	PARAllel FACTor analysis
PAR	Photosynthetically Active Radiation
pCO <sub>2</sub>	CO <sub>2</sub> partial pressure
PO <sub>4</sub> <sup>3-</sup>	Phosphate
POC	Particulate Organic Carbon
POM	Particulate Organic Matter
QSU	Quinine Sulfate Units
R.U.	Raman Units
SiO <sub>2</sub>	Silicate
S <sub>R</sub>	Slope Ratio
TOC	Total Organic Carbon
UV	Ultra Violet radiation



# Chapter 1

## Introduction





## 1.1. – The marine carbon cycle

Life in our planet is based on the stoichiometry of organic matter. The different compartments in which the Earth is divided (biosphere, geosphere, hydrosphere and atmosphere) exchange carbon in the form of countless reactive chemical species, making all ecosystems capable of sustaining life. This movement entails the use and recycling of inorganic (e.g.  $\text{CO}_2$ ,  $\text{CaCO}_3$ ...) and organic (e.g.  $\text{C}_6\text{H}_{12}\text{O}_6$ ,  $\text{CH}_4$ ...) forms of carbon, and it is named biogeochemical carbon cycle. These carbon fluxes determine sources and sinks (reservoirs) of inorganic and organic carbon.

The present-day global inventory of carbon on Earth is dominated firstly by geological rock formations ( $100 \cdot 10^6$  Pg C; **Figure 1.1**; Globe Carbon Cycle Project, 2010), and secondly by the fraction of inorganic carbon dissolved in the aquatic ecosystems (DIC;  $\sim 38 \cdot 10^3$  Pg C; Houghton, 2007; IPCC, 2007). The majority of this DIC is stored in the intermediate and deep layers of the ocean (**Figure 1.1**). Moreover, the carbon included in extractable resources of fossil fuels ( $5 \cdot 10^3$  Pg C) and in plants and soils ( $\sim 2 \cdot 10^3$  Pg C) are, respectively, an order of magnitude lower than the DIC (**Figure 1.1**). Complementary to these reservoirs, the oceans also contain organic carbon in a) the recently deposited marine sediments (150 Pg C; **Figure 1.1**) and in b) through the water column in the form of dissolved (DOM; 660 Pg C; Hansell *et al.*, 2009) and particulate organic matter (POM; 20-25 Pg C; Hedges, 2000; Jiao *et al.*, 2010). DOM is one of the largest pools of reduced carbon on Earth, comparable to the  $\text{CO}_2$  accumulated in the atmosphere (750 Pg C; **Figure 1.1**).

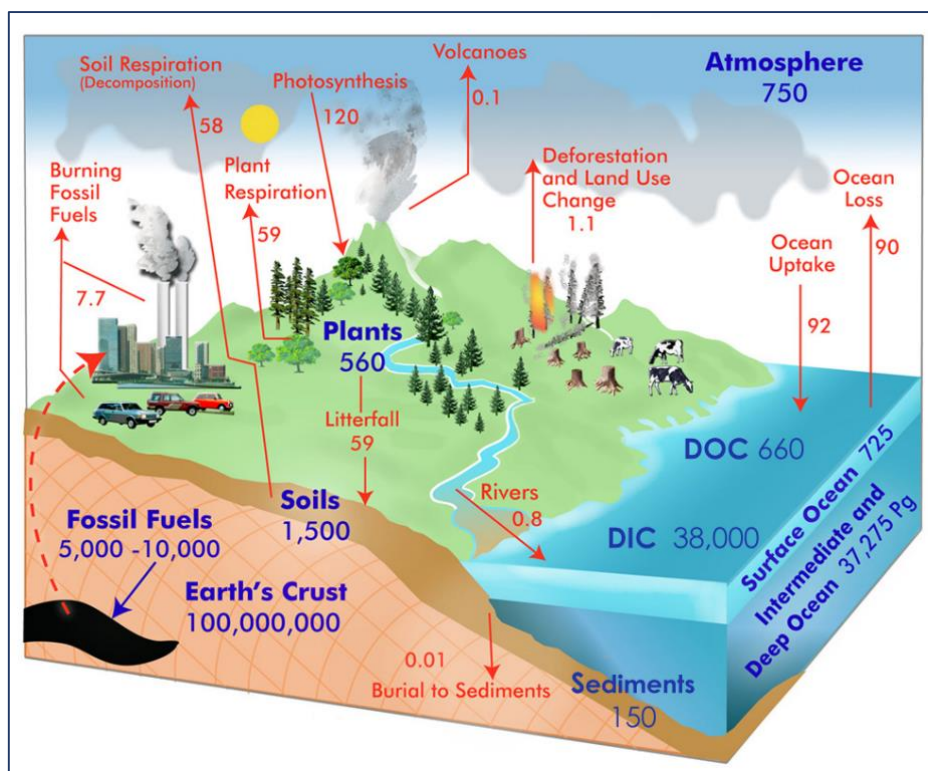


**Figure 1.1.** The global carbon cycle. Blue text represents carbon pools (units expressed in Pg C). Red text and arrows represent carbon fluxes (units expressed in Pg C year<sup>-1</sup>). Figure modified from The Globe Carbon Cycle Project (2010).

The oceans cover approximately the 75% of the total surface of the planet and, globally, this system acts as a sink of CO<sub>2</sub>. The imbalance in the CO<sub>2</sub> partial pressure (pCO<sub>2</sub>) between the atmosphere and the oceans generate a rapid exchange of this gas between the two media, meaning that atmospheric pCO<sub>2</sub> is highly responsive to changes in surface DIC, which stresses the importance of the oceans in the global carbon cycle, even beyond its relative total carbon mass.

The carbon flux between the surface ocean and the ocean interior is explained by four conceptual pumps (Ridgwell and Arndt, 2015). All four pumps act primarily by vertically relocating carbon away from the surface to the deep ocean:

- a) The solubility pump (Figure 1.2). Once the atmospheric CO<sub>2</sub> enters into the aqueous media, the speciation of DIC starts to vary between the free dissolved CO<sub>2</sub> (aq), the bicarbonate ion (HCO<sub>3</sub><sup>-</sup>) and the carbonate ion (CO<sub>3</sub><sup>2-</sup>). The stoichiometric re-adjustments of these three species of inorganic carbon will entail changes in the alkalinity and the pH of the seawater (Volk and Hoffert, 1985; Zeebe, 2012; Hönisch *et al.*, 2012). The partitioning of DIC between surface (globally ~1·10<sup>3</sup> Pg C; Figure 1.1) and deep waters (globally ~37·10<sup>3</sup> Pg C; Figure 1.1) is mainly controlled by the temperature of the water body. As CO<sub>2</sub> is more soluble in colder seawater, the downwelling areas of the oceans efficiently redistribute C from the atmosphere to the deep ocean (Figure 1.2).

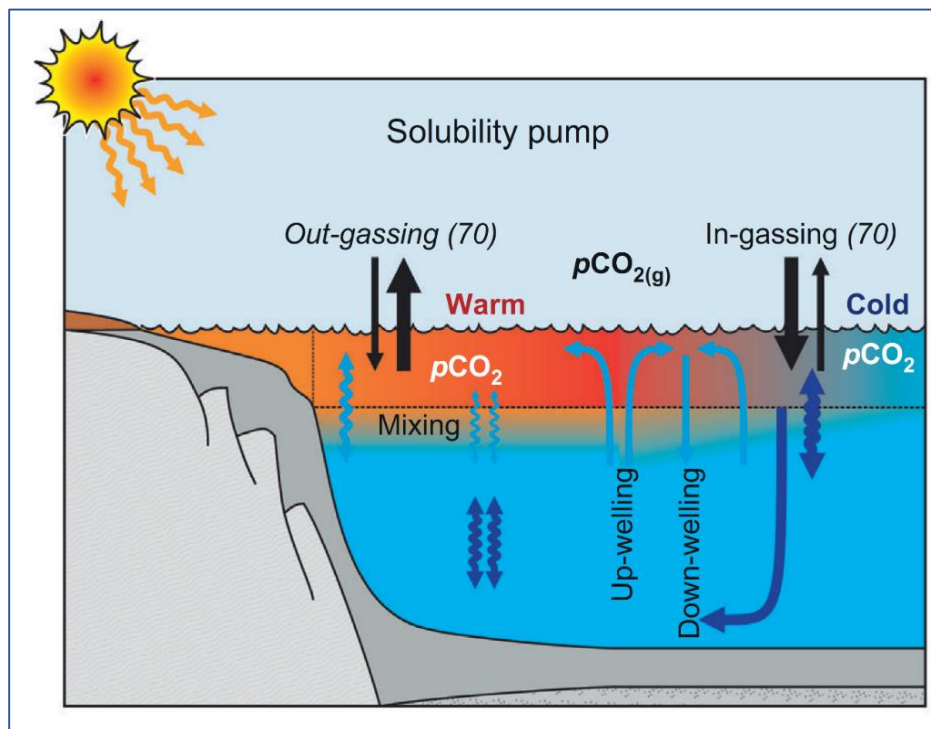


**Figure 1.2.** Illustration of the primary reservoirs and processes constituting the solubility pump. Carbon fluxes into the ocean are shown in normal font and sinks in italics, which were quantified following Hönisch *et al.* (2012), shown in Pg C year<sup>-1</sup> units. Figure taken from Ridgwell and Arndt (2015).

- b) The organic carbon pump (Figure 1.3). It comprises the combination of a) the processes involving the fixation of inorganic carbon into organic matter during photosynthesis, b) food web processes, c) physical mixing, and d) transport and gravitational settling (Volk and Hoffert, 1985; Passow and Carlson, 2012; Honjo *et al.*, 2014). Surface organic matter is mainly carried down within a rain of particles, which includes fecal pellets from zooplankton, shells from dead plankton, and other bits of organic material from dead or dying microorganisms. Particles can travel to the deep ocean floor in spans of days or weeks. Based in this sinking mechanism, the organic carbon pump controls nutrient cycling in the ocean by enriching the deep waters in inorganic nutrients that are redistributed by global circulation.

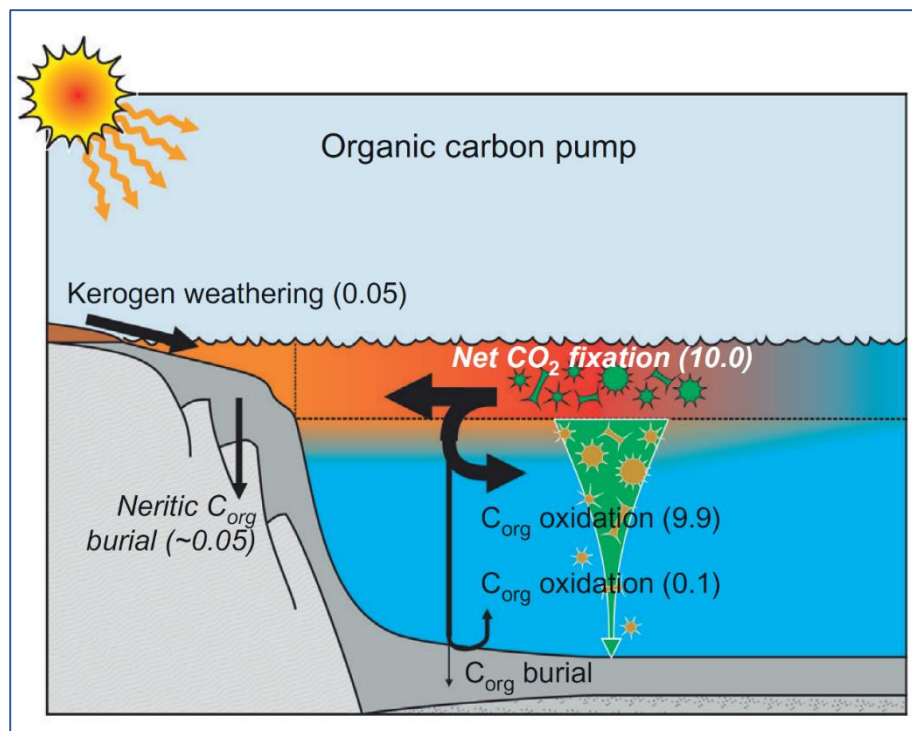


**Figure 1.3.** Illustration of the primary reservoirs and processes constituting the organic carbon pump. Carbon fluxes into the ocean are shown in normal font and sinks in italics, which were quantified following Hönisch *et al.* (2012), shown in Pg C year<sup>-1</sup> units. Figure taken from Ridgwell and Arndt (2015).

- c) The carbonate pump (**Figure 1.4**). This pump reflects the biological precipitation of calcium carbonate ( $\text{CaCO}_3$ ), supersaturating these upper layers with respect to  $\text{CaCO}_3$  (calcite or aragonite). When calcifying organisms die, their carbonated structures are transported down through gravitational settling and active bio-transport (Elderfield, 2002). Carbonate dissolution occurs during this downward transport. Under conditions favorable to biogenic calcium carbonate preservation, sediments become richer in  $\text{CaCO}_3$ , locking away large amounts of carbon for millions of years in the form of chalk deposits. Approximately, the 20% of the total carbonate that sinks in the oceans is able to evade dissolution and it is buried in the sediment (Feely *et al.*, 2004).

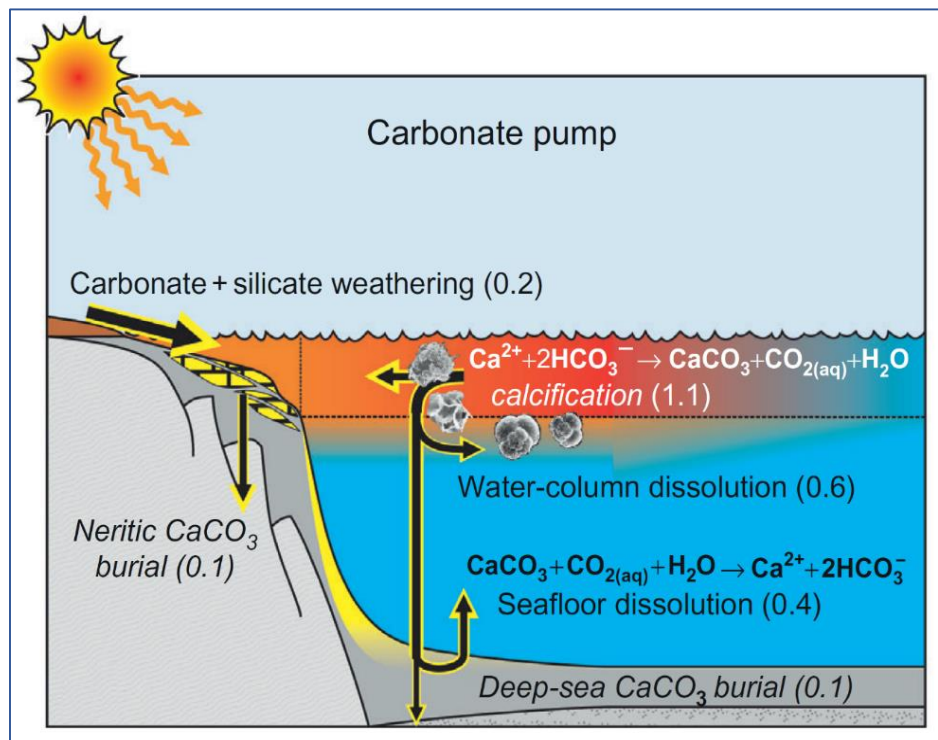


**Figure 1.4.** Illustration of the primary pools and processes constituting the carbonate pump. Carbon fluxes into the ocean are shown in normal font and sinks in italics, which were quantified following Hönisch *et al.* (2012), shown in  $\text{Pg C year}^{-1}$  units. Figure taken from Ridgwell and Arndt (2015).

- d) The microbial carbon pump (MCP; **Figure 1.5**). The MCP emphasizes the role of bacteria, archaea and viruses in generating refractory DOM (RDOM) as a sub-product of the remineralization/respiration processes. Because of its recalcitrant nature, the compounds generated would remain stored in the water column for millennia, representing a new sequestration process of the CO<sub>2</sub>. Therefore, this pump is a further mechanism that distributes carbon among the non-geological reservoirs. The interest in this relatively recent-defined concept has increased rapidly over last years. (Jiao *et al.*, 2010; Legendre *et al.*, 2015).

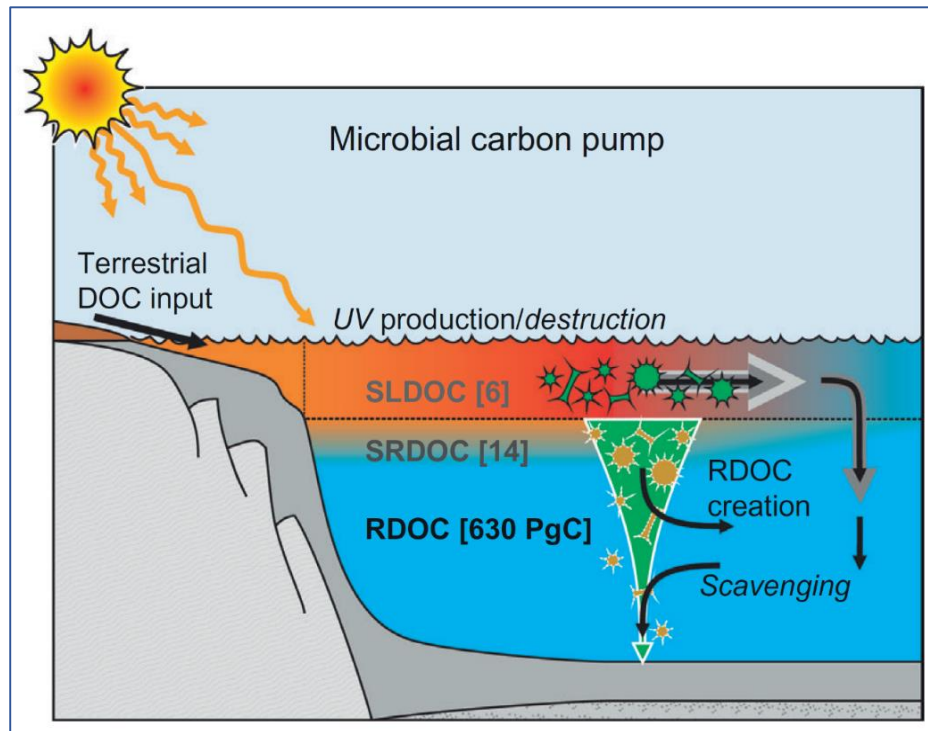


**Figure 1.5.** Illustration of the primary reservoirs and processes constituting the microbial carbon pump. Reservoir inventories, in brackets, are from Hansell (2013). Fluxes of DOC are broken down into semi-labile (light gray) and semi-refractory (dark gray), neither of which are transported far into the ocean interior. Fluxes of refractory DOC (RDOC) are indicated with black arrows. Carbon fluxes into the ocean are shown in normal font and sinks in italics, which were quantified following Hönisch *et al.* (2012), shown in Pg C year<sup>-1</sup> units. Figure taken from Ridgwell and Arndt (2015).

## 1.2. – Dissolved Organic Matter

### 1.2.1. – DOM distribution in the world wide oceans

In the marine ecosystems, most of the DOM is respired by marine microheterotrophs, oxidized by photochemical processes or buried in the sediments (Carlson and Hansell, 2015). Nonetheless, as explained in the previous section, a significant fraction is stored in the water column where it participates in multiple biogeochemical processes over time scales ranging from hours to millennia. The time interval that the DOM is able to remain in the water column is directly linked to its inherent reactivity. Therefore, relatively high concentrations of DOC ( $70\text{--}80\ \mu\text{mol kg}^{-1}\ \text{C}$ ) can be found at the ocean surface in the tropical and subtropical biogeographic provinces ( $40^\circ\text{N}$  to  $40^\circ\text{S}$ ) because its accumulation is favored by the vertical stratification (Figure 1.6a; Hansell *et al.*, 2009). Instead, lower concentrations of about  $40\text{--}60\ \mu\text{mol kg}^{-1}\ \text{C}$  can be observed at the surface in equatorial regions, in subpolar seas and in the Southern Ocean ( $>50^\circ\text{S}$ ), where low-DOC deep ocean waters surge to the surface. DOC concentrations in the worldwide deep oceans ( $<3000\ \text{m}$ ) are further depleted to  $\sim 39\ \mu\text{mol kg}^{-1}$  at  $25^\circ\text{--}50^\circ\text{S}$  (Figure 1.6b; Hansell *et al.*, 2009)

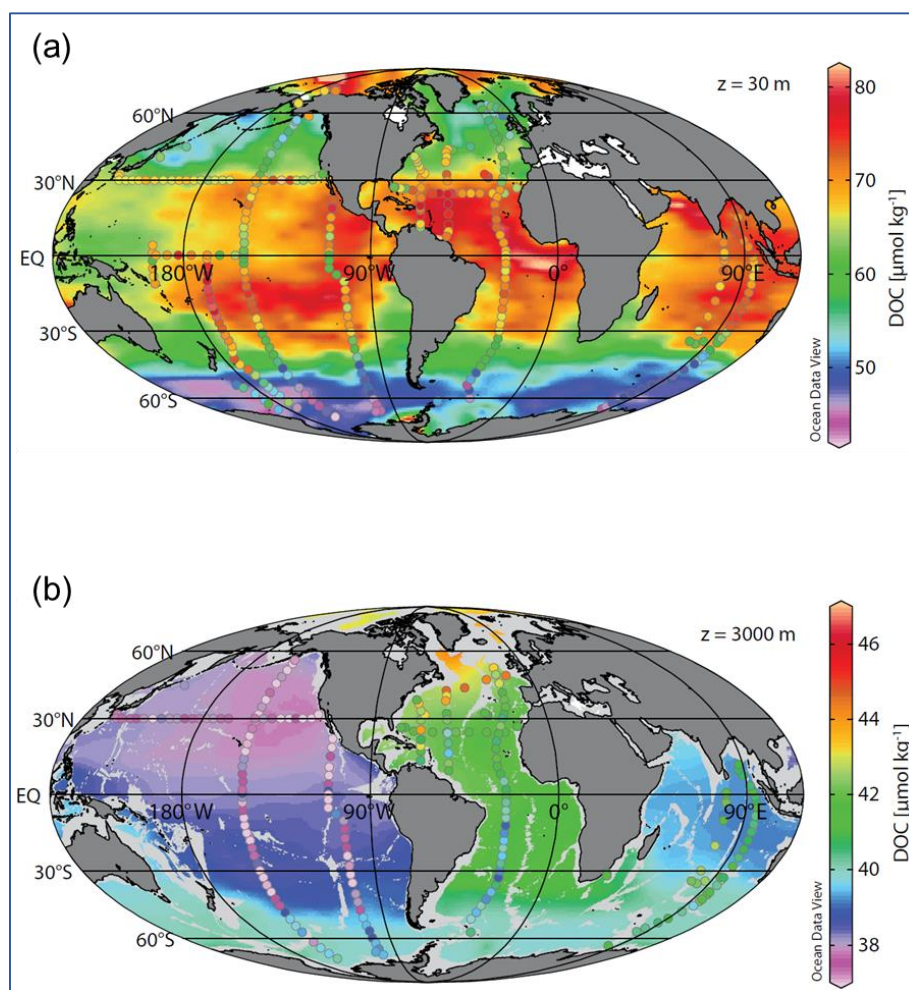


**Figure 1.6.** Distributions of dissolved organic carbon (in  $\mu\text{mol kg}^{-1}$ ) at (a) 30 m and (b) 3000 m. Meridional and zonal lines of data are observed values, while the background field is modeled. Taken from Hansell *et al.* (2009).

### 1.2.2. – DOM sources and reactivity

There are two main sources of dissolved organic matter in the ocean:

- a) From allocthonous origin. Coming from terrestrial and atmospheric inputs, this fraction of the DOM has a low contribution to the total oceanic pool (2-3%), but the terrestrial supply is considered one of the main sources in marine coastal ecosystems (Opsahl and Benner, 1997, Herut *et al.*, 2005; Pey *et al.*, 2010).
- b) From autochthonous origin. Accounts for more than the 95% of the total organic matter and, therefore, it is the core source. This *in situ* production is mainly due to extracellular release by:
  - i) Phytoplankton (Marañón *et al.*, 2005; Romera-Castillo *et al.*, 2010).
  - ii) Grazing and egestion by protists (Nagata and Kirchman, 1992; Jiao *et al.*, 2010).
  - iii) Release via cell lysis (both viral and bacterial; Brusaard *et al.*, 2004; Jiao *et al.*, 2010; Weinbauer *et al.*, 2011).
  - iv) Release of metabolites by microbes for nutrient acquisition (e.g., metal-binding ligands for metal acquisition; Ito and Butler, 2005), for communication (e.g., acyl homoserine lactones for quorum sensing; Gram *et al.*, 2002), or for chemical defense (e.g., polyunsaturated aldehydes for grazing inhibition; Wichard *et al.*, 2008).
  - v) Programmed cell death of microalgae and prokaryotes (Bidle and Falkowski, 2004; Orellana *et al.*, 2013).

The chemical structure of the DOM is mainly determined by the origin of the material, and, in turn, the nature of this chemical structure is the prime factor determining DOM reactivity. Consequently, the bio-reactivity of the DOM pool makes reference to the chemical structure and also to the residence time of the different compounds. **Figure 1.7** illustrates the composition of the five major fractions of the oceanic DOC pool according to reactivity (Hansell, 2013; Carlson & Hansell, 2015): labile (LDOC), semi-labile (SLDOC), semi-refractory (SRDOC), refractory (RDOC) and ultra-refractory (URDOC) dissolved organic carbon. LDOC, represents only a small fraction of the DOC pool as it is quickly assimilated by the marine microorganisms (from hours to days), supporting the metabolic energy and the nutrient demand of heterotrophic prokaryotes (Carlson & Hansell, 2015). The LDOC fraction comprises organic phosphorous and sulfur compounds, lipids, amino acids and monosaccharides, as well as hydrolysable high molecular weight (HMW) compounds (Amon and Benner, 1996; Benner, 2002). The SLDOC fraction is more resistant than LDOC to microbial degradation (larger proteins, polysaccharides...), therefore it can persist for months to years in the water mass. Consequently, it is exportable from the euphotic zone to deeper layers (Nagata, 2008) and it is distributed throughout the global ocean (Aluwihare *et al.*, 1997). The SRDOC is mainly constituted by DOM of intermediate reactivity, remaining in the oceans for decades (Hansell *et al.*, 2009). The RDOC, is resistant to biological degradation and dominates the organic matter pool in deep waters, with residence times of centuries to millennia, (Hansell, 2013). Recently, using worldwide data, Catalá *et al.* (2015) estimated the turnover time of humic-like compounds, ranging between 435 and 610 years, which indicates the recalcitrant

character of these fluorescent compounds. Finally, the URDOC is a small fraction of the RDOC (~2%) and its lifetime can be larger than 40000 years as inferred from radiocarbon and molecular composition analyses (Dittmar and Koch, 2006; Dittmar and Paeng, 2009; Ziolkowski & Druffel, 2010).

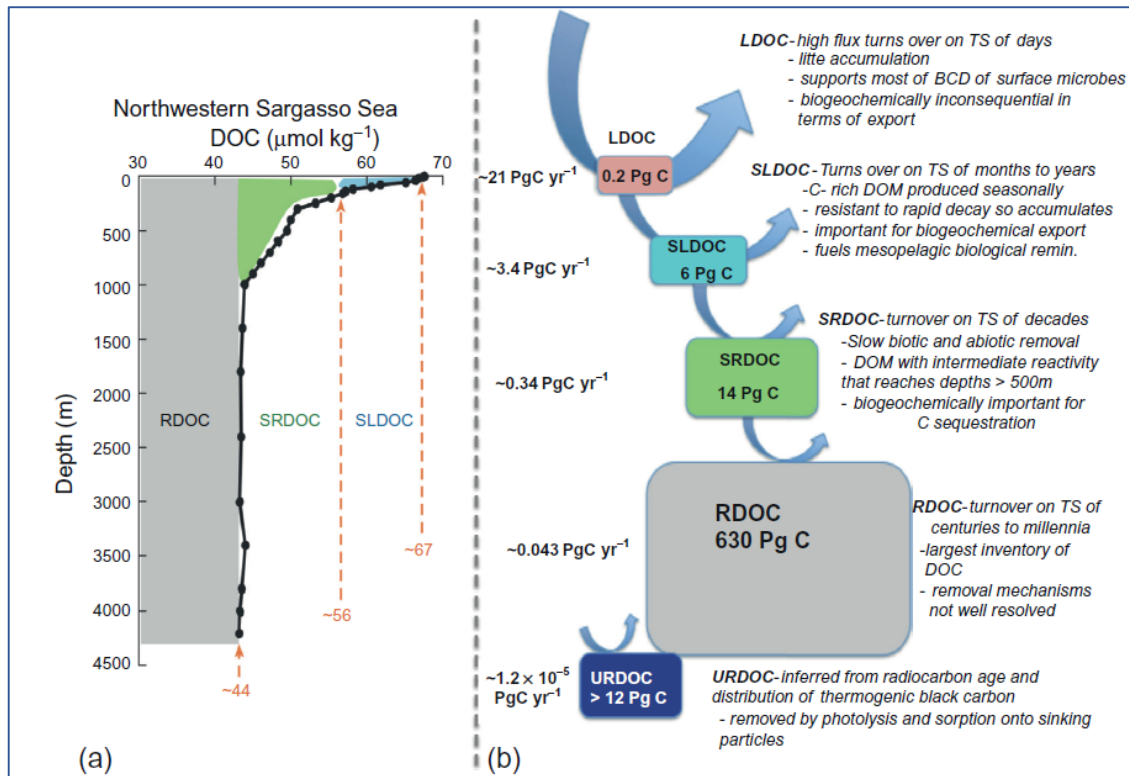


**Figure 1.7.** DOC fractions, defined by reactivity, found in the oceanic water column. (a) Vertical distribution of the RDOC, SRDOC and SLDOC pool (shaded areas) and the estimate range of DOC concentrations observed within those pools in stratified oligotrophic waters such as of the Northwestern Sargasso Sea. (b) Estimated inventories (in boxes) and removal rates of each fraction of DOM. Acronym 'TS' means time scale. Taken from Carlson & Hansell (2015).

In 2015, Dittmar proposed three hypotheses to account for the constrained total remineralization in deep oceanic waters, one of them is precisely related to the high percentage of recalcitrant DOM present in these waters, while the other two deal with the lack of any indispensable environmental component and the dilution or diversity factor:

- The 'intrinsic stability hypothesis' suggests that the stability of DOM is due to resistant molecular structures synthesized by living organisms (e.g. molecular subunits of peptidoglycan membranes) or abiotic transformations (e.g. photobleaching).
- The 'environment hypothesis' defends that DOM mineralization is limited by the availability of essential resources such as electron acceptors (e.g. oxygen, sulfate...) or essential elements (e.g. phosphorus, iron...).
- The 'molecular diversity hypothesis' proposes that the extremely dilute concentrations of a high diversity of substrate molecules could restrain the activation of the metabolic prokaryote machinery pathways. A recent experimental study by Arrieta *et al.* (2015) showed that when autochthonous RDOM was added in excess, prokaryote growth

increased, thus indicating that the low microbial activity in the deep waters could be caused by a dilution factor.

On the other hand, this RDOM from deep waters reaches the surface ocean when it is transported by upwelling processes. Once in shallow layers, sunlight radiation transforms part of this recalcitrant fraction into labile DOM that becomes available for microbes, re-starting the cycle (Obernosterer *et al.*, 2001; Nieto-Cid *et al.*, 2006). At the surface, not only labile DOM but also inorganic carbon (CO<sub>2</sub>/CO) and nitrogen are produced by the photo-degradation of the RDOM. It has been estimated that about 2-3% of the oceanic DOM pool is lost by photochemical degradation per year (Moran and Zepp, 1997).

### 1.2.3. – How to measure DOM

Recent methodological improvements have shed light in the composition of the DOM through the use of a broad range of analytical tools, including isotopic tracers (Hood *et al.*, 2005), mass spectrometry (Gonsior *et al.* 2009; Stubbins *et al.*, 2010) and spectroscopic tools (Coble, 1996; Stedmon *et al.*, 2003; Fellman *et al.*, 2010). The most common techniques used to characterize DOM do not fully reveal the chemical composition of open ocean DOM, although they are offering novel insights of DOM molecular understanding (Stubbins *et al.*, 2014). Up to date, the approaches to characterize DOM have been gathered into two categories: a) bulk measurements as for example DOC and CDOM concentration and b) more specific ones to identify lignins, amino acids, sugars, proteins, nucleic acids, and other biomolecules (Mopper *et al.*, 2007). While these approaches have yielded significant advances, as demonstrated by the quantity and scope of the current DOM literature, the techniques remain limited. The most common advanced instrumental approaches for an exhaustive, although not specific, molecular characterization of marine DOM are the nuclear magnetic resonance (NMR; Amon and Benner, 1996; Clark *et al.*, 1998; Aluwihare *et al.*, 2005) and ultrahigh resolution Fourier transform ion cyclotron mass spectrometry (FT ICR MS; Koch *et al.*, 2005; Dittmar and Koch, 2006; Mopper *et al.*, 2007; Kujawinski *et al.*, 2009; Repeta, 2015).

In addition to the advances acquired at the molecular level using these novel methodologies, the spectroscopic techniques have profoundly improved the identification of DOM and its transformations during the last decade (McKnight *et al.*, 2001, Stedmon *et al.*, 2003). These tools are relatively fast, inexpensive and easy to implement in comparison with other analytical procedures, allowing their use in a broad range of temporal and spatial scales (Jaffé *et al.*, 2008, Fellman *et al.*, 2010). Specifically, absorbance and fluorescence measurements of seawater samples provide extended information on the chemical properties of DOM (Stedmon and Markager, 2005, Jaffé *et al.*, 2008, Fellman *et al.*, 2010). Therefore, two fractions of DOM are defined based on the optical properties of the organic compounds (**Figure 1.8**; Stedmon and Álvarez-Salgado, 2011): a fraction that absorbs ultraviolet (UV) and visible light (chromophoric

DOM; CDOM) and a fraction that is able to re-emit light after absorbing it (fluorescent DOM, FDOM; Ewald *et al.*,1983).

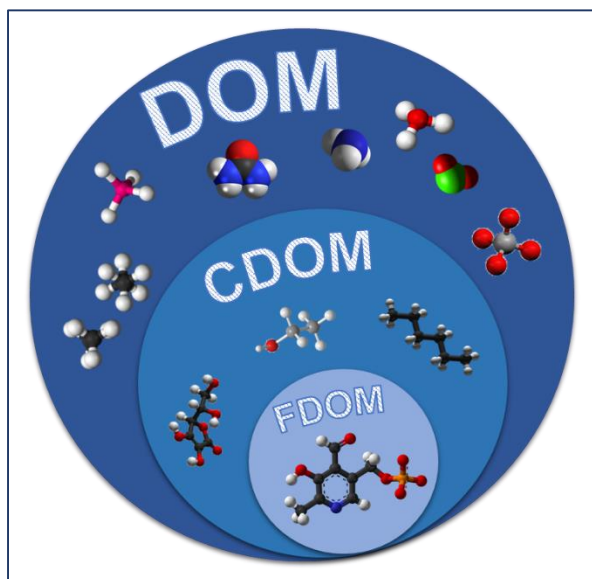


**Figure 1.8.** Representation of chromophoric and fluorescent dissolved organic matter (CDOM and FDOM, respectively) as sub-fractions of the total DOM pool. Different organic molecules forming part of all three fractions have been represented. Figure modified from Stedmon and Álvarez-Salgado (2011).

The processes behind the absorption and emission of light are illustrated by the Jablonski diagram (Figure 1.9). The singlet ground and the first and second electronic states are depicted by  $S_0$ ,  $S_1$ , and  $S_2$ , respectively. At each of these electronic energy levels the fluorophores can exist in a number of vibrational energy levels, depicted by 0, 1, 2, etc. When a beam of light incises in the sample, a fluorophore is usually excited to some higher vibrational level of either  $S_1$  or  $S_2$ . With a few rare exceptions, molecules in condensed phases rapidly relax to the lowest vibrational level of  $S_1$ . Once the electron is excited, emits radiation and subsequently returns to its ground state after first losing energy.

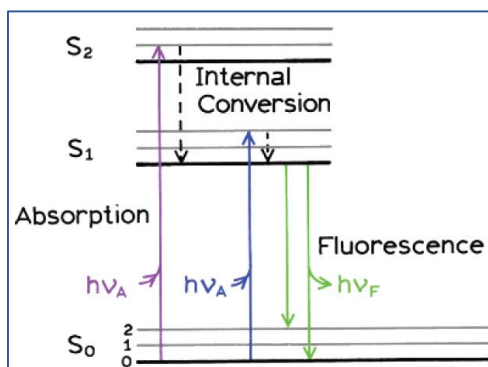


**Figure 1.9.** Jablonski diagram. Taken from Lakowicz (2006).

### 1.2.3.1. – CDOM measurements

The absorption properties of CDOM are measured on a spectrophotometer as absorbance ( $Abs_{\lambda}$ ), a unitless ratio of spectral radiant power transmitted through the sample across the path-length (Braslavsky, 2007).  $Abs_{\lambda}$  is then converted to (Napierian) absorption coefficients ( $a_{\lambda}$ ,  $m^{-1}$ ) according to Eq 1:

$$a_{\lambda} = \frac{2.303 \cdot Abs_{\lambda}}{l} \quad (1)$$

where  $l$  is the path-length (in meters) and 2.303 is the factor to convert a base-10 to a natural logarithm.

The CDOM absorbance spectrum can be fairly adjust to a negative exponential function throughout the UV and visible light, hence showing maxima of absorbance in the UV and blue portions (Figure 1.10; Bricaud *et al.*, 1981). In addition, diverse absorption indices can be extracted from these spectra:

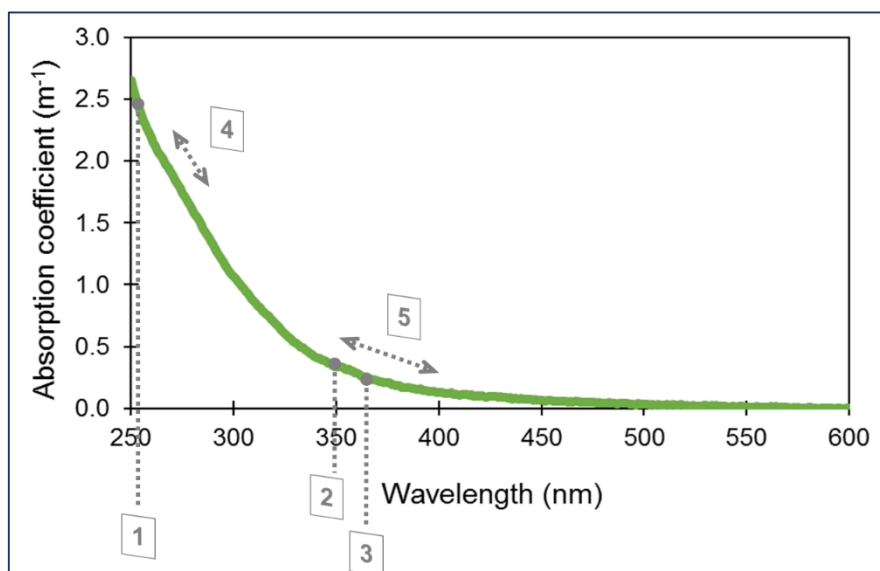


**Figure 1.10.** Absorption spectrum from a seawater sample taken at the Estartit Oceanographic Station at 0.5 m deep on April 2012. Different absorption spectra-derived indices are indicated: (1) absorption coefficient at a wavelength of 254 nm ( $a_{254}$ ); (2) absorption coefficient at a wavelength of 350 nm ( $a_{350}$ ); (3) absorption coefficient at a wavelength of 365 nm ( $a_{365}$ ); (4) spectral slope over the range 275 to 295 nm ( $S_{275-295}$ ); and (5) spectral slope over the range 350 to 400 nm ( $S_{350-400}$ ).

The base-10 logarithm of the absorption at 254 nm normalized to dissolved organic carbon (DOC) allows to obtain the specific UV absorbance (SUVA, Weishaar *et al.* (2003)). SUVA values are correlated with DOM aromaticity providing information about the complexity of molecules (Helms *et al.*, 2008; Weishaar *et al.*, 2003). The absorption coefficient at 350 nm ( $a_{350}$ ) can be considered as a proxy for tracing refractory DOC (Lønborg *et al.*, 2010). The 254 nm to 365 nm absorption coefficients ratio ( $a_{254}:a_{365}$ ; Dalzell *et al.*, 2009) are inversely correlated to the molecular size of the substances. Furthermore, the spectral slope of the wavelength interval between 275 and 295 nm region ( $S_{275-295}$ ) has been used to trace terrestrial DOM (Fichot and Benner, 2012).

Additionally, the ratio between this and the slope between 350 and 400 nm region ( $S_{350-400}$ ), constitutes the  $S_R$ , the dimensionless slope ratio.  $S_R$  provides information about DOM molecular weight and photochemically induced alterations (Helms *et al.*, 2013).

### 1.2.3.2. – FDOM measurements

The fluorescence properties of FDOM are limited to excitation wavelengths of 240-500 nm and emission wavelengths of 300-600 nm. A combined plot of the fluorescence emission/excitation scans is referred to as excitation-emission matrices (EEM; Coble *et al.*, 1990). In natural aquatic systems, EEMs are characterized by several signals that have been classified in two main groups: protein- and humic-like fluorophores (Figure 1.11; Coble, 2007). Protein-like fluorescence signal is originated mainly by fluorescent amino acids such as tryptophan (Try; peak-T, Coble, 1996), tyrosine (Tyr; peak-B, Coble, 1996) and phenylalanine (Phe, Yamashita and Tanoue, 2003). In their free water-dissolved form, these amino acids present fluorescence maxima at, Ex/Em 280/350 nm, 275/310 nm and 240/280 nm, respectively (Eisinger and Lamola, 1971). In this thesis we have mainly focused on the evolution of peak-T (Try) because peak-B (Tyr) can be affected by the Raman scattering band of water and the fluorescence of the Phe is often found quenched by Tyr if they bound in the same protein, making measurements of these two last amino acids not reliable. On the other hand, the humic-like fluorescence has traditionally been identified as different peaks, commonly referred to as peak-A, peak-C and peak-M, that have excitation/emission pairs at 250/435 nm, 340/440 nm and 320/410 nm, respectively. While peak-C has traditionally been attributed to a group of compounds of terrestrial origin, organic compounds fluorescing at peak-M has been typically related to *in situ* production in marine environments.

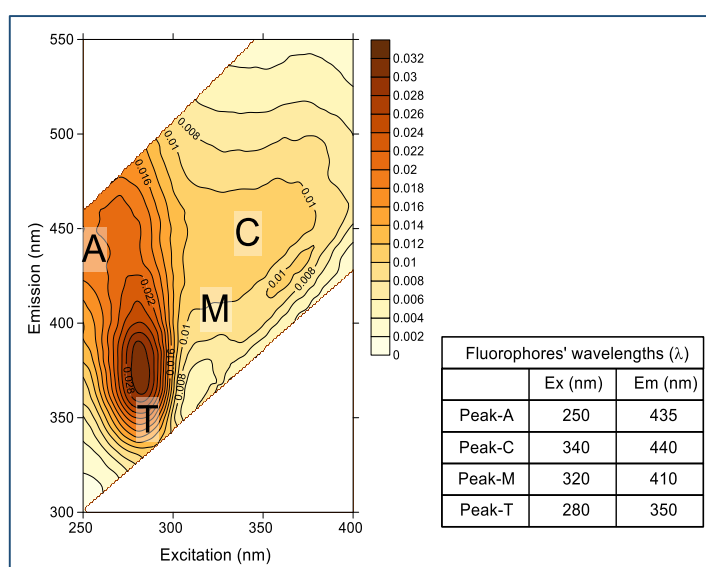


**Figure 1.11.** Excitation-emission matrix (EEM) of a seawater sample from the Atlantic Ocean enriched with an amino acids solution. The position of the four main fluorophores is indicated. Values expressed in Raman Units (R.U.)

With the proliferation of the EEMs measurements, the PARAllel FACtor analysis (PARAFAC) has become popular in the last decade. This approach is based on a multivariate statistical technique that decomposes the combined fluorescence signal into underlying individual, independently variable fluorescent signals (Bro, 1997; Stedmon *et al.*, 2003; Stedmon and Bro, 2008; Murphy *et al.*, 2013a, 2014a). The popularity of PARAFAC stems from its ability to mathematically separate the spectra of overlapping fluorescence components. PARAFAC of a three-way data set decomposes the data signal into a set of trilinear terms and a residual array:

$$x_{ijk} = \sum_{f=1}^F a_{if} b_{jf} c_{kf} + e_{ijk} \quad (2)$$

$$i = 1, \dots, I; j = 1, \dots, J; k = 1, \dots, K$$

where  $x_{ijk}$  is the intensity of the  $i^{\text{th}}$  sample at the  $j^{\text{th}}$  emission value and at the  $k^{\text{th}}$  excitation value (Figure 1.12).

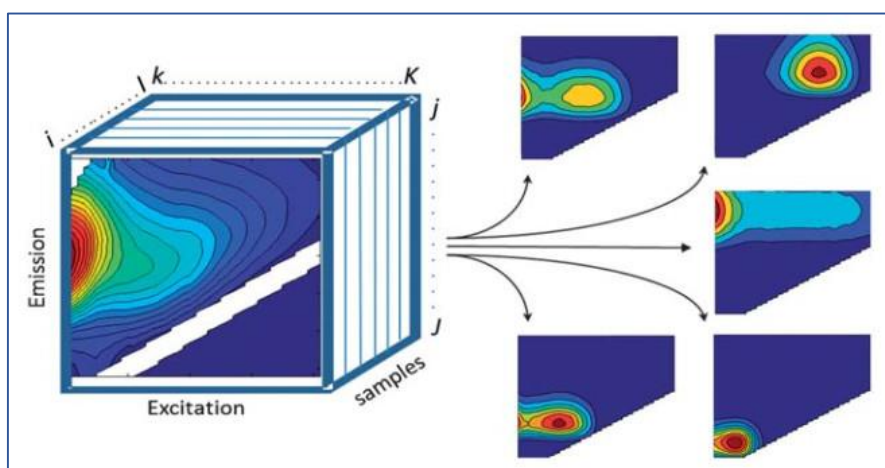
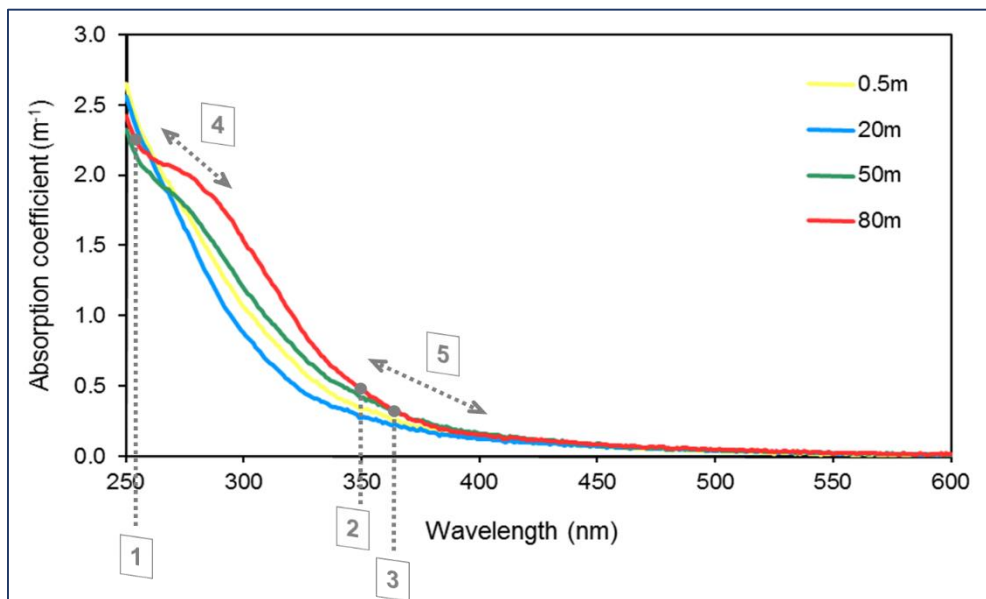


Figure 1.12. EEM dataset arranged in a three-way structure and decomposed into five PARAFAC components. Taken from Murphy *et al.* (2013a).

PARAFAC models use three important assumptions: a) variability, two chemical components cannot present identical excitation or emission spectra or have concentrations that are perfectly correlated (an example could be a set of diluted samples); b) tri-linearity, emission spectra of a component do not vary across excitation wavelengths, excitation spectra do not vary across emission wavelengths, and fluorescence increases approximately linearly with concentration; and c) additivity, fluorescence is due to the linear superposition of a fixed number of components (Bro, 1997). In the case where data consists of a three-way array of EEMs (sample  $\times$  emission  $\times$  excitation), PARAFAC has been shown to be able of recovering accurate spectra and concentrations of known fluorescent materials in mixtures, even in the presence of uncalibrated spectral interferences (Bro, 1997). The chemical interpretation of a PARAFAC model relies on the right number of components being specified by the user.

### 1.3. – Using optical signatures to trace DOM transformations

CDOM and FDOM signatures depend on DOM quality and origin, suffering changes as the organic material experiences biological and photochemical processes. Consequently, the study of the variability of these signatures gives valuable information about the processes that drive the dynamics of the DOM. For example, we can observe the transformation of the shape of the absorption spectra along the water column at the Estartit Oceanographic Station (**Figure 1.13**) and how different are the signal intensities of the fluorescent compounds in samples from surface (5 m) and deep (3000 m) waters of a South Atlantic station (40° 42' 46.021" N; 74° 0' 21.388" W; **Figure 1.14**).



**Figure 1.13.** Examples of absorption spectra of seawater samples taken from the Estartit Oceanographic Station at 0.5, 20, 50 and 80 m deep on April 2012. Different absorption spectra-derived indices are indicated: (1) absorption coefficient at a wavelength of 254 nm ( $a_{254}$ ); (2) absorption coefficient at a wavelength of 350 nm ( $a_{350}$ ); (3) absorption coefficient at a wavelength of 365 nm ( $a_{365}$ ); (4) spectral slope over the range 275 to 295 nm ( $S_{275-295}$ ); (5) spectral slope over the range 350 to 400 nm ( $S_{350-400}$ ).

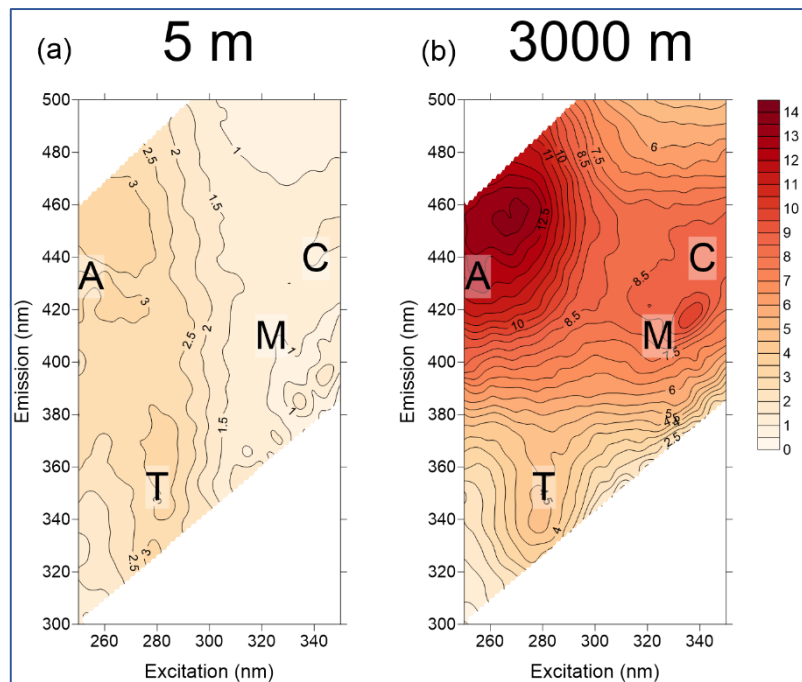


**Figure 1.14.** Excitation-emission matrices (EEM) of two Atlantic Ocean seawater samples (a) 0.5 m deep and (b) 3000 m deep at station 61 of the XV<sup>th</sup> FICARAM cruise on April 2013. The position of the four main fluorophores is indicated. Values expressed in Raman Units (R.U.) x 1000.

### 1.3.1. – FDOM: dynamics and origin of DOM in marine systems

Romera-Castillo *et al.* (2010) demonstrated, for the first time, that phytoplankton can exudate organic compounds fluorescing mainly at peak-M, that are later consumed by prokaryotes and transformed into metabolic by-products that fluoresce at peak-C. Since compounds fluorescing at peak-C and peak-M are known to present more resistance to microbial degradation (lower lability) than those fluorescing at peak-T, recent studies have used the optical characterization to outline inputs of DOM coming from dust aerosols in coastal areas (Sánchez-Pérez *et al.*, 2015). In addition, previous research works have demonstrated the appropriateness of measuring DOM fluorescence signals as a tracer for different water masses (Nieto-Cid *et al.*, 2005; Álvarez-Salgado *et al.*, 2013; Jørgensen *et al.*, 2014a). Moreover, field studies have found a positive linear relationship between the variability of oxygen consumption, also known as apparent oxygen utilization (AOU), and the increase in FDOM signal (Yamashita and Tanoue, 2008; Álvarez-Salgado *et al.*, 2013). This trend was observed to be general for the deep Atlantic Ocean when the origin of the water mass factor was not taken into account (De la Fuente *et al.*, 2014) altogether indicating a positive relationship between FDOM in situ generation and respiration. Other studies highlighted that the availability of precursors is a requisite for a new production of these aromatic compounds. In 2013, Andrew and collaborators demonstrated that, to generate terrestrial humic-like compounds (peak-C fluorophore), it was necessary having, at least, a very small fraction of specific precursors of humic compounds to allow microorganisms inhabiting the deep ocean to generate material of the same quality.

### 1.3.2. – FDOM indices: quality and alterations of DOM in marine systems

In addition to direct optical measurements of organic matter, additional derived variables have been described to better interpret the DOM bulk composition. These indices are, among others, a) C/M ratio, which has been used to examine the proportion of terrestrial-origin DOM respect to *in situ* DOM production in surface waters of coastal systems, and also as a proxy for prokaryotic respiration in deep waters (Chapter 5); b) the humification index (HIX), which describes the diagenetic state of the DOM, for example, aromatic humic acids of high molecular weight are characterized by high HIX (calculated by dividing the peak area under the emission spectra 435-480 nm and the peak area under the emission spectra 300-345 nm, at an excitation of 254 nm; Zsolnay *et al.*, 2003; Giering *et al.*, 2014); c) the biological index BIX, which is an indicator of recent biological activity (Huguet *et al.*, 2009) or recently produced DOM (Wilson and Xenopoulos, 2009) and it is calculated as the ratio of the emission intensities at 380/430 nm for an excitation of 310 nm (Huguet *et al.*, 2009); iv) the fluorescence index (FI), which is a marker to distinguish between terrestrial-plant derived (low FI of ~1.2) and microbial-algal derived (high FI of ~1.4) DOM (Jaffé *et al.*, 2008; Fellman *et al.*, 2010). It is calculated as the ratio of the emission intensities at 470/520 nm respect to the excitation at 370 nm (Cory & McKnight, 2005).

### 1.4. – Hypothesis and Objectives of this thesis

As has been mentioned before, the fluorescence of DOM is being used for multiple purposes. In this thesis we explore the appropriateness of applying fluorescence methods to track the DOM dynamics in marine waters subjected to experimentally-induced or natural perturbations.

#### Experimental work

Two main questions were addressed in our experimental work:

a) Will the availability of humic precursors induce changes in the production of new humic compounds by microbial activity? We tested this question with natural microbial assemblages subjected to different organic enrichments. We performed these experiments with deep water communities because it is known that microbial activity in the deep ocean could be limited by the quality and quantity of the organic matter (see section 1.2.2). Therefore, with these experiments we could explore simultaneously the importance of the quality of the precursors and also the possible priming effect when labile material is provided. In other words, we could test simultaneously the assumptions and hypotheses proposed in Andrew *et al.* (2013) and Dittmar (2015).

b) Will the predicted increase on acidification and eutrophication modify the percentage of recalcitrant organic matter? It has been reported that a reduction of pH and an increase in eutrophication could increase the photosynthesis activity and, consequently, the phytoplanktonic particulate and dissolved organic production (Riebesell *et al.*, 2007), but could these stressors modify the DOM quality? To address this question we performed experiments by enclosing

surface coastal water from the NW Mediterranean Sea in two different seasons of the year. During approximately 10 days, we followed, not only the transformations of FDOM, but also the changes that ruled the succession in the planktonic communities subjected to different pH and nutrient amendments (Chapter 3 and 4). We examined this question in surface coastal waters because this is the layer more directly affected by the increases of  $p\text{CO}_2$  and also because the predicted eutrophication would heavily impact the coastal areas.

#### Field work

Aiming to better monitor and trace the changes that Mediterranean ecosystems would suffer under unstoppable eutrophication processes, a sampling site in the NW Mediterranean Sea was studied for a period of four years. During this period, we simultaneously sampled biological and chemical variables, as well as scrutinized the meteorological time series dataset (Chapter 5). The presence of recurrent upwelling effects induced by severe wind regimes, conditioned the dynamics and transformations of the DOM in the whole water column sampled.

**In summary**, in this thesis, we use CDOM and FDOM as tracers to study the role of the organic precursors in the formation of humic-like DOM in the deep ocean. Moreover, we explore the suitability of using these optical properties as a tool for tracking the transformations that this DOM will suffer in future projected scenarios affected by human-induced impacts, such as acidification and eutrophication. In the field, we examine the variability of DOM in a coastal sampling site along with the variations of other environmental parameters to identify the major drivers of DOM dynamics.



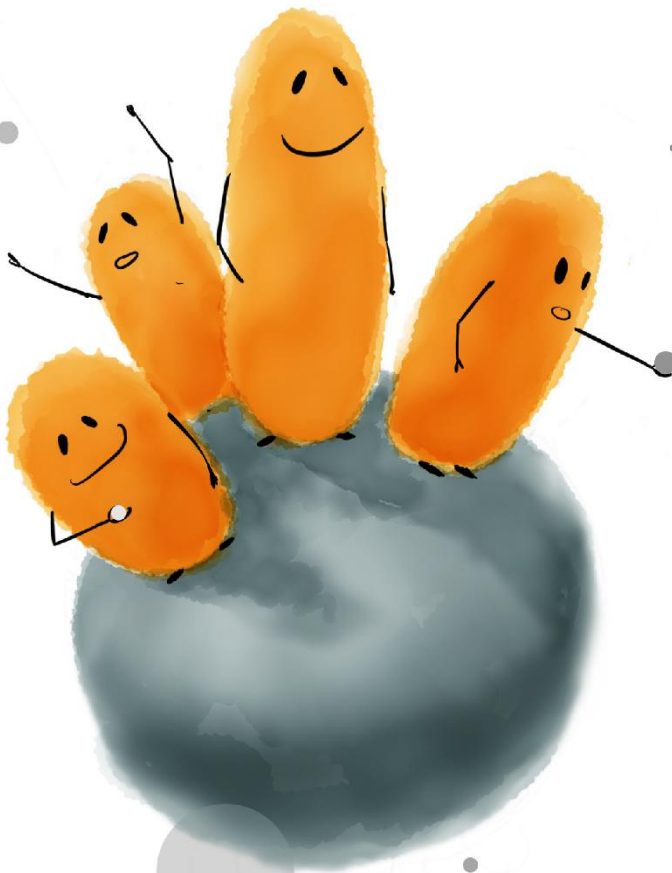
## List of spectroscopic indices used in this thesis

Index	Units	Description	Reference/s
Peak-A	QSU or R.U.	Fluorescence intensity peak at Ex: 250 nm Em: 435 nm	Coble (1996, 2007)
Peak-C	QSU or R.U.	Fluorescence intensity peak at Ex: 340 nm Em: 440 nm	Coble (1996, 2007)
Peak-M	QSU or R.U.	Fluorescence intensity peak at Ex: 320 nm Em: 410 nm	Coble (1996, 2007)
Peak-T	QSU or R.U.	Fluorescence intensity peak at Ex: 280 nm Em: 350 nm	Coble (1996, 2007)
Peak-C/Peak-M	-	Peak-C to peak-M ratio	Aparicio <i>et al.</i> (2016)
Peak-M/DOC or Peak-C/DOC	QSU (or R.U.) L $\mu\text{mol}^{-1}$	Humic-like fluorescence at peak- M o peak-C per carbon unit	Nieto-Cid <i>et al.</i> (2006); Sánchez- Pérez <i>et al.</i> (2015)
HIX	-	Area under the emission spectra 435-480 nm divided by that of 300-345 nm, at an excitation of 254 nm	Zsolnay (2003)
BIX	-	Ratio of the emission intensities at 380/430 nm at an excitation of 310 nm	Huguet <i>et al.</i> (2009)
SUVA	L $\text{mg}^{-1} \text{m}^{-1}$	Absorbance coefficient (base-10 logarithm) at 254 nm per carbon unit	Weishaar <i>et al.</i> (2003)
S <sub>275-295</sub>	-	Absorbance slope between 275 and 295 nm	Helms <i>et al.</i> (2008)
S <sub>350-400</sub>	-	Absorbance slope between 350 and 400 nm	Helms <i>et al.</i> (2008)
S <sub>R</sub>	-	Slope ratio: S <sub>275-295</sub> to S <sub>350-400</sub> ratio	Helms <i>et al.</i> (2008)
DOC/Chl <i>a</i>	$\mu\text{mol } \mu\text{g C}^{-1}$	DOC to chlorophyll ratio	Morán <i>et al.</i> (2002); Hargreaves (2003)



## Chapter 2

Microbially-mediated fluorescent organic matter transformations in the deep ocean. Do the chemical precursors matter?





## 2.1. – Introduction

An important issue to be considered when exploring the role of the ocean in carbon sequestration is the biogeochemical fate of the organic matter. Conventionally, it is known that the biological and solubility pumps combined are important for the transfer of carbon (C) from the atmosphere to the ocean interior, resulting in the temporary or permanent storage of carbon (Legendre *et al.*, 2015; Honjo *et al.*, 2014; Volk and Hoffert, 1985). The recently introduced concept of the microbial carbon pump (MCP) postulates mechanisms by which dissolved refractory organic matter is produced and accumulated in the ocean through microbial activity, underlying the role that this refractory pool plays in carbon sequestration in marine systems (Jiao *et al.*, 2010).

The mechanisms that produce dissolved organic matter (DOM) are, among others: phytoplankton exudation (Sarmiento *et al.*, 2013; Romera-Castillo *et al.*, 2010; Hopkinson *et al.*, 2002), release by viral lysis (Motegi *et al.*, 2009; Brussaard, 2004), sloppy feeding and the solubilization of particulate organic matter (POM) by bacterial and archaeal hydrolases (Sala and Güde, 2004; Nagata *et al.*, 2000). These various mechanisms condition not only DOM production but also its quality, and consequently its ultimate fate.

The study of DOM in the ocean interior has been in the spotlight for several years. A fraction of this pool, called chromophoric dissolved organic matter (CDOM; Coble, 1996), absorbs light at both ultraviolet (UV) and visible wavelengths. A sub-fraction of this CDOM, the fluorescent DOM (FDOM; Coble, 2007, 1996), fluoresces when irradiated with UV light. In 1961, Weber described a technique to elucidate the main fluorescing groups of compounds, i.e. fluorophores, by varying the excitation and emission wavelengths and constructing a matrix of the resulting intensities. This technique generates the so-called fluorescence excitation-emission matrix (EEM) which was first applied by Coble *et al.* (1990) to characterize marine FDOM. This technique, however, does not permit the quantification of specific molecules. A better understanding of specific molecules has become possible with the recently developed Fourier transform ion cyclotron resonance mass spectrometry (FT-ICR-MS), a methodology that offers novel insights for molecular-level characterization of the complex composition and structure of DOM (Repeta, 2015; Stubbins *et al.*, 2014; Koprivnjak *et al.*, 2009; Koch *et al.*, 2005; Kim *et al.*, 2003). Nevertheless, the most exhaustive analysis that has been performed to date (Hertkorn *et al.*, 2006) could only identify 8% of the molecules composing the DOM pool. These authors combined multidimensional nuclear magnetic resonance (NMR) with FT-ICR-MS on solid phase extracted dissolved organic matter (SPE-DOM), and their results indicate that carboxylic-rich alicyclic molecules (CRAM) are the major component of DOM. Great efforts are being performed in recent years to relate molecular formulas to the optical measurements of DOM in order to associate fluorescent signatures to single molecules (Reader *et al.*, 2015; Stubbins *et al.*, 2014). Nevertheless, the challenge of identifying and revealing the composition of DOM remains still incomplete. With that said, fluorescence spectroscopy methods, being rapid and inexpensive, are convenient for certain

studies focused on humic- and protein like compounds that require large coverage, spatial or temporal.

Marine DOM is composed of a large variety of substances owning different turnover rates and residence times. The turnover times of some FDOM components have been estimated to be, on average, higher than the deep ocean water renewal, and thus the fluorescence measurements have been proposed as a proxy to study the cycling of DOM that is resistant at centennial time scales (Catalá *et al.*, 2015). In water masses exhausted in labile or semi-labile fractions of DOM, bacteria could 'prime' the recalcitrant compounds decomposition if labile compounds are added to the media (Bianchi, 2012; Carlson *et al.*, 2002). The 'priming effect' (PE), bacterial remineralization of unreactive organic carbon substrates when labile sources are available, was described for the first time in soil sciences in 1926 by Löhnis. The PE has been experimentally observed in a variety of environments and with additions of different carbon compounds: in soils (Kuzyakov, 2002; Fontaine *et al.*, 2004); fresh water ecosystems (De Haan, 1977; Shimp and Pfaender, 1985; Bianchi *et al.*, 2015; Catalán *et al.*, 2015); and also in marine ecosystems, mainly using mesocosm experiments (Guenet *et al.*, 2014; Fonte *et al.*, 2013; Carlson *et al.*, 2002). However, as it was mentioned before, the mechanisms that hinder the complete remineralization of DOM, causing the relative permanence of part of this pool, from months to millennia, are not really well understood.

Despite the several studies conducted during the last years to assess the spatial and temporal variability of DOM quality (Kothawala *et al.*, 2014; Gontikaki *et al.*, 2013; Koehler *et al.*, 2012; Yamashita *et al.*, 2011), little is known about how the reactivity of DOM varies across landscapes (rivers, lakes, estuaries, coastal ocean, deep ocean). Most of these studies have recognized that DOM reactivity is not only inherently linked to its chemical composition, but also depends on ecosystem properties (Dittmar, 2015). A better understanding of microbial FDOM transformations in the deep ocean is required before FDOM can be consistently applied as a water mass tracer or as a proxy for a fraction of the DOM.

Recent studies have found a high correlation between apparent oxygen utilization (AOU) and the generation of humic-like compounds, indicating that humic-DOM in the dark ocean could originate from in situ microbial respiration (Jørgensen *et al.*, 2014a; De La Fuente *et al.*, 2014; Yamashita and Tanoue, 2008), which agrees with the MCP concept proposed by Jiao *et al.* (2010). Furthermore, Andrew *et al.* (2013) suggested that the production of humic-like fluorescence signal is favored when terrestrial chemical precursors are present. In order to gain insight into the microbially-mediated FDOM variability, the present study examines how the quality and quantity of the organic substrates influence simultaneously the generation of humic fluorescence signal and the microbial activity. This was carried out by performing incubation experiments using water samples from the deep Atlantic Ocean. These calculations are key to understand the particularities of deep waters C storage and the functioning of the microbial carbon pump.

## 2.2. – Materials & Methods

### 2.2.1. – Sample collection and experimental strategy

We conducted three experiments (DEEP I, DEEP II and DEEP III) with natural prokaryotic communities from deep waters of the South Atlantic Ocean. Seawater was taken during the FICARAM-15 cruise, carried out from the 20<sup>th</sup> of March to the 22<sup>nd</sup> of May 2013, following a track from Punta Arenas (Chile) to Cartagena (Spain). Experiment DEEP I was performed with water taken from station 5 (48° 18' 18.6" S; 54° 54' 35.4" W) at 4500 m while in experiments DEEP II and DEEP III we used 3000 m water from stations 18 (40° 30' 0" S; 48°, 5' 28" W) and 53 (17° 50' 1.21" S; 31° 38' 2.4" W), respectively (**Figure 2.1**).

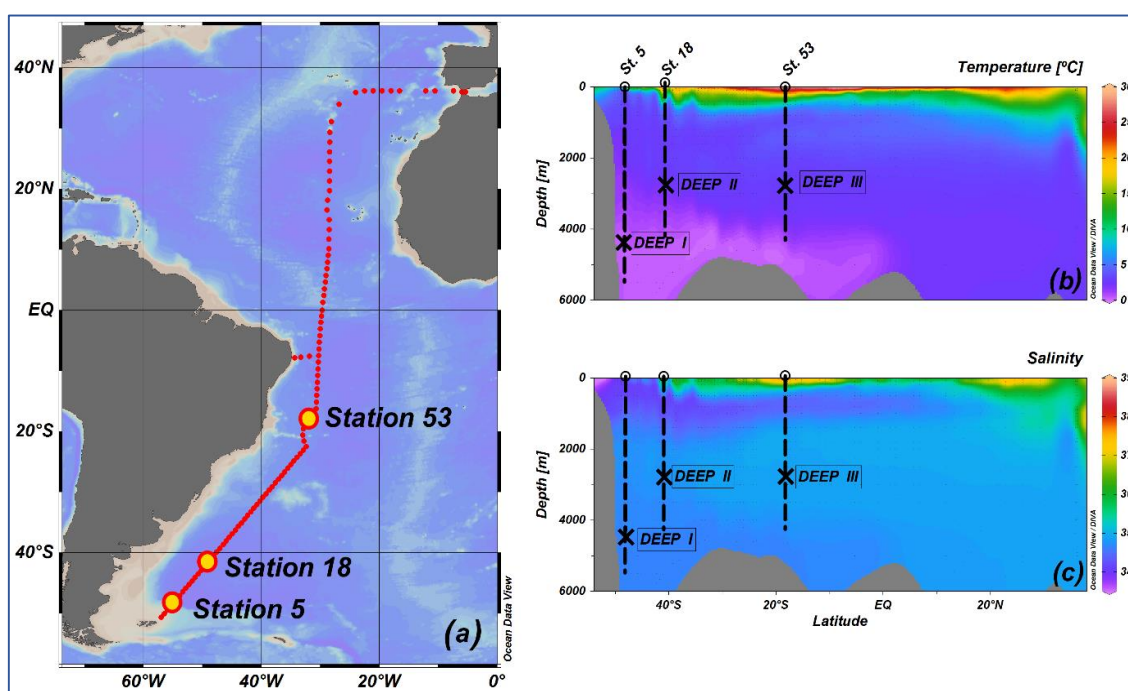


**Figure 2.1.** Graphic summary of the XIV<sup>th</sup> FICARAM cruise: cruise track followed on board the Spanish R/V *Hespérides* (a), contour plot of temperature expressed in °C (b), and contour plot of salinity (c). Panels include information about the sampling station and depths for each experiment. Ocean Data View was used for mapping (Schlitzer, 2016).

In each experiment, sample filtration through 0.6 µm pore-size polycarbonate filters started within 20 minutes after collection. Then, the water was distributed into four 20 L fluorinated polyethylene carboys. The first container was kept as a control (K). Acetate and glucose (both had been found to be very labile compounds with turnover times of hours to days in marine waters (Azam and Hodson, 1981; Ho *et al.*, 2002), were added to the second container (CL). A combination of carbon-based substances was added to the third container (CM). In this case, not only glucose and acetate were added, but also a mixture of compounds of different lability, including terrestrial humic acids and amino acids, which are known to be essential for prokaryotic metabolism, (see **Table 2.1**). In the last carboy (CR), Suwannee River humic acids (Ref. 2R101N) provided by the International Humic Substances Society (IHSS) was added. All the organic carbon (OC)

substrates were dissolved in 50 mL of Milli-Q water prior to the addition into the carboys. In the case of Suwannee River humic acids, a pH of 12 was needed to favor the dilution, thus we previously added the material in a solution of NaOH and later we compensate the pH adding  $\text{HCO}_3^-$ .

**Table 2.1.** A list of the compounds added to each experimental treatment (Sigma-Aldrich Co. LLC.)

Compound	Molecular formulae	Final estimated concentration ( $\mu\text{mol C L}^{-1}$ ) per treatment		
		CL	CM	CR
<i>D-glucose</i>	$\text{C}_6\text{H}_{12}\text{O}_6$	15	3.33	
<i>Sodium acetate</i>	$\text{C}_2\text{H}_3\text{O}_2\text{Na}$	15	3.33	
<i>Sodium pyruvate</i>	$\text{C}_3\text{H}_3\text{NaO}_3$		3.33	
<i>Humic acids</i>	-Unknown-		3.33	30
<i>Cellulose</i>	$(\text{C}_6\text{H}_{10}\text{O}_5)_n$		3.33	
<i>Chitin</i>	$(\text{C}_8\text{H}_{15}\text{NO}_6)_n$		3.33	
<i>D-aspartic</i>	$\text{C}_4\text{H}_7\text{NO}_4$		3.33	
<i>N-acetyl-D-glucosamine</i>	$\text{C}_8\text{H}_{15}\text{NO}_6$		3.33	
<i>L-arginine hydrochloride</i>	$\text{C}_6\text{H}_{14}\text{N}_4\text{O}_2$		0.33	
<i>L-histidine hydrochloride</i>	$\text{C}_6\text{H}_9\text{N}_3\text{O}_2 \cdot \text{HCl}$		0.33	
<i>L-isoleucine</i>	$\text{C}_6\text{H}_{13}\text{NO}_2$		0.33	
<i>L-leucine</i>	$\text{C}_6\text{H}_{13}\text{NO}_2$		0.33	
<i>L-lysine hydrochloride</i>	$\text{C}_6\text{H}_{14}\text{N}_2\text{O}_2$		0.33	
<i>L-methionine</i>	$\text{C}_5\text{H}_{11}\text{NO}_2\text{S}$		0.33	
<i>L-phenylalanine</i>	$\text{C}_9\text{H}_{11}\text{NO}_2$		0.33	
<i>L-threonine</i>	$\text{C}_4\text{H}_9\text{NO}_3$		0.33	
<i>L-tryptophan</i>	$\text{C}_{11}\text{H}_{12}\text{N}_2\text{O}_2$		0.33	
<i>L-valine</i>	$\text{C}_5\text{H}_{11}\text{NO}_2$		0.33	

All carbon amendments were calculated to result in an approximately 30  $\mu\text{mol C}$  increase in dissolved organic carbon (DOC) concentration. After the additions, the containers were manually shaken and kept one hour at 4 °C before sampling the initial point ( $t_0$ ) in order to assure homogenization. At  $t_0$ , water from each of the experimental conditions was distributed among 72 acid clean 250 mL glass bottles (18 bottles per treatment). Three glass bottles per experimental condition were harvested at every sampling date, and the three bottles were considered experimental replicates. The experiments were conducted on board in a dark temperature-controlled chamber at 4 °C and monitored for a total of 35 days. Intensive samplings were scheduled for days: 0, 5, 10, 15, 25 and 35, where the variables measured were: prokaryotic abundance, FDOM and CDOM. Furthermore, after day 3 ( $t_3$ ), one bottle of each condition was sampled daily to monitor prokaryote abundances. This subsampled bottle was then considered replicate number 1 in the following intensive sampling.

### 2.2.2. – Measurements

The ship's rosette was equipped with a SBE11plus (Sea-Bird Electronics) CTD probe, recording, at each station, profiles of temperature, conductivity and oxygen. Analyses of dissolved inorganic nutrient concentrations, nitrate ( $\text{NO}_3$ ), phosphate ( $\text{PO}_4$ ) and silicate ( $\text{SiO}_2$ ), were done on board by standard segmented flow analyses with colorimetric detection (Hansen and Grasshoff, 1983) using a Skalar Autoanalyzer. Precisions were  $\pm 0.01 \mu\text{mol kg}^{-1} \text{NO}_3$ ,  $\pm 0.02 \mu\text{mol kg}^{-1} \text{PO}_4$ , and  $\pm 0.01 \mu\text{mol kg}^{-1} \text{SiO}_2$ . DOC samples were collected in 10 mL precombusted (450 °C, 24 h) glass ampoules. After acidification with 50  $\mu\text{L}$  of 25%  $\text{H}_3\text{PO}_4$  to  $\text{pH} < 2$ , the ampoules were heat-sealed and stored in the dark at 4 °C until examination. Analyses were carried out in a Shimadzu TOC-CSV organic carbon analyzer. Three to five injections of 150  $\mu\text{L}$  were performed per replicate. DOC concentration in each replicate was calculated by first subtracting a Milli-Q blank and then dividing by the slope of a daily standard curve made from potassium hydrogen phthalate. The precision of measurements was  $\pm 0.7 \mu\text{mol L}^{-1}$ . All samples were checked against deep Sargasso Sea reference water (2600 m) provided by D. Hansell (U. of Miami).

FDOM was measured using a Perkin Elmer LS55 luminescence spectrometer equipped with a xenon discharge lamp (20 kW/8  $\mu\text{s}$ ). A red sensitive R928 photodiode multiplier worked as a reference detector. The running parameters for the instrument were set as follows: scan speed at 250  $\text{nm min}^{-1}$  and slit widths (for excitation and emission wavelengths) at 10 nm, at a constant room temperature of 20 °C in a 1 cm quartz fluorescence cell. Excitation-emission matrices were performed by concatenating 21 excitation/emission spectra of the sample, obtained at a constant offset of 10 nm between the excitation and emission wavelengths. The spectra were collected starting from the highest excitation wavelength, to minimize the exposure of the sample to low-wavelength radiation and thereby minimize photodegradation. Following Lawaetz and Stedmon (2009), fluorescence measurements were expressed in Raman Units (R.U.) by normalization to the integrated water Raman scattering band of Milli-Q water freshly generated on board every day.

To better characterize the dynamics of the FDOM, PARAFAC modelling of the EEM datasets was conducted using the drEEM toolbox (Murphy *et al.*, 2013b) in the Matlab® software package. The dataset for PARAFAC modelling was composed of 289 samples collected during the cruise to increase the consistency of the model, 64 of them belonging to the DEEP water experiments. In order to organize the data for the modelling process, regions of no fluorescence or scatter were removed. By doing so, our EEMs ranged from 250 to 450 nm along the excitation axis, and from 350 to 550 nm along the emission axis. The model was run with non-negativity constraints. A series of PARAFAC models were tested with 3 to 7 components fitted to the data. Split-half validation was used to divide the data into six random halves of equal size and the model run independently on the halves. A four-component PARAFAC model was validated. According to the residual analyses, we could confirm that less than 10% of the fluorescence was left unexplained (subtraction of the modelled from the measured spectra yielded a residual fluorescence an order

of magnitude lower than the measured EEMs). The characteristics of the four components of the PARAFAC model are shown in **Figure 2.2**. Their excitation and emission maxima are specified in **Table 2.2** and they are associated to components already detected in previous studies. Three out of the four components identified (FIC1, FIC2 and FIC4) are placed in humic-like fluorescence regions and one of them (FIC3) in the protein-like area.

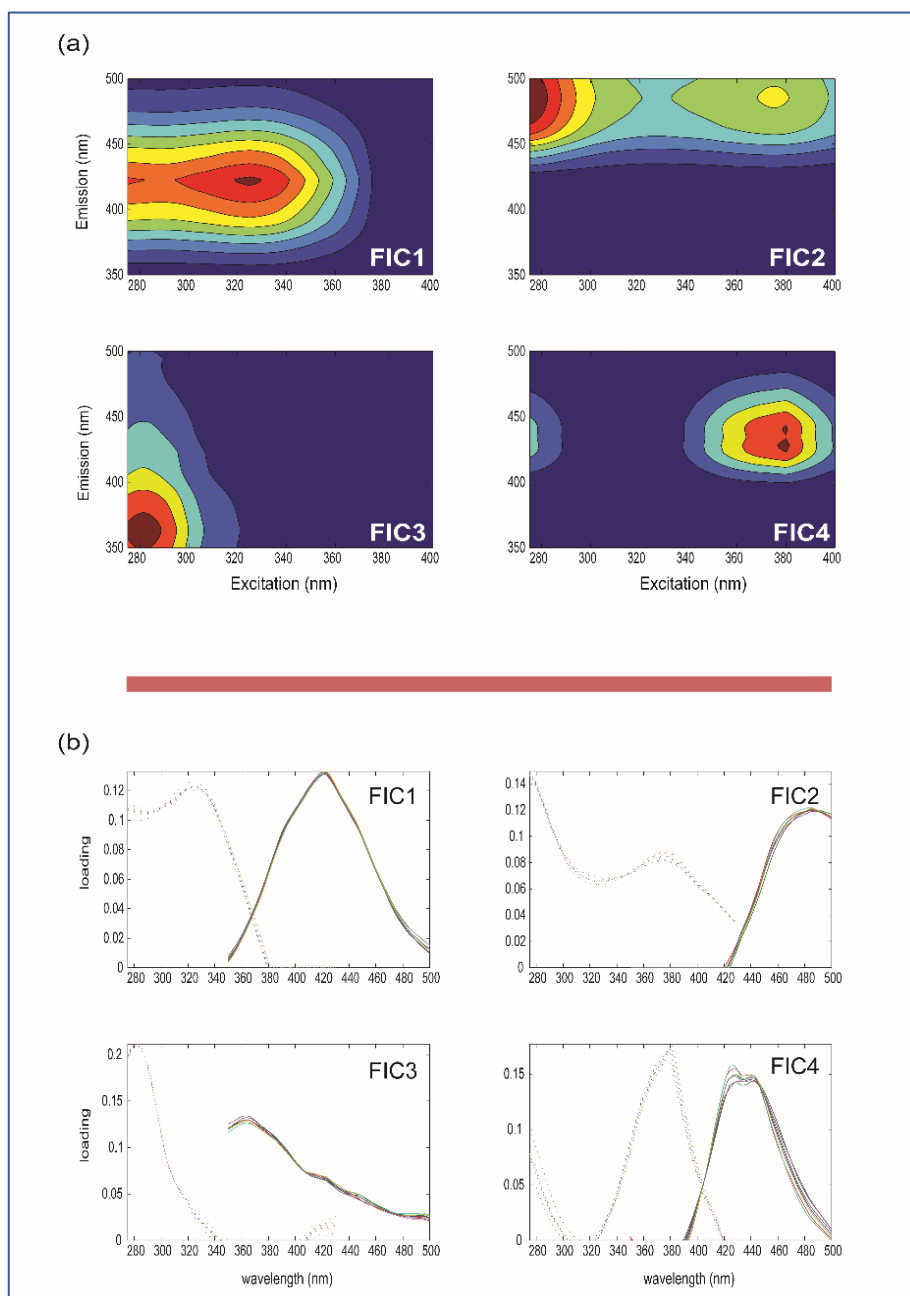


**Figure 2.2.** (a) Fluorescence signatures of the four PARAFAC components (FIC1 to FIC4) identified during the experiments. (b) Line plots showing split-half validations in which each component's excitation (left) and emission (right) spectra are estimated from independent halves of the dataset.

**Table 2.1.** Optical characteristics of five components derived from the PARAFAC and their comparison with the results from previous studies available in the OpenFluor database (Murphy *et al.*, 2014b). For all comparisons Tucker's Congruence Coefficient (TCC) was > 0.95.

Comp	Ex (nm)	Em (nm)	Assignment					
			Murphy <i>et al.</i> (2008)	Walker <i>et al.</i> (2009)	Yamashita <i>et al.</i> (2010a)	Kothawala <i>et al.</i> (2012)	Graeber <i>et al.</i> (2012)	Brym <i>et al.</i> (2014)
<b>FIC1</b>	325	423	C3	BERC3*	C1		C1*/C4	
<b>FIC2</b>	275	468	C2/C4*			CX		
<b>FIC3</b>	<281	363			C6*	CT	C5	C1*
<b>FIC4</b>	380	428	P3*					C3

\*Component does not completely match

Heterotrophic prokaryotes were enumerated with a FACSCalibur (Becton Dickinson) flow cytometer equipped with a 15 mW argon-ion laser (488 nm emission) as described by Gasol and del Giorgio (2000). Samples (1.8 mL) were immediately fixed with 1% paraformaldehyde plus 0.05% glutaraldehyde (final concentrations), incubated for 10 min at room temperature, frozen in liquid nitrogen and stored at -80 °C. Before analysis, samples were unfrozen, stained with SYBRGreen I (Molecular Probes) at a final concentration of 10 µM and left in the dark for about 15 min. Each sample was then run at low speed (approx. 12 µL min<sup>-1</sup>) for 2 minutes with Milli-Q water as a sheath fluid. We added 10 µL per sample of a solution of yellow-green 0.92 µm Polysciences latex beads (10<sup>6</sup> beads mL<sup>-1</sup>) as an internal standard. Bacteria were detected by their signature in a plot of side scatter versus FL1 (green fluorescence). Data analysis was performed with the Paint-A-Gate software (Becton Dickinson).

### 2.2.3. – Statistical analyses

The software SigmaPlot v11.0 (Systat Software Inc.) was used to perform the statistical analyses applied in this work. Two-way ANOVA was carried out to test if differences between conditions and experiments were significant and t-tests to discriminate if the temporal evolution of the different variables measured in an experiment could be considered significant. For both types of tests, significance was set to *p*-value < 0.05.

## 2.3. – Results

### 2.3.1. – Initial conditions

The physical and chemical signatures of the water masses used in each experiment, Antarctic Bottom Water (AABW) in experiment DEEP I, Circumpolar Deep Water (CDW) in experiment DEEP II and North Atlantic Deep Water (NADW) in experiment DEEP III, are listed in **Table 2.3**. AABW presented the lowest temperature and highest concentration of nutrients. As shown in **Figure 2.1**, the temperature and salinity of the deep Atlantic Ocean increased as latitude

decreased, whereas DOC decrease values ranging from 40 to 45  $\mu\text{mol L}^{-1}$ , in agreement with previous observations of deep ocean DOC (Hansell *et al.*, 2009).

**Table 2.2.** Physical and chemical signatures of the water masses used in each of the three DEEP experiments.

Station (experiment)	5 (DEEP I)	18 (DEEP II)	53 (DEEP III)
Depth (m)	4500	3000	3000
Water mass	Antarctic Bottom Water (AABW)	Circumpolar Deep Water (CDW)	North Atlantic Deep Water (NADW)
Temperature ( $^{\circ}\text{C}$ )	0.27	1.84	2.78
Salinity	34.67	34.76	34.91
Nitrate ( $\mu\text{mol kg}^{-1}$ )	32.82	29.28	20.51
Phosphate ( $\mu\text{mol kg}^{-1}$ )	2.27	1.98	1.21
Silicate ( $\mu\text{mol kg}^{-1}$ )	128.37	90.75	32.51
Oxygen ( $\mu\text{mol kg}^{-1}$ )	221.3	204.9	250.4
DOC ( $\mu\text{mol L}^{-1}$ )	47.5	45.8	41.8

A compilation of excitation-emission matrices acquired at the beginning of each experiment ( $t_0$ ) is presented in **Figure 2.3**. Clearly different patterns, depending on the treatment, are apparent. When comparing the EEMs for the control (K, no carbon addition, **Figure 2.3a-c**) among experiments, the starting points for the different water samples are similar, reflecting the limited range in DOC values between sites. High fluorescence values ( $>0.01$  R.U.) were located around the FIC2 maxima at Ex/Em wavelengths (275 nm/468 nm) while the other humic-like fluorophores (325 nm/423 nm and 380 nm/428 nm) had lower intensities (0.006~0.008 R.U.). Signals for protein-like material (281 nm/363 nm) were even lower ( $\sim 0.004$  R.U.). Likewise, the fluorescence intensities for the labile carbon treatments (CL) at  $t_0$  (**Figure 2.3d-f**) did not reach values higher than 0.01 R.U., indicating that the added compounds did not influence the initial fluorescence signal. As expected, in the mixed substrate treatment (CM, **Figure 2.3g-i**), the addition of amino acids and humic acids increased remarkably the initial fluorescence values. The addition of pure amino acids was the main reason behind the high values observed within the protein-like region ( $\sim 0.03$  R.U.), while the addition of Suwannee River natural organic matter caused higher values within the humic-like regions of the EEM, e.g. up to  $\sim 0.021$  R.U. at the FIC2 maximum area and around 0.018 R.U. for the rest of the humic-like fluorophores. Finally, the initial EEMs of the CR treatments (refractory carbon, **Figure 2.3j-l**) also showed a similar trend for the three experiments. The Suwannee River humics additions altered only the visible wavelength emission enhancing humic-like intensities (up to  $\sim 0.06$  R.U.), a reflection of the terrestrial nature of the added compounds.

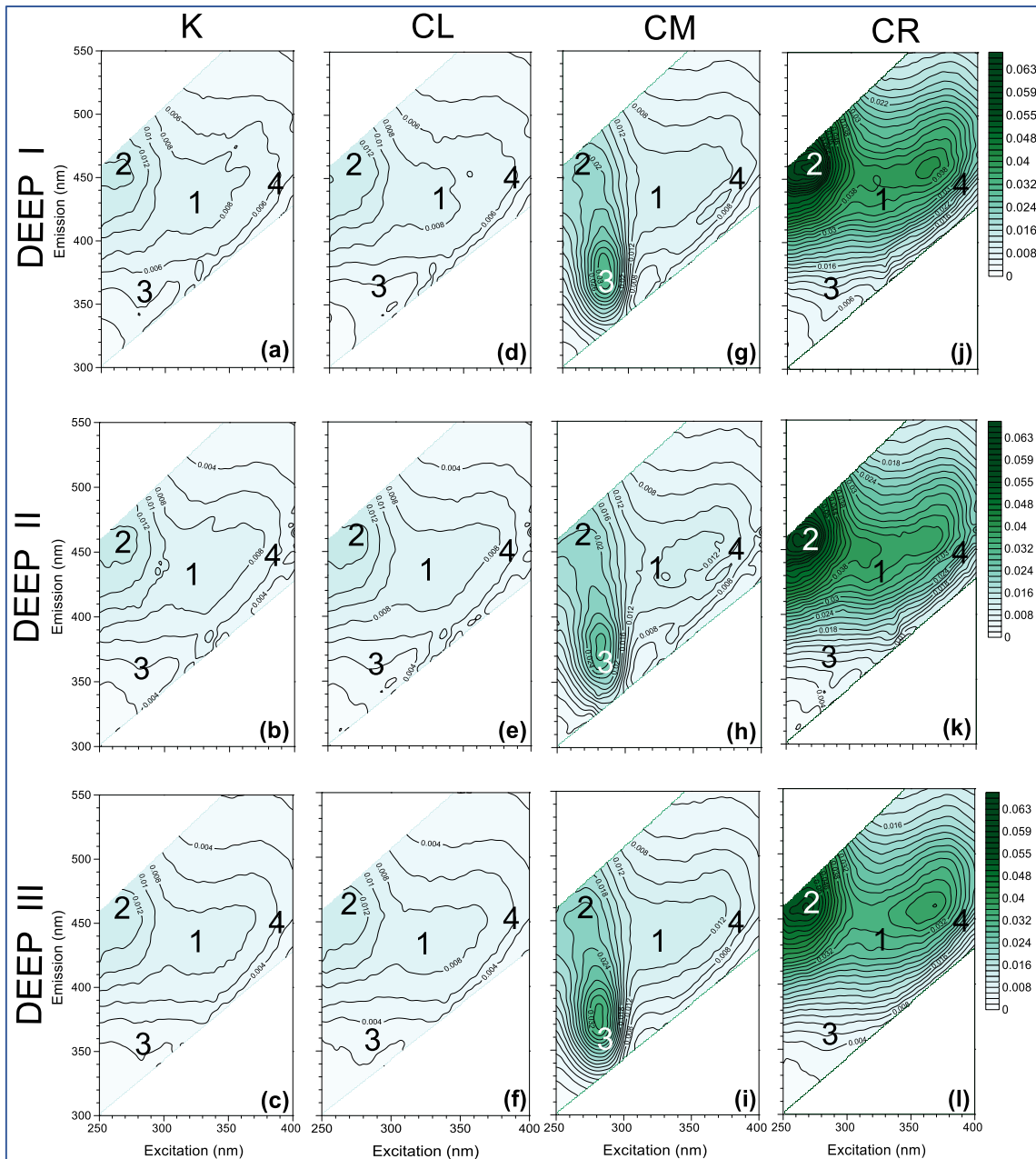


**Figure 2.3.** FDOM characterization (EEMs) of all the initial ( $t_0$ ) water samples. From left to right: K conditions for DEEP I (a), DEEP II (b) and DEEP III (c); CL conditions for DEEP I (d), DEEP II (e) and DEEP III (f); CM conditions for DEEP I (g), DEEP II (h) and DEEP III (i); and lastly, CR conditions for DEEP I (j), DEEP II (k) and DEEP III (l). Location of the excitation and emission maxima of the four PARAFAC components identified is indicated by the numbers attributed (1, FIC1 Ex/Em: 325 nm/423 nm; 2, FIC2 Ex/Em: 275 nm/468 nm; 3, FIC3 Ex/Em: 281 nm/363 nm; 4, FIC4 Ex/Em: 380 nm/428 nm). Values expressed in R.U.

## 2.3.2. – Responses to treatments

### 2.3.2.1. – Dynamics of the prokaryotic community

Prokaryotic abundance increased throughout the first five days of the incubation following the same trend in the three experiments (Figure 2.4). Prokaryotic abundance at  $t_0$  was about  $8.0 \cdot 10^3$ ,  $2.3 \cdot 10^4$  and  $1.1 \cdot 10^4$  cells  $\text{mL}^{-1}$  for experiments DEEP I, DEEP II and DEEP III, respectively. The stationary phase was reached after 10 days of incubation in all experiments. Prokaryote concentration at the end of the exponential growth phase ranged from  $6.9 \cdot 10^4$  to  $8.0 \cdot 10^4$  cells  $\text{mL}^{-1}$  in the K treatments, from  $7.8 \cdot 10^5$  to  $9.2 \cdot 10^5$  cells  $\text{mL}^{-1}$  in the CL conditions, from  $5.8 \cdot 10^5$  to

$6.1 \cdot 10^5$  cells  $\text{mL}^{-1}$  in the CM incubations and from  $6.5 \cdot 10^4$  to  $1.3 \cdot 10^5$  cells  $\text{mL}^{-1}$  in the CR conditions. During the first days of experiment the slopes of the curves indicated faster growth rates for the CM treatments than for the rest of them, although the number of cells in the CL treatment reached the highest values at the end of the exponential-growth phase. After  $t_{10}$ , the prokaryotic communities in all the experiments entered stationary phase. This lasted until the end of the experimental period.

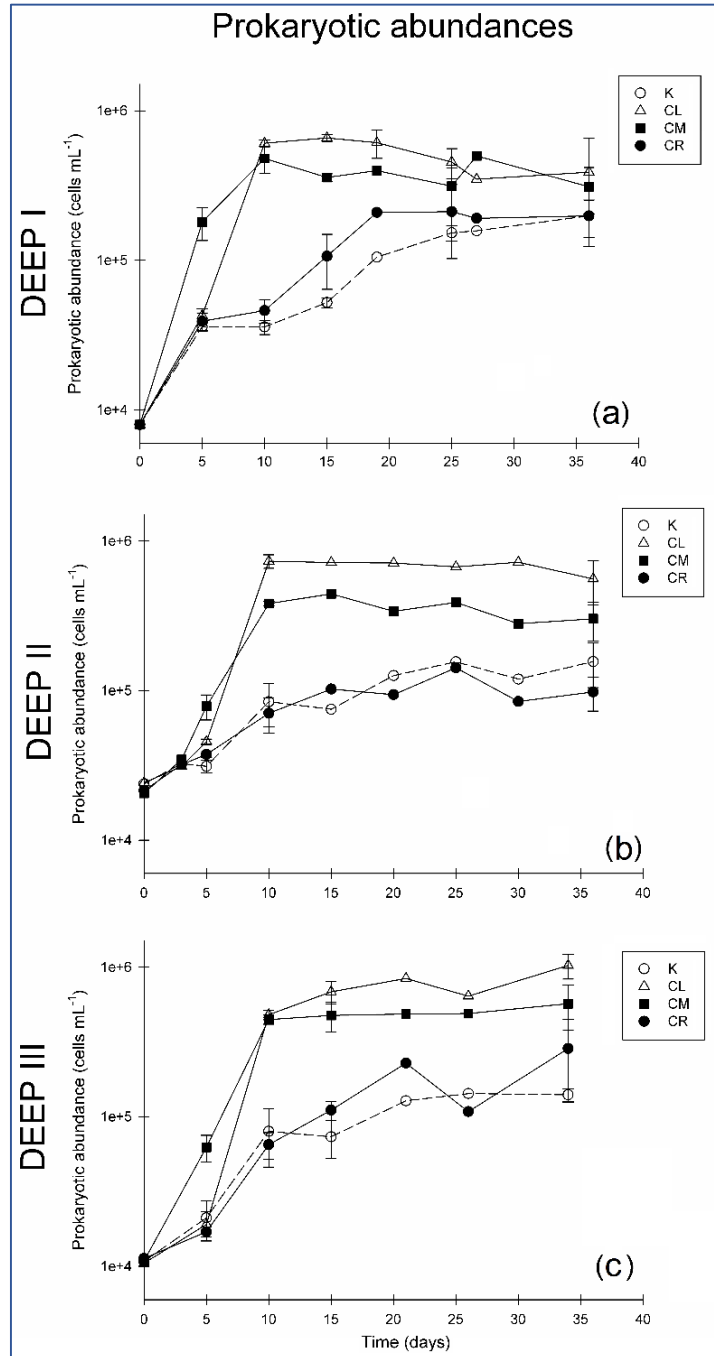


**Figure 2.4.** Prokaryote abundances (in cells  $\text{mL}^{-1}$ ) during experiments DEEP I (a), DEEP II (b), and DEEP III (c). Vertical lines show standard deviations of 3 replicates.

### 2.3.2.2. – Fluorescence characterization

To easily visualize the net change in the humic-like and the protein-like fractions of the FDOM during the exponential-growth and stationary phases of the experiments, we subtracted the fluorescence intensities at  $t_0$  from those measured at  $t_{10}$  and also the values at  $t_{10}$  from those measured at  $t_{\text{final}}$ . We also divided the resultant values by the number of days each phase lasted. The bar charts in **Figure 2.5** show fluorescence intensity increases/decreases for each humic-like component in each experiment. The resultant fluorescence intensities during the exponential-growth phase and the stationary phase were similar for experiments DEEP II and DEEP III, but DEEP I presented divergent patterns. In DEEP I, FIC1, FIC2 and FIC4 intensities decreased for all treatments during the exponential-growth phase (**Figures 2.5a, d and g**). The largest decreases during this phase were observed in the CR conditions followed by the decreases in the CM conditions. On the contrary, we found increases during the same time period in DEEP II and DEEP III, the highest being again detected in the CR and CM conditions, with the exception of the FIC4 signal in the CM and CL conditions in DEEP III, which decreased (**Figures 2.5b-c, 2.5e-f and 2.5h-i**). During the stationary phase of the three experiments the fluorescence signals tended to increase in all treatments. The values of this increase were always the highest for the CR conditions, regardless of the experiment, except in one case, for the FIC4 component.

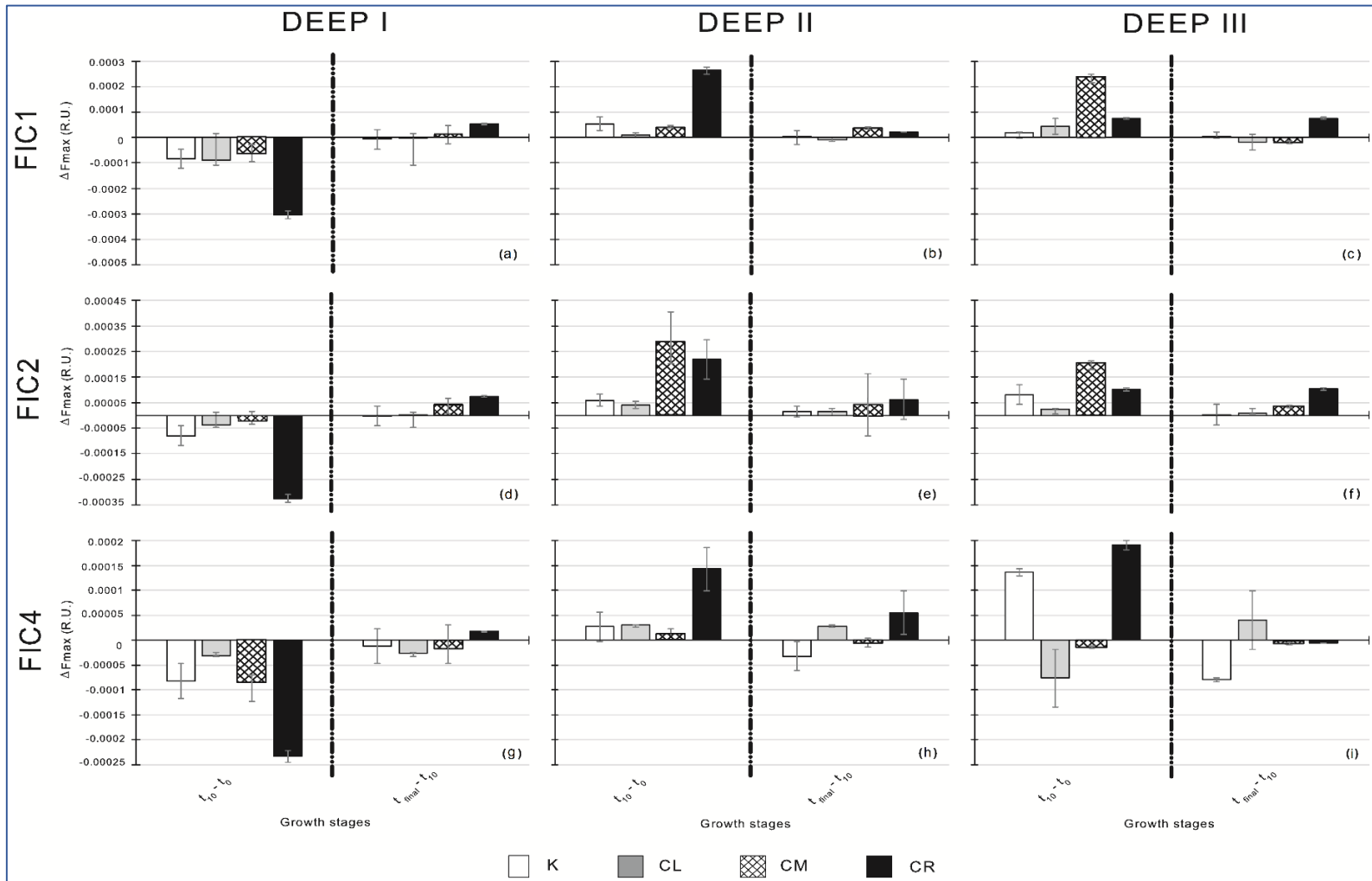


**Figure 2.5.** Variations of each humic-like component in the four experimental conditions of the three experiments. From top to bottom: variations of FIC1 for DEEP I (a), DEEP II (b) and DEEP III (c); variations of FIC2 for DEEP I (d), DEEP II (e) and DEEP III (f); and variations of FIC4 for DEEP I (g), DEEP II (h) and DEEP III (i). Exponential-growth and stationary phases are separated in the graphs. Values expressed in R.U.

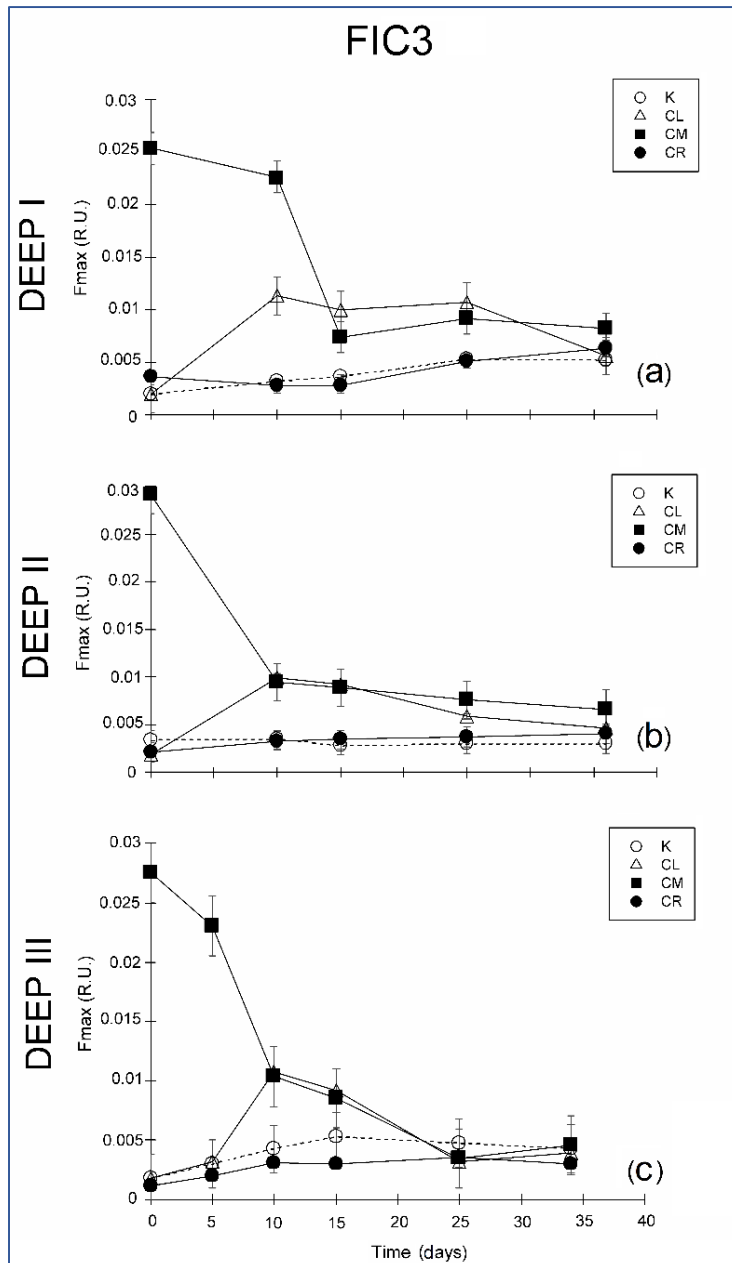


**Figure 2.6.** Temporal evolution of FIC3 component in (a) DEEP I, (b) DEEP II and (c) DEEP III for the four experimental conditions. Values expressed in R.U.

A different temporal dynamic was observed for protein-like substances, FIC3 (Figure 2.6). All the experiments showed similar trends in K, CL and CR treatments. The FIC3 component signal was very low at the beginning of the experiments for the K, CL and CR treatments, while in the CM condition the added amino acids induced elevated values of protein-like fluorescence (Figure 2.6). FIC3 intensity coupled to prokaryotic abundance in all treatments except in that amended with protein-like precursors (CM). The decay of FIC3 signal in DEEP II and DEEP III experiments was higher than the decrease detected for this component in DEEP I. We hypothesized that the FIC3 increase in K, CL and CR is due to bacterial growth while in the CM treatment, the consumption of the added fluorescent protein-like substances overcame FIC3 production.

To examine the relative importance of FIC3 consumption with respect to FIC3 generation in CM, we estimated the production in this treatment using an empirical model based on the relationship between FIC3 fluorescence and prokaryotic abundance (Figure 2.7). The model was constructed with the data pooled from the treatments with no amino acid amendments (K, CL and CR) and where FIC3 fluorescence increased with time, as prokaryotes grew (Figure 2.6).

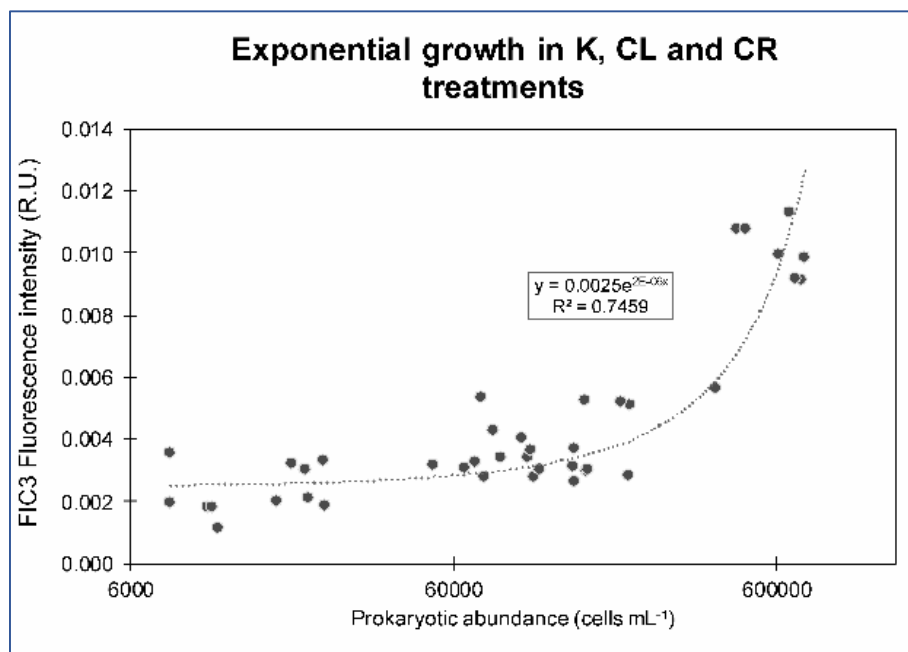


**Figure 2.7.** Exponential growth model of FIC3 intensity versus bacterial abundances for all the K, CL and CR treatments together. Prokaryotic abundances are expressed in cells mL<sup>-1</sup> and fluorescence intensities in R.U.

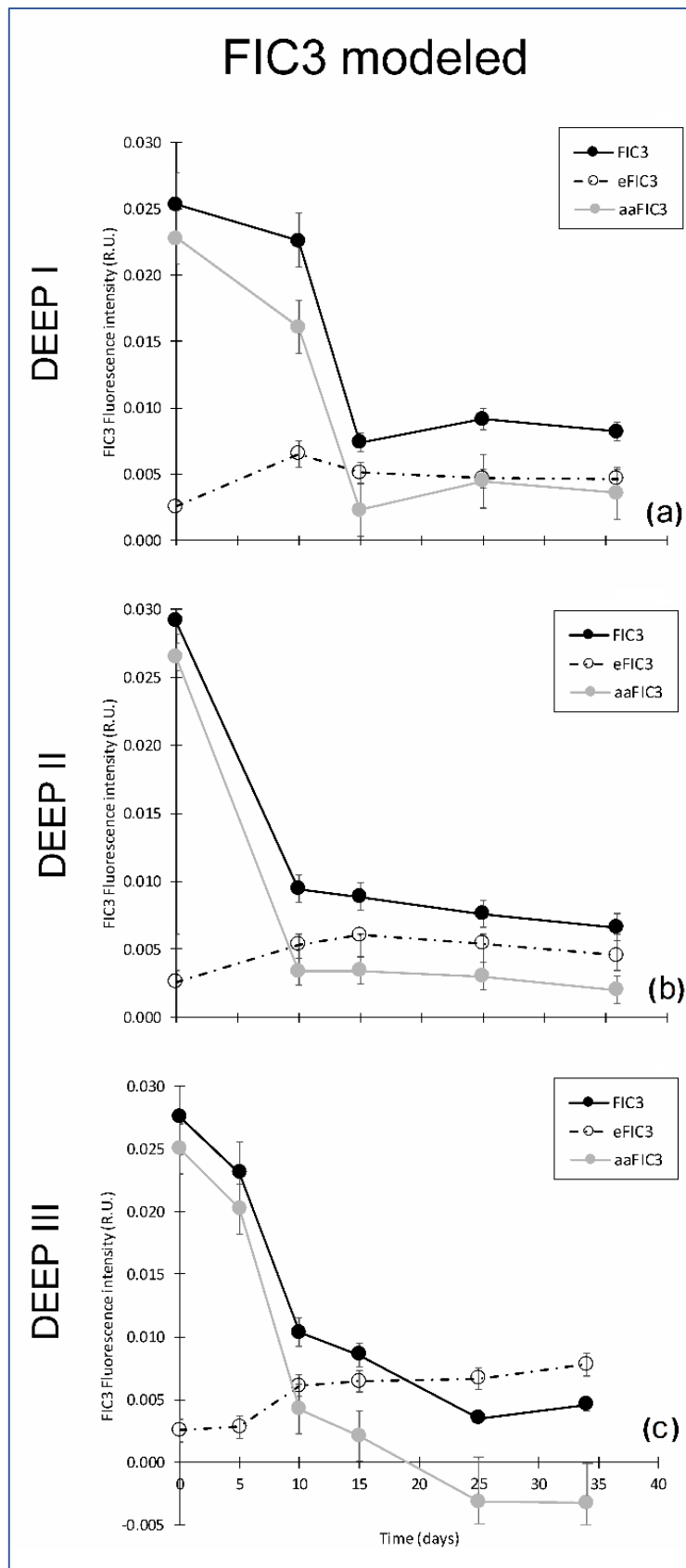


**Figure 2.8.** Temporal evolution of: i) observed FIC3 fluorescence intensity (black dots), ii) protein-like fluorescence due to prokaryotic growth estimated following the model described in Figure 1.7 (eFIC3) (dashed line and empty dots), and iii) fraction of the FIC3 signal due to the amended amino acids (aaFIC3) in CM treatment (grey dots) for experiments DEEP I (a), DEEP II (b), and DEEP III (c). Values expressed in R.U.

Using the equation described by this empirical model (**Figure 2.7**) ( $R^2 \approx 0.75$ ,  $N = 41$ ), we have estimated the protein-like fluorescence (eFIC3) due to prokaryotic growth for each sampling day of the CM condition. Comparing these values with the observed FIC3 intensity, we could estimate the fraction of the signal due to the original amino acids amended to this condition (aaFIC3), which decreased with time (**Figure 2.8**).

## **2.4. – Discussion**

### **2.4.1. – PARAFAC component source identification**

The OpenFluor spectral database (Murphy *et al.*, 2014b), was used to identify the different PARAFAC components present in our incubations. Two out of four components (FIC1 and FIC2) were clearly placed in areas traditionally related to humic-like fluorescence (Coble, 1996). FIC1 has recently been reported as a constituent of terrestrial and aquatic fulvic acids. Different studies devoted to track the origin of the organic compounds using their optical properties have found it in coastal areas around the globe, from Florida (Brym *et al.*, 2014; Yamashita *et al.*, 2010b) to Australia (Cawley *et al.*, 2012), including Arctic rivers estuaries (Walker *et al.*, 2013), the Bay of Liverpool (Yamashita *et al.*, 2011) and even the ballast water of different commercial ships (Murphy *et al.*, 2006). The fluorescent intensity of FIC2 is very similar to the traditional peak-A (Coble, 1996) a humic-like material found in rivers and sensitive to photodegradation (Lapierre and del Giorgio, 2014; Walker *et al.*, 2009; Stedmon *et al.*, 2007; Søndergaard *et al.*, 2003). The FIC3 component showed characteristics of tryptophan-like fluorescence and was similar to other previously reported PARAFAC components, which have been associated to tryptophan-like, protein-bound and free amino acids (Kowalczyk *et al.*, 2013; Kothawala *et al.*, 2012; Murphy *et al.*, 2008; Stedmon and Markager, 2005; Yamashita and Tanoue, 2003). The spectral characteristics of FIC4 have not been traditionally defined (Coble, 1996) but it occupies a region very close to those of the humic-like substances. Other studies that have found this component, mainly in the watershed of tropical rivers (Yamashita *et al.*, 2010a) and its estuaries (Brym *et al.*, 2014), have assigned it to a microbial reduced quinone-like substance (Cory and McKnight, 2005; Ariese *et al.*, 2004).

### **2.4.2. – Dynamics of humic-like fluorescence in response to different types of organic matter additions**

Since the incubations were performed in the dark, thus preventing photo bleaching, the changes in concentration and quality of FDOM humic-like compounds should exclusively be induced by prokaryotic metabolism, abiotic condensation or viral life cycles. With the exception of the exponential-growth phase in DEEP I, we observed an accumulation of the humic-like fraction across all treatments in the three experiments (**Figure 2.5**). In general, the increase in humic-like substances was higher in the conditions where humic precursors were added. These results would be in accordance with the hypothesis postulated by Andrew *et al.* (2013) about the requirement of polyphenolic terrestrial precursor material to generate additional humic

fluorescence signal. The overall picture fits with the expectations that the quality of the precursor material is a significant factor determining the characteristics of the generated DOM. It is remarkable that, in CM and CR conditions, a production of humic-like substances in the stationary phase was recorded in the three experiments. These results agree with the trends observed in earlier studies that reported the accumulation of humic-like fluorescence during the development of incubation experiments. Most of these experiments were performed with the addition of different C sources to the media as phytoplankton exudates added to sea water tanks (Romera-Castillo *et al.*, 2011a; Stedmon and Markager, 2005; Rochelle-Newall and Fisher, 2002) . Our results also agree with other studies that found a positive correlation between in-situ microbial respiration and humic-like FDOM generation in the deep (Guerrero-Feijóo *et al.*, 2014; Jørgensen *et al.*, 2014a; De La Fuente *et al.*, 2014; Lønborg and Álvarez-Salgado, 2014) as the three humic-like components showed an increase of intensity during the stationary phase.

In two out of the three experiments (DEEP II and III), the main trend of the humic-like compounds showed the same pattern for the total extent ( $t_{\text{final}} - t_0$ ). Yet, when we related these FDOM increases to prokaryotic abundance, the cell-specific production of FDOM components (**Table 2.4**) differed depending on the available source of organic matter. This result indicates that the quality of the precursor material is a significant factor determining the characteristics of the generated DOM and also modifies the organisms' activity. In fact, in the CR condition, where lower prokaryotic abundances were observed, the humic FDOM production per cell turned out to be significantly higher than in the other treatments.

Our results (**Figure 2.5** and **Table 2.4**) allow us: i) to reinforce Andrew *et al.* (2013) theory (previously stated), and ii) to demonstrate the (Jørgensen *et al.*, 2014b) hypothesis, who highlighted the idea that the less labile the precursor material is, the more humic fluorescence is generated. In addition, these results emphasize the appropriateness of distinguishing between different growth stages to better understand the dynamics of produced/consumed DOM.

**Table 2.3.** Overall production/consumption of humic-like fluorescence per cell [(FDOM at  $t_{final}$  – FDOM at  $t_0$ ) · (prokaryotes at  $t_{final}$  – prokaryotes at  $t_0$ )<sup>-1</sup>] for all the different treatments during the experiments (in R.U. · cells<sup>-1</sup> · d<sup>-1</sup>).

		K	CL	CM	CR
DEEP I	FIC1	$-5.22 \pm 0.02 \cdot 10^{-9}$	$-2.34 \pm 0.06 \cdot 10^{-9}$	$-1.16 \pm 0.03 \cdot 10^{-9}$	$-8.90 \pm 0.05 \cdot 10^{-9}$
	FIC2	$-4.48 \pm 3.02 \cdot 10^{-9}$	$-8.56 \pm 0.11 \cdot 10^{-10}$	$3.18 \pm 0.01 \cdot 10^{-9}$	$-7.42 \pm 0.02 \cdot 10^{-9}$
	FIC4	$-6.05 \pm 3.06 \cdot 10^{-9}$	$-2.59 \pm 0.02 \cdot 10^{-9}$	$-3.55 \pm 0.11 \cdot 10^{-9}$	$-1.00 \pm 0.05 \cdot 10^{-8}$
DEEP II	FIC1	$4.17 \pm 2.10 \cdot 10^{-9}$	$-1.48 \pm 0.01 \cdot 10^{-10}$	$4.88 \pm 1.01 \cdot 10^{-9}$	$4.17 \pm 1.03 \cdot 10^{-8}$
	FIC2	$7.39 \pm 3.06 \cdot 10^{-9}$	$1.44 \pm 0.04 \cdot 10^{-9}$	$1.37 \pm 0.02 \cdot 10^{-8}$	$4.94 \pm 2.05 \cdot 10^{-8}$
	FIC4	$-4.15 \pm 1.02 \cdot 10^{-9}$	$1.84 \pm 0.33 \cdot 10^{-9}$	$2.16 \pm 0.12 \cdot 10^{-11}$	$3.65 \pm 0.02 \cdot 10^{-8}$
DEEP III	FIC1	$2.01 \pm 0.1 \cdot 10^{-9}$	$-4.28 \pm 2.00 \cdot 10^{-9}$	$3.72 \pm 0.01 \cdot 10^{-9}$	$9.75 \pm 3.03 \cdot 10^{-9}$
	FIC2	$-1.13 \pm 0.00 \cdot 10^{-9}$	$4.60 \pm 0.00 \cdot 10^{-9}$	$3.44 \pm 0.02 \cdot 10^{-9}$	$1.32 \pm 0.02 \cdot 10^{-8}$
	FIC4	$-4.81 \pm 1.45 \cdot 10^{-9}$	$2.24 \pm 0.00 \cdot 10^{-10}$	$-2.80 \pm 0.06 \cdot 10^{-9}$	$1.48 \pm 0.07 \cdot 10^{-8}$

Concerning humic FDOM dynamics, some discrepancies were observed between the DEEP I and the other two experiments, i.e. an assimilation of the humic-like components in DEEP I versus an accumulation in DEEP II and III. We are aware that the characteristics of the water masses differed, and that this is perhaps the main reason behind the different responses. Seawater temperature for experiment DEEP I was 0.27 °C while the temperatures for the DEEP II and DEEP III experiments were 1.84 and 2.78 °C, respectively. Although all three temperatures were low, the DEEP I samples suffered the most substantial change when located at the temperature control chamber, set to 4 °C. This fact could explain the steepest slope detected in the prokaryotes' growth curves for all conditions in the DEEP I experiment during the first 10 days of incubation (Figure 2.4). The prokaryotic growth rate turned out to be approximately two times higher during the first days in DEEP I compared to DEEP II and III. The relevance of temperature in controlling the degradation of organic matter by microbes has been highlighted many times before (Vázquez-Domínguez *et al.*, 2007; Delille, 2004; Leahy and Colwell, 1990). It is known that the metabolism of cold tolerant prokaryotes is adapted to regulate cellular activities at low temperatures (Feller *et al.*, 1996), however a sudden relatively relevant increase of temperature combined with the availability of DOM sources in excess, and the nature of the DOM already present in the media

may cause differences in the behavior of cells while incorporating nutrients (Pomeroy and Wiebe, 2001). In DEEP I experiment, this change in the metabolism could have promoted a fast growth of the bacteria, supporting the use of the humic-like substances instead of its production. We are also aware that the prokaryotic diversity found in AABW differed from those present in NADW and CDW (M. Sebastián, personal communication). For that reason, we cannot reject the hypothesis that the different groups of microorganisms present in the water could have experienced a faster growth in DEEP I, and thus changing the consumption/production ratio of the humic-like substances.

### **2.4.3. – Dynamics of protein-like fluorescence in response to different types of organic matter additions**

The large initial drop detected in FIC3 fluorescence in the CM treatments is likely due to the utilization of the added amino acids by prokaryotes, while the signal increase in the K, CL and CR conditions could be attributed: i) to an increase in prokaryotic biomass, as microbial cells have protein-like fluorescence themselves (Determann *et al.*, 1998) or ii) to prokaryotic by-products that fluoresce in the protein-like region (Yamashita and Tanoue, 2003). The differences between the CM and the other conditions were caused by the different origin of the carbon sources available for prokaryotic consumption. In previous experiments where the only source of carbon was glucose, a selective release of amino acids (D-alanine) and an increase of other components (glucosamine and muramic acid) was observed, associated to prokaryotic growth (Azúa *et al.*, 2014; Jørgensen *et al.*, 2014b; Kawasaki and Benner, 2006). These findings concur with the increase of protein-like fluorescence observed in the K, CL and CR treatments in our experiments. On the other hand, using data from Bermuda (BATS) and Hawaii (HOT) time series, Kaiser and Benner (2009) found that carbohydrates and amino acids were preferentially used during microbial decomposition of marine organic matter.

We suggest that, in our CM conditions, prokaryotes may have been using the available amino acids for growth. Thus, the drop in the fluorescence signal would correspond to the balance between production and assimilation microbial processes. In order to evaluate the relative importance of these two processes, we estimated the FIC3 signal produced by prokaryotes in the CM condition by applying an exponential model (**Figure 2.7**).

According to the model calculations, approximately 90% of the fluorescence detected at  $t_0$  was due to the added amino acids in the CM treatment, while this percentage decreased down to about 2% of the total fluorescence detected at  $t_{10}$  or  $t_{15}$  (**Figure 2.8**), implying that bacteria used the amino acids added to supply their metabolic requirements until they reached the end of the exponential growth phase. This is in accordance with prior results obtained in degradation experiments (Nieto-Cid *et al.*, 2006) where they observed a rapid consumption of recently produced dissolved protein-like material which was accumulated in the water column only when gross primary production exceeded a threshold value. Nevertheless, during the stationary phase,

values of eFIC3 remained practically unaltered, suggesting that the prokaryotic community would have entered in a low-anabolic activity stage. In this regard, our results indicate that prokaryotic heterotrophic activity participates in both consumption and production of protein-like fluorescent substances, although production tends to surpass consumption during the exponential phase when labile/refractory substances are present.

## **2.5. – Conclusions**

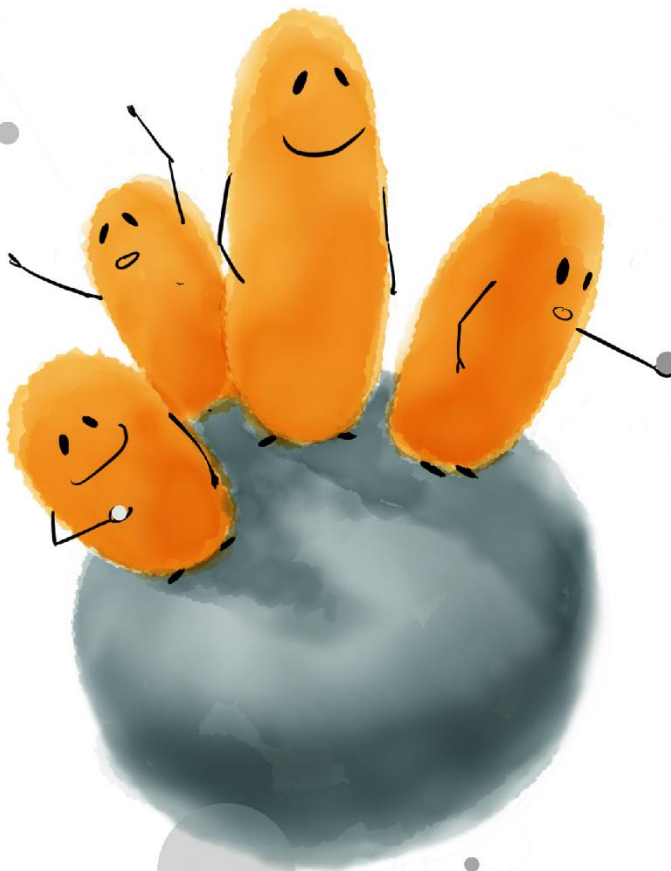
Recently, Arrieta *et al.* (2015) found that deep sea prokaryotic growth was stimulated when organisms were exposed to increasing concentrations of autochthonous DOM. Our results demonstrated that the quality also influences prokaryotic activity.

In addition, we found that both the quality of organic matter added, and the initial biotic and abiotic conditions can modify the microbial net production and consumption of FDOM. A clear FDOM net consumption was only observed in the experiment with Antarctic Bottom Water (AABW). To better understand the final fate of organic matter, further experiments should include analyses of organic matter at molecular levels (e.g. with spectrometry methods) and microbial gene diversity.

Based on our findings we conclude that, although mechanisms that hinder DOC total remineralization in deep waters are still poorly understood, the sequestration of OC in the deep ocean can significantly be reduced when labile substrates become available.

## Chapter 3

Eutrophication and acidification:  
Do they induce changes in the  
dissolved organic matter dynamics  
in the coastal Mediterranean Sea?





### 3.1. – Introduction

As a result of human activities, atmospheric CO<sub>2</sub> levels have increased from approximately 280 ppm in pre-industrial times to 395 ppm in 2013 (Le Quéré *et al.*, 2015 and references therein). A large portion of the atmospheric CO<sub>2</sub> is dissolved in the ocean and, thanks to the 'solubility pump', it is transported from the ocean's surface to its interior in form of dissolved inorganic carbon (Volk and Hoffert, 1985). In addition to this passive diffusion of CO<sub>2</sub> into the ocean, marine biota plays an active role in the uptake of carbon dioxide from the atmosphere in what is known as the 'biological pump' which refers to the processes that involve the biologically-mediated uptake and transport of carbon from the upper to the deep ocean (Volk and Hoffert, 1985; Passow and Carlson, 2012). Thus, marine ecosystems play an important role in regulating atmospheric CO<sub>2</sub> concentrations and, in this way, in moderating climate change. However, the physical, chemical, and biological mechanisms governing the fluxes between the different carbon compartments in the marine system are still poorly understood.

The diffusion of CO<sub>2</sub> into the ocean is determined by temperature and salinity that provide a dependent solubility coefficient (Henry's law, Henry, 1803). When a CO<sub>2</sub> molecule is finally taken up by the ocean, two main paths may follow: i) it may remain in a dissolved inorganic form, altering the marine carbonate chemistry equilibrium and leading to ocean acidification (Hönisch *et al.*, 2012; Zeebe, 2012), or ii) may be captured by a photosynthetic marine organism, fixing it in the form of organic carbon. The pathways that this new biologically generated organic molecule may follow within the trophic chain are very diverse and vary from being incorporated into a larger organism (reaching higher trophic levels) to being excreted or respired as part of a variety of metabolic processes. The size of the excreted compounds varies widely, contributing to both the particulate organic matter (POM) and the dissolved organic matter (DOM) fractions. Regarding the DOM, this pool is mainly produced by phytoplankton exudation (Hopkinson *et al.*, 2002; Romera-Castillo *et al.*, 2011a; Sarmiento *et al.*, 2013), viral lysis (Brussaard, 2004; Motegi *et al.*, 2009), the sloppy feeding carried out by protists and metazoans grazers and the POM solubilization by bacterial and archaeal hydrolases (Nagata *et al.*, 2000; Sala and Güde, 2004). These mechanisms determine the quantity and the complexity of the molecules contained in the DOM, as well as their fate along the biogeochemical cycles.

The estimations of oceanic CO<sub>2</sub> assimilation by phytoplankton to generate cellular structures or its subsequent release of C as exudates (particulate and dissolved primary production, respectively) range between 3 and 4 Pmol C year<sup>-1</sup> (Berger, 1989; Antoine and Morel, 1996; Behrenfeld and Falkowski, 1997; Chavez *et al.*, 2011). Research undertaken in the context of the US Joint Global Ocean Flux Study (Schlitzer *et al.*, 2003) concluded that a fraction of this carbon is rapidly removed from surface waters and exported to the ocean's interior. In addition, Jiao *et al.* (2010) emphasized the role of oceanic in transforming POM and DOM into recalcitrant DOM, material susceptible of staying sequestered in the ocean for long periods of time. The processes

that transform labile organic matter into refractory compounds are termed 'microbial carbon pump' (MCP, Jiao *et al.*, 2010).

The chromophoric dissolved organic fraction (CDOM; Coble, 1996) of the DOM pool absorbs light at both ultraviolet (UV) and visible wavelengths. A sub-fraction of this CDOM, the fluorescent DOM (FDOM; (Coble, 2007, 1996), fluoresces when irradiated with UV light. Since 1990, (Coble *et al.*, 1990) the characterization of marine DOM has been performed by applying fluorescence excitation-emission matrices (EEM). Although this technique does not permit the quantification of specific molecules, it has been extensively used to track the origin and transformations of DOM (Coble *et al.*, 1990; Cory and McKnight, 2005; Nieto-Cid *et al.*, 2005; Romera-Castillo *et al.*, 2011b, Catalá *et al.*, 2015) because it is relatively inexpensive, low-time consuming and provides valuable information about the quality of the DOM.

As it has been shown over the last years, ocean acidification affects marine organisms and ecosystems in several ways (Gattuso *et al.*, 2015 and references therein). In addition, nitrogen (N) and phosphorous (P) pollution has increased over the past decades, primarily due to the utilization of active N and P for fertilizer use (Galloway *et al.*, 2004). This utilization has enhanced the nutrient loads from land to coastal zones and may favor an increase of eutrophication episodes in the near future (Howarth & Marino, 2006). Since the beginning of the 20<sup>th</sup> century, eutrophication has been a persistent problem and a subject of different studies. Bio-assay experiments in lake and coastal systems were done to test the effect of eutrophication on phytoplankton dynamics in the seventies and eighties (Pomeroy *et al.*, 1972; Carpenter & Capone, 1983). Since then, numerous studies have been addressed this issue in different aquatic systems (Statham, 2012 and references therein).

A convenient procedure to gain insight on the possible changes that ocean acidification and eutrophication may induce on marine systems is the deployment of mesocosms experiments (Kim *et al.*, 2011; Teeling *et al.*, 2012; Riebesell *et al.*, 2007, 2013; Bunse *et al.*, 2016). Three recent mesocosms studies (Yamada *et al.*, 2013; Riebesell *et al.*, 2013; Zark *et al.*, 2015) have examined the effects of ocean acidification on DOM transformation processes. Yamada *et al.* (2013) did not find a significant effect of increased CO<sub>2</sub> concentration on the short-term decomposition of labile DOM in Sagami Bay (Japan), yet the study did not look at the possible changes in organic matter quality. The study conducted by Riebesell and collaborators (2013) in Svalbard (Norway) shed light on the pathways that the organic matter followed when the system was amended with nutrients and increased in pCO<sub>2</sub>. They found that the combination of these two stressors triggered a synergistic effect inducing an increase in the dissolved organic carbon fraction. The study of Zark *et al.* (2015) tracked the transformations suffered by DOM molecules in a mesocosms study using Fourier transform ion cyclotron resonance mass spectrometry (FT-ICR-MS) and they concluded that ocean acidification alone did not induce changes in the composition of the DOM pool in the Gullmar Fjord (Sweden).

We investigated the effects of increasing pCO<sub>2</sub> and its synergy with increasing nutrient availability on the dynamics of organic matter in a Mediterranean coastal area. We particularly examined the optically active fractions of the DOM, since they can be used as indicators of recalcitrant material and can provide useful information about DOM transformations. In addition, the study of these fractions is of remarkable interest in the Mediterranean waters where the CDOM to chlorophyll ratio is higher than the global average (Morel & Gentili, 2009; Claustre *et al.*, 2002). We enclosed coastal water in mesocosms and performed two experimental studies in which we manipulated pCO<sub>2</sub> and nutrient concentrations. In order to assess the importance of the initial conditions in regulating the responses to reducing pH and increasing nutrients, one mesocosm experiment was performed in winter and the other in summer, displaying contrasting initial oceanographic and biological characteristics.

## **3.2. - Materials and methods**

### **3.2.1. - Experimental setup and initial conditions at the sampling site**

Two experiments were conducted in winter 2010 and summer 2011 to examine the dynamics of microbial communities and organic matter under different pH conditions and nutrient levels. Natural seawater from the Blanes Bay Microbial Observatory, NW Mediterranean (BBMO; 41°40'0" N, 2°48'0" E; Gasol *et al.*, 2012), was enclosed in eight 200 L tanks and maintained in a temperature-controlled chamber, with a 12:12 h light:dark cycle. Gro-lux and cool-white lamps were positioned in the walls of the chamber surrounding the tanks. Light intensity inside the containers was  $121.3 \pm 3.5 \mu\text{mol m}^{-2} \text{s}^{-1}$  during the winter experiment and  $230 \pm 25 \mu\text{mol m}^{-2} \text{s}^{-1}$  during the summer experiment, measured using a spherical radiometer (Biospherical Instruments Inc., Model QSL 2100, San Diego, CA).

Four experimental conditions were randomly assigned to duplicated containers: K1 and K2 (controls), KA1 and KA2 (reduced pH) N1 and N2 (nutrient amended), and NA1 and NA2 (nutrient amended and reduced pH). The pH in the KA and NA treatments was manually adjusted by bubbling CO<sub>2</sub> every morning in a controlled way, to lower their pH in approximately 0.2 units respect to the controls, so as to simulate future conditions in a medium-level mitigation scenario such as the Representative Concentration Pathway (RCP) 4.5 (Taylor *et al.*, 2016). For reproducibility, the control tanks were also bubbled with compressed air at current atmospheric CO<sub>2</sub> concentrations.

The seasonal cycle in Blanes Bay is characterized by a late winter phytoplankton bloom dominated mostly by diatoms (Guadayol *et al.*, 2009). In contrast, during summer, when nutrient concentrations are lower, picophytoplankton is the most representative group (Alonso-Sáez *et al.*, 2008). Moreover, DOC accumulates during summer, while annual minimum concentrations are found in winter (Vila-Reixach *et al.*, 2012; Romera-Castillo *et al.*, 2013). Due to this seasonality, the initial seawater of the winter experiment was relatively rich in inorganic nutrients and poor in

DOC. On the contrary, in summer the water was depleted of inorganic nutrients and enriched in DOC, generated via metabolic pathways during the bloom phase within the previous spring season (Romera-Castillo *et al.*, 2013). The summer nutrient depletion limits the bacterial activity, reducing the microbial degradation of DOM and leading to a DOC accumulation in this season (Thingstad *et al.*, 1997) Thus, the starting point conditions of the experiments differed in the original concentrations of organic matter and inorganic nutrients.

### 3.2.2. – Measured variables

Measurements of the following variables were taken every day during 9 days. Duplicate containers for each of the four treatments were simultaneously and independently sampled. Temperature was monitored daily using a digital thermometer VWR 8202-156 (VWR International, LLC). This variable was set to  $14 \pm 1$  °C and to  $22 \pm 1$  °C for W and S experiments, respectively. The pH in the mesocosms was determined every morning by spectrophotometry in the laboratory, following standard procedures (Clayton and Byrne, 1993). In addition, pH was continuously recorded using glass electrodes (Ecotrode Plus, Metrohm) connected to a D130 data logger (Consort, Belgium) that were calibrated on a daily basis with a Tris buffer following standard procedures (SOP6a of Dickson *et al.*, 2007). Chlorophyll a (Chl a) was measured according to Yentsch and Menzel (1963): seawater (50 mL) was filtered through Whatman GF/F glass fiber filters, which were subsequently placed in 90% acetone at 4 °C for 24 h and the fluorescence of the extract measured using a fluorometer (Turner Designs, Sunnyvale, CA).

Dissolved inorganic nutrient concentrations, nitrate ( $\text{NO}_3^-$ ), phosphate ( $\text{PO}_4^{3-}$ ) and silicate ( $\text{SiO}_2$ ), were determined by standard segmented flow analyses with colorimetric detection (Hansen & Grasshoff 1983) using a CFA Bran + Luebbe autoanalyser. Precisions were  $\pm 0.01 \mu\text{mol kg}^{-1} \text{NO}_3^-$ ,  $\pm 0.02 \mu\text{mol kg}^{-1} \text{PO}_4^{3-}$ , and  $\pm 0.01 \mu\text{mol kg}^{-1} \text{SiO}_2$ . Inorganic nutrients were added to N and NA treatments to reach a final P:N:Si molar concentration of 1:16:30 and 0.25:4:8 in the winter and summer experiments, respectively. Initial and post-addition nutrient concentrations are summarized in [Table 3.1](#). In both cases, the nitrogen enrichment was increased at least eight times from the seasonal average concentration measured in the BBMO during the last 10 years. Nitrogen and phosphorus were added at a Redfield ratio, whereas silicate was added in excess, so diatom growth was not affected by lack of elemental compounds.

**Table 3.1.** Concentrations of the main inorganic nutrients measured before and after the additions. Values are expressed in  $\mu\text{M}$ . The standard deviations were calculated using duplicated containers of the same experimental condition.

	Winter		Summer	
	Before addition	After addition	Before addition	After addition
<b>NO<sub>3</sub><sup>-</sup></b>	2.55 ± 0.00	17.38 ± 0.45	0.10 ± 0.01	4.70 ± 0.06
<b>PO<sub>4</sub><sup>3-</sup></b>	0.11 ± 0.00	1.14 ± 0.07	0.03 ± 0.00	0.24 ± 0.03
<b>SiO<sub>2</sub></b>	2.33 ± 0.00	31.41 ± 0.79	0.37 ± 0.03	6.51 ± 0.13

Samples for dissolved organic carbon (DOC), FDOM and CDOM were prefiltered under reduced pressure through precombusted (450 °C, 4h) Whatman glass fiber filters (GF/F). DOC samples were collected in 10 mL precombusted (450 °C, 24 h) glass ampoules, acidified with 50  $\mu\text{L}$  25% H<sub>3</sub>PO<sub>4</sub> to pH <2 and heat-sealed and stored in the dark at 4 °C until analysis. A Shimadzu TOC-CSV organic carbon analyzer was used to carry out analysis. Three to five injections of 150  $\mu\text{L}$  per sample were performed, and DOC concentrations were calculated by subtracting a Milli-Q blank and dividing by the slope of a daily standard curve of potassium hydrogen phthalate. The precision of these measurements was  $\pm 0.7 \mu\text{M}$ . All samples were checked against deep Sargasso Sea reference water (2600 m).

CDOM absorption spectra were determined from 250 to 600 nm using a Varian Cary 100 Bio spectrophotometer equipped with 10 cm quartz-cells. Milli-Q water was used as a blank. Absorbance was converted into napierian absorption coefficient ( $a_\lambda$ , Green and Blough, 1994) using the equation:

$$a_\lambda = \frac{2.303 \cdot \text{Abs}_\lambda}{l} \quad (1)$$

where  $\text{Abs}_\lambda$  is the absorbance at a given wavelength, the factor 2.303 converts from decadic to natural logarithms, and  $l$  is the cell path-length in meters. In addition, the UV absorption at 254 nm was also normalized to the dissolved organic carbon (DOC) concentration to obtain the specific UV absorbance coefficient (SUVA, in  $\text{m}^{-1} \text{mg}^{-1} \text{L}$ ) following Weishaar *et al.* (2003). SUVA values are correlated with DOM aromaticity and provide information on the complexity of molecules (Helms *et al.*, 2008; Weishaar *et al.*, 2003). Furthermore, the dimensionless slope ratio of a short wavelength region (275-295 nm) to that of a longer wavelength region (350-400 nm) was determined ( $S_R$ ; Helms *et al.*, 2013).  $S_R$  is inversely correlated to SUVA and is related to the molecular weight of the DOM (Helms *et al.*, 2013).

A Perkin Elmer LS55 luminescence spectrometer was used to measure FDOM. This instrument was equipped with a xenon discharge lamp equivalent to 20 kW for an 8- $\mu$ s duration. Both, single point measurements and emission excitation matrices of the samples were acquired. The scan speed was set at 250 nm min<sup>-1</sup> and slit widths for the excitation and emission wavelengths were fixed at 10 nm. Measurements were performed in a 1 cm quartz fluorescence cell. Following Coble 1996, the Ex/Em wavelengths used for the single point measurements were: Ex/Em 280 nm/350 nm (peak-T) indicative of the presence of protein-like compounds, Ex/Em 320 nm/410 nm (peak-M) as indicator of marine humic-like substances, Ex/Em 340 nm/440 nm (peak-C) to trace terrestrial humic-like substances and Ex/Em 250 nm/435 nm (peak-A) to track humic materials in general. Additionally, EEMs were obtained by concatenating 21 excitation/emission spectra of the sample. The fluorescence intensities were reported as quinine sulfate units (QSU) by calibrating the instrument at Ex/Em: 350 nm/450 nm against a quinine sulfate dehydrate (QS) standard made up in 0.05 mol L<sup>-1</sup> sulfuric acid. Optical analyses of tryptophan (Try) dissolved in seawater at different levels of pH were performed to test the pH influence in the fluorescence properties of the protein-like substances.

The humification index (HIX) describes the diagenetic state of the DOM and it was calculated by dividing the peak area under the emission spectra at 435-480 nm by the peak area under the emission spectra at 300-345 nm, at an excitation of 254 nm. The aromatic humic acids are known to have high HIX values (Zsolnay, 2003; Giering *et al.*, 2014).

Heterotrophic prokaryotes were enumerated with a FACSCalibur (Becton Dickinson) flow cytometer equipped with a 15 mW argon-ion laser (488 nm emission) as described by Gasol and del Giorgio (2000). Samples (1.8 mL) were immediately fixed with 1% paraformaldehyde plus 0.05% glutaraldehyde (final concentrations), incubated for 10 min at room temperature, frozen in liquid nitrogen and stored at -80 °C. Before analysis, samples were unfrozen, stained with SYBRGreen I (Molecular Probes) at a final concentration of 10  $\mu$ M and left in the dark for about 15 min. Each sample was then run at low speed ( $\sim$ 12  $\mu$ L min<sup>-1</sup>) for 2 minutes with Milli-Q water as a sheath fluid. We added 10  $\mu$ L per sample of a solution of yellow-green 0.92  $\mu$ m Polysciences latex beads (10<sup>6</sup> beads mL<sup>-1</sup>) as an internal standard. Bacteria were detected by their signature in a plot of side scatter versus FL1 (green fluorescence). Data analysis was performed with the Paint-A-Gate software (Becton Dickinson).

### **3.2.3. – Statistical analyses**

The software SigmaPlot v11.0 (Systat Software Inc.) was used to perform the two-way ANOVA and the t-tests. Two-way ANOVA was carried out to test if differences between conditions and experiments were significant and t-tests to discriminate if the temporal evolution of the different variables measured in an experiment (winter or summer) could be considered significant. The software XLSTAT 2016 (Addinsoft ©) was used to perform Mantel tests. The Pearson correlation implemented in the Mantel tests was performed to discriminate if changes in the intensity of the

fluorophores were significant between conditions. p-values were set to  $p < 0.05$  for all types of test.

### 3.3.- Results

#### 3.3.1. – Plankton dynamics

**Figure 3.1** shows the differences between prokaryotic abundances and Chl *a* levels for the different treatments during winter and summer experiments. Prokaryotic abundances started at  $5.0 \pm 0.1 \cdot 10^5$  cells mL<sup>-1</sup> at  $t_0$  in the winter experiment. Between  $t_3$  and  $t_4$ , the abundances in K and KA conditions reached the highest numbers  $4.0 \pm 0.2$  and  $3.7 \pm 0.4 \cdot 10^6$  cells mL<sup>-1</sup>, respectively. Within a short time lag, slightly higher values were reached in N and NA tanks ( $4.4 \pm 0.3$  and  $4.0 \pm 0.3 \cdot 10^6$  cells mL<sup>-1</sup>, respectively). Between  $t_5$  and  $t_7$ , prokaryotic abundances decreased markedly and, by the end of the experiment the abundances increased again in all conditions (**Figure 3.1a**). Prokaryotic abundances at  $t_0$  ranged from  $7.3 \pm 0.2$  to  $8.4 \pm 0.2 \cdot 10^5$  cells mL<sup>-1</sup> in the summer experiment (**Figure 3.1b**). An initial drop was observed in all conditions, reaching the lowest values at  $t_3$ . After this time point, the prokaryotic populations started to increase in all treatments. Prokaryotic numbers in K and KA treatments were lower than those in treatments N and NA. Chl *a* concentrations varied in a similar way in both the winter and summer cases: Chl *a* under N and NA experimental conditions (**Figure 3.1e, f**) reached higher concentrations than under K and KA treatments (**Figure 3.1c, d**). The Chl *a* values were about three to eight times higher in the winter experiment, which relates to the higher nutrient enrichment induced in that experiment.

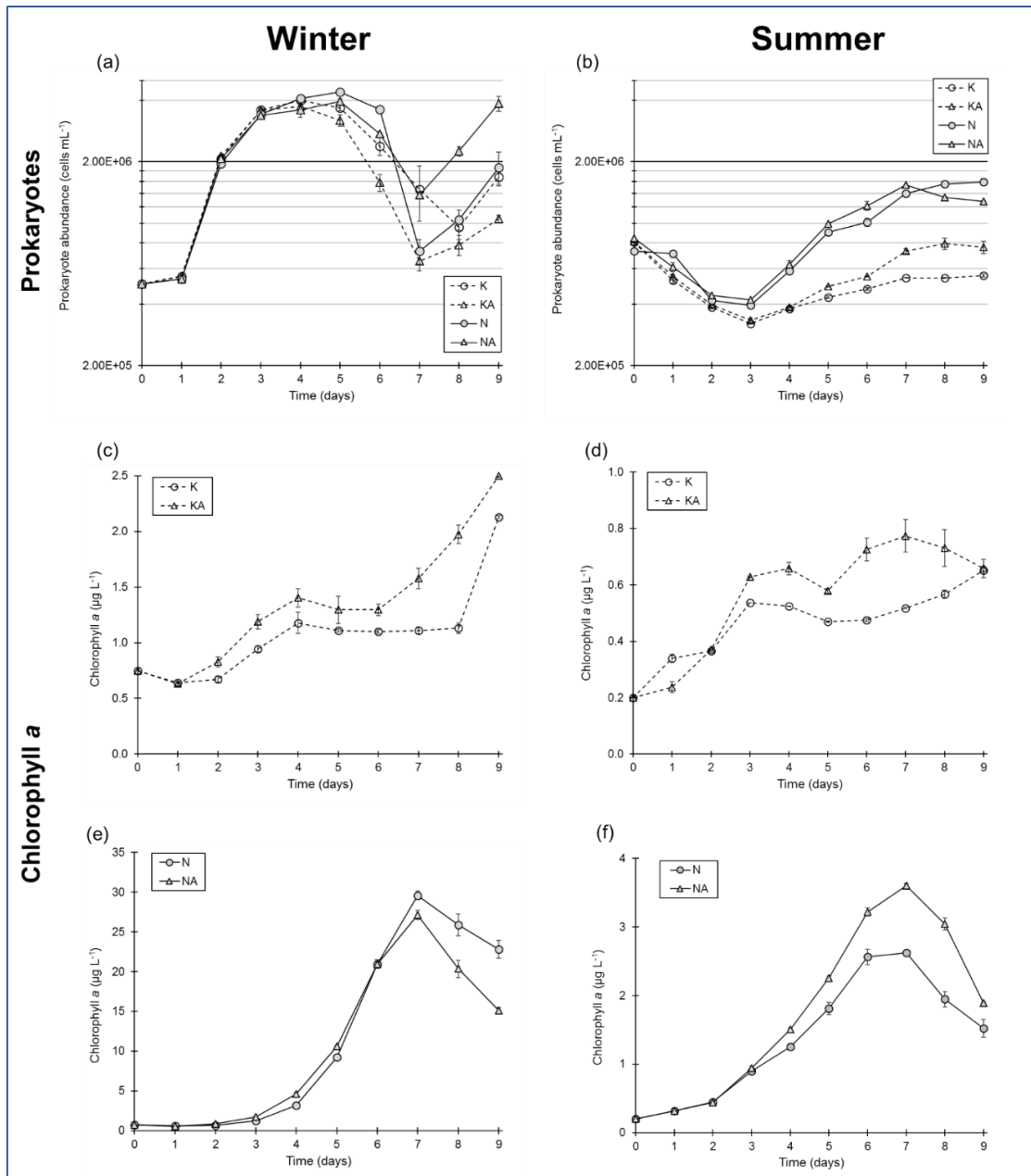


**Figure 3.1.** Temporal dynamics of prokaryote abundances (cells mL<sup>-1</sup>) in (a) winter and in (b) summer; chlorophyll a pigment concentration (μg L<sup>-1</sup>) for K and KA treatments in (c) winter and (d) summer; chlorophyll a pigment concentration (μg L<sup>-1</sup>) for N and NA treatments in (e) winter and (f) summer. Note that, in (c), (d), (e) and (f) panels, the scales of the vertical axes are different. Error bars indicate the standard error of 2 replicates.

### 3.2. – DOC

DOC concentration in the winter experiment increased in the four treatments (Figure 3.2a) reaching maximum values at  $t_7$  in treatments K and KA, and  $t_9$  in N and NA. From  $t_7$  to  $t_9$ , DOC decreased in both K and KA treatments, while DOC concentration kept increasing in N and NA conditions, coinciding with the decay of phytoplankton bloom. During the summer experiment, small variations in DOC concentration were observed (Figure 3.2b). In general, a positive trend to higher concentrations was identified during the entire incubation. The starting point conditions were about 80-85  $\mu\text{mol L}^{-1}$  and the final concentrations increased to 90-95  $\mu\text{mol L}^{-1}$ . Regarding nitrate concentrations, they generally decreased from the beginning of the experiment in the N and NA tanks. Similar patterns were found for phosphate concentrations in these enriched conditions, while small variations occurred during the whole experimental period in the control treatments.

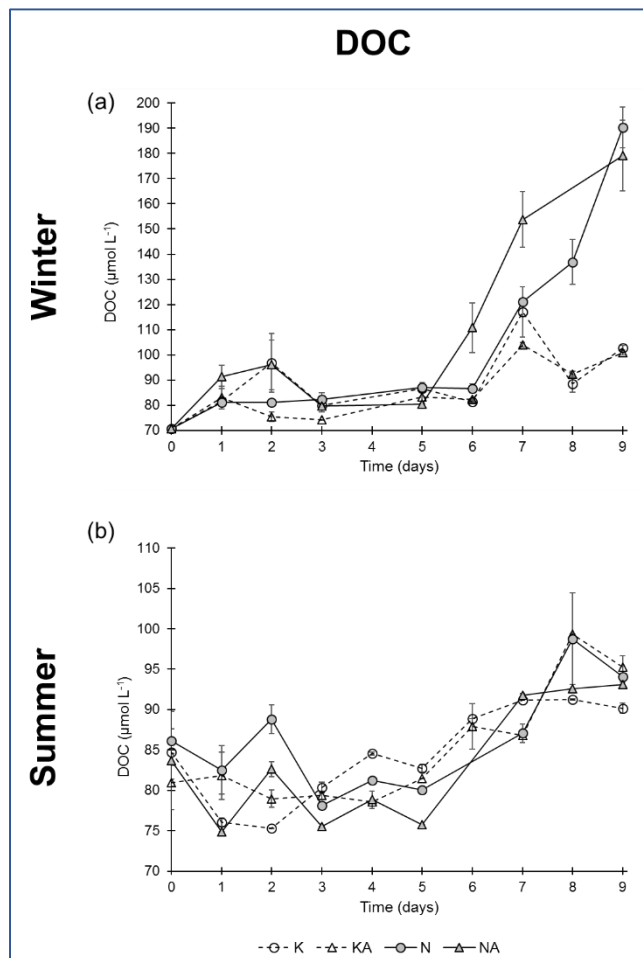


**Figure 3.2.** Changes in DOC concentrations ( $\mu\text{mol L}^{-1}$ ) in the (a) winter and in the (b) summer experiments. Open symbols represent control (K) conditions and filled colored symbols nutrient-amended (N) conditions. Note the change of scale in vertical axes. Error bars indicate the error of 2 replicates.

### 3.3. – Optical analyses of the DOM

Fluorescence intensities during the experiments were measured to track changes in the quality of organic matter. We visualized the differences by subtracting the EEMs at  $t_0$  from those at  $t_9$  (Figure 3.3). In the winter experiment, the most remarkable feature was the increase in the fluorescence signal of the protein-like material (peak-T) in all treatments, including the control, which reached 2.3 QSU (Figure 3.3a). However, in the acidified scenario (Figure 3.3b), the increase was slightly smaller in the non-enriched treatments (~1.6 QSU). Regarding the enriched mesocosms (N and NA, Figure 3.3c, d), we also observed slighter increases of the fluorescence signal of the humic-like compounds (A, C and M regions), in addition to those of the peak-T.

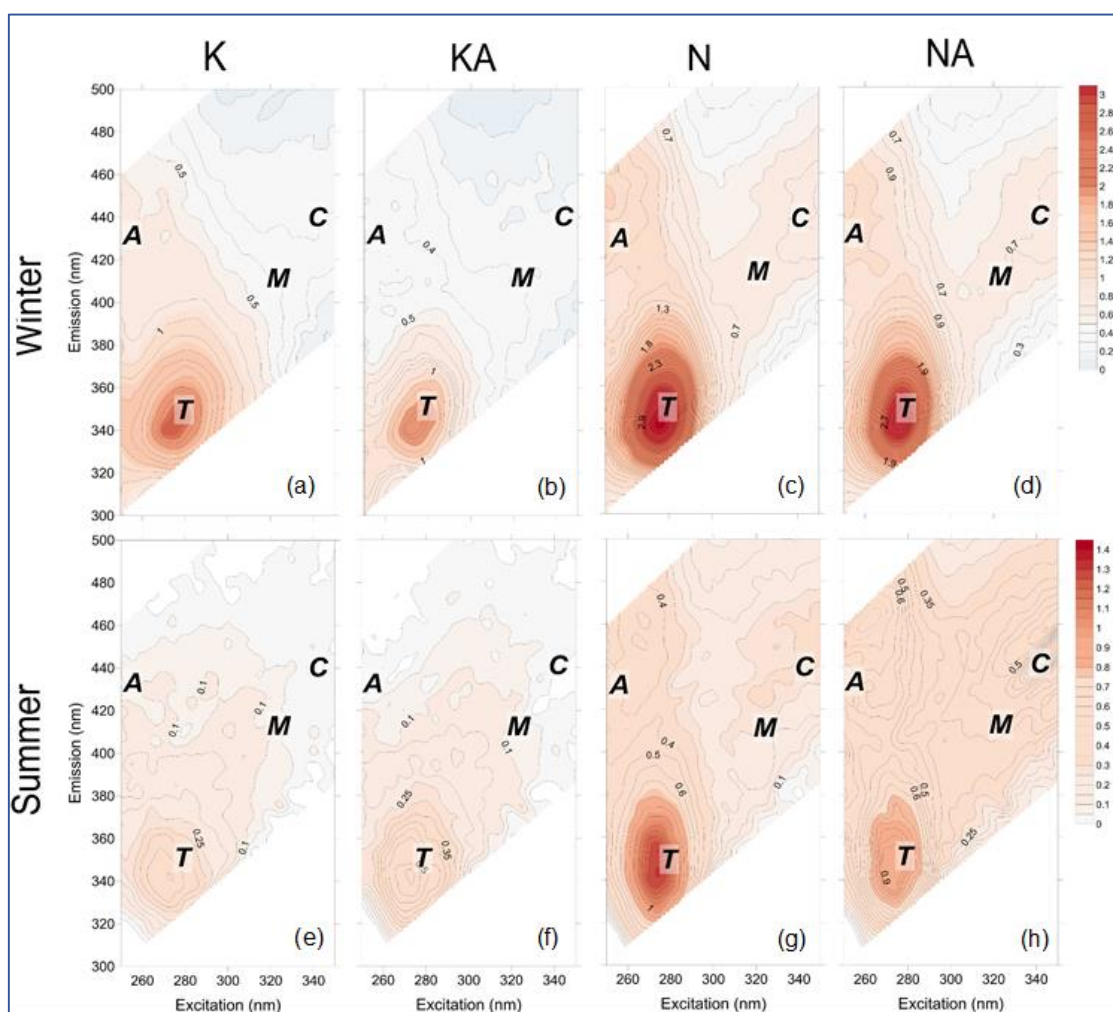


**Figure 3.3.** EEMs showing increases/decreases in fluorescence intensity over the 9 days of the mesocosm experiments ( $\Delta EEM = EEM_{t_9} - EEM_{t_0}$ ) for the different fluorophores in winter (a-d) and summer (e-h). Values reported as quinine sulfate units (QSU). Humic-like fluorophores indicated as A, C and M; protein-like fluorophore indicated as T. Note the change in scale between the winter and summer experiments.

The patterns identified in summer and winter were similar: the main changes were found around the protein-like fluorescence region, which increased in all four conditions (~0.5 QSU in K and KA to ~1.4 in N and ~1.0 QSU in NA). Again, slight increases of humic-like fluorescence were detected during the experiments, mainly in the nutrient-enriched treatments (Figure 3.3g, h).

The temporal evolution of peak-C to peak-M ratio (peak-C/peak-M) helped us to explore, in more detail, the changes experienced by the humic-like substances (**Figure 3.4a, b**). In general, the ratios were lower in winter than in summer, but both experiments showed the highest ratios in the N and NA tanks at the end of the experiment. In K and KA conditions, no clear trends were identified in winter, while the evolution of the non-nutrient-enriched and nutrient-enriched tanks was relatively parallel in summer. After a decrease observed from  $t_0$  to  $t_1$ , the values tended to increase until the end of the experiment reaching higher values in the enriched conditions. The SUVA evolution (**Figure 3.4c, d**) did not show a clear temporal pattern in the winter experiment, although by  $t_9$  NA and N conditions presented the highest increase in relation to the initial values. In summer, after  $t_3$ , the enriched- and non-enriched treatments diverged, reaching significantly higher values in the N-conditions (p-value < 0.05) and, again, the highest increase at the end of the experiment occurred in the NA treatment ( $0.040 \pm 0.004 \text{ m}^{-1} \text{ mg}^{-1} \text{ L}$ ) followed by the N treatment ( $0.030 \pm 0.005 \text{ m}^{-1} \text{ mg}^{-1} \text{ L}$ ). In winter the K treatment displayed higher increases in SUVA than the acidified control condition (KA) but this fact was not observed in summer. The temporal evolution of HIX differed during the first days of the experiment between the winter and summer scenarios, this index decreased until  $t_5$  and then increased until  $t_9$  in winter, whereas it increased during the whole experiment in summer. The HIX values reached at the end of the incubation were always higher in the nutrient enriched conditions than in the non-enriched ones. Furthermore, the values of the NA treatments were higher than the N ones in both experiments.

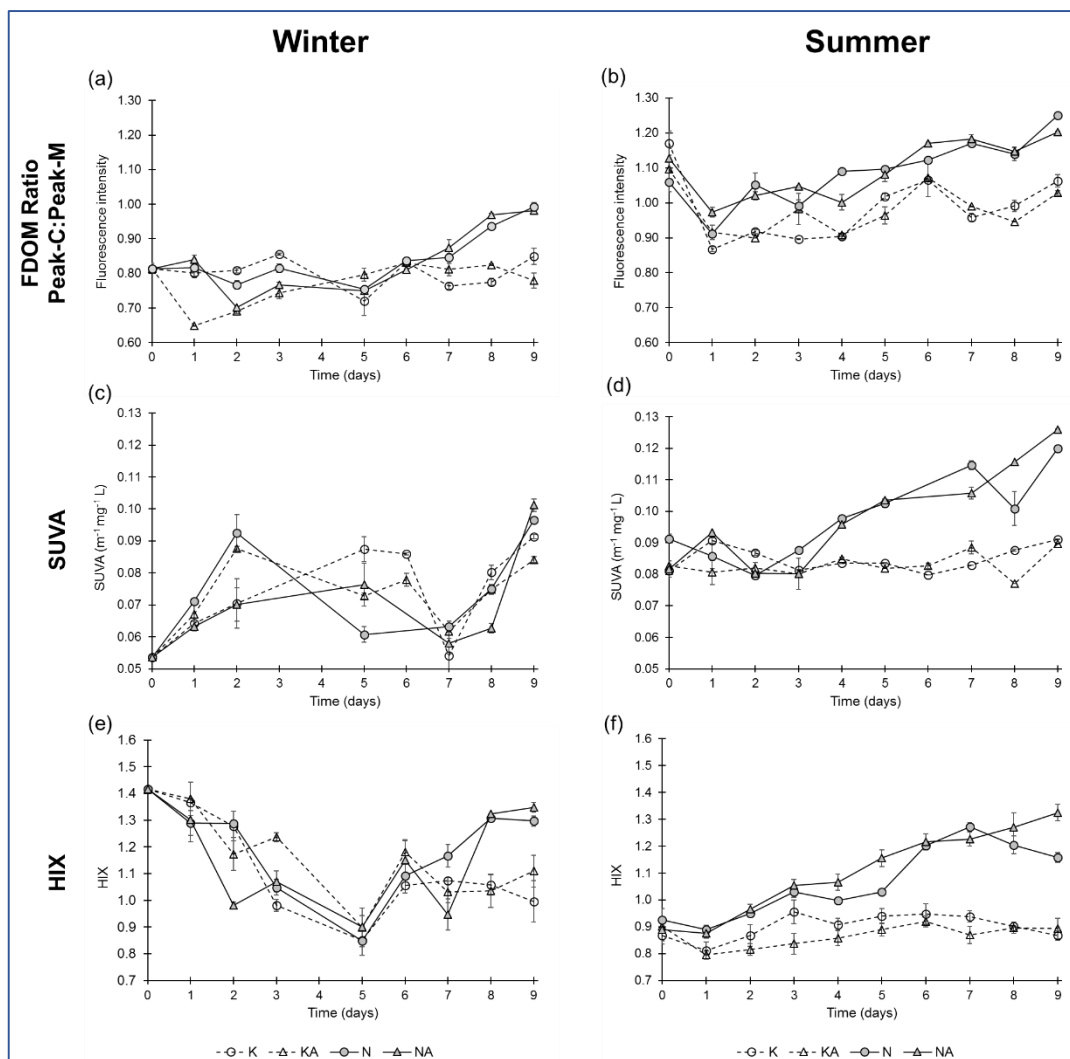


**Figure 3.4.** Time evolution of the quotient between peak-C and peak-M in (a) winter and (b) summer; specific UV absorbance at 254 nm (SUVA) in (c) winter and (d) summer; and humification index (HIX) in (e) winter and (f) summer. Peak-C/peak-M ratio and HIX are dimensionless variables. Error bars indicate the standard error of 2 replicates.

### 3.4. – Discussion

#### 3.4.1. - DOC dynamics

DOC net accumulation occurred always after the end of the exponential-growth phase (coinciding with the phytoplankton post-bloom phase) either with high or low pCO<sub>2</sub> levels (Figures 3.1, 3.2). Thus, the production of DOC, without distinction of the seasonality or the addition of nutrients, was not significantly different between the non-acidified and acidified tanks (K and N with respect to KA and NA, p-value < 0.05). In the same way, MacGilchrist *et al.* (2014) found no significant effect of pCO<sub>2</sub> on the DOC dynamics in five shipboard bioassay experiments in the northwest European shelf seas. These results are also in agreement with the mesocosm study by Maugendre *et al.* (2014) in the Bay of Villefranche (France, NW Mediterranean Sea), where no significant effects of elevated temperature and/or CO<sub>2</sub> were found on most biological parameters and processes, including the generation of DOM. On the other hand, Yoshimura *et al.* (2010)

conducted incubation experiments with sea surface water (depleted in nutrients) from the Sea of Okhotsk and detected a decrease in the generation of DOC when pCO<sub>2</sub> levels were >480 µatm.

The evolution of DOC and nutrient dynamics in previous mesocosm experiments, can be contradictory. In 2007, Riebesell and collaborators found that although the CO<sub>2</sub> uptake was higher in conditions with elevated pCO<sub>2</sub>, no differences in the phytoplankton POC flux were observed. Thus, they suggested that the extra CO<sub>2</sub> incorporated was lost as DOC or respiration. More recently, in 2013, a mesocosm experiment was conducted in Svalbard to examine the influence of high pCO<sub>2</sub> and nutrient availability on microbial activities (Riebesell *et al.*, 2013). In that experiment, pico-phytoplankton growth and DOC exudation increased at elevated CO<sub>2</sub> concentrations after inorganic nutrients were supplied. Another mesocosm experiment conducted in waters off the Baltic Sea during 4 weeks in the summer season (Paul *et al.*, 2015) revealed that under high pCO<sub>2</sub> an important percentage of the organic matter production was in dissolved form. In our study, the abundance of small phytoplankton (pico- and nanoeukaryotes) was stimulated in the enriched conditions of the summer experiment (Sala *et al.*, 2016). However, this stimulation was not accompanied by a net increase of DOM. In the nutrient-enriched conditions of the winter scenario, we found an increase of DOC due to the phytoplankton bloom (dominated by diatoms) reaching discrete higher values (although not significant) during the bloom phase when high pCO<sub>2</sub> were induced. Moreover, the experiments performed by Kim *et al.* (2011) with mesocosm enclosures in Korean coastal waters, showed that when the pCO<sub>2</sub> and temperature increased, the production of DOC was enhanced. A different study conducted by Yoshimura *et al.* (2013) in the sub-Arctic Pacific obtained higher concentrations of DOC in the lowest pCO<sub>2</sub> treatment (300 µatm) over the first 10 days of incubation. Thus, in discordance with Kim *et al.* (2011), Riebesell *et al.* (2013), Yoshimura *et al.* (2013) and Paul *et al.* (2015), no significant differences were observed in DOC dynamics between acidified and non-acidified conditions.

Looking in further detail to the relationship between DOC and phytoplankton biomass (DOC/Chl *a* ratio, **Figure 3.5**), the highest values of this ratio were found under non-enriched conditions in both experiments. This fact could be due to a nutrient limitation of prokaryote growth as it has been described in open and coastal Mediterranean waters during low nutrient concentration episodes (Thingstad *et al.*, 1997; Sala *et al.*, 2002). Besides, for the non-enriched conditions, we found higher values of this ratio in the acidified conditions in winter, while the opposite pattern was observed in summer. The high values found for this ratio in summer have been

previously discussed in different studies conducted in Mediterranean waters (Morel and Gentili, 2009; Organelli *et al.*, 2014).

As described in the work of Romera-Castillo *et al.* (2013), at the Blanes Bay sampling site, the DOC accumulates during summer when the degradation of organic matter by heterotrophic prokaryotes is reduced due to the depletion of inorganic nutrients. In that scenario, DOC accumulates and the ratio DOC/Chl *a*, increases with respect to winter.

### 3.4.3. – FDOM dynamics

Since fluorescence excitation-emission matrices are spectral signatures of the FDOM, they are useful to track the changes of different DOM constituents over time. As explained above, previous studies have hypothesized that the increasing concentration of CO<sub>2</sub> in seawater could channel the extra organic carbon fixed by photosynthesis into the dissolved fraction. Despite not finding accumulation of DOC in the treatments amended with high pCO<sub>2</sub>, we consistently observed changes in the quality of DOM (**Figure 3.3**). The temporal evolution of the four main fluorophores

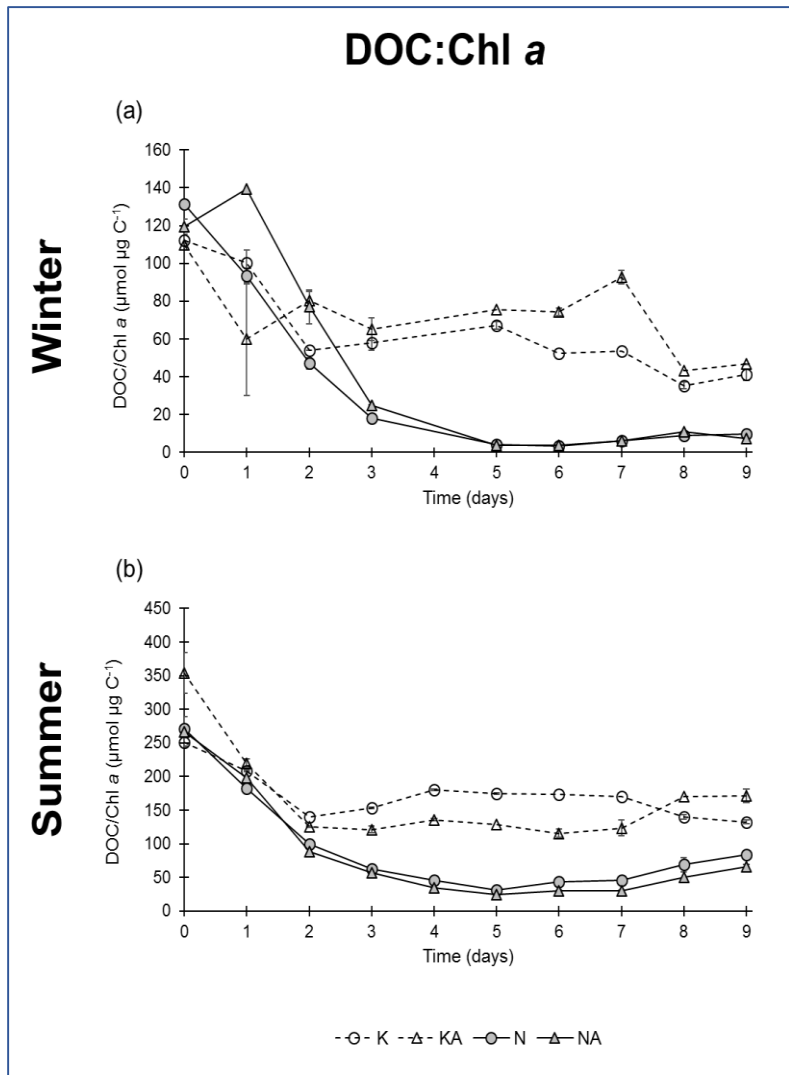


**Figure 3.5.** Time evolution of the quotient between DOC and Chl *a* in (a) winter and (b) summer. Units are expressed in  $\mu\text{mol } \mu\text{g } \text{C}^{-1}$ . Error bars indicate the standard error of 2 replicates.

revealed an increase with time, so no net consumption of FDOM was detected in any of the treatments. Data depicted in **Figure 3.3**, confirms that the increase in the humic-like fluorescent signal was greater in the tanks where nutrients were added than in the non-enriched tanks. This would agree with the increase of CDOM compounds after enrichment with nitrate found in the experiments performed by Lekunberri *et al.* (2012) and by Yuan *et al.* (2016) in the Mediterranean Sea and the South China Sea, respectively.

Lowered-pH conditions could potentially alter the optical properties of the protein- and humic-like portions of FDOM. Previous studies indicated that only pH levels above and below specific values (i.e., a pH <5 or >8) have potential to significantly change the structure of the DOM and thus induce a reduction of the fluorescence efficiency of the humic-like molecules (Laane, 1982; Dryer *et al.*, 2008; Yan *et al.*, 2013). Equally, it has been reported that the fluorescence signal of protein-like compounds as tyrosine and tryptophan can be only altered above and below specific pH values (i.e., a pH < 3 or >9; White, 1959). Consequently, given that the pH values achieved in KA and NA conditions were ~7.81 and ~7.76 for winter and summer, respectively, and that the original seawater pH values were 7.99 in winter and 8.02 in summer, we can discard that the changes in fluorescence were due to the alterations caused directly by the pH levels reached. In addition, we also tested the possible effects of pH on FDOM measurements (see Material & Methods section). And, as expected, we found no differences of FDOM intensities within the range of pH observed in our experiments. Therefore, we can assume that the changes in FDOM intensity were induced only by biological activity (i.e. FDOM intensities were not affected by pH).

The increment in peak-T fluorescence (**Figure 3.3**) indicated the generation of protein-like compounds in all the experimental conditions. It is common to find this type of fluorescence increases when studying microbial assemblages because it is associated to high productivity periods (Coble, 1996, 2007). Also, since microbial cells have protein-like fluorescence themselves (Determann *et al.*, 1998), several authors have found a positive direct relationship between fluorescence intensities and microbial biomass, in estuaries (Boyd and Osburn, 2004; Chen *et al.*, 2004; Nieto-Cid *et al.*, 2006; Huguet *et al.*, 2009), coastal waters (Para *et al.*, 2010; Romera-Castillo *et al.*, 2011b, 2010), open ocean (Yamashita and Tanoue, 2003; Aparicio *et al.*, 2015) or lakes (Yao *et al.*, 2011; Catalán *et al.*, 2013). The increase in peak-T intensity was lower in acidified conditions (**Figure 3.3**) except for the non-enriched summer conditions. However, the Pearson correlation performed in the Mantel tests revealed that differences between acidified and non-acidified treatments were not significant (p-value < 0.05). We found a significant correlation between prokaryote abundance and peak-T in summer experiment but not in winter, probably due to a larger influence of other variables not measured here, such as grazing on bacteria.

Although the production of protein-like material was the most relevant fluorescence feature in both experiments, the generation of humic-like substances (peak-A, -C and -M) was also notable. Nutrient enriched mesocosms (N and NA) presented an important increase in humic signals

regardless of the experiment. This is consistent with these humic signals being by-products of the microbial respiration processes (Niето-Cid *et al.*, 2005; Coble, 2007; Romera-Castillo *et al.*, 2011b, 2013; Jørgensen *et al.*, 2011, 2014a; Catalá *et al.*, 2015). In order to elucidate whether the presence of higher fluorescent signals in the humic-like substances area was accompanied by a change in the quality of the FDOM, we made use of three different fluorescent indices that are related to the quality of the DOM. The temporal trend of the peak-C/peak-M ratio (**Figure 3.4a, b**) indicated that nutrient additions affected the quality of the fluorescent organic matter, however changes in pCO<sub>2</sub> did not induce significant changes in the quantity nor in the quality of the fluorescent organic material (p-value < 0.05). It has been previously demonstrated that the fluorescence in the peak-C region is associated with prokaryote respiration (Lønborg *et al.*, 2010) and exudation of prokaryote by-products (Romera-Castillo *et al.*, 2011a). Therefore the high peak-C/peak-M ratios found at the end of the nutrient enriched experiments, compared to the non-nutrient amended, could be linked to an increase of prokaryote respiration which would be induced by the elevated nutrient availability.

The high pCO<sub>2</sub> did not seem to influence the SUVA index. However, the nutrient addition generated an increase of the SUVA values with respect to the non-amended mesocosms, but only in the summer season. This contrasting response to nutrient additions in summer could have resulted from differences in the initial quality of the DOM (note the initial values of the three indices tested, **Figure 3.4**). The generation of high molecular weight aromatic humic acids in the enriched mesocosms was distinguishable by the increase in HIX values at the end of the experiment. The HIX starting values in the two experiments differed between seasons and, most likely due to the intense solar radiation, we found lower values of HIX in the summer experiment. It has been demonstrated that photobleaching of humic-like materials results a loss of aromaticity and a decrease in the molecular weight of irradiated organic matter (Moran and Zepp, 1997; Osburn *et al.*, 2001; Rochelle-Newall and Fisher, 2002; Helms *et al.*, 2008; Para *et al.*, 2010; Catalán *et al.*, 2013). Nevertheless, because our mesocosms were not exposed to UV radiation (only photosynthetically active radiation -PAR- was provided) changes in HIX values were most parsimoniously ascribed to differences in biological activity.

It is clear that the evolution of the optical indices differed between seasons (**Figure 3.4**). In winter, nutrient and control conditions showed differences, but only in the last days of the experiment. In summer these differences were observed already at the beginning of the incubations, although the differences were statistically significant (p-value < 0.05) from t<sub>4</sub> (for SUVA and HIX indices) and from t<sub>6</sub> (peak-C/peak-M ratio). In this way, the normalization of the FDOM to DOC (peak-C/DOC and peak-M/DOC; **Figure 3.6**) also revealed that the quality of the DOM was highly influenced by the initial conditions. Although the starting values were similar for all the conditions, the different initial microbial populations could have conditioned the evolution of the DOC and FDOM dynamics. Diatoms clearly predominated over other phytoplanktonic group during winter, in the four tanks, whereas, during the summer experiment, this group was only present at small

proportions in N and NA conditions and almost inexistent in the control conditions (Sala *et al.*, 2016). Thus, a synergistic effect can be extracted from our results regarding the composition of the initial microbial population and the nutrient availability. These results agreed with those obtained in the work of Zark and collaborators (2015), indicating that the ocean acidification *per se* does not influence the accumulation of DOM in coastal environments.

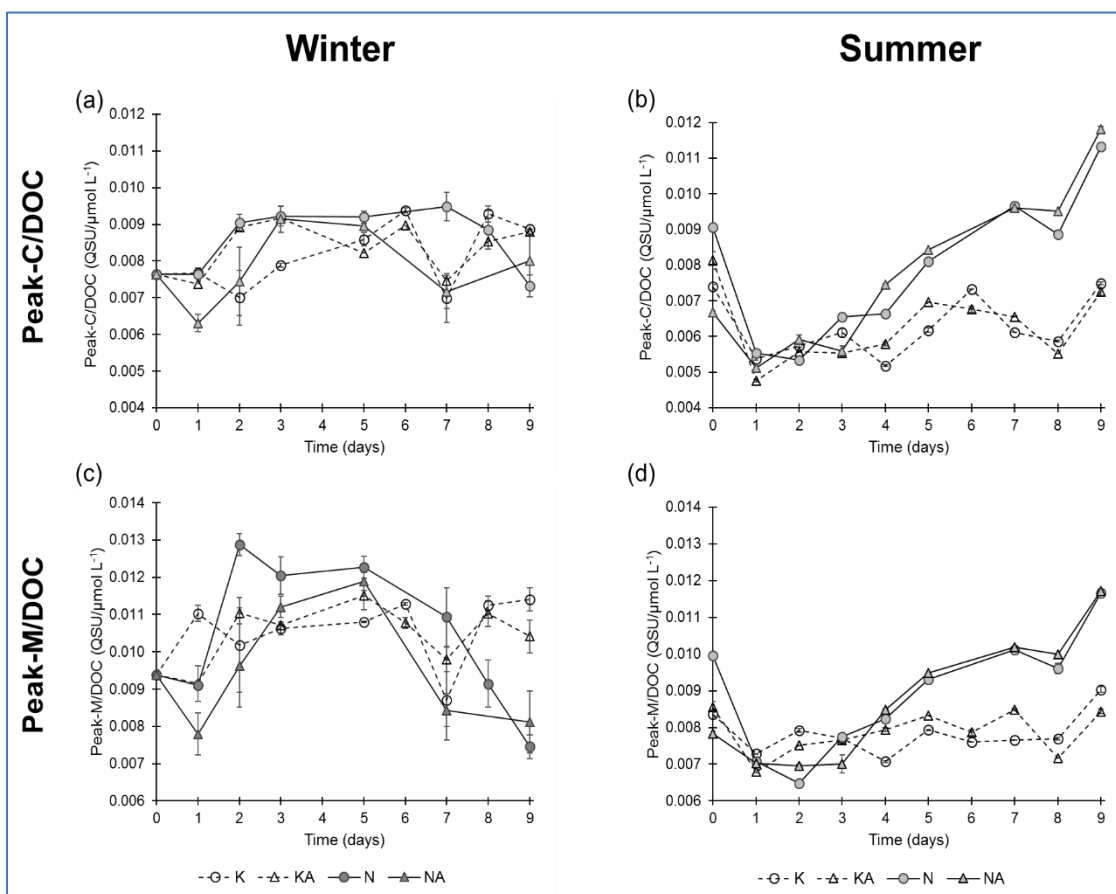


**Figure 3.6.** Time evolution of the quotient between peak-C and DOC in (a) winter and (b) summer; quotient between peak-M and DOC in (c) winter and (d) summer. Units are expressed in  $\text{QSU}/\mu\text{mol L}^{-1}$ . Error bars indicate the standard error of 2 replicates.

### **3.5. – Conclusions**

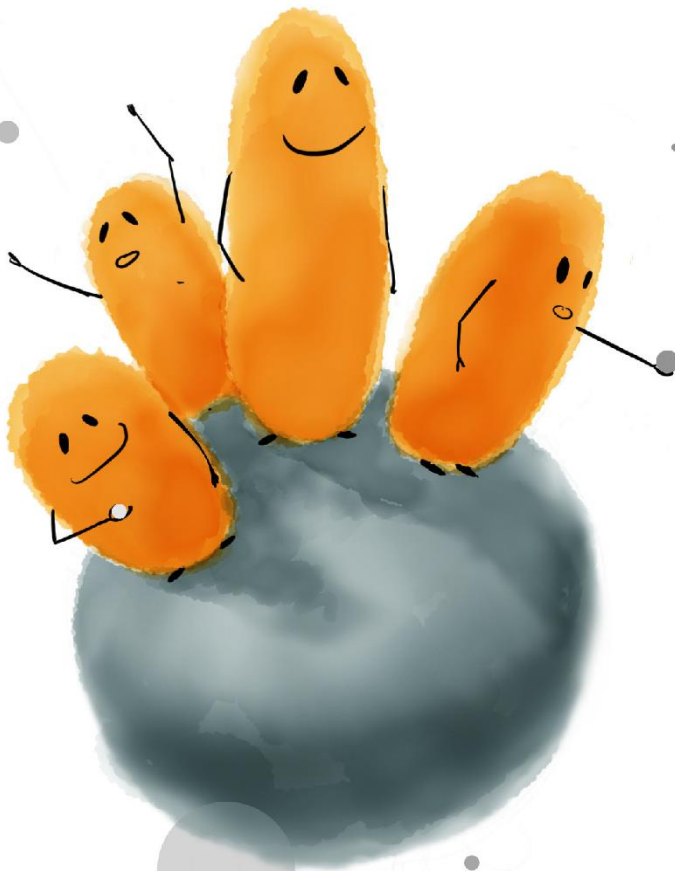
The results extracted from this study highlight the value of mesocosm experiments as a way to assess possible responses of DOM dynamics to future environmental changes. To our knowledge, this is the first study that quantifies the influence of high levels of pCO<sub>2</sub> on the fluorescent properties of DOM in the Mediterranean Sea.

Although we found, in general, higher phytoplankton biomass under high-pCO<sub>2</sub> conditions, we did not observe differences in the DOC dynamics between acidified and non-acidified treatments.

The transformations of DOM composition traced from the changes in its optical properties (absorbance and fluorescence) indicated that eutrophication modified the structure of the organic matter into more complex material, while a weak aromatization of the DOM was observed under higher pCO<sub>2</sub> conditions.

The effects of eutrophication, in terms of quantity and quality of organic matter, varied depending on the initial conditions, which highlights the importance of conducting experiments under different seasons/regimes to account for temporal variability in the response of the ecosystem to the studied variables.

**Chapter 4**  
Contrasting effects of ocean  
acidification on the microbial food web  
under different trophic conditions





## 4.1. - Introduction

Human activity is currently emitting around 10 Pg C in the form of CO<sub>2</sub> into the atmosphere every year (Peters *et al.*, 2012). About 30% of this CO<sub>2</sub> dissolves in the upper layers of the oceans, leading to a lowering of pH and, consequently, to fundamental changes in the chemistry of seawater (Doney *et al.*, 2009; Pelejero *et al.*, 2010). Marine organisms show a wide range of responses to this ocean acidification (OA) (e.g. Kroeker *et al.*, 2010; Harvey *et al.*, 2013).

Many of the studies performed to understand OA effects on picoplankton have used cultures (see Liu *et al.*, 2010 for a review). However, culture-based experiments, which are necessary to understand important physiological aspects, might not reflect the indirect effects that occur through biological interactions. Assays with natural communities in containers that are as large as possible would be an appropriate tool, and mesocosm experiments have been identified as a good approach to ecosystem studies (Lawton, 1995; Duarte *et al.*, 2000; Thingstad *et al.*, 2007).

Until now, few such mesocosm experiments have addressed OA effects on picoplankton (**Table 4.1**). Although comparative analyses are difficult because of differences between experimental set-ups, in general these experiments show a stimulatory effect of OA on photosynthetic picoeukaryotes and nanoeukaryotes (Paulino *et al.*, 2008; Newbold *et al.*, 2012; Brussaard *et al.*, 2013) and complex responses of heterotrophic prokaryotes, which often follow the dynamics of large phytoplankton (Grossart *et al.*, 2006; Allgaier *et al.*, 2008; Arnosti *et al.*, 2011). However, most of these experiments were conducted under high nutrient concentrations, either because they were high in the initial water (Lindh *et al.*, 2013) or because nutrient was added to produce a phytoplankton bloom (e.g. Riebesell *et al.*, 2013). Therefore, these experiments have provided important information on the effects of OA under eutrophic conditions, but not under oligotrophic conditions, which are those that prevail throughout the year in most open-ocean surface waters. Furthermore, mesocosm experiments to test the effects of OA on natural microbial planktonic communities have mostly been conducted at high latitudes (e.g. in the Arctic (Ray *et al.*, 2012) and in the Baltic Sea (Lindh *et al.*, 2013)), while at lower latitudes only two experiments have been published (Hama *et al.*, 2012; Kim *et al.*, 2013; **Table 4.1**). Our knowledge of the responses of microbes to acidification in medium- or low-latitude oligotrophic oceans is still very poor (Maugendre *et al.*, 2015).

**Table 4.1.** Selection of representative published mesocosm experiments testing the effect of ocean acidification on microbes.

Site	Season	pCO <sub>2</sub> or pH levels assayed	Nutrients added	pH manip.	References
Coastal, North Sea	June 2011	Decrease of 0.4 pH units	NO <sub>3</sub> +PO <sub>4</sub> +Si	CO <sub>2</sub>	Calbet <i>et al.</i> , 2014
Coastal, Greenland Sea	May 2010	145-1050 ppm	NO <sub>3</sub> +PO <sub>4</sub> +Si	CO <sub>2</sub>	Motegi <i>et al.</i> , 2013; Roy <i>et al.</i> , 2013; Piontek <i>et al.</i> , 2013; Schulz <i>et al.</i> , 2013; Brussaard <i>et al.</i> , 2013
Open ocean, Greenland Sea	June 2009	250-400 ppm	NO <sub>3</sub> +PO <sub>4</sub> +Si	Acid	Ray <i>et al.</i> , 2012
Coastal, East China Sea	January 2009	800 & 1200 ppm	NO <sub>3</sub> +PO <sub>4</sub> +Si	CO <sub>2</sub>	Hama <i>et al.</i> , 2012
Coastal, East China Sea	November 2008	400 & 900 ppm	NO <sub>3</sub> +NO <sub>2</sub> +PO <sub>4</sub> +Si	CO <sub>2</sub>	Kim <i>et al.</i> , 2013
Coastal, Baltic Sea	March 2008	Decrease of 0.4 pH units	None	CO <sub>2</sub>	Lindh <i>et al.</i> , 2013
Coastal, North Sea	May 2006	750 ppm	NO <sub>3</sub> +PO <sub>4</sub>	CO <sub>2</sub>	Newbold <i>et al.</i> , 2012; Meakin and Wyman, 2011
Coastal, North Sea	May 2005	350-1050 ppm	NO <sub>3</sub> +PO <sub>4</sub>	CO <sub>2</sub>	Allgaier <i>et al.</i> , 2008; Paulino <i>et al.</i> , 2008
Coastal, North Sea	Spring 2003	190-750 ppm	NO <sub>3</sub> +PO <sub>4</sub> +Si	CO <sub>2</sub>	Grossart <i>et al.</i> , 2006; Engel <i>et al.</i> , 2008; Arnosti <i>et al.</i> , 2011
Coastal, NW Med Sea	February 2010 & July 2011	7.5-8.3 units in pH, variable pH, see <a href="#">Figure 4.1</a>	None/NO <sub>3</sub> +PO <sub>4</sub> +Si	CO <sub>2</sub>	This study

The NW Mediterranean is an oligotrophic temperate sea that exhibits contrasting seasonal nutrient and phytoplankton levels in winter vs. summer (Gasol *et al.*, 2012). The planktonic phytoplankton communities also show contrasting composition: while in winter microphytoplankton are dominant, in summer nano- and picoplankton phototrophs are dominant. The high alkalinity and active overturning circulation of this area compared with the global oceans

must involve higher absorption and penetration of anthropogenic CO<sub>2</sub>, although it is not clear whether this high penetration translates into a pH decrease (Palmiéri *et al.*, 2015). These characteristics (oligotrophy, seasonality and high alkalinity) might very well be fundamental in determining the effects of acidification on microbes, but no results have been presented on the variability of the response of the Mediterranean microbial communities to OA in different seasons.

To gain insight into the consequences of acidification of marine ecosystems, we evaluated the effects of OA on microbial dynamics experimentally in NW Mediterranean waters, and determined the importance of contrasting community composition (i.e. winter vs summer communities) and different levels of nutrient concentrations on the observed responses. We will use the abbreviation OA throughout the manuscript to refer to a high pCO<sub>2</sub> level.

## **4.2. - Materials and methods**

### **4.2.1. - Experimental setup**

We conducted two experiments: one in winter 2010, during the period of maximum chlorophyll *a* (Chl *a*) concentration in the area, and one in summer 2011, when Chl *a* is at its annual low in the area (Gasol *et al.*, 2012). Common features of the two experiments were the following: Eight 200-L polyethylene tanks were filled with coastal surface water from the Blanes Bay Microbial Observatory (BBMO), NW Mediterranean, 1 km offshore (41°40'N 2°48'E). The experiments were conducted in a temperature-controlled chamber, set at in situ temperature and with a light:dark cycle of 12:12 h. The light conditions were set by a combination of cool-white and GRO-LUX lamps, which mimic the quality of natural light. The pH manipulation was performed by bubbling very small amounts of CO<sub>2</sub> (99.9% purity) directly into the mesocosms. This addition was performed manually every morning, in order to maintain the levels of pH in the acidified tanks ~0.25 to 0.30 pH units lower than the controls. This pH lowering is equivalent to that expected by the end of the century with atmospheric CO<sub>2</sub> concentrations of 750-800 ppm (Joos *et al.*, 2011). The lowering of pH was closely monitored using glass electrodes (LL Ecotrode plus - Metrohm), which were calibrated on a daily basis with a Tris buffer, following standard procedures (SOP6a of Dickson *et al.*, 2007). The pH in the tanks was continuously recorded by a D130 data logger (Consort, Belgium). In order to mimic the physical perturbation associated with CO<sub>2</sub> bubbling, the control tanks were also bubbled with similar small amounts of compressed air at current atmospheric CO<sub>2</sub> concentrations.

Four experimental conditions were randomly assigned to duplicated tanks: K1 and K2 (controls), KA1 and KA2 (pH-modified), N1 and N2 (nutrient-amended), and NA1 and NA2 (nutrient-amended and pH-modified). We gradually modified the pH (in the A treatments) starting immediately after mesocosm filling, and the following day we added inorganic nutrients (to the N treatments) to reach a final molar ratio of 1:16:30 and 0.25:4:8 (P:N:Si) in the winter and summer experiments, respectively (Table 4.2). In both cases, the nitrogen enrichment was close to 8x the monthly average concentration measured in the BBMO during the last 10 years. Nitrogen and

phosphorus were added at the Redfield ratio, whereas silicate was added in excess to assure no limitation for diatoms.

**Table 4.2.** Summary of the in situ and experimental conditions. Initial conditions are variables measured in Blanes Bay at the time of sampling on the dates of the experiments: winter (17 February 2010) and summer (6 July 2011). Experimental conditions are the temperature of the incubation chamber, the light intensity measured inside the microcosms, nutrient concentrations added in the N treatments, and the average lowering of pH in the acidified treatments vs controls (days 2-9).

	Winter		Summer	
<b>In situ conditions</b>				
Temperature (°C)	13		22	
Light intensity ( $\mu\text{mol m}^{-2} \text{s}^{-1}$ )	110		1001	
pH	8.045		8.069	
Salinity	37.92		37.83	
Total alkalinity ( $\mu\text{mol kg}^{-1}$ )	2533		2540	
Chl a ( $\mu\text{g L}^{-1}$ )	0.96		0.20	
<b>Experimental conditions</b>				
Temperature (°C)	14		22	
Light intensity ( $\mu\text{mol m}^{-2} \text{s}^{-1}$ )	121		217-261	
	<b>K</b>	<b>N</b>	<b>K</b>	<b>N</b>
Average pH lowering	0.18	0.13	0.28	0.28
NO <sub>3</sub> concentration ( $\mu\text{mol L}^{-1}$ )	3.11	16.8	0.39	4.69
PO <sub>4</sub> <sup>3-</sup> concentration ( $\mu\text{mol L}^{-1}$ )	0.14	1.14	0.02	0.24
SiO <sub>2</sub> concentration ( $\mu\text{mol L}^{-1}$ )	2.01	31.0	0.34	6.51

In the winter experiment (see initial conditions of the experiments in [Table 4.2](#)), the temperature of the chamber was set to  $14 \pm 1$  °C, and the measured light intensity inside of the containers was  $121.3 \pm 3.5$   $\mu\text{mol m}^{-2} \text{s}^{-1}$ . In the summer experiment temperature was set to  $22 \pm 1$  °C, and the actual light intensity in the tanks ranged from 217 to 261  $\mu\text{mol m}^{-2} \text{s}^{-1}$ .

The pH in the acidified treatments was lowered initially to values around 7.81 units in the winter experiment, which were achieved in the third day, and later they were manipulated to mimic the evolution of the corresponding control (with and without nutrients), but around 0.2 pH units lower. In the summer experiment, pH was progressively lowered in the acidified treatments with the aim of maintaining a relatively constant offset of around 0.2-0.3 units in pH in comparison with the controls.

#### 4.2.2. - Chemical parameters

Prior to each morning's controlled addition of CO<sub>2</sub>, we measured pH and alkalinity precisely in all the mesocosms. pH was measured by spectrophotometry after the addition of m-cresol purple (Clayton and Byrne, 1993) and alkalinity was determined with a fast, single-point potentiometric titration (Perez *et al.*, 2000). Samples for inorganic nutrients were kept frozen at -20 °C until analysis, which was performed using a CFA Bran +Luebbe autoanalyser following the methods described by Hansen and Koroleff (1999).

Chl *a* was measured according to the procedure of Yentsch and Menzel (1963). Briefly, 50 mL were filtered through Whatman GF/F glass fibre filters. The filters were placed in 90% acetone at 4 °C for 24 h and the fluorescence of the extract was measured using a Turner Designs fluorometer.

#### **4.2.3. – Microbial abundances**

Pico- and nanophytoplankton and bacterial abundance was determined by flow cytometry (Gasol and del Giorgio, 2000). For pico- and nanophytoplankton, the samples were analysed without addition of fixative and run at high speed (ca. 100  $\mu\text{L min}^{-1}$ ). Phototrophic populations (*Prochlorococcus*, *Synechococcus*, two groups of picoeukaryotes [small and large] and nanoeukaryotes) were discriminated according to their scatter and fluorescence signals. For heterotrophic bacteria, abundances were estimated after fixing 1.2-mL samples with a 1% paraformaldehyde + 0.05% glutaraldehyde solution, and deep-freezing in liquid N<sub>2</sub>. Afterwards, the samples were unfrozen, stained with SybrGreen at a 10x dilution and run at low speed (ca. 15  $\mu\text{L min}^{-1}$ ). Cells were identified in plots of side scatter versus green fluorescence and green vs red fluorescence.

Microphytoplankton counts were performed after fixing the sample with formalin-hexamine (0.4% final concentration). Afterwards, 50 mL of each sample were placed in sedimentation columns for 24 h. The sedimentation chamber was then scanned in an inverted microscope at 100x and 400x magnification.

#### **4.2.4. – Bacterial activity**

Bacterial heterotrophic activity was estimated using the <sup>3</sup>H-leucine incorporation method (Kirchman *et al.*, 1985). Quadruplicate aliquots of 1.2 mL and two trichloroacetic acid (TCA)–killed controls were taken immediately after sample collection. The samples were incubated with 40 nM <sup>3</sup>H-leucine (final concentration) for about 1.5 h in the dark in a temperature-regulated room. The incorporation was stopped with the addition of 120  $\mu\text{L}$  of cold TCA 50% to each replicate and the samples were kept frozen at -20 °C until processing, which was carried out by the centrifugation method described by Smith and Azam (1992).

#### **4.2.5. - Extracellular enzyme activities**

Samples were assayed for the activity of five hydrolytic enzymes, using fluorogenic substrates that are molecules linked to 4-methylumbelliferone (MUF) or 4-methylcoumarinyl-7-amide (MCA), following the method described in Sala *et al.* (1999) and adapted to the use of microplates. The enzymes studied were  $\alpha$ -glucosidase,  $\beta$ -glucosidase, chitinase and leu-aminopeptidase; and the substrates used were 4-methylumbelliferyl  $\alpha$ -D-glucopyranoside, 4-methylumbelliferyl  $\beta$ -D-glucopyranoside, 4-methylumbelliferyl N-acetyl- $\beta$ -D-glucosaminide and L-Leucine-7-amido-4-methyl coumarin. The assays were arrayed in black, 96-well microplates using a protocol similar

to that in Sala *et al.* (2010). For each enzyme, 350  $\mu\text{L}$  of the sample was added to a well together with 50  $\mu\text{L}$  of substrate solution. Each assay was replicated in four wells. The substrate solutions were prepared in sterile deionized water and methanol 1% at a final concentration of 1 mM, yielding a final substrate concentration of 125  $\mu\text{M}$  in the assay wells. Fluorescence was measured regularly at different times for 5 hours using a Modulus microplate reader set to an excitation wavelength of 365 nm and an emission wavelength of 450 nm. Fluorescence units were transformed into activity using a standard curve prepared with the end product of the reactions: 7-amido-4-methylcoumarin for leu-aminopeptidase and 4-methylumbelliferone for the rest of the enzymes.

#### **4.2.6. - Statistical analysis**

We used STATISTICA version 8.0 (StatSoft, Inc. 2007) for the statistical analyses. To test the hypothesis that there were no effects of acidification within treatments of the same experiment and nutrient addition, we used independent two-tailed t-tests. The overall differences between acidified and control treatments were tested with sign tests (**Figure 4.2**). Data from day 3 to 9 were chosen for both analyses because it was during this period that the effects of acidification were more conspicuous.

#### **4.3. – Results**

A difference in pH in the range of 0.1-0.5 was maintained between the acidified and control mesocosms in both experiments (**Figure 4.1a, b**). In summer, pH varied only slightly between the nutrient-enriched and non-enriched conditions. However, in winter, the intense phytoplankton bloom in the nutrient-enriched treatments (up to 29.6  $\mu\text{g Chl a L}^{-1}$ , **Figure 4.1**) induced an increase of pH on day 5, reaching levels of up to 8.3 pH units in the non-acidified enriched treatment.

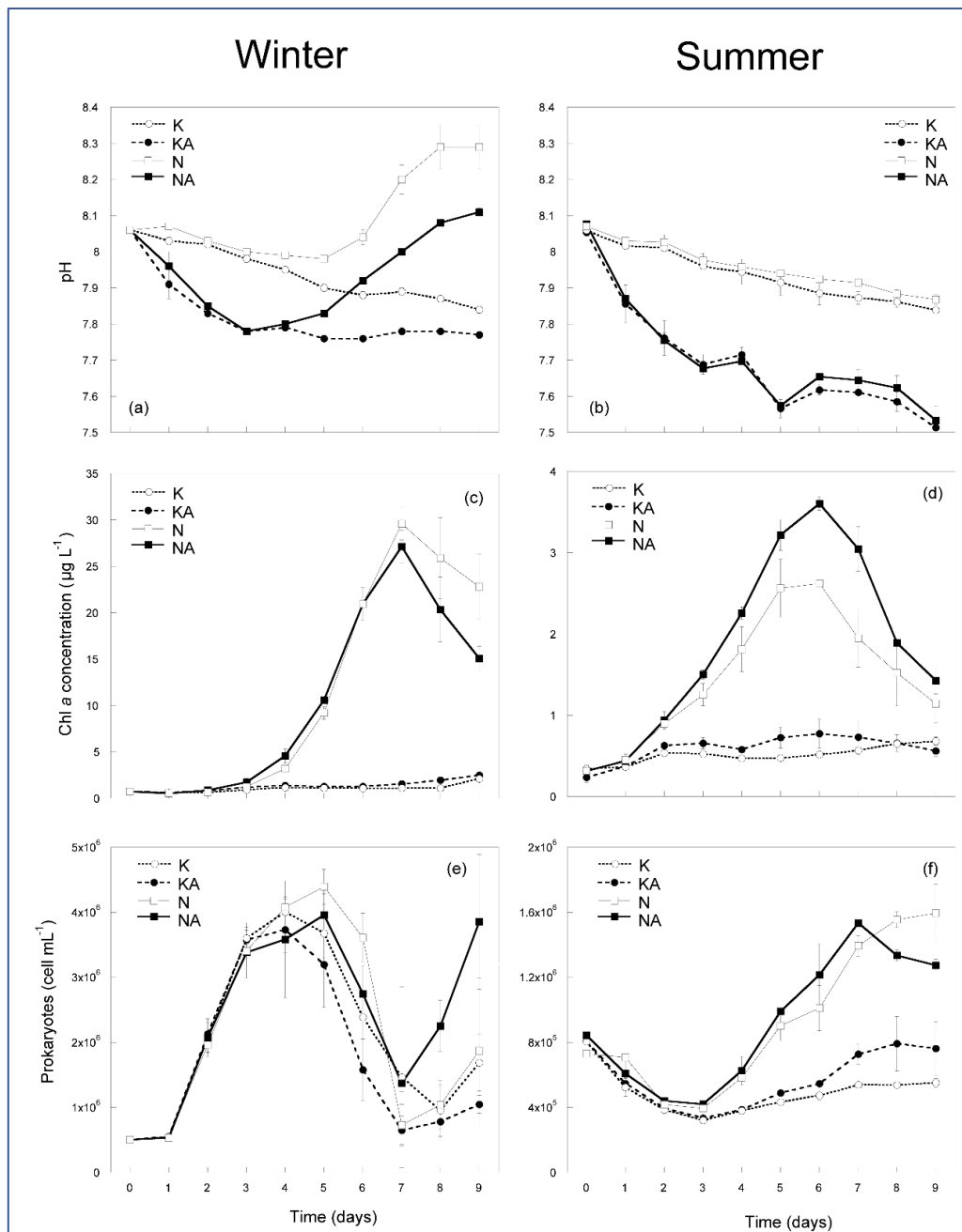


**Figure 4.1.** Evolution of pH, Chl *a* concentration and prokaryote abundances in the winter (a, c and e panels) and summer (b, d and f panels). Squares, nutrient-amended treatments; circles, controls without nutrient additions; full symbols, acidified treatments; empty symbols, non-acidified treatments. Error bars denote standard deviations for duplicate treatments.

We examined the effects of pH in our set of measured parameters with independent t-tests (Table 4.3). Chl *a* concentration was positively affected by acidification (Figure 4.1c, d) except in the nutrient-enriched treatment of the winter experiment, in which no effects were observed (Table 4.3). The composition of the winter and summer blooms also differed considerably: diatoms of the genus *Thalassiosira*, *Chaetoceros*, and *Pseudo-nitzschia* dominated the winter bloom (80% of the abundance of the phytoplankton community), whereas the summer community was mostly composed of small pico- and nanoflagellates. No effect of acidification on diatoms was observed, and both positive and negative effects on dinoflagellates were observed (Table 4.3). The

abundances of phototrophic nanoeukaryotes and of large picoeukaryotes were consistently positively affected by acidification (**Table 4.3**), with significant differences in both experiments.

Although the initial abundances of heterotrophic bacteria were similar in both seasons ( $5-8 \times 10^5$  cells mL<sup>-1</sup>), their concentration during the experiment increased more in winter than in summer, to maximum values of  $4.5 \times 10^6$  cells mL<sup>-1</sup> (**Figure 4.1**). The abundance of the different groups of prokaryotes (heterotrophic bacteria, *Synechococcus* and *Prochlorococcus*) and leucine incorporation showed a stimulation effect in non-enriched conditions in summer. However, we also found a negative effect of acidification in winter with the nutrient-enriched treatment for *Synechococcus* (**Table 4.3**).

**Table 4.3.** Results of independent t-tests for various abundance and microbial activity data.

PARAMETER	WINTER		SUMMER	
	-NUTS	+NUTS	-NUTS	+NUTS
Chl a ( $\mu\text{g L}^{-1}$ )	0.041		0.007	0.046
Chl a <3 $\mu\text{m}$ ( $\mu\text{g L}^{-1}$ )				
MICROPLANKTON (cell L <sup>-1</sup> )				
Diatoms				
Dinoflagellates		0.031	0.004	
PICOPLANKTON (cell mL <sup>-1</sup> )				
Nanoeukaryotes	<0.001	0.014		
Large picoeukaryotes			0.002	0.049
Small picoeukaryotes				
PROKARYOTES (cell mL <sup>-1</sup> )				
<i>Synechococcus</i>		<0.001	<0.001	
<i>Prochlorococcus</i>			0.020	
Heterotrophic bacteria			0.050	
PROKARYOTIC ACTIVITY				
Leucine incorporation			0.001	
Leu-aminopeptidase				
Chitobiase				
$\alpha$ -Glucosidase			0.050	
$\beta$ -Glucosidase			0.010	<0.000

Among the four bacterial extracellular enzyme activities tested,  $\alpha$ - and  $\beta$ -glucosidase were affected by acidification in summer (**Table 4.3**). The other enzyme activities, leu-aminopeptidase and chitinase, were not affected by acidification under any of the conditions tested.

To summarize the main results obtained, **Figure 4.2** shows a comparison of the abundances of the main groups of organisms between the control and acidified pairs of mesocosms in the two experiments (filled circle, winter; empty circle, summer). In order to compare the general trends of the effects of acidification on the measured variables, we performed a sign test, i.e. a non-parametric test aimed at comparing pairs of data of acidified vs non-acidified treatments. The sign test revealed no significant global differences between treatments for heterotrophic bacteria and *Synechococcus* (a negative sign of acidification effect in winter neutralized the positive sign in summer). By contrast, significantly higher concentrations were found in acidified treatments for nanoeukaryotes ( $n = 56$ ;  $p < 0.001$ ), large picoeukaryotes ( $n = 56$ ;  $p < 0.001$ ) and Chl *a* concentrations ( $n = 54$ ;  $p < 0.001$ ) (**Figure 4.2**)

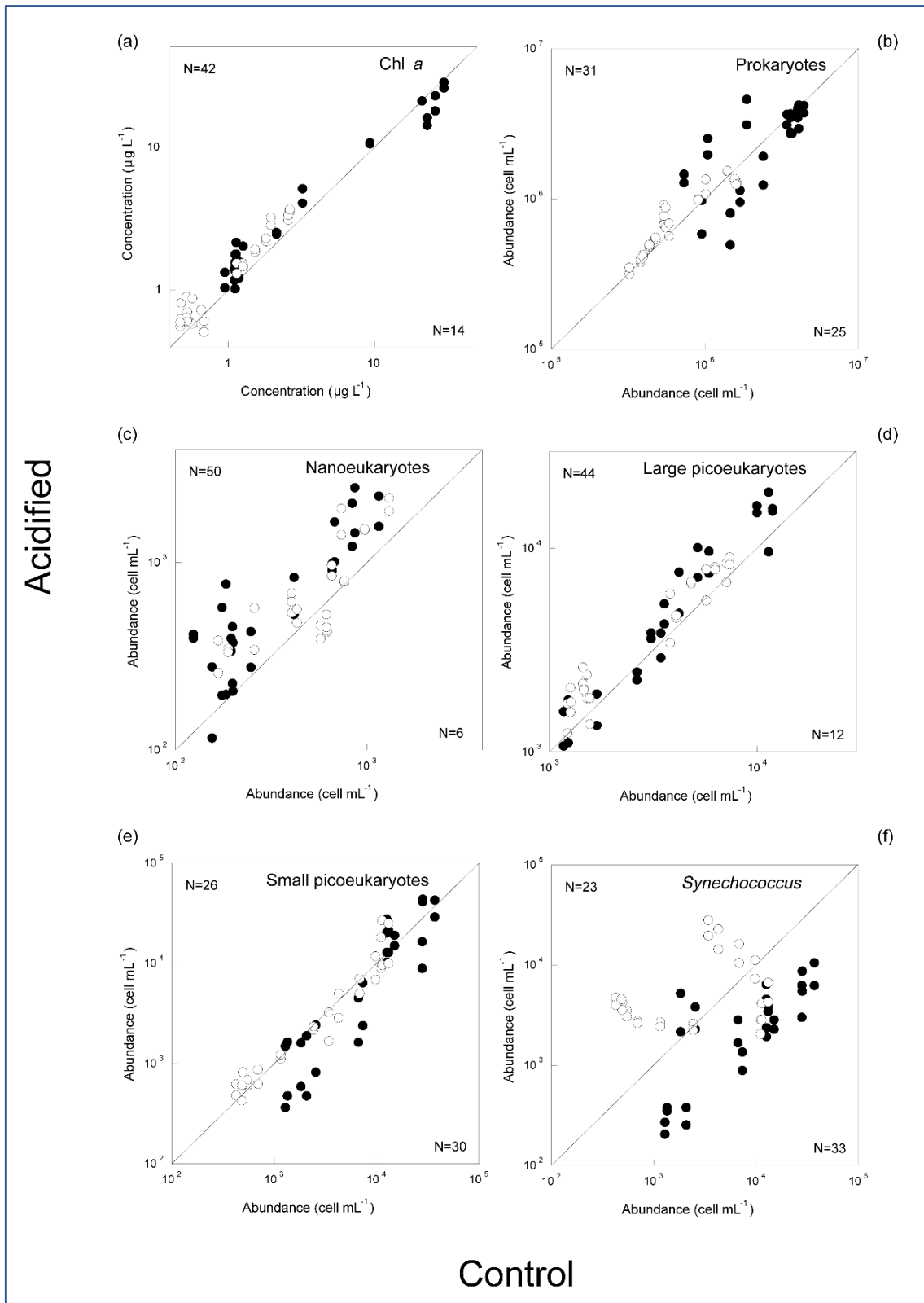


**Figure 4.2.** Concentrations of Chl a (a), prokaryotes (b) and photosynthetic picoplankton groups (c-f) in acidified vs non-acidified treatments. Empty symbols, summer experiment; full symbols, winter experiment. The N in the upper left corner corresponds to the number of cases in which the value of the acidified treatment is higher than that of the non-acidified treatment. The N in the lower right corner is the number of cases with values lower in the non-acidified than in the acidified treatment.

#### 4.4. - Discussion

We assessed the response of the microbial community to a decrease in pH in the Mediterranean. Because in the likely future ocean the response of the microbial planktonic community to OA will interact with other stressors linked to global change, such as eutrophication and increased temperature, we tried to deepen our understanding of possible OA-eutrophication interactions. The major findings of this study are 1) phototrophic pico- and nanoeukaryotes were consistently stimulated by acidification; 2) prokaryotic picoplankton and phototrophic microplankton exhibited different responses to acidification in winter and summer; and 3) overall, the magnitude of the acidification effects was lower under nutrient-rich conditions.

##### 4.4.1. - Effects of acidification on phototrophic pico- and nanoeukaryotes

We observed a consistent stimulation of the large pico- and nanoeukaryotic phototrophic communities in both winter and summer and in conditions with high and low nutrient levels (i.e. treatments). Stimulation of pico- or nanoeukaryotes by acidification has previously been reported in some mesocosm studies (Engel *et al.*, 2008, Newbold *et al.*, 2012, Brussard *et al.*, 2013, Calbet *et al.*, 2014), although no effect or a negative effect has also been observed (Paulino *et al.*, 2008, Calbet *et al.*, 2014). Here, the positive effect found in most of the experimental conditions contrasts with the negative effect observed in dinoflagellates in the winter, nutrient-enriched conditions. These divergent results might be due to differences in the species-specific sensitivities to CO<sub>2</sub> in accordance with different carbon concentration mechanisms (CCMs; Rost *et al.*, 2003). Eutrophication and pH decreases are predicted in coastal waters for the near future (IPCC, 2013). In such scenarios, our results suggest that small phototrophic organisms will show a relative increase in comparison with large ones. Temperature rises will also promote small-sized organisms (Morán *et al.*, 2009). These changes in size distribution will affect food web interactions and sedimentation processes (Legendre and Lefèvre, 1991), which should be considered when it is attempted to predict the likely communities of a future ocean.

##### 4.4.2. - Effects of acidification in winter vs summer

The number of variables affected by acidification in the controls was lower in winter than in summer, and the sign of the responses was always positive in summer, whereas in winter it was negative for *Synechococcus* and dinoflagellates (Table 4.3). This differential response to acidification in the two experiments suggests a clear role of the initial community composition and environmental trophic conditions. Blanes Bay surface waters exhibit a temperate seasonal cycle with a winter phytoplankton bloom driven in part by elevated nutrient concentrations, typically with diatom dominance, and a summer period dominated by picophytoplankton, microheterotrophs and low inorganic nutrient concentrations (Alonso-Sáez *et al.*, 2008; Gasol *et al.*, 2012). Contrasting with phototrophic pico- and nanoeukaryotes, which showed a similar number of positive responses in both seasons, all prokaryotes were affected positively in summer and no effects, or negative effects, were detected in winter (Table 4.3). The only study that evaluated the

planktonic community response to OA in different seasons, conducted in 1-L bottles in the Baltic Sea, showed no clear differences in acidification effects on bacterial abundance and diversity during the year (Krause *et al.*, 2012). Ours is the first study to show differences between winter and summer in the prokaryote response to OA. The higher number of effects of acidification in summer than in winter may be related to differences in initial species composition, but also to the different nutrient levels or to a combination of both factors (see next section).

Cyanobacteria are known to use CCMs to actively transport inorganic C species and maintain their growth even at low external dissolved inorganic carbon concentrations (Badger and Price, 2003). Therefore, it is reasonable to assume that, at increased CO<sub>2</sub>, the need for CCMs would decrease, and this would result in energy savings that could be allocated to growth. Indeed, several culture-based studies have found a stimulation of the growth rate or CO<sub>2</sub> fixation in cyanobacteria with acidification (Fu *et al.*, 2007; Hutchins *et al.*, 2007). However, negative responses to acidification were found in our winter experiment and also in some previous mesocosm studies (Paulino *et al.*, 2008).

The recent literature tends to suggest that the impact of OA on bacterioplankton community composition is negligible (Ray *et al.*, 2012; Roy *et al.*, 2013), but compositional shifts (Lindh *et al.*, 2012; Krause *et al.*, 2012) and strain-dependent effects (Teira *et al.*, 2012) have also been encountered. Studies in nutrient-enriched mesocosms have reported decreases (Rochelle-Newall *et al.*, 2004; Grossart *et al.*, 2006) or lack of effects (Allgaier *et al.*, 2008) in bacterial abundance in acidified conditions. In addition, contrasting results were also found in the magnitude and direction of the effect of OA on bacterial activity (Allgaier *et al.*, 2008; Grossart *et al.*, 2006; Motegi *et al.*, 2013).

We also looked at specific functions mediated by heterotrophic bacteria, such as the extracellular enzymatic activities which mediate important biogeochemical processes such as the decomposition and transformation of organic carbon and the release of nutrients (Hoppe, 1983). Still very little is known about the direct effects of OA on extracellular enzyme activities, but effects could be expected since changes in pH have direct effects on the functioning of enzymes in bacterial cultures (Page *et al.*, 1988). However, the results to date have been controversial (see Cunha *et al.*, 2010 for a review). Some authors have found that OA stimulated the activity of a set of extracellular enzymes in different environments (Grossart *et al.*, 2006; Piontek *et al.*, 2010, 2013; Mass *et al.*, 2013), but others reported a lack of stimulation (Arnosti *et al.*, 2011; Engel *et al.*, 2014). In our study, the only enzyme activities for which we found some effect were  $\alpha$ - and  $\beta$ -glucosidases, which mediate the final step of the hydrolysis of polysaccharides. Similar to the bulk heterotrophic activity, both glucosidase activities were higher in summer under acidified treatments; Piontek *et al.* (2010) and Maas *et al.* (2013) similarly observed increased  $\beta$ -glucosidase activities under OA. These results suggest higher hydrolysis of carbohydrates. Since carbohydrates represent a large fraction in the composition of organic aggregates of marine

ecosystems, an increase in glucosidase activities might contribute to changes in the degradation patterns of different types of organic matter, which could eventually lead to a reduction of the strength of the biological pump in the future ocean.

#### **4.4.3. - Effects of nutrient addition on OA**

In general, effects of OA on plankton communities have been studied under high nutrient concentrations, either induced or natural (**Table 4.1**), and the combined effects of extra inorganic carbon and nutrients promoted phytoplankton growth on most occasions. It is noteworthy that in our experiments the effects of acidification on bacterial abundance and production were more evident in the treatments with the lowest nutrient concentrations. Moreover, the amendment with nutrients altered the responses of phototrophic picoeukaryotes and microplankton. Overall, the compilation of variables that were significantly affected by acidification in our experiment (**Table 4.3**) shows that the treatment with the clearly lowest nutrient concentrations (summer non-enriched, see **Table 4.2**) had a higher number of variables with significant responses to acidification (n=9) than the other treatments (n= 2-3).

The most similar approximation to our study in terms of nutrient dynamics is the EPOCA mesocosm experiment, in which a set of very large enclosures manipulated with CO<sub>2</sub> were enriched in nutrients only after day 14 (Riebesell *et al.*, 2013). In that study, unlike in ours, no significant effects on the abundance of any of the analysed planktonic groups were observed before nutrient addition. However, contrasting responses of phytoplankton abundance and activity to OA (from positive to negative) were observed between the first and the second bloom phases of their study. In the EPOCA experiment, nutrients were added at a point when treatments might have evolved differently during the first few days of the experiment. Although their results cannot be directly compared with ours, the present findings corroborate their conclusions about the importance of examining the effect of acidification in contrasting stages of plankton community succession. They evaluated different phases of succession by conducting longer experiments than ours (one month), whereas we collected natural water in two different seasons with divergent community structures. The initial percentage of diatoms with respect to the total phytoplankton cells was 22% in winter and 2% in summer, a finding that could explain the clear positive response of chlorophyll in summer in contrast with the low response in winter. This result agrees with those of Riebesell *et al.* (2013), in which diatoms responded negatively to acidification. Different photosynthetic groups reacting in opposite ways and indirect effects mediated by changes in prey biochemical composition (i.e. changing the food quality of prey; Schoo *et al.*, 2012) would induce changes in the community structure of grazers, which in turn would feed back on their prey. For instance, if different predators are favoured, then a different nutrient competition could be established between prokaryotes and microphytoplankton, etc. The existence of these complex interdependences requires further research on multiple trophic interactions when ecosystem responses to acidification are evaluated.

At a smaller scale (4-L bottles), a recent study in the Mediterranean reported a very limited impact of OA on the planktonic communities of nutrient-depleted waters (Maugendre *et al.*, in press). This experiment could be closely related to our work because of the area of study, although the original community may have been different. The species-specific responses to nutrient additions and acidification, usually veiled by bulk analyses (chlorophyll, cytometry, etc), may be the key to explaining the discrepancies between that study and ours. As seen above, many groups benefit from nutrient additions and OA. Others, however, may be outcompeted by faster-growing species with better capabilities of incorporating and accumulating CO<sub>2</sub>.

The fact that we observed a larger number of effects of acidification under low nutrient concentrations emphasizes the importance of running experiments under natural conditions. When the effects of OA on very productive communities need to be investigated, it would be advisable to conduct the experiments during natural bloom situations, rather than generating an artificial one. In addition, to better represent the natural environmental conditions, we advise that research should focus on communities of areas of great importance that remain mostly unexplored so far, such as the oligotrophic ocean.

The duration of the mesocosm experiment is an additional important variable to consider. Normally, mesocosm studies on planktonic communities have been conducted over timescales ranging from days to one month. Experimentation over longer periods of time would be interesting to address issues related to acclimation and adaptation. However, prolonging mesocosm experiments for too long is not trivial, and there is an inherent danger of driving the community away from the real world over time (i.e. due to wall effects, unreal water mixing, etc.). In our case, though the nine-day experiment is too short to be meaningful for assessing potential acclimation/adaptation, it is set up over a temporal pH variability that parallels the real world, particularly in the coastal areas. These environments often exhibit natural short-term changes in seawater at scales of days or even hours of similar magnitude to that induced in our experiments. Furthermore, progressive OA due to anthropogenic CO<sub>2</sub> emissions superimposed on these short-term pH changes will induce similar changes to those experienced by our mesocosm communities.

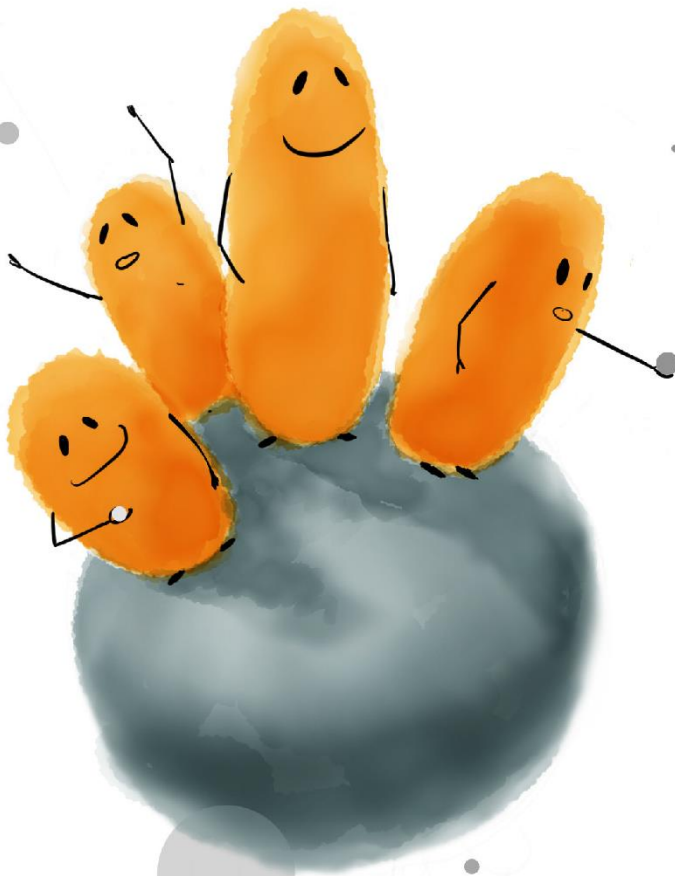
Further understanding of OA effects on plankton communities will come from the integration of single-species studies, short mesocosm experiments such as the present one, field observations in naturally or artificially acidified environments and ecosystem modelling, together with data on potential acclimation and adaptation through multi-generational studies.

As a general trend, in our study we observed a stimulatory effect of ocean acidification on the abundance of small phytoplankton (pico- and nanoeukaryotes) independently of the nutrients added. Considering the effects of combining acidification and eutrophication, our observations point towards a lower sensitivity of the microbial community to OA under eutrophic conditions,

which may have implications on the interpretation of the effects of OA in coastal and more nutrient-rich systems compared with oligotrophic open-ocean environments. They also highlight the need for comparative experimental studies during different periods of the year and with different levels of nutrient concentrations to provide a broader assessment of the effects of acidification on marine ecosystems.



**Chapter 5**  
Wind-induced changes in the  
FDOM dynamics of a NW  
Mediterranean sampling station





## 5.1.- Introduction

The Mediterranean Sea is considered the largest semi-enclosed basin on Earth and also one of the most complex marine environments (Santinelli, 2015). From a biogeochemical perspective, it is defined as a low-nutrient, low-chlorophyll system (Durrieu de Madron *et al.*, 2011 and references therein). The specific geographic location of the Mediterranean Sea in the globe and the fact that it is surrounded by three continents with contrasting coastal orography (Europe, Africa and Asia) make it prone to large cyclonic and anticyclonic gyres, elevated evaporation quotas, unequal precipitation rates between basins and abundant eddies with regional and local impacts (Robinson *et al.*, 2001; Santinelli, 2015).

In the NW Mediterranean coast, severe winds blowing during the winter season bring cold and dry continental air over the warmer ocean, generating intense air-sea heat exchanges and cooling the surface waters (Flamant *et al.*, 2003; Millot and Taupier-Letage, 2005). The loss of heat and buoyancy, coupled with mixing mechanisms, induce two main physical processes: i) dense water formation during winter and early spring, that may trigger deep ocean convection (Béthoux *et al.*, 2002; Marshall and Schott, 1999), and ii) upwelling processes due to the wind-induced displacement of surface waters, which rise deep waters towards shallower layers (Millot, 1979; Millot and Taupier-Letage, 2005; Vila-Reixach *et al.*, 2012).

Additionally, since Mediterranean climate is characterized by long dry summer seasons and scarce precipitations and mild temperature in winter (Rana and Katerji, 2000), the inputs of freshwater associated to rain are expected to be seasonal and intermittent, mainly occurring in spring and autumn. These inputs constitute a high contribution to the dissolved organic matter (DOM) supply to the marine ecosystems within the area (Cauwet, 2002).

The origin of DOM in marine waters can be allochthonous (mainly from terrestrial origin, as for example leachates from terrestrial plants, wetland drainage and aerosol depositions; Coble, 2007; Murphy *et al.*, 2008; Pey *et al.*, 2010) but also autochthonous (as, for example, the by-products from the metabolism of marine organisms, such as phytoplankton extracellular release, particulate organic matter dissolution into DOM, or the release via cell lysis; Jiao *et al.*, 2010; Romera-Castillo *et al.*, 2010; Turner, 2015) covering a high diversity of structures and lability. The study of the DOM distribution and transformations in marine systems, along with its role in the carbon cycle, has been in the spotlight during the last two decades because the marine DOC constitutes one of the greatest reservoirs of organic carbon on Earth (Hansell *et al.*, 2009).

A portion of this DOM, able to absorb light at ultraviolet and visible wavelengths, is named chromophoric dissolved matter (CDOM), and a sub-fraction of this pool, known as fluorescent dissolved organic matter (FDOM), can also, after absorbing light, re-emit it in form of fluorescent energy (Coble, 1996). The different optical properties of the DOM are useful tracers of the nature, origin and possible fate of the DOM in aquatic ecosystems. Thus, some groups of compounds

can be detected by its characteristic fluorescence signal, as for example the humic-like substances (Coble, 1996). The fluorescence of the humic-like fraction of DOM usually presents a shift to long wavelengths (Coble, 1996), which is mainly associated with higher aromaticity. This complexity in their molecular structure confers refractory characteristics to the humic-like compounds. The more refractory a compound is, the more difficult to be remineralized by organisms (Hansell *et al.*, 2009), facilitating its accumulation in the ocean for longer time scales (Chen and Bada, 1994; Jiao *et al.*, 2010). The presence of fluorescent humic-like material in marine coastal systems has been related mainly to allochthonous inputs (Boyd and Osburn, 2004; Nieto-Cid *et al.*, 2005; Para *et al.*, 2010; Romera-Castillo *et al.*, 2011b), but also to microbial respiration processes (Nieto-Cid *et al.*, 2006; Romera-Castillo *et al.*, 2010). The monitoring of humic-like compounds in the particular case of Mediterranean coastal areas has shown different temporal patterns that go from weak to strong seasonality (Para *et al.*, 2010; Romera-Castillo *et al.*, 2013). The fluctuations of carbon fluxes among the different compartments (atmospheric-terrestrial-marine) are still poorly understood and more research is needed to elucidate whether seasonal processes in coastal systems act as a source or a sink of refractory DOM.

The present study aims to examine the seasonal cycle of DOM in a NW Mediterranean coastal site. Previous time-series studies in Mediterranean coastal areas have been focused on seasonal cycles of DOM: Vila-Reixach *et al.* (2012) and Romera-Castillo *et al.* (2013) in the Blanes Bay Microbial Observatory (BBMO), Sánchez-Pérez (2015) in the bay of Banyuls-sur-mer (SE France) and Tedetti *et al.* (2012) in the bay of Marseilles (SE France). One big advance of our study with respect to these previous ones is that we have performed samplings through the water column, allowing the study of the possible influence of oceanic water intrusions into the shallower coastal waters. We hypothesize that the proximity to l'Estartit village, the Ter river estuary and the intrusion of high salinity water into surface coastal waters may condition the DOM dynamics in the study area.

## **5.2. – Methodology**

### **5.2.1. – Location of the sampling point**

The Estartit Oceanographic Station (EOS) is located in the NW Mediterranean Sea (42.05 N, 3.25 E, [Figure 5.1](#)). The bathymetry at the sampling point is ~90 m deep. EOS presents several singular features: i) it is located close to an urban area (L'Estartit village) and to the Ter river estuary; ii) it is affected by an extreme variability of the wind regime throughout the year; and iii) it is placed inside of a natural marine reserve (*El Parc Natural del Montgrí, les Illes Medes i el Baix Ter*). This park is protected under law 15/2010 enacted the 21<sup>st</sup> May 2010 by the Spanish Ministry of Environment, which cataloged it as a Specially Protected Area of Mediterranean Importance (SPAMI zone). In addition, L'Estartit village presents a very marked seasonality in terms of population density because of the large influx of tourists during the summer months, multiplying its number of residents by 25 (source: Institut d'Estadística de Catalunya – IDESCAT –).

In this context, seawater samples were taken monthly from January 2011 to December 2014, collected with 5 L Niskin bottles at four depths: 0.5 m (surface), 20 m, 50 m and 80 m. Once on board, water was filtered through a 200  $\mu\text{m}$  nylon mesh to remove large planktonic organisms and samples were kept in 8 L polyethylene carboys, covered with black plastic bags to avoid photo-degradation. Samples were carried to the laboratory in Barcelona and analyzed within 4 h. Due to adverse weather conditions, a few months were not sampled during the four-year period.

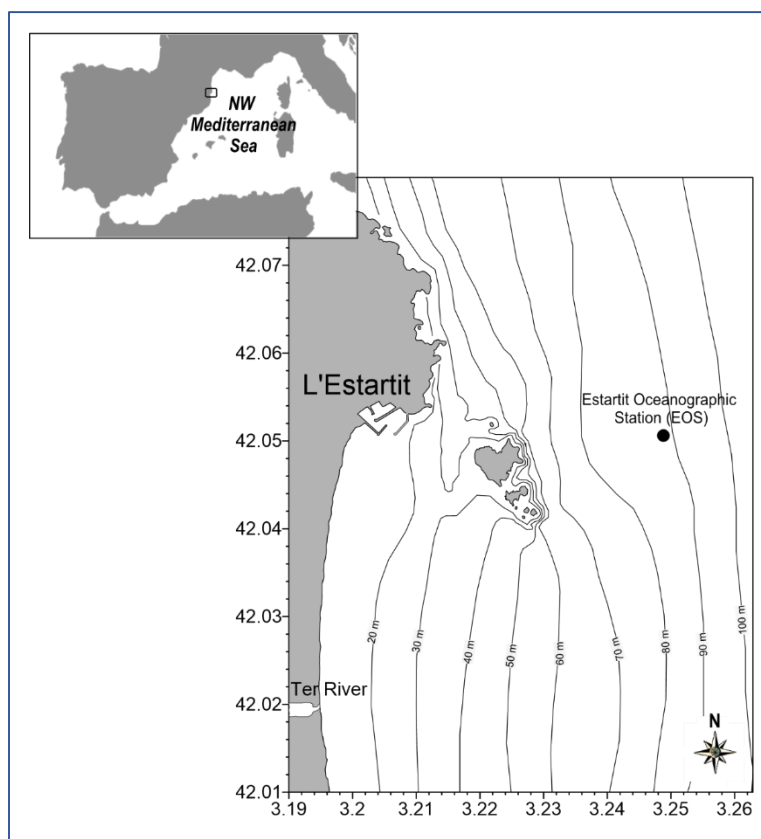


**Figure 5.1.** Map of the study area. The Estartit Oceanographic Station (EOS) is represented by a black circle.

### 5.2.2. – Variables measured

Monthly measurements of salinity and temperature were carried out *in situ* with a CTD probe (model SD204, SAIV A/S). Additional, daily measurements of temperature were performed using calibrated Richter and Weise reversing thermometers. Chlorophyll a (Chl a) was measured by filtering 100 mL of seawater through a glass fiber filter (GF/F Whatman) and following the methodology used by Welschmeyer (1994). The filter was immersed in acetone solution (90%, v/v) in the dark at 4 °C for 24 h. Fluorescence signal at 670 nm was measured with a fluorometer (Turner Designs).

Samples for inorganic nutrient, nitrate ( $\text{NO}_3^-$ ), phosphate ( $\text{PO}_4^{3-}$ ) and silicate ( $\text{SiO}_2$ ), were collected in 15 mL polyethylene vials and kept frozen (-20 °C) until analysis. The concentrations were determined by standard continuous flow analysis with colorimetric detection (Hansen & Grasshoff

1983) using a Bran + Luebbe autoanalyser. Precisions were  $\pm 0.01 \mu\text{mol kg}^{-1} \text{NO}_3^-$ ,  $\pm 0.02 \mu\text{mol kg}^{-1} \text{PO}_4^{3-}$ , and  $\pm 0.01 \mu\text{mol kg}^{-1} \text{SiO}_2$ .

DOC samples were collected in 10 mL precombusted (450 °C, 24 h) glass ampoules. After acidification to pH <2 with 50  $\mu\text{L}$  of 25%  $\text{H}_3\text{PO}_4$ , the ampoules were heat-sealed and stored in the dark at 4 °C until analysis. Measurements were carried out using a Shimadzu TOC-CSV organic carbon analyzer. Per replicate, three to five injections of 150  $\mu\text{L}$  were performed. DOC concentration contained in each replicate was calculated by subtracting a Milli-Q blank and dividing by the slope of a daily standard curve made from potassium hydrogen phthalate. All samples were checked against deep Sargasso Sea reference water (2600 m).

The fluorescent properties of DOM were measured using a Perkin Elmer LS55 luminescence spectrometer equipped with a xenon discharge lamp equivalent to 20 kW for an 8- $\mu\text{s}$  duration. A red sensitive R928 photodiode multiplier worked as a reference detector. Single measurements and emission excitation matrices (EEMs) were performed. Measurements were performed in a 1 cm quartz fluorescence cell at a constant room temperature. Following Coble (1996), the Ex/Em wavelengths used for the single point measurements were: Ex/Em 320 nm/410 nm (peak-M) and Ex/Em 340 nm/440 nm (peak-C) as indicators of marine and terrestrial humic-like substances, respectively. The running instructions for the EEM data acquisition were set as follows: scan speed at 250 nm  $\text{min}^{-1}$ , slit widths for the excitation and emission wavelengths at 10 nm. The fluorescence intensities were expressed in quinine sulfate units (QSU) by calibrating the instrument at Ex/Em: 350 nm/450 nm against a quinine sulfate dehydrate standard made up in 0.05 mol  $\text{L}^{-1}$  sulfuric acid.

The humification index (HIX) was calculated according to Zsolnay (2003) as the ratio between the areas under the emission spectra of 435-480 nm and 300-345 nm, recorded at an excitation of 254 nm. Also, the biological index (BIX) was estimated as the ratio of fluorescence intensities at 380 nm and 430 nm, using 308 nm as excitation wavelength (Huguet *et al.*, 2009).

### **5.2.3. – Meteorological data**

Precipitation data was collected from a meteorological station (supported by the Spanish Agencia Estatal de Meteorología, AEMET) located at the seafront of the l'Estartit village (0 m above the sea level). On the other hand, wind data was collected from a different meteorological station (also supported by AEMET) situated on the top of Roca Maura hill (228 m above sea level, behind l'Estartit village), to avoid buildings interferences.

### **5.2.4. – Graphical tools and Statistical analyses**

Depth-profile plots were represented using the software Ocean Data View 4.7.6 (ODV, Schlitzer, 2016). Wind rose plots were drawn using the software WRPLOT View™ 7.0 (Lakes

Environmental). All other plots were performed making use of the software Sigma Plot 11.0 (Systat Software Inc.).

The software XLSTAT 2016 (Addinsoft ©) was used to perform the statistical methodologies applied in this work. Man-Kendall tests were applied to find out if the data sets presented seasonality. Pearson coefficient was calculated to ascertain possible correlations between pairs of variables (p-values were set to  $p < 0.05$  and  $p < 0.01$ ).

## **5.3. - Results**

### **5.3.1. – Physical monitoring**

#### **5.3.1.1. – Temperature**

The temporal evolution of the temperature in the water column is represented in [Figure 5.2a](#). Sampling frequency and depths were more profuse for temperature than for any other variable analyzed as we included the daily monitoring program conducted at EOS by J. Pascual. In general, no stratification of the water column was detected from January to April, thus favoring a complete vertical mixing. The 'reflux arrow' symbols ([Figure 5.2](#)) mark these periods exhibiting the presence of a uniform water body at EOS. During these cold periods, the temperature in the water column oscillated from 12 to 14 °C in the whole 4-year period studied. Later in the year, in parallel to the increase of light hours per day, the seawater became warmer. This phenomenon led to the formation of less dense, upper water layers, thus stratifying the water column. From the beginning of May to the end of June, water temperature increased up to 20 °C and the thermocline was established around 50 m deep in 2011, 2012 and 2014 and around 40 m deep in 2013. The summer period (July, August and mid-September) exhibited surface temperatures higher than 23 °C. Over the study period, an intrusion of cold water from the deep layers was also detected, mainly during the months of July and August. The 'up arrow' symbols indicate the sub-periods when these surge features were detected ([Figure 5.2](#)). Normally, the water stratification lasted until the end of October, and from then to end of December the whole water column presented a temperature around 17.5 °C. This situation contrasts with the temperatures observed in the whole water column during the months of November and December of 2012 and 2013 (below 15 °C).

#### **5.3.1.2. – Salinity**

In contrast to temperature, salinity did not show a clear seasonal variability ([Figure 5.2b](#)). Low values (<37.5) were found in April-May 2011, May-June 2012, March-April and August-September 2013, usually detected in the first 20 m of the water column. The only exception was the feature of 2011, when the decrease in salinity was observed in the whole water column. On the other hand, high salinity values (>38) were found at the bottom layer (80 m) in March and April 2011 and July-September 2013, in the whole water column in March and April 2012, and at 50 and 80 m deep in July-September 2012.

## **5.3.2. – Inorganic nutrients at the study site**

### **5.3.2.1. – Nitrate**

Nitrate concentrations, ranged from 0.25 to 5.25  $\mu\text{mol L}^{-1}$  (**Figure 5.2c**) during the 4-year sampling period. High levels of nitrate were mainly present when temperatures were lower than 15 °C (during the winter season). From January to March, nitrate concentrations were always higher than 1.00  $\mu\text{mol L}^{-1}$  in the entire water column. Each year, when temperatures increased and the stratification progressed (spring season), nitrate concentrations decreased. At surface (<20 m), values were kept down to 0.50-1.00  $\mu\text{mol L}^{-1}$ , but below 20 m deep, concentrations increased as the stratification of the water column disappeared. The lowest levels of nitrate in surface waters were detected in summer (~0.25  $\mu\text{mol L}^{-1}$ ), while at 20 m deep the concentration varied around 0.50 to 0.75  $\mu\text{mol L}^{-1}$ . Nevertheless, just below the thermocline, concentrations were always higher than 1.25  $\mu\text{mol L}^{-1}$ , except for 2013 and 2014, when we found the lowest concentrations. At 80 m deep concentrations were always higher than 1.5  $\mu\text{mol L}^{-1}$ .

### **5.3.2.2. – Phosphate**

The variability of phosphate did not seem to follow any pattern during the studied period (**Figure 5.2d**). Concentrations fluctuated between 0.05 and 0.25  $\mu\text{mol L}^{-1}$  in the water column all year long. In general, increases in salinity brought out elevated concentrations of phosphate (winter-summer 2012 and summer-autumn 2013).

### **5.3.2.3. – Silicate**

Silicate followed a distribution very similar to phosphate, so again, different to nitrate (**Figure 5.2e**). Values in the water column during the four-year monitoring program ranged up to 5.00  $\mu\text{mol L}^{-1}$ . In parallel to phosphate, high variability was mainly found in winter-summer 2012 and in summer-autumn 2013.

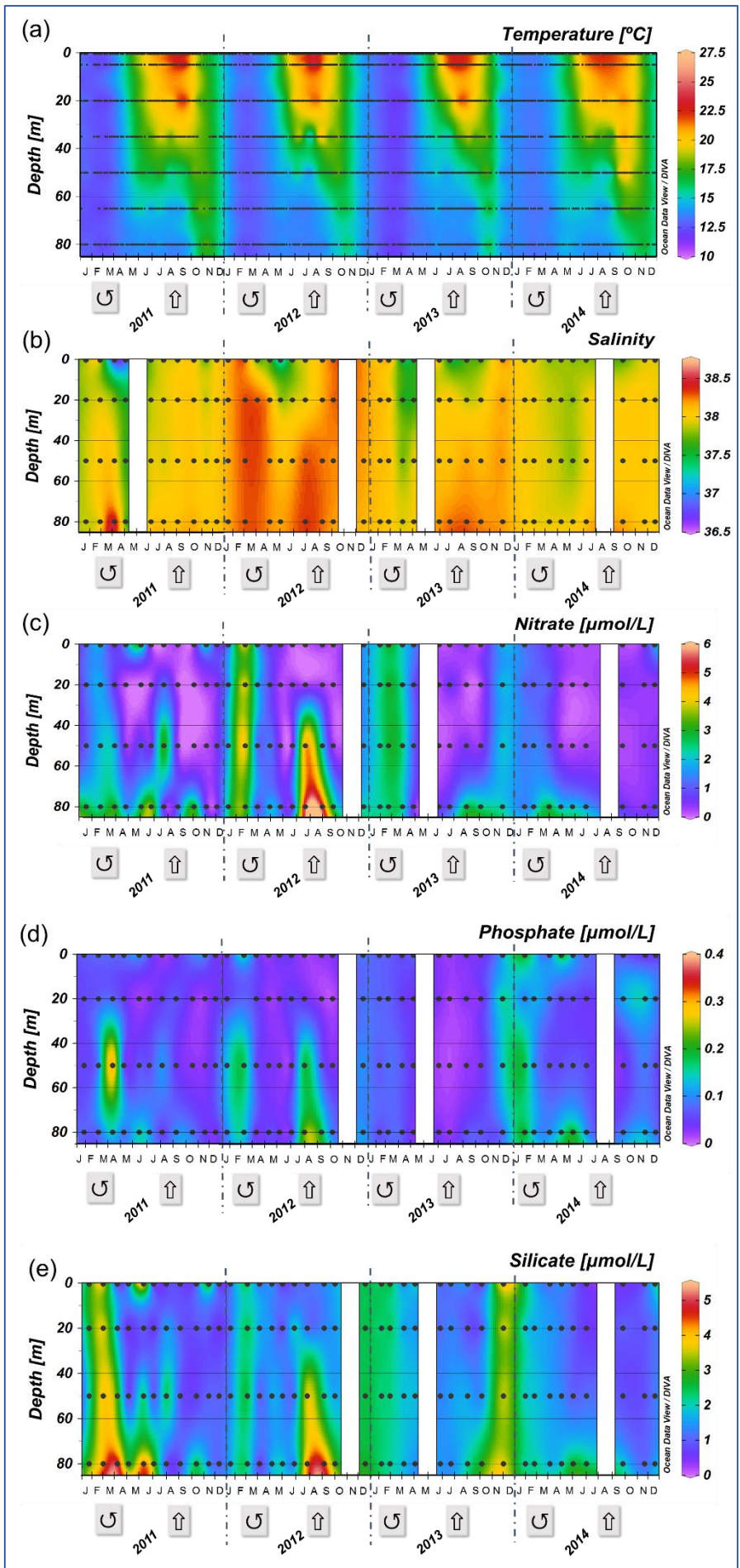


**Figure 5.2.** Water column distribution of a) temperature ( $^{\circ}\text{C}$ ), b) salinity, c) nitrate ( $\mu\text{mol L}^{-1}$ ), d) phosphate ( $\mu\text{mol L}^{-1}$ ) and e) silicate ( $\mu\text{mol L}^{-1}$ ) from January 2011 to December 2014. Black dots represent sampling points. Temperature samplings were performed daily. Blank spaces represent periods when the weather conditions did not allow the sampling. 'Reflux arrow' symbols in the bottom of the plots indicate processes of vertical mixing in the whole water column whereas 'up arrow' symbols indicate upwelling processes detected at the study area.

### 5.3.3. – Biotic variables at the study site

#### 5.3.3.1. – Chlorophyll a

The distribution of Chl a at different depths during the 4-year monitoring program is represented in **Figure 5.3**. A seasonal trend can be appreciated in the upper layers (<20 m). Blooming periods were registered at the end of autumn and at the beginning of spring, when Chl a concentrations reached values from 1.0 to 1.4  $\mu\text{g L}^{-1}$ . In general, during the summer periods, Chl a values were lower than 0.2  $\mu\text{g L}^{-1}$  concurring with the lack of inorganic nutrients. Below 50 m, Chl a concentrations were always lower than 0.6  $\mu\text{g L}^{-1}$ , except for the first bloom episode of 2012.

#### 5.3.3.2. – DOC

Additionally, DOC variability by depth is depicted in **Figure 5.3** as overlapped lines to Chl a concentrations, showing that seasonal trends cannot be extracted from the four-years monitoring program. However, DOC accumulations in surface waters were frequently detected at the end of each summer. Furthermore, DOC concentrations (>90  $\mu\text{mol L}^{-1}$ ) were found in bottom waters in many of the samplings.

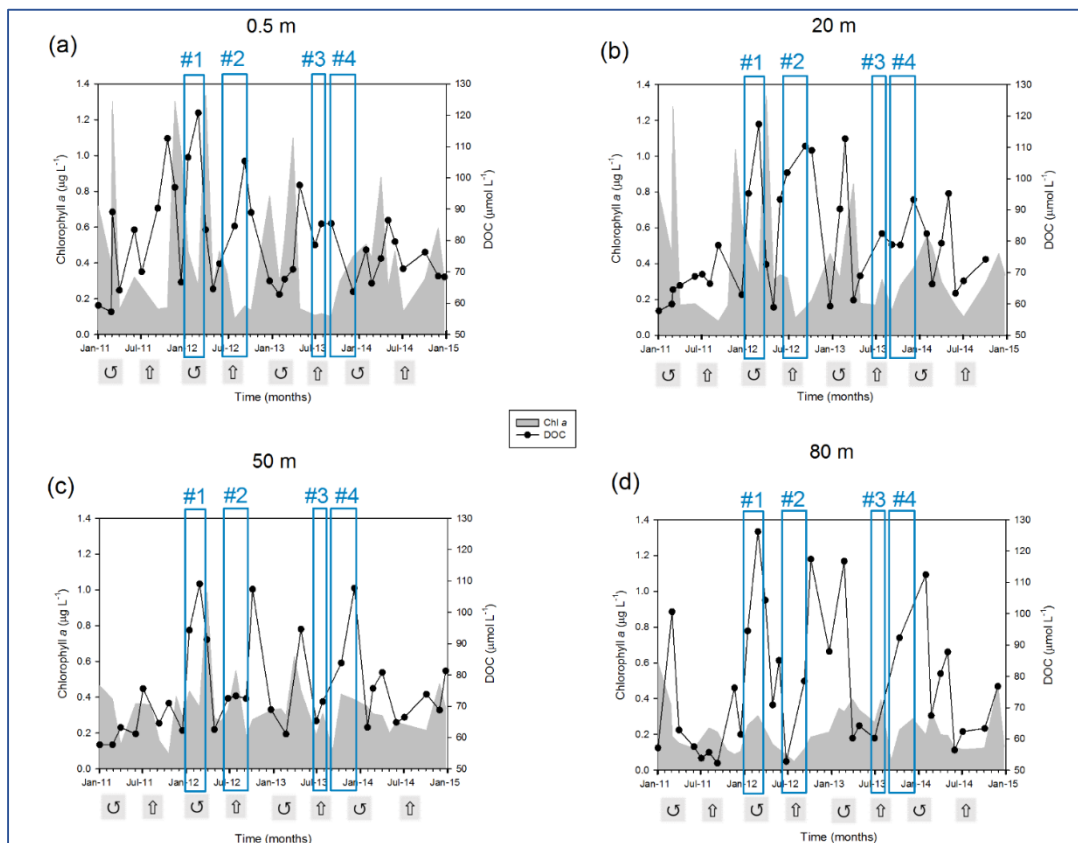


**Figure 5.3.** Chlorophyll a (in  $\mu\text{g L}^{-1}$ , solid grey area) overlapped to DOC (in  $\mu\text{mol L}^{-1}$ , black dots) at a) 0.5 m, b) 20 m, c) 50 m and d) 80 m deep during the four-years study period. Blue rectangles indicate the occurrence of different wind events. 'Reflux arrow' symbols and 'up arrow' symbols below the plots represent processes of vertical mixing and upwelling processes, respectively.

### 5.3.4. – Optically-active DOM fractions

#### 5.3.4.1. – Humic-like compounds

Figure 5.4 represents the ratio between terrestrial (peak-C) and marine (peak-M) humic-like fluorophores, related to salinity values. Overall, seasonal trends were not appreciated, however it appears that the increases in salinity entailed decreases in the humic-like fluorophores ratio. Thus, episodes of high-salinity water intrusion coincided with low peak-C/peak-M ratios, pointing to bottom waters with higher contribution of peak-M fluorophores. Fluctuations in salinity and peak-C/peak-M ratio were higher in shallower layers (<20 m deep). A remarkable feature was detected in July 2013 in surface waters, when salinity and peak-C/peak-M ratio both decreased.

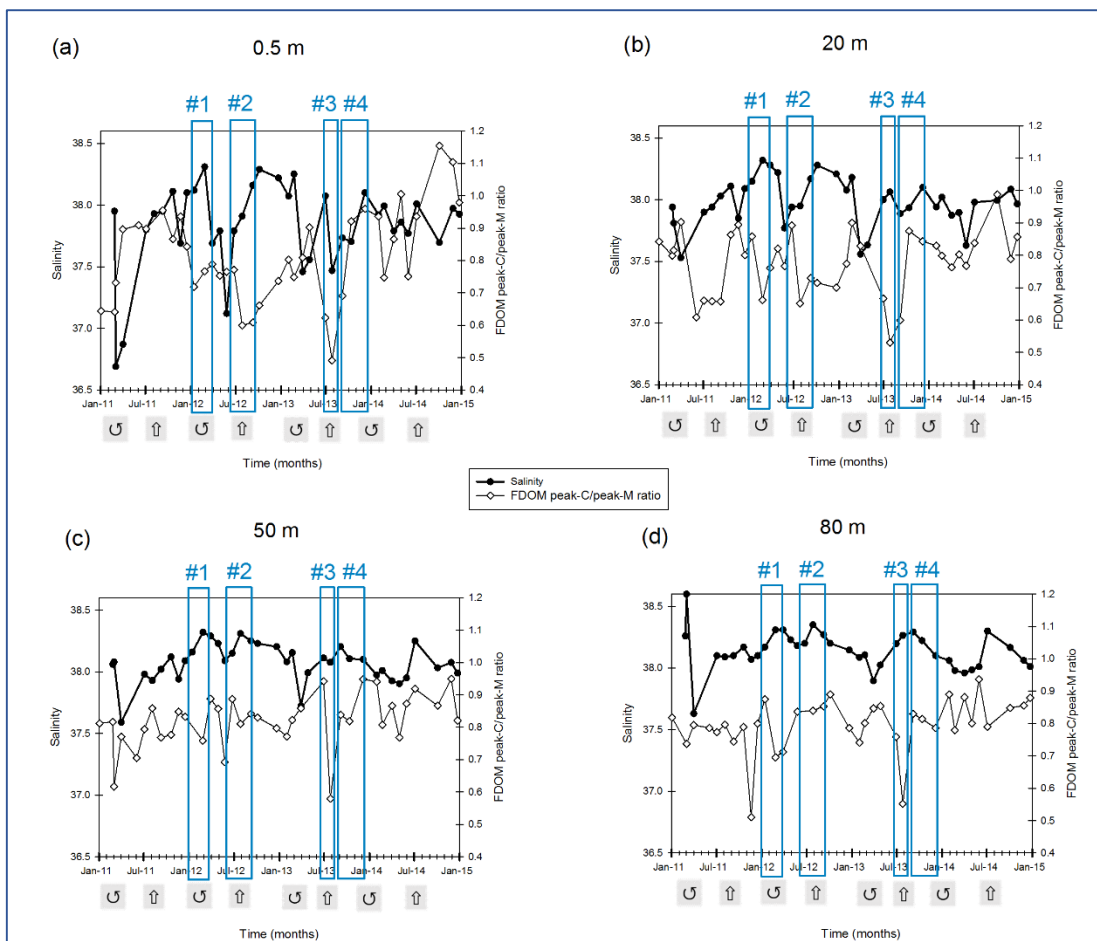
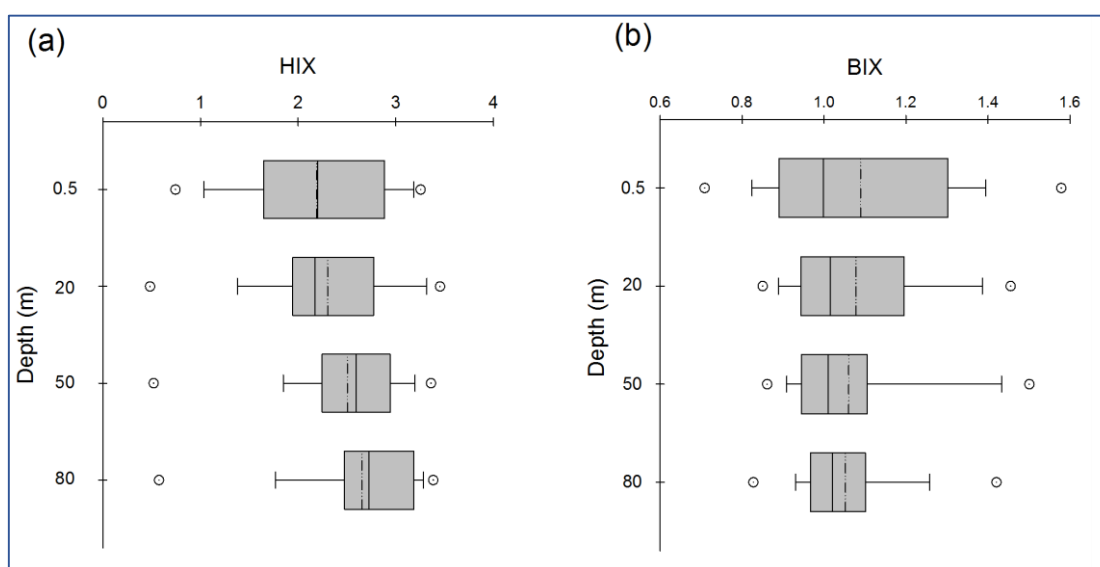


Figure 5.4. Salinity (black dots) and peak-C to peak-M ratio (white dots) overlapped plots at a) 0.5 m, b) 20 m, c) 50 m and d) 80 m deep during the four-years study period. Blue rectangles indicate the occurrence of different wind events. 'Reflux arrow' symbols and 'up arrow' symbols below the plots represent processes of vertical mixing and upwelling processes, respectively.

### 5.3.4.2. – Additional fluorescence indices

Changes in DOM quality during the 4-year monitoring were also assessed by exploring additional optical indices (Figure 5.5). HIX values clearly increase with depth, thus the humification index was higher at the bottom layer (Figure 5.5a). No clear trend was observed for BIX (Figure 5.5b). Regardless the statistical parameters, values of BIX mean (dashed line) and median (solid line) remained almost unaltered, whereas for HIX, these two statistical indicators tended to increase with depth. Both indices presented more variability at the shallower layers. Interestingly, for both indicators, atypical high outliers occurred in July 2013 while unusual low outliers correspond to February 2012.



**Figure 5.5.** Box and whisker plots of a) humification index (HIX) and b) biological index (BIX) for the studied period (4 years) along the water column. White circles represent outliers above and below 95<sup>th</sup> and 5<sup>th</sup> percentiles. HIX and BIX are dimensionless variables.

## 5.4. - Discussion

### 5.4.1. – Lack of seasonality

Since the Mediterranean is a microtidal environment, the variability found in the inner-shelf of the Catalan Sea is predominantly driven by storm-induced fluctuations and forcing mechanisms acting primarily at seasonal scales (Grifoll *et al.*, 2013). The meteorological seasonal cycle of the NW Mediterranean Sea is characterized by dry summers with stable atmospheric conditions, mild temperatures in winter and an elevated number of precipitation events during spring and autumn (Bolaños *et al.*, 2009). However, the application of the Man-Kendall tests to our different data sets revealed that no one of the 10 measured variables presented a monotonic trend during the four-years study ( $p < 0.05$ ).

### 5.4.2. – Environmental parameters and wind forcing

The distribution of the temperature across the water column and through the years showed the following pattern: during the cold season temperatures below 14 °C were homogeneously distributed due to mixing processes, and during summer high temperatures were observed in superficial layers due to stratification processes (Figure 5.2a). Winter temperatures were not significantly different from the range of surface temperatures registered in the NW Mediterranean, between 12-13 °C (Durrieu de Madron *et al.*, 2011). However, we perceived that the establishment of warm upper layers of water did not have the same duration each year. Notably, in 2011 and 2014 the temperature remained warm longer after the summer season than in 2012 or 2013. In addition, 2014 was the warmest of the 4-year study and the temperatures recorded during this year were above the monthly-average temperature of the last forty years (Figure 5.6). The study of Coma *et al.* (2009) reported that the whole water column at this sampling station has been showing a temperature increasing trend since 1974. The same behavior was reported in NW Mediterranean Sea waters at the DYFAMED sampling station (Marty and Chiavérini, 2010) in a study period comprised from 1995 to 2007. The studies conducted by Sánchez-Pérez (2015) at SOLA (coastal) and MOLA (oceanic) stations revealed that temperatures and other variables raised in 2013 and 2014 above the values obtained during the last decade.

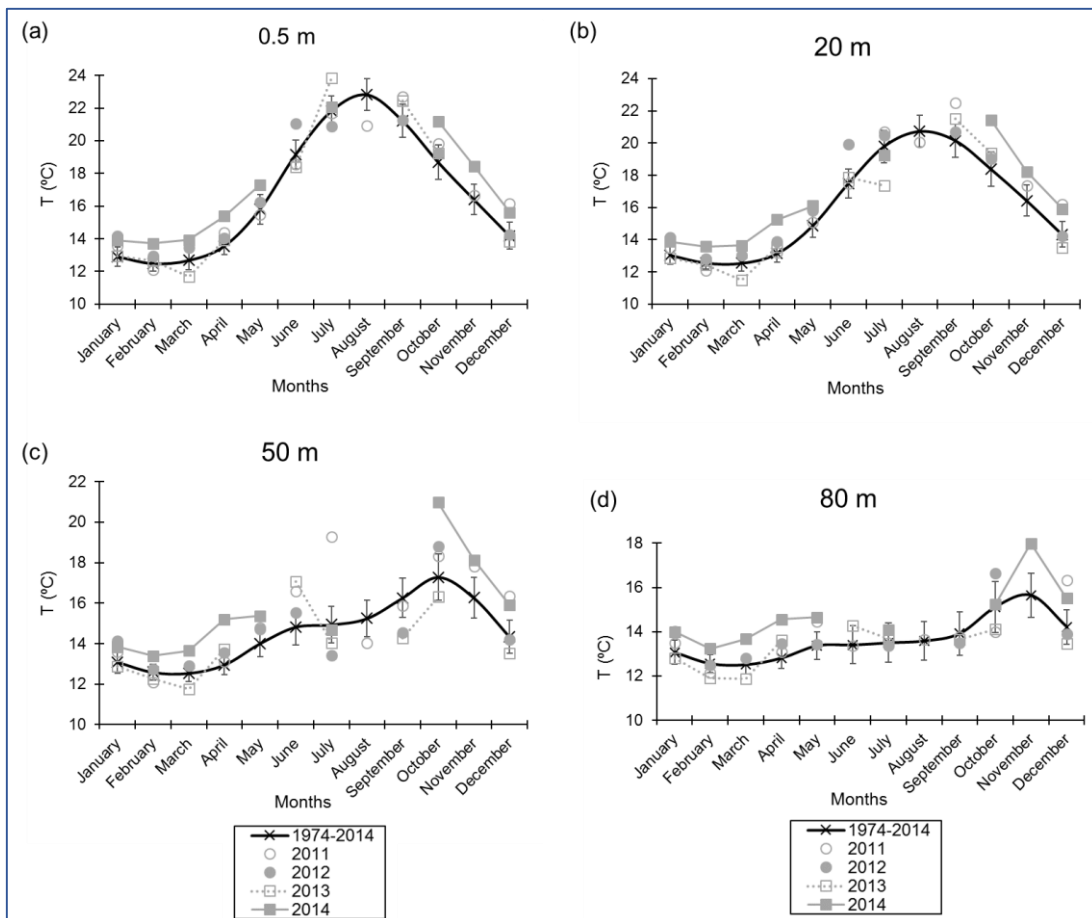


**Figure 5.6.** Temperature plots (in °C) at the different sampling depths a) 0.5 m, b) 20 m, c) 50 m and d) 80 m. Black solid line represents the average temperature from 1974 to 2014 records. The meaning of the symbols meaning is described in the figure legend.

During the 4-year period, bloom episodes (high values of Chl *a*) were linked to surface salinity minimum (**Figure 5.3a** and **Figure 5.4a**). As the Mediterranean is eminently an oligotrophic sea, the coastal systems in the NW basin essentially receive nutrients during stormy periods. This fact was also reported by Guadayol *et al.* (2009) and Romera-Castillo *et al.* (2013) in the bay of Blanes (Spain) and by Sánchez-Pérez (2015) in the bay of Banyuls-sur-mer (France). As previously evidenced in the bay of Blanes (Alonso-Sáez *et al.*, 2008), the summer water stratification prevents the income of new inorganic nutrients to the system, leading to the establishment of oligotrophic conditions. Consequently, in addition to nutrient consumption by microorganisms during the bloom episodes occurring in spring, this fact leads to concentrations almost exhausted at the surface (<20 m) at the EOS site during the warm season. The concentrations of nitrate and phosphate were  $\sim 0.3 \mu\text{mol L}^{-1}$  and  $0.03 \mu\text{mol L}^{-1}$ , respectively, in accordance with the concentrations found by Romera-Castillo *et al.* (2013) in the bay of Blanes. Every year, when the stratification of the water column progressively disappeared, winter deep convection events promoted the replenishment of nutrients, reaching the surface layers (Schroeder *et al.*, 2010).

The analysis of wind data collection revealed that mainly two major wind types occur at EOS (**Figure 5.7**). From late autumn to the end of winter, winds blow from the N and NW (locally known as “Tramuntana” and “Mestral” winds, respectively), whereas winds coming from the S and SW are registered during spring and summer (locally called “Migjorn” and “Garbí” winds, respectively). Guadayol *et al.* (2006) previously assessed that the predominant winds in our coastal section were mainly northerlies (“Tramuntana” winds).

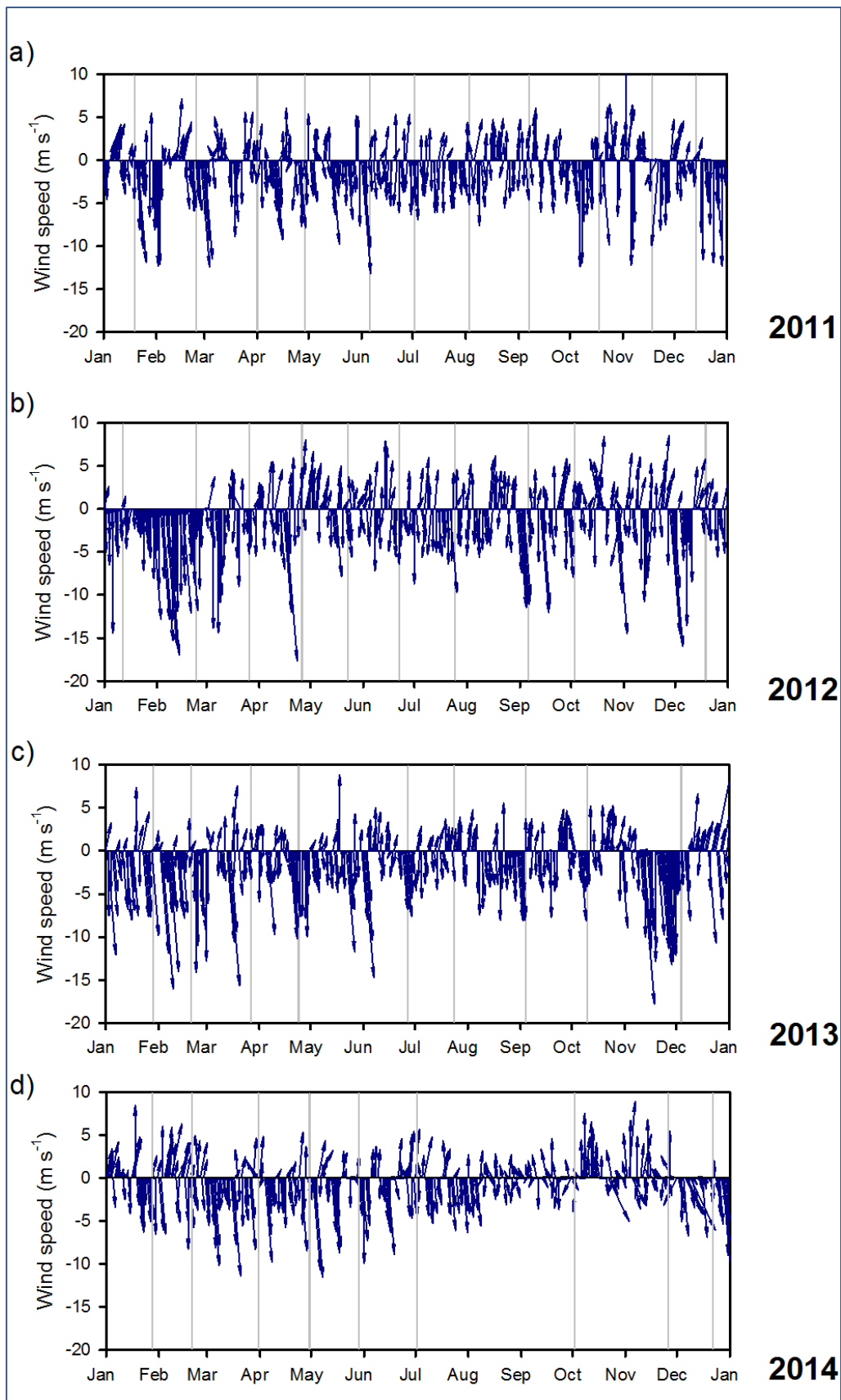


**Figure 5.7.** Wind velocity and direction feather plots of: a) 2011, b) 2012, c) 2013 and d) 2014. Arrows represent the direction towards the winds are blowing. Arrow lengths indicate the velocity reached by the winds. Grey vertical lines represent sampling dates.

Remarkably, wind-related phenomena appeared to be responsible for the different annual periods, depicted by water column mixing/stratification. Rectangles marked as #1, #2, #3 and #4 in **Figures 5.3, 5.4** and **5.10** represent four of the typical events detected at EOS from 2011 to 2014 based on intense wind features (wind speeds of 4-8 m/s blowing ~50% of the time during the 4 days before the sampling date; **Figures 5.8** and **5.9**), which altered the vertical distribution of the studied variables. Generally, during the 4-year monitoring program, when “Tramuntana” winds predominate the water column was mixed (not stratified; **Figure 5.2a**, wind scenario #1, **Figure 5.8a, b**) or slightly stratified (**Figure 5.2a**, wind scenario #4, **Figure 5.9b, c**). On the contrary, S-SW winds usually prevailed during the hotter months of the year, when the water column was highly stratified and oceanic waters were tracked rising from deeper layers (**Figure 5.2a**, wind episodes #2 and #3; **Figure 5.8c** and **Figure 5.9a**).

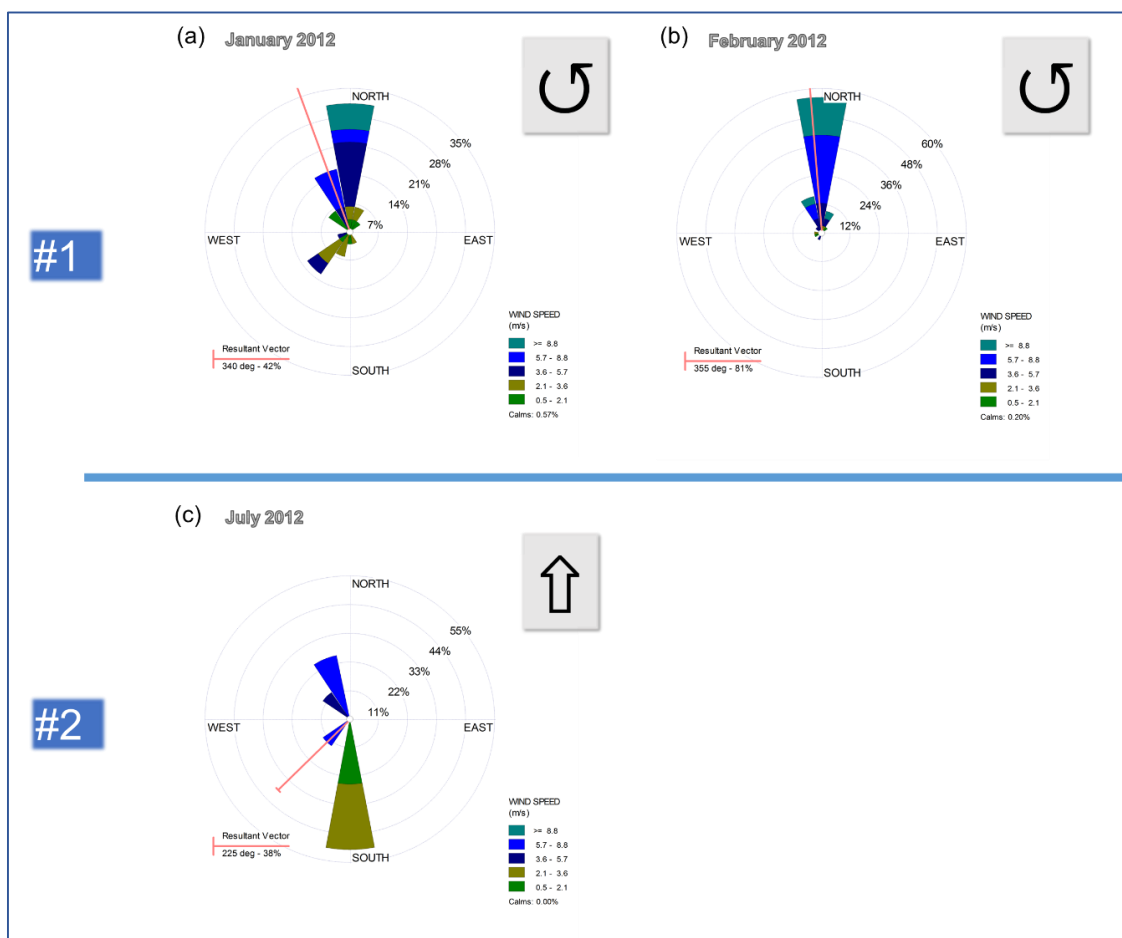


**Figure 5.8.** Wind rose plots (direction and intensity) of winds at the study site representing the 4-days time period previous to samplings: a) January 2012 (part of event #1), b) February 2012 (part of event #1), and c) July 2012 (event #2). The resultant vector of the average wind direction is also indicated. Colour scales represent wind speeds in m/s. ‘Reflux arrow’ and ‘up arrow’ symbols indicate whether the wind event developed a vertical mixing of the water column or an upwelling process.

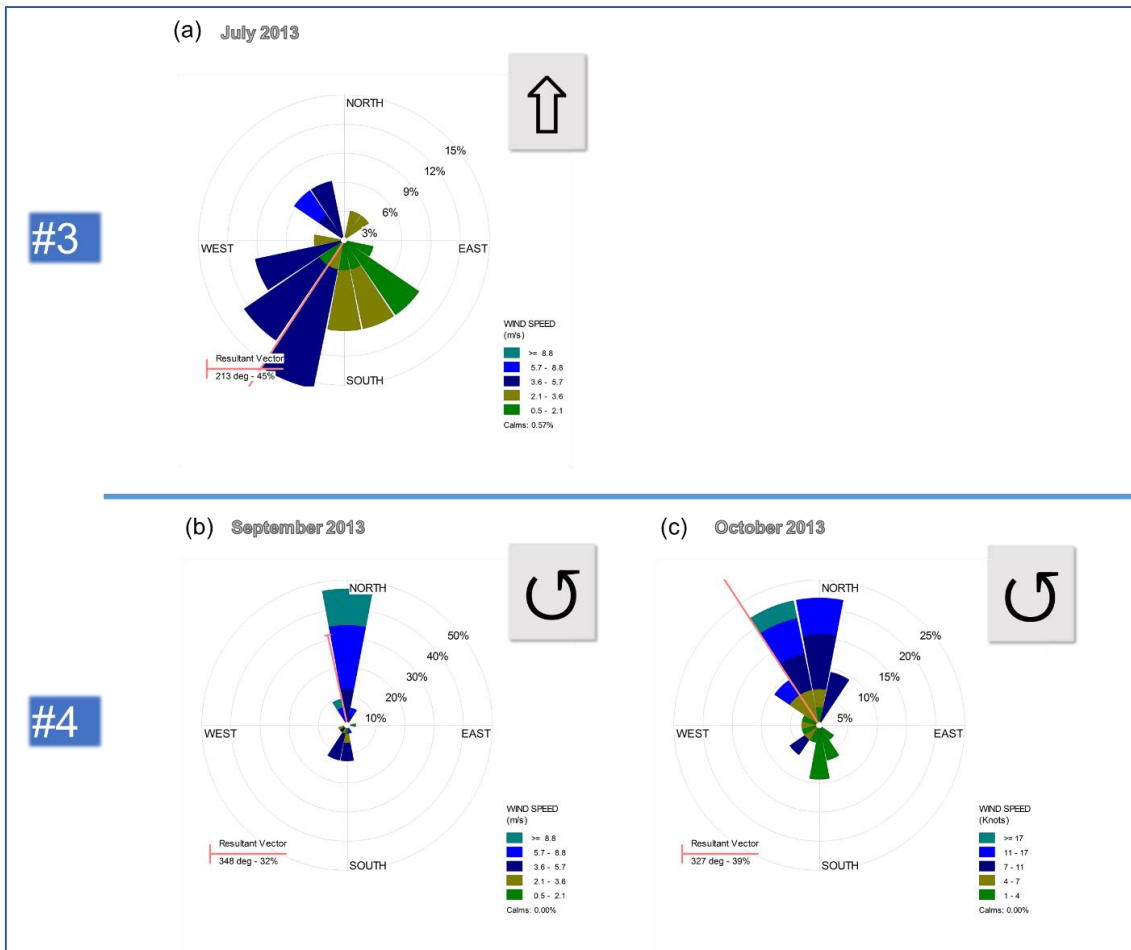


**Figure 5.9.** Wind rose plots (direction and intensity) of winds at the study site representing the 4-days time period previous to samplings: a) July 2013 (event #3), b) October 2013 (part of event #4) and c) October 2013 (part of event #4). The resultant vector of the average wind direction is also indicated. Colour scales represent wind speeds in m/s. 'Reflux arrow' and 'up arrow' symbols indicate whether the wind event developed a vertical mixing of the water column or an upwelling process.

Based in this wind data and *in situ* water measurements, we can outline the surface water movement depending on the direction of the predominant winds (**Figure 5.10**). Therefore, when “Tramuntana” winds (N) blow (**Figure 5.10a**), surface seawater tends to move along in the same direction, however the Coriolis effect (Ekman transport) produces a 90° clockwise gyre, thus making surface waters moving towards the coastline and causing the complete vertical mixing of the whole non-stratified water column. In a related way, when S-SW winds blow from sea to land (**Figure 5.10b**), the surface water moves along in this direction, again the Coriolis effect (Ekman transport) displaces the water body 90° clockwise generating a water movement away from land. If these winds are intense enough, the movement of warm surface water produces the upwelling of cold deep oceanic water that, eventually, breaks the thermocline and reaches the shallower layers, as for example in summer of 2011 (**Figure 5.11**).

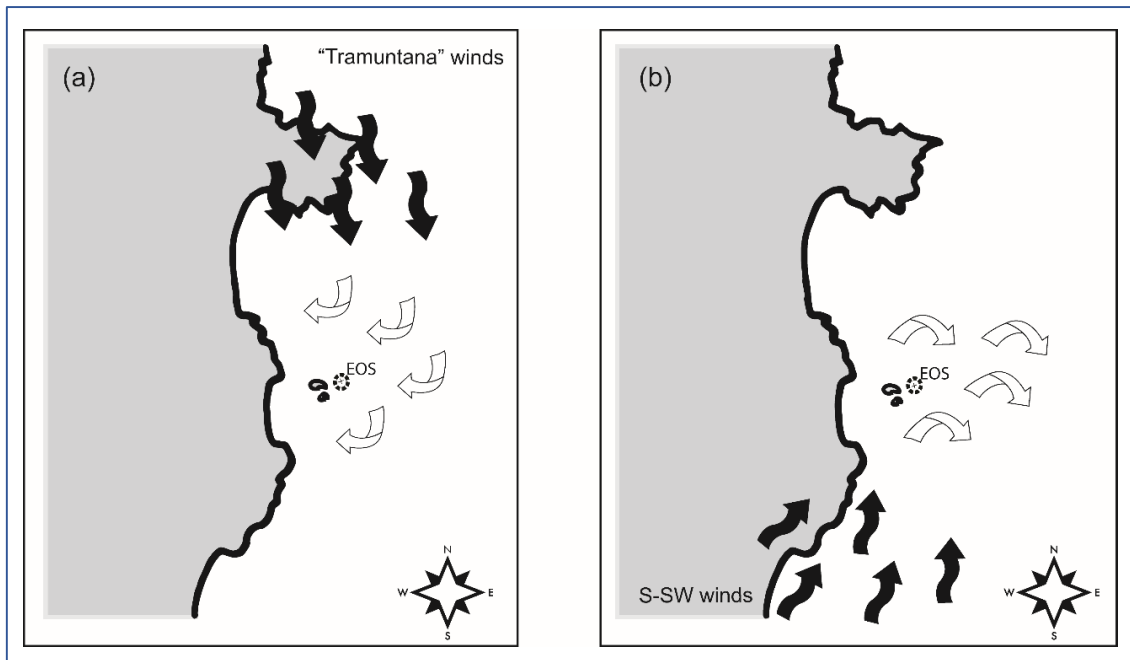


**Figure 5.10.** Aerial scheme of the northern Catalan coast under a) "Tramuntana" wind regime (northerlies) and b) S-SW winds. Black arrows represent wind direction and white arrows indicate the displacement of superficial seawater due to the Coriolis effect (Ekman transport). EOS location is indicated.

During January and February of 2011 and 2014, corresponding with long warm season years, the influence of S-SW winds was more intense than in 2012 and 2013, which seems to cause a reduction of the vertical mixing of inorganic nutrients. Other studies have previously observed that weak winter convections cause an inefficient uplift of nutrients (Marty and Chiavérini, 2010; Sánchez-Pérez, 2015). In addition, decreases in temperature and increases in salinity and nutrients from the bottom to the upper layers are caused by the upwelling events generated by S-SW wind regimes during July and August. Large drops of temperature were detected in three of the four upwelling events at 50 m (red circles; [Figure 5.11](#)), and small decreases in July 2014 at 80 m, in two events at 20 m and in just at one at the surface (orange circles; [Figure 5.11](#)). In summer 2014, Northern winds were more intense than in previous years causing the weakness of the upwelling processes ([Figures 5.2c, 5.7 and 5.11](#)). Overall, nutrients and salinity seem to be coupled regardless of water column conditions, fact reinforced by the significant positive correlations found at 20, 50 and 80 m deep during the 4-year study period ( $p$ -value < 0.05; [Tables 5.1-5.4](#)).

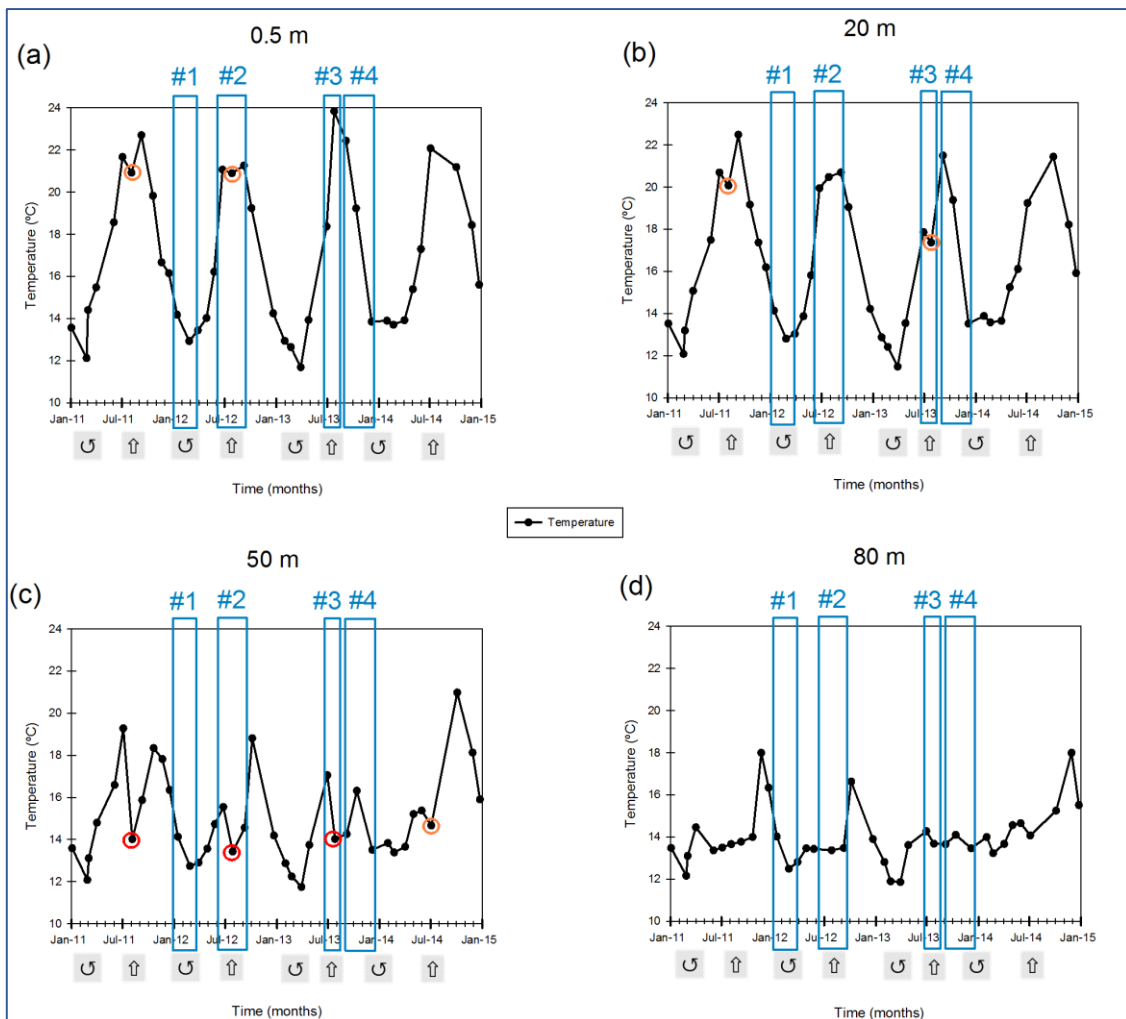


**Figure 5.11.** Temperature values at a) 0.5 m, b) 20 m, c) 50 m and d) 80 m deep during the four-years study period. Units expressed in °C. Blue rectangles indicate the occurrence of distinctive wind events. Red open dots indicate samplings in which a sudden decrease in temperature was detected. 'Reflux arrow' symbols and 'up arrow' symbols below the framed wind events represent processes of vertical mixing and upwelling processes, respectively.

### 5.4.3. – Biogeochemical variables and influence of precipitation events

As defined by Coble (1996) and also identified in other studies (Nieto-Cid *et al.*, 2006; Lønborg *et al.*, 2010; Romera-Castillo *et al.*, 2011a, 2013), peak-M is associated with humic-like compounds produced *in situ*, mainly as by-products of the prokaryote metabolism. On the other hand, peak-C has been defined as a tracer for humic-substances of terrestrial origin (Coble, 1996). Therefore, the proportion of peak-C with respect to peak-M fluorescent signal could be a tracer of the terrestrial vs marine origin of the DOM. During upwelling events, increases in salinity coincided with decreases in peak-C/peak-M ratio, indicating that the humic-like material reaching surface could have been produced *in situ* at deep layers (Figure 5.4). This fact was reinforced with prokaryote abundances: the proportion of HNA bacteria in relation to total bacteria was higher during the upwelling events than in other periods of the year (data not shown).

Concentrations of DOC and FDOM in coastal areas are usually very influenced by terrestrially-derived inputs such as rain events and river drainage (Romera-Castillo *et al.*, 2013; Sánchez-

Pérez *et al.*, 2015). Nevertheless, we could not appreciate this link in our study, perhaps due to the fact that monthly samplings do not have enough resolution to capture the effect of these sporadic events in this area. Indeed, comparing rain episodes and sampling dates, we detected that only a few (~6) samplings were carried out just 1-3 days after significant precipitation events (**Figure 5.12**). However, we observed a DOC accumulation in surface waters by the end of summer (**Figure 5.3**) as mentioned in other studies conducted in the NW Mediterranean (Goutx *et al.*, 2009; Tedetti *et al.*, 2012). Furthermore, we detected that the majority of Chl *a* blooms occurred before rain events. For this reason, we suggest that winter Chl *a* peaks were favored by vertical mixing of the water column propitiated by winds and cooling down process at surface waters rather than by rain events.

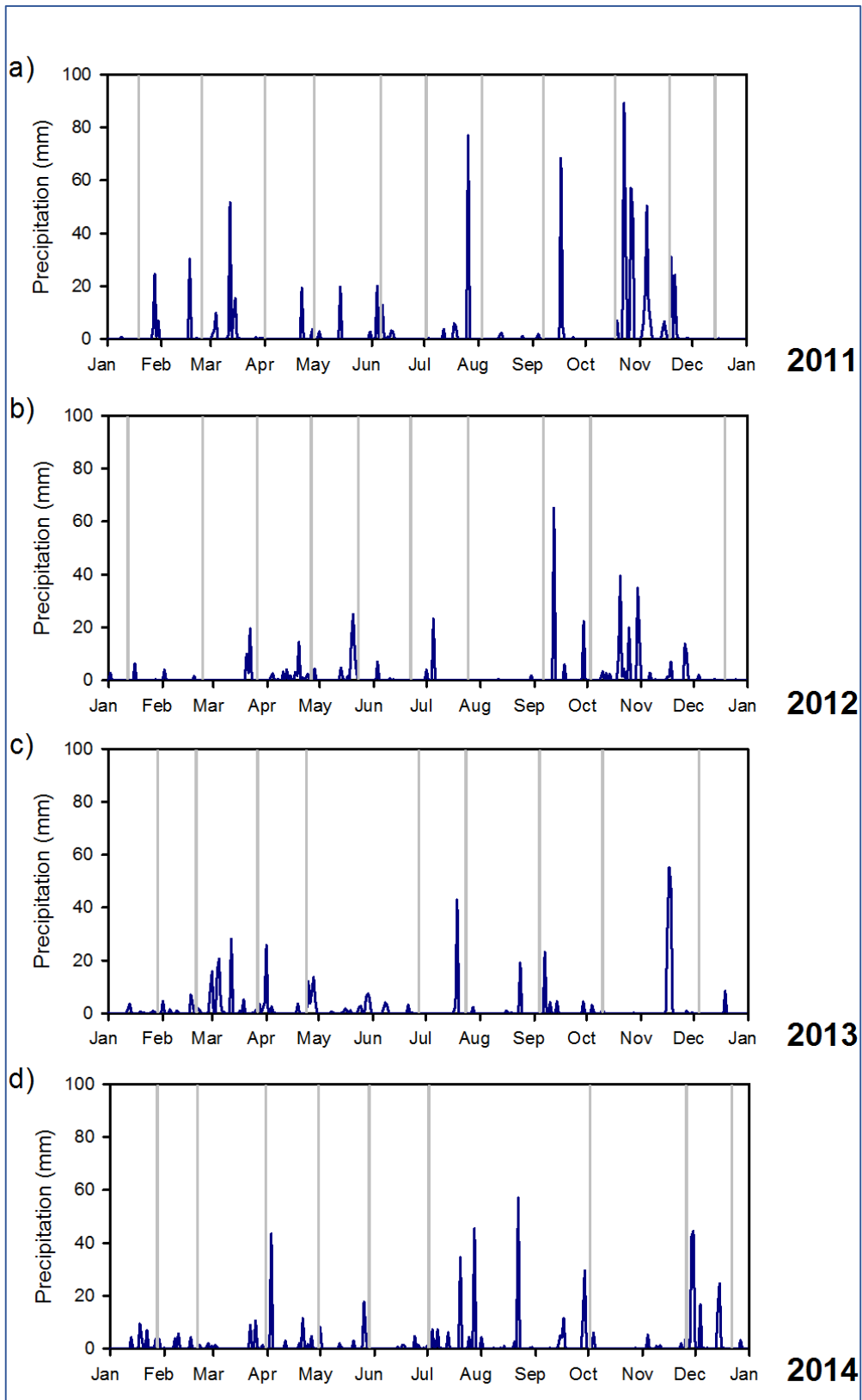


Figure 5.12. L'Estartit village hyetographs of: a) 2011, b) 2012, c) 2013 and d) 2014. Grey vertical lines indicate sampling dates. Units expressed in mm.

It has been documented that terrestrial inputs such as river discharges, can act as sources of humic-like materials, traced by fluorescence at peak-C (Romera-Castillo *et al.*, 2013). In contrast to the results obtained by Romera-Castillo *et al.* (2013), we did not find an accumulation of humic-like material in any of the winter seasons. We suggest that the presence of the Ter river estuary, located southwards, does not influence the seawater properties at the sampling station mainly because of the direction of the Liguro-Provençal current, which flows from north to south.

The hyetographs registered during the four-years sampling period revealed that, in general, storms were sporadic and did not show any annually-repeated pattern (**Figure 5.12**). As mentioned before, only 6 samplings were performed within a few days after significant rain events hit the coast off l'Estartit (**Figure 5.12**): July 2011, May and October 2012, July 2013, and May and October 2014. Nevertheless, the way this rain events influenced the water column was conditioned by the actual wind regime occurring at each sampling:

- On July 2011 and October 2012, "Tramuntana" winds confined surface water towards the coast, avoiding the presence of low-salinity waters at EOS.
- Conversely, in May 2012 and July 2013, low salinity values were detected at the surface. S-SW winds were dominant during these events causing the upwelling of relatively cold, salty and nutrient-rich deep water and the corresponding off-coast surface circulation. However, in July 2013, high intensity of the peak-M fluorescence (low peak-C/peak-M ratio; **Figure 5.4**) was also found in the entire water column, including the surface, and also extreme values for fluorescent HIX and BIX indices (high-end outliers in **Figure 5.5**). This pattern could be due to two different factors depending on the depth: i) at 0.5 m the fluorescent DOM is affected by photodegradation; ii) from 20 m deep and below, the peak-C/peak-M ratio decreased and HIX/BIX increased because of the upwelling of deep oceanic waters.
- Low salinity values were found at the surface in May and October 2014, following the two last rain events sampled during the 4-year period. The wind direction and intensity was very variable during both samplings, without dominance of "Tramuntana" winds, which permitted the freshwater to reach the EOS site. Therefore, the increase in the peak-C/peak-M ratio detected in October 2014 at surface, in parallel to the decrease in salinity (**Figure 5.4a**), was due to the high percentage of terrestrially-derived DOM in the continental inputs.

Regarding the complexity of the fluorescent DOM over time, at surface HIX was affected mainly by photobleaching processes, where values were more variable than at deeper layers (Aparicio *et al.*, 2016). At 50 and 80 m deep, HIX values increased far from the insolation effect mainly because of prokaryotic metabolism (**Figure 5.5a**). In accordance to previous works (Vacher, 2004; Parlanti *et al.*, 2006; Huguet *et al.*, 2009), BIX values (mostly higher than 1.0; **Figure 5.5b**) indicated that the source of the DOM was predominantly *in situ* bacterial production. In **Figure 5.5b** it can be appreciated a high variability in surface respect to deeper waters, this can be associated to a higher temporal biological variability in surface waters. Besides, low outliers

identified in winter 2012 for both fluorescence indices were attributed to the water column homogenization during intense 'Tramuntana' winds that drove a decrease in the values.

It is interesting to remark that peak C and peak M correlated significantly ( $p < 0.01$ ) in the entire water column except for the bottom layer (80 m; [Tables 5.1-5.4](#)), where the humic fluorophores were unconnected. In addition, a significant correlation ( $p < 0.05$ ) was found between DOC and nitrate at this depth, together with unusually high DOC concentrations. Considering that 80 m is rather close to the ocean floor at this station (90 m), all these facts could be related with sediment resuspension processes due to the mixing/stratification/upwelling events, however, the relatively low sampling frequency did not allow us to confirm this point.

## **5.5. – Conclusions**

This monitoring program underscores the importance of performing samplings at different depths in coastal and oceanographic stations and also emphasizes the necessity of increasing the sampling frequency to fully study the coupling between environmental variables and all the main meteorological features, specially to assess seasonality and the effect of rain events. Interestingly, although the location of EOS is close to other sampling sites in Blanes (NW Spain) and Banyuls-sur-mer (SE France), this site presented several differences: contrary to these previous studies, land-derived inputs were not representative for the FDOM dynamics, while the interaction with the oceanic seawater played an important role as responsible for the variations of the humic-like DOM. In summer, when the water column is highly stratified, S-SW winds get to displace surface waters off l'Estartit coast and incentive upsurge processes. This upwelling episodes has been identified at EOS as one of the mechanisms to provide a surplus of humic-like material and inorganic nutrients from deep waters. In a related way, during the winter, strong "Tramuntana" winds favor the movement of superficial oceanic water towards the coast, promoting the confinement of the continental inputs towards the coast and to the south and the homogenization of the entire water column.

**Table 5.1.** Pearson correlation coefficients ( $R^2$ ) as a result of multiple correlation tests between variables at 0.5 m deep. Dark grey colored cells indicate  $p$ -values  $\leq 0.01$  while light grey colored cells indicate  $p$ -values  $\leq 0.05$ .

0.5 m Variables	Temp.	Sal.	Chl a	NO <sub>3</sub> <sup>2-</sup>	PO <sub>4</sub> <sup>3-</sup>	SiO <sub>2</sub>	DOC	FDOM Peak-C	FDOM Peak-M	HIX	BIX
Temperature	<b>1</b>										
Salinity	0.1334	<b>1</b>									
Chl a	0.1415	0.0154	<b>1</b>								
NO <sub>3</sub> <sup>2-</sup>	<b>0.4593</b>	0.0269	0.1665	<b>1</b>							
PO <sub>4</sub> <sup>3-</sup>	0.0100	0.1166	0.0311	0.0182	<b>1</b>						
SiO <sub>2</sub>	<b>0.2641</b>	0.0888	0.0003	<b>0.6045</b>	0.0003	<b>1</b>					
DOC	0.1555	0.2123	0.0396	0.0033	0.0206	0.1253	<b>1</b>				
FDOM Peak-C	0.0080	0.1753	0.1179	0.0839	0.1122	0.0083	0.0032	<b>1</b>			
FDOM Peak-M	0.0784	<b>0.4321</b>	0.0000	0.0002	0.2052	0.0011	0.0188	<b>0.5685</b>	<b>1</b>		
HIX	<b>0.5468</b>	<b>0.2515</b>	0.2068	<b>0.3504</b>	0.0489	0.1693	0.0790	0.0007	<b>0.2969</b>	<b>1</b>	
BIX	<b>0.3716</b>	<b>0.3677</b>	0.1107	0.0752	0.0781	0.0100	0.0370	0.0065	<b>0.4232</b>	<b>0.7033</b>	<b>1</b>

**Table 5.2.** Pearson correlation coefficients ( $R^2$ ) as a result of multiple correlation tests between variables at 20 m deep. Dark grey colored cells indicate  $p$ -values  $\leq 0.01$  while light grey colored cells indicate  $p$ -values  $\leq 0.05$ .

20 m Variables	Temp.	Sal.	Chl a	NO <sub>3</sub> <sup>2-</sup>	PO <sub>4</sub> <sup>3-</sup>	SiO <sub>2</sub>	DOC	FDOM Peak-C	FDOM Peak-M	HIX	BIX
Temperature	<b>1</b>										
Salinity	0.1325	<b>1</b>									
Chl a	0.1106	0.1267	<b>1</b>								
NO <sub>3</sub> <sup>2-</sup>	<b>0.4593</b>	<b>0.5396</b>	0.0082	<b>1</b>							
PO <sub>4</sub> <sup>3-</sup>	0.2962	<b>0.5132</b>	0.0012	<b>0.7923</b>	<b>1</b>						
SiO <sub>2</sub>	0.2908	0.1811	0.0034	<b>0.4098</b>	0.1687	<b>1</b>					
DOC	0.0820	0.0468	0.0822	0.0636	0.1540	0.0334	<b>1</b>				
FDOM Peak-C	0.0829	0.0531	0.0450	0.2511	<b>0.3589</b>	0.0083	0.2269	<b>1</b>			
FDOM Peak-M	0.1672	0.1350	0.0472	<b>0.4483</b>	<b>0.5556</b>	0.0166	0.1230	<b>0.8979</b>	<b>1</b>		
HIX	0.0687	0.1620	0.0179	0.2218	0.2260	0.0032	0.0013	<b>0.4964</b>	<b>0.5840</b>	<b>1</b>	
BIX	0.2749	0.1688	0.0365	<b>0.6245</b>	<b>0.3575</b>	0.1943	0.0022	0.2220	<b>0.4074</b>	<b>0.4745</b>	<b>1</b>

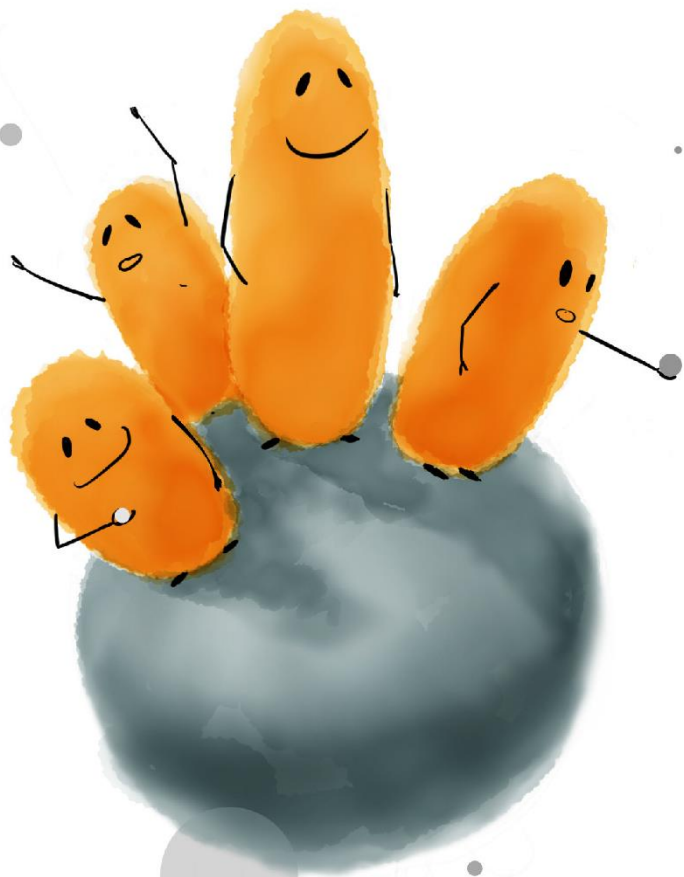
**Table 5.3.** Pearson correlation coefficients ( $R^2$ ) as a result of multiple correlation tests between variables at 50 m deep. Dark grey colored cells indicate  $p$ -values  $\leq 0.01$  while light grey colored cells indicate  $p$ -values  $\leq 0.05$ .

50 m Variables	Temp.	Sal.	Chl a	NO <sub>3</sub> <sup>2-</sup>	PO <sub>4</sub> <sup>3-</sup>	SiO <sub>2</sub>	DOC	FDOM Peak-C	FDOM Peak-M	HIX	BIX
Temperature	<b>1</b>										
Salinity	0.0359	<b>1</b>									
Chl a	0.0795	0.0831	<b>1</b>								
NO <sub>3</sub> <sup>2-</sup>	<b>0.4607</b>	<b>0.4472</b>	0.2123	<b>1</b>							
PO <sub>4</sub> <sup>3-</sup>	<b>0.2820</b>	0.1193	<b>0.2542</b>	<b>0.6042</b>	<b>1</b>						
SiO <sub>2</sub>	<b>0.6342</b>	<b>0.2718</b>	0.2273	<b>0.6459</b>	<b>0.3552</b>	<b>1</b>					
DOC	0.0440	0.1421	0.0070	0.1965	0.0911	0.0063	<b>1</b>				
FDOM Peak-C	0.0040	0.0269	0.0036	0.0259	0.0552	0.0413	0.0088	<b>1</b>			
FDOM Peak-M	0.0096	0.0984	0.0000	0.0790	0.0682	0.0628	0.0068	<b>0.8804</b>	<b>1</b>		
HIX	0.2012	0.0110	0.0712	<b>0.2475</b>	<b>0.2714</b>	<b>0.3212</b>	0.0422	<b>0.3140</b>	<b>0.2965</b>	<b>1</b>	
BIX	0.0955	0.0006	0.0046	0.0026	0.0247	0.0180	0.0057	0.0020	0.0046	0.0058	<b>1</b>

**Table 5.4.** Pearson correlation coefficients ( $R^2$ ) as a result of multiple correlation tests between variables at 80 m deep. Dark grey colored cells indicate  $p$ -values  $\leq 0.01$  while light grey colored cells indicate  $p$ -values  $\leq 0.05$ .

80 m Variables	Temp.	Sal.	Chl a	NO <sub>3</sub> <sup>2-</sup>	PO <sub>4</sub> <sup>3-</sup>	SiO <sub>2</sub>	DOC	FDOM Peak-C	FDOM Peak-M	HIX	BIX
Temperature	<b>1</b>										
Salinity	0.1303	<b>1</b>									
Chl a	<b>0.5750</b>	0.0520	<b>1</b>								
NO <sub>3</sub> <sup>2-</sup>	0.2980	<b>0.4265</b>	0.0092	<b>1</b>							
PO <sub>4</sub> <sup>3-</sup>	0.0772	0.0140	0.0802	<b>0.4774</b>	<b>1</b>						
SiO <sub>2</sub>	0.2447	<b>0.3449</b>	0.0035	<b>0.6489</b>	<b>0.3470</b>	<b>1</b>					
DOC	0.0459	0.2244	0.0034	<b>0.3743</b>	0.1013	0.1311	<b>1</b>				
FDOM Peak-C	0.0152	0.0002	0.0050	0.0390	0.0212	0.1222	0.0691	<b>1</b>			
FDOM Peak-M	0.1519	0.0300	0.0253	0.0253	0.0304	0.0021	0.0861	0.2802	<b>1</b>		
HIX	0.0087	0.1369	0.0435	0.0474	0.0908	0.0857	0.0282	<b>0.3743</b>	0.0016	<b>1</b>	
BIX	0.0080	0.3078	0.0474	0.0000	0.2261	0.0001	0.1800	0.0099	0.2780	0.2936	<b>1</b>

**Chapter 6**  
**Discussion**





## 6. – Discussion

Every chapter of this thesis already contains a section incorporating the specific debate regarding each study. This general discussion aims to provide a global and transversal overview of the results included in the different chapters. To attain this synthesis, we also comment on some additional results and methodological considerations.

### 6.1. – DOM transformations in natural and experimentally controlled conditions

Contrary to what happens with other major reservoirs of carbon on Earth, dissolved organic matter (DOM) is not trapped in an uninhabitable environment. Nevertheless, ocean bacterioplankton that decompose organic matter is surrounded by a pool of organic material that appears to remain unaltered for millennia (Moran *et al.*, 2016). If the capability of prokaryotes to decompose freshly produced DOM is high, why this pool is not completely remineralized in the deep ocean?

Several authors have pointed out different hypotheses to explain the reduced DOM remineralization in deep waters, proposing that the low DOM concentration and the recalcitrant character of the organic material are key factors controlling this reduction (Arrieta *et al.*, 2015; Dittmar, 2015). Yet, during upwelling events, deep-water meets surface layers of the ocean where the lability and the concentration of DOM are, generally, higher. Would these characteristics act as priming effects for DOM remineralization? Without the intention of mimicking the natural scenario, we performed the experiments described in Chapter 2. In surface upwelling scenarios, the sunlight may induce molecular transformations of the DOM and thus affecting the lability degree (Dittmar and Paeng, 2009; Helms *et al.*, 2013; Dainard *et al.*, 2015). In our experiments, to avoid possible interaction-effects between light and microbial DOM transformations, we kept the incubations in dark conditions. By doing so, we observed that the addition of labile DOM fueled the growth rates of prokaryote populations in higher proportion than when an assortment of recalcitrant humic acids was added (**Figure 2.2**). However, the cell-specific production of humic-like FDOM components was highest when humic-precursors were added to the media (**Table 2.4**). In supplementary experiments we found out that increasing recalcitrant material (humic acids) stimulated the prokaryotic growth (**Figure 6.1**). These results are in accordance with those of Arrieta *et al.*, 2015, who examined the response of deep prokaryotic assemblages to experimental additions of different quantities of in situ DOM concentrate, indicating that, not only the structure of the organic compounds but also the concentration, are crucial for microbial growth.

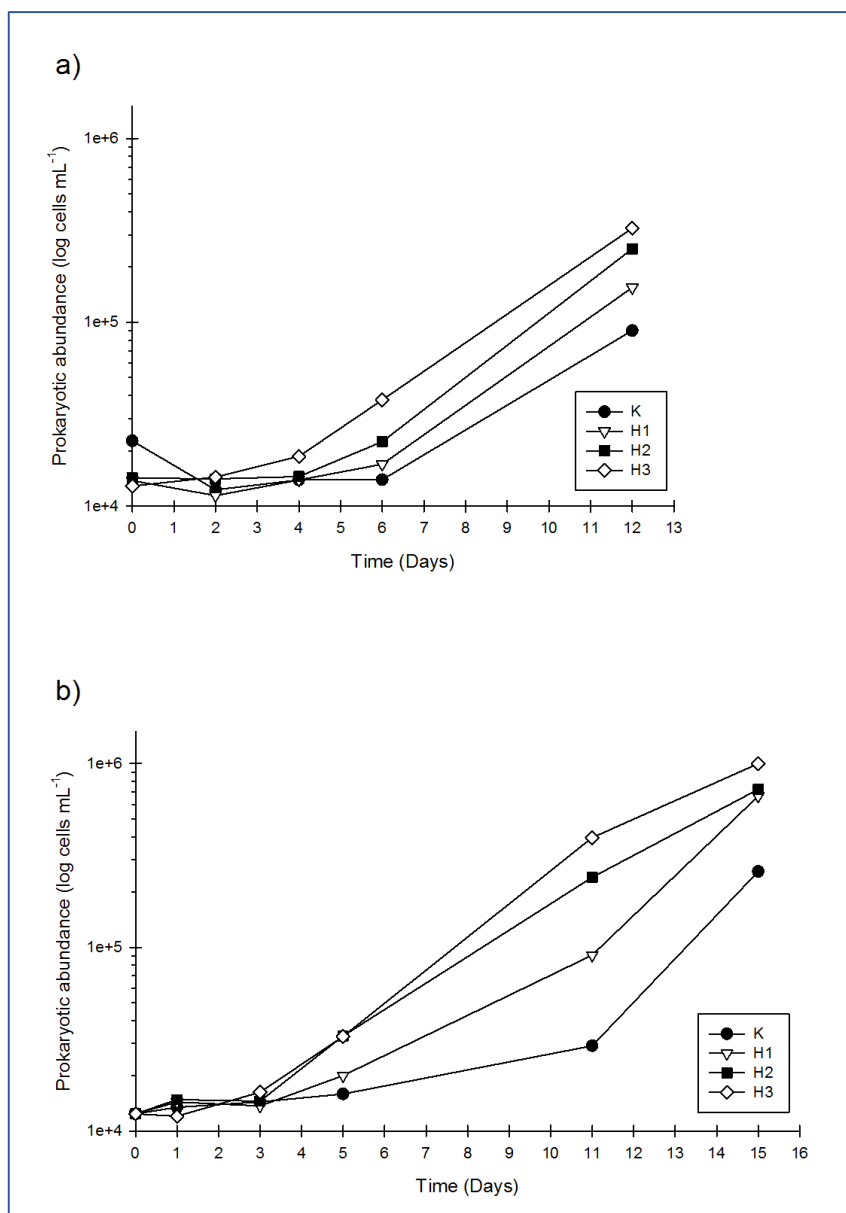


**Figure 6.1.** Prokaryotic abundances reached in additional incubation experiments (a) and (b) performed with Atlantic Ocean water from 3500 m deep. Legend acronyms stand for different background concentrations of Suwannee River humic acids (2R101N): K (control, no addition); H1 ( $30 \mu\text{mol L}^{-1}$ ); H2 ( $60 \mu\text{mol L}^{-1}$ ) and H3 ( $90 \mu\text{mol L}^{-1}$ ).

The interpretation of these findings could be somehow controversial because small quantities of labile compounds might have been also added in both studies. However, additional analyses performed on these experiments using mass spectrometry techniques (FT ICR MS, data not shown) demonstrated that recalcitrant organic compounds (defined in our experiment as molecules that persisted until the end of the experiment) in the control treatments were different from the refractory substances preserved in all the other carbon-enriched conditions. Therefore, when extra sources of carbon (labile or not) were added, most of the apparent recalcitrant compounds were microbially altered. Altogether, we consider that a combination of both factors, dilution and DOM chemical structure, could modulate the remineralization in deep ocean as it has been also postulated by Koch *et al.* (2005) and Dittmar (2015).

At surface layers, the arrival of waters from the deeper strata (with relatively high proportion of recalcitrant material) is quite frequent; we observed it in several occasions during the Estartit Oceanographic Station (EOS) monitoring (Chapter 5). This phenomenon was associated with strong winds blowing from the S-SW. Unfortunately, our sampling frequency did not allow us to follow the subsequent transformations of the raised water. However, in the light of the results discussed here, it is plausible that the availability of fresh labile carbon, as a result of photosynthesis activities, together with the light exposure in surface waters, would favor the remineralization of some of the highly refractory organic compounds from the upwelled waters.

Coastal systems, in addition to be subjected to those natural perturbations mentioned above, are highly influenced by human activities, for instance the increase of inhabitants in these areas give rise to eutrophication conditions. Could the eutrophication alter the recalcitrant degree of DOM? Our experimental studies, combining changes in pH with different availability of inorganic nutrient as stressors, indicated that eutrophication conditions, independently of changes in pH, would increase the proportion of fluorescent organic materials respect to dissolved organic carbon (DOC) production. Considering the fluorescence of DOM (FDOM) as a proxy of recalcitrant material we suggest that eutrophication could alter the functioning of the carbon recycling machinery, strengthening the microbial carbon pump as it is visualized in the flowchart of **Figure 6.2**.

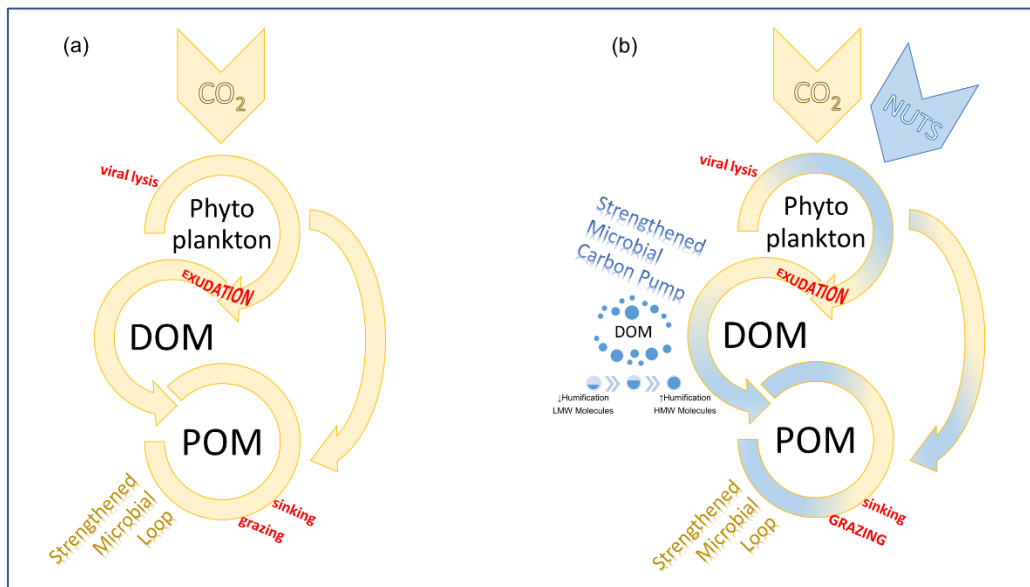


**Figure 6.2.** Flowchart representing the transformations of carbon through the trophic chain when: (a) the system is amended only with CO<sub>2</sub>, and (b) the system is amended with increasing concentrations of nutrients and CO<sub>2</sub>. Processes that mediate the exchanges of the carbon between fractions are indicated in red. In each panel, key processes are written in capital letters, while the less significant are shown in lowercase characters. Figure modified from Riebesell et al. (2013).

## 6.2. – Singularities of the fluorescence measurements

### 6.2.1. – Effect of pH variations on the results from fluorescence analyses

As described in Chapter 3, the influence of pH on the dissociation or protonation of the aromatic constituents of the fluorophores only occurs above or below specific pH values. These structural changes on the fluorescent compounds can result in a shift in the fluorescence emission caused by the alteration of the ground-electronic-states relative separation (Reynolds, 2014). These specific thresholds were not reached in our experiments because the current future projections of acidification do not contemplate that scenario yet. Consequently, our fluorescence measurements should not be affected by these structural transformations. Nevertheless, to evaluate the susceptibility of the peak-T, peak-C and peak-M fluorophores to changes in pH, we analyzed a subset of samples at the pH used in Chapter 3. Since the pH values reached in the winter experiment were 8.28 and 7.77, and 8.1 and 7.5 in summer, four levels of pH were selected to test the possible fluorescence perturbations in seawater: 8.27, 8.04, 7.76 and 7.44. The fluorescence values obtained at each pH are listed in [Table 6.1](#) and the resultant EEMs are depicted in [Figure 6.2](#).

*Table 6.4. Summary of the fluorescence intensities at different pH values studied at each of the four experimental treatments in winter. Fluorescence intensity values are expressed in quinine sulfate units (QSU). The standard deviation represents the variation between two replicates.*

Code	pH value	FDOM peak-T	FDOM peak-C	FDOM peak-M
K	8.27	0.72 ± 0.03	0.74 ± 0.01	0.75 ± 0.02
KA1	8.04	0.71 ± 0.04	0.70 ± 0.02	0.73 ± 0.03
KA2	7.76	0.71 ± 0.01	0.71 ± 0.03	0.70 ± 0.06
KA3	7.44	0.72 ± 0.01	0.73 ± 0.03	0.72 ± 0.01

No significant differences were found among the experimental treatments for any of the fluorophores (unpaired *t*-test; *p*-value < 0.05), confirming that, for the pH range reached in the experiments, all significant changes in fluorescence should be associated to chemical and biological processes instead of methodological artifices.

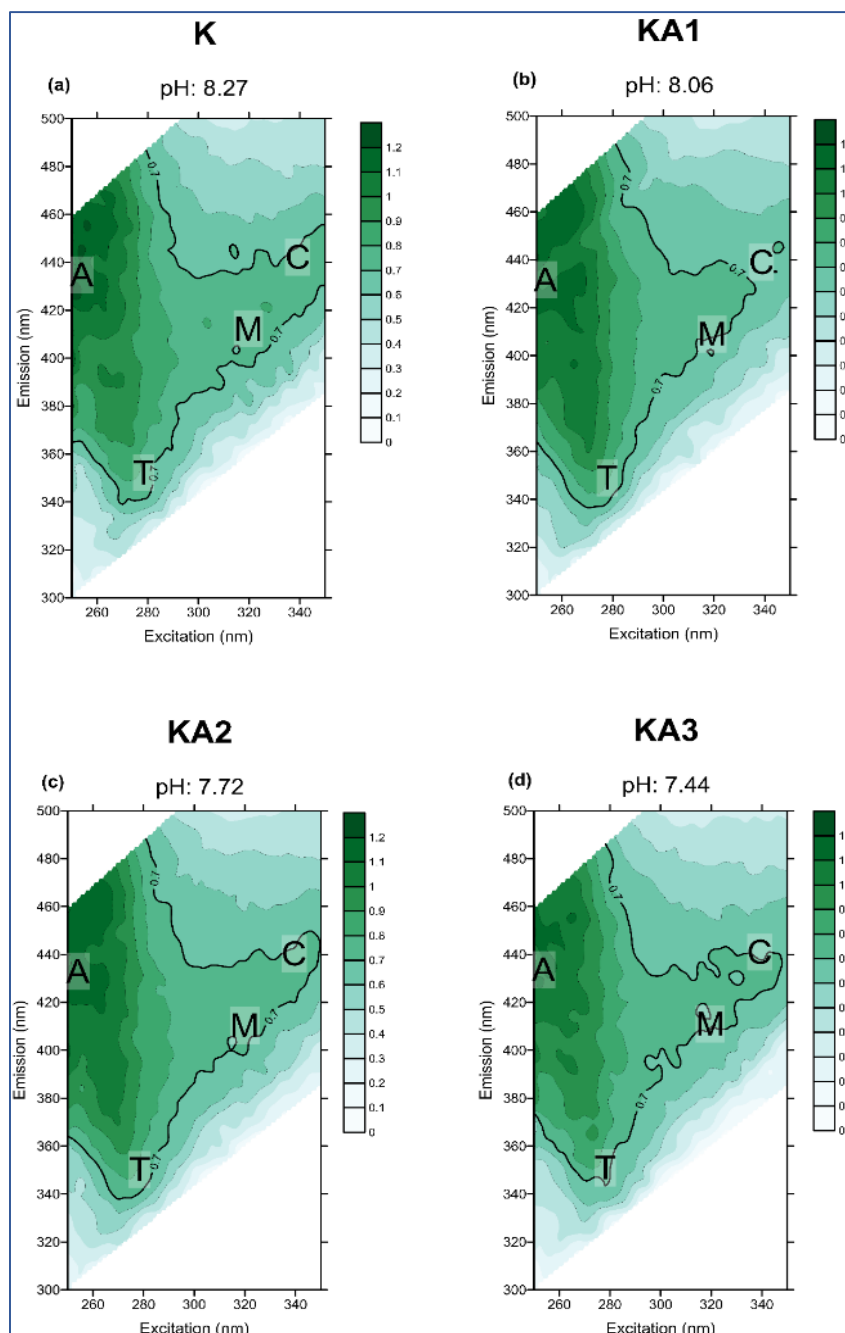


**Figure 6.2.** EEMs showing the fluorescent intensities of the four main fluorophores (A, C, M and T) in experimental treatments at (a) pH = 8.27, (b) pH = 8.06, (c) pH = 7.72 and (d) pH = 7.44. Units expressed in QSU.

## 6.2.2. – Fluorescence units

In Chapter 2 of this thesis, the fluorescence measurements were expressed in Raman units (R.U.) whereas in the rest of the chapters, the results were provided in quinine sulfate units (QSU). The main advantages and disadvantages of each normalization procedure made us opt for one instead of another in each occasion.

For expressing the results in R.U. it is necessary to calibrate the arbitrary fluorescence units (A.U.) given by default by the instrument against the Raman peak area of Milli-Q water sample. When

the A.U. are divided by the Raman peak area of the Milli-Q water blank, the conversion into R.U. is complete. However, the Raman peak area can experience subtle modifications between daily samplings, it is recommended to implement emission scans previously to the sampling analyses in order to account for a proper conversion factor.

Since each instrument can also introduce certain deviances due to manufacturer specifications, in 2009, Lawaetz and Stedmon published a study in which compared the Raman calibration procedure among three different types of spectrofluorometers. They concluded that the normalization procedure to R.U. was universal. Nevertheless, in our experiments we have found that the Raman peak can vary its location depending on the intensity signal of the lamp and its hours of operation. For this reason, while the comparison procedure using R.U. can be universal, we cautiously recommend to use it when the normalization to QSU can not be performed.

Conversely, the normalization to QSU needs the calibration of the spectrofluorometer against a quinine sulfate standard made up in 0.05 mol L<sup>-1</sup> sulfuric acid. The calibration curve obtained with the fluorescence measurements at an Ex/Em 350 nm/ 450 nm of the previous solution, provides a reliable information about possible signal drifts. The use of a calibration curve protocol, favors the reproducibility of this analysis and thus makes feasible the comparison of data among different studies performed elsewhere (Yamashita and Tanoue, 2003; Maie *et al.*, 2012;). Nevertheless, this normalization is based in the fluorescence properties of peak-C. The utilization of chemicals used in this calibration method (e.g. H<sub>2</sub>SO<sub>4</sub>), was one of the arguments that made Lawaetz and Stedmon (2009) proposing the use of the Raman calibration instead of the quinine sulfate approach.

While it is true that each standardization can be applied depending on particular circumstances, a novel normalization protocol should be applied in further studies, the normalized fluorescence intensity units (NFIU). This technique compares the fluorescent intensities of each peak by applying calibration curves with two standard solutions, one for the humic-like components (quinine sulfate) and another for the protein-like substances (tryptophan), as proposed by Nieto-Cid *et al.* (2005).

### **6.2.3. – Data interpretation challenges using PARAFAC**

As explained in Chapter 1, the parallel factor analysis (PARAFAC) decomposes the overlapping fluorescent signals into independent spectra (Stedmon and Bro, 2008; Murphy *et al.*, 2013a). It was initially applied in the field of psychometrics when it was termed canonical decomposition (CANDECOMP; Harshman and Lundy, 1994). Its first application to DOM fluorescence has been relatively recent, in 2003 (Søndergaard *et al.*, 2003; Stedmon *et al.*, 2003). While the technique can be easily applied to a large number of samples regardless of their origin (lakes, rivers soils, coastal, open ocean), we have noticed that the chemical interpretation entails certain difficulty. In this section we examine the pros and cons of using PARAFAC components versus single-point

measurements at the traditional fluorophores (Coble 1996) to characterize the aquatic DOM samples (Table 6.2).

**Table 6.2.** Summary of advantages and disadvantages of PARAFAC components with respect to the traditional fluorophores (Coble, 1996).

PARAFAC vs SINGLE-POINT	
Cons	Pros
Fluorescence data pre-treatment	
Need to achieve the three main assumptions	Allows the inclusion of a high number of samples into the same model
Manually determination of the number of components	
The comparison with components obtained in other studies is sometimes not precise	Opportunity for finding new fluorophores
Correspondence with traditional fluorescent peaks	

### 1. Fluorescence data pre-treatment.

Before applying PARAFAC, a pre-treatment of the fluorescence data is needed depending on the data output. Square matrices are needed to work with the drEEM toolbox in the Matlab® software package. When using the Aqualog FLUOROMAX (J-Y, Horiba®), the data output is ready to export to Matlab®.

### 2. Accomplishment of the main three assumptions.

A successful implementation of a PARAFAC model relies on its three assumptions:

- a) Variability (not two components with identical spectra).
- b) Trilinearity (for each component emission and excitation spectra do not vary and fluorescence increases linearly with concentration).
- c) Additivity (the total signal is due to the linear superposition of a fixed number of components).

According to the previous premises, PARAFAC would not be suitable for calibration procedures, like the quinine-sulfate (QS) standard curves that are necessary to apply in order to check the instrument against a reference material. By the same token, PARAFAC cannot be applied when the number of samples is low. Although the study of Hall and Kenny (2007) identified as much as 5 components with only 18 samples, the consistency of the modelisation highly increases with large data sets.

ℒ **The inclusion of high number of samples is allowed (almost recommended)**

As a chemometric technique, PARAFAC can deal with large data sets. During the validation process, independent halves of a data set are modeled separately. The

model is validated when the same components are found in each half-data set. The use of numerous EEMs is recommended to ensure that the components are in all halves, thus giving consistency to the model. In Chapter 3 of this thesis, PARAFAC was not applied because the number of EEMs performed was considered too low to run a PARAFAC model.

**3. The determination of the number of components must be assigned manually.**

The chemical interpretation of a PARAFAC model relies on the right number of components being specified by the user. When models are under- or over-specified, the number of components are not properly representing the fluorescent moieties present at detectable levels. In these cases, two or more PARAFAC components may be used to represent a single fluorophore often in combination with noise, or components not chemically meaningful may be included.

**4. The comparison to match PARAFAC components is often not precise.**

As can be seen in Table 2.2 (Chapter 2) and also in Table 6.3, in several occasions the fluorescence spectra of components identified in different studies did not perfectly overlap. In this sense, authors must advertise that the attribution is not completely accurate. The existence of the OpenFluor database ([www.openfluor.org](http://www.openfluor.org); Murphy *et al.*, 2014b) facilitates an on-line search for equivalences between components. Currently, OpenFluor identifies as similar spectra those having a Tucker congruence factor exceeding 0.95 on the excitation and emission spectra simultaneously. Nevertheless, it is worth to mention that many fluorophores could have very similar spectra, so identifying similar PARAFAC components in two different studies does not guarantee that the same compounds are responsible in both cases.

In Chapter 5, despite the data set of EOS accounted with more than 100 EEMs, we decided not to include the PARAFAC modelisation. A six-component PARAFAC model was validated with a 99.49% of the variability explained. The five components identified by the PARAFAC model were referred to as E1 – E6 (**Figure 6.3**) and their spectral characteristics were compared to previous studies that detected the same EEM fluorescence regions (**Table 6.3**). Two of the components were mainly of protein origin (E3 and E4), three presented fluorescence properties similar to humic-like compounds (E1, E2 and E5) and one was situated in the fluorescence range of organic pollutants (E6). Although E5 was vaguely mentioned in the literature (Yu *et al.*, 2010; Murphy *et al.*, 2011).

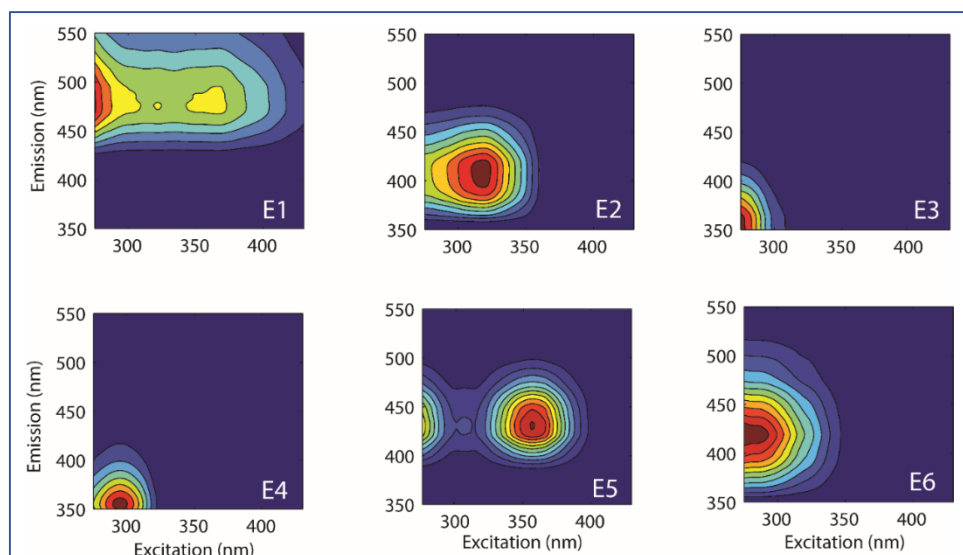


**Figure 6.3.** Fluorescence signatures of the six PARAFAC components (E1 to E6) identified during the monitoring program at EOS.

**Table 6.3.** Characteristics of the six components derived from the PARAFAC model compared with previous studies.

Comp	Ex. max (nm)	Em. max (nm)	Assignment				
			Yamashita <i>et al.</i> , 2010b	Murphy <i>et al.</i> , 2011	Cawley <i>et al.</i> , 2012	Zeri <i>et al.</i> , 2014	Ferretto <i>et al.</i> , 2014
E1	<275 & 365	475		G1* (Terr)		C1* (Hum)	
E2	319	411	C3* (Hum)	G2* (Mar)			
E3	275	358		G7* (a.a.)	C5* (a.a.)	C2* (a.a.)	
E4	295	355	C8 (a.a.)	G6 (a.a.)			Thi
E5	356	431		G3* (w.w.)			
E6	284	420					Pho

\*Component does not exact match. <sup>a</sup>Hum, Terr, Mar, a.a. and w.w. indicate: humic composition, terrestrial-, marine-, protein-like origin and waste water tracer, respectively. <sup>b</sup>Abbreviates for pesticides: Thi (Thiabendazole) and Pho (2-Phenylphenol).

Components E1 and E2 were assimilated to peak-A and peak-C, respectively. As reported in previous studies (Zeri *et al.*, 2014; Dainard *et al.*, 2015) these components were of humic nature, easily photodegraded and ubiquitous to a wide range of environments.

The fluorescence spectra of E3 and E4 were similar to the excitation and emission wavelength range of free or protein bound amino acids. Actually, E3 occupied the area where tryptophan-like compounds fluoresce while E4 was situated –with a slight shift in the emission wavelength- in the zone where tyrosine-like compounds fluoresce. As found in previous studies (Stedmon *et al.*, 2007; Murphy *et al.*, 2011; Tedetti *et al.*, 2012) these components are susceptible to biological degradation and are mainly located in coastal areas but also in open ocean areas around the world.

Interestingly, the work of Ferretto *et al.* (2014) with samples from the Bay of Marseilles (France, NW Mediterranean) registered a fluorescent component in their PARAFAC model that fluoresced at the wavelengths of our E4 but was identified as a pesticide (Thiabendazole, Thi). In addition, component E5, was associated with microbial degradation processes and was identified as a wastewater/nutrient enrichment tracer (Murphy *et al.*, 2011; Yu *et al.*, 2010). Lastly, the fluorescence characteristics of component E6 were perfectly matched with those of the 2-Phenylphenol (Pho) detected in the study of Ferretto *et al.* (2014) in the NW Mediterranean. This organic compound consists of a phenolic hydroxyl group and two linked benzene rings. The assimilations of these last components (E4 to E6) revealed that possible sources for E4 (Thi) and E6 (Pho) were estuaries of rivers whose riverbeds crossed agricultural plains, being common to detect the presence of agricultural fungicides and antibiotics. Since the presence of land-derived inputs was not detected at EOS, we suggested that the identification of these compounds at our sampling site could be due to a misleading comparison procedure performed at the OpenFluor webpage. Furthermore, we brought in question the presence of the E5 component firstly because the lookup in the bibliography was not a straightforward task as it was found only in two studies; and secondly because it was mainly identified as a nutrient enrichment tracer and no presence of eutrophication effect was found at EOS.

#### ↳ **Availability of categorizing the identified spectra.**

Although the lack of correlation between components and peaks made us to change our minds for this study, the identification of component E4 demonstrated the possible strengths that PARAFAC can provide for advancing in the identification of aquatic sciences. Due to its proximity to a protein-like fluorophore, E4 component (Ex/Em 295 nm/395 nm) was identified as an amino acid derived source (Yamashita *et al.*, 2010b; Murphy *et al.*, 2011). Nevertheless, in the study of Ferretto *et al.* (2014) it was associated to a pesticide (Thi). Further investigation into the molecular composition of this material, applying FT ICR MS would be needed to ascertain the nature of this compound.

### **5. Correspondence with traditional fluorescent peaks.**

In addition to the misleading information provided by the E4 to E6 components, a different argument against the use of PARAFAC in this work arose when we performed a correlation between the E3 component and the traditional fluorophore peak-T (**Figure 6.4**). We expected to obtain a significant linear relationship as both measurements provided information of the same fluorescent region, with the same Ex/Em pair of wavelengths. However, a significant linear relationship was not found (**Figure 6.4**). More studies need to be done in this sense, to explain this uncoupling between the two measurements.

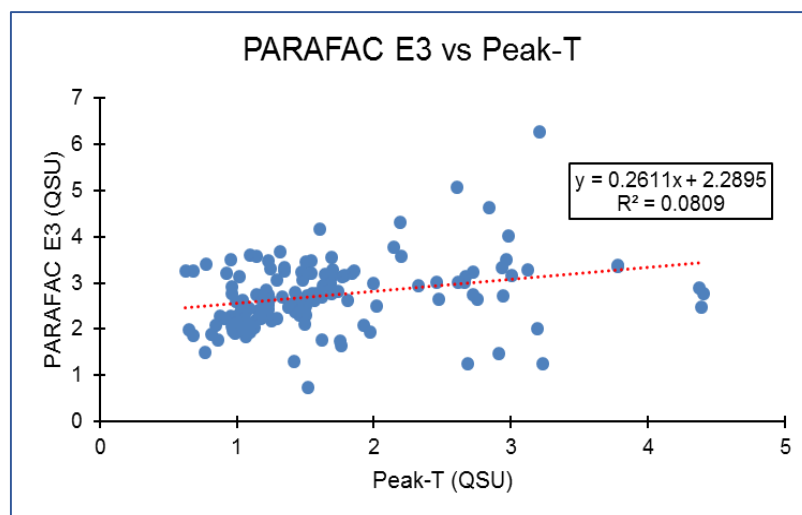


**Figure 6.4.** Correlation between E3 component fluorescence maxima values (Y axis) and peak-T (X axis). Values expressed in quinine sulfate units (QSU).

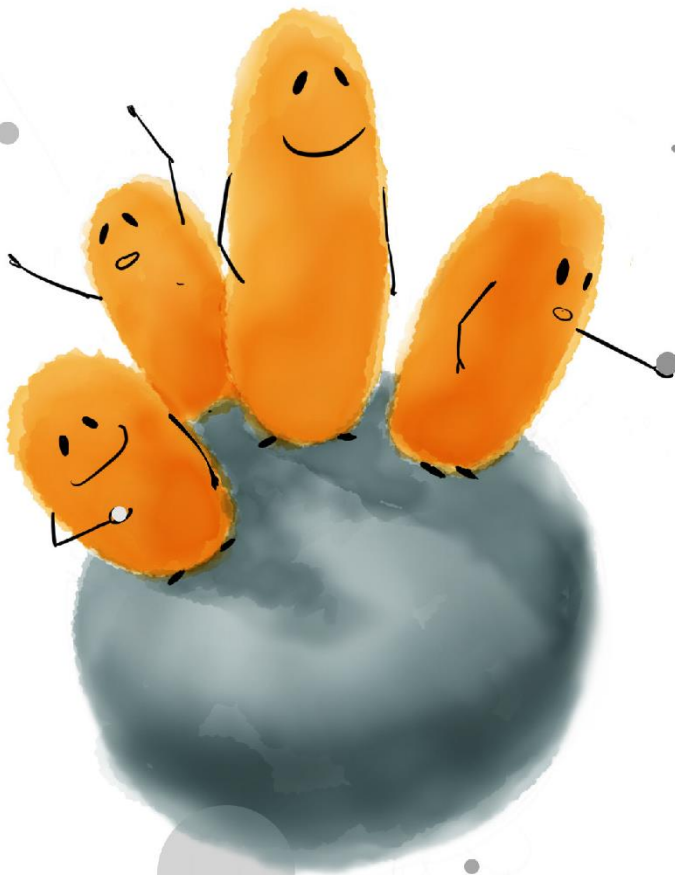
As an exploratory novel technique, PARAFAC is still improving with each new dataset that is modeled. Its ability (and also its strength) to statistically treat a vast amount of data can also become a weakness because it leaves the operator with a limited leeway once the number of components have been chosen. (Murphy *et al.*, 2014a, 2014b), impellers of the PARAFAC methodology, also recognized its limitations in the interpretation of DOM models and its application in a predictive capacity. They characterized PARAFAC as a “developing science necessitating a cautious investigative approach”.

New analyzing tools are emerging to develop pattern recognition methods, capable of detecting and isolating the signal of the different fluorescing moieties of DOM in a given sample. The ‘Self-Organising Maps’ technique (SOM) is one of them. SOM is an artificial neural network algorithm capable of recognizing patterns in complex data sets due to its unsupervised self-learning capacity. Although it has been increasingly used within analytical chemistry in recent years (Bieroza *et al.*, 2009) it has not been until now that SOM has been used to analyze EEM data sets (Bieroza *et al.*, 2012; Brereton, 2012). The recent work of Ejarque-González and Butturini (2014) analyzed a large and heterogeneous data set of riverine EEMs using SOM instead of PARAFAC. They relied on the robustness of SOM because of the presence of outlier samples. Thus, samples with very distinct features were discerned while having little effect on the ordination and classification of the global set.



# Chapter 7

## Conclusions





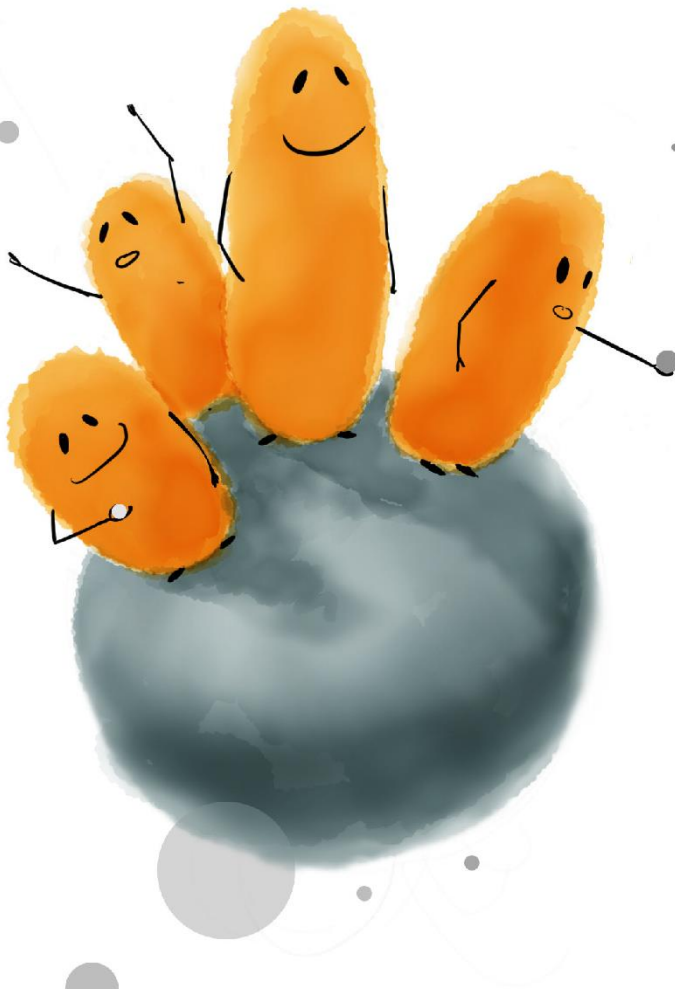
## Conclusions

The main conclusions extracted from this dissertation are the following:

1. The diversity and quantity of DOM reaching the deep ocean influence the posterior respiration by marine prokaryotes. The influx of extra humic-like substances (precursors) to the bottom layers enhances prokaryote metabolic pathways generating more humic-like substances. Whereas, the addition of labile compounds, including a mixture of essential amino acids, favors remineralization processes, reducing the sequestration of organic carbon in the deep ocean.
2. The acidification levels expected for the next century in the oceans will not affect the quality of the DOM pool in Mediterranean coastal waters. In contrast, the predicted ocean eutrophication is expected to influence the microbial communities, favoring metabolic processes that transform DOM into more recalcitrant material.
3. Acidification will stimulate the growth of phototrophic pico- and nanoeukaryotes. The prokaryote community was positively affected by acidification during summer but no clear effects were observed during winter. The impact of acidification on plankton communities is more evident and significant when the background concentration of inorganic nutrients of the media is low.
4. Wind regimes strongly influence the dynamics of DOM in the entire water column at EOS. In winter, "Tramuntana" winds (N) favor the movement of surface seawater towards the coast promoting the homogenization of the inorganic and organic nutrients concentration along the water column. In summer, the intensity of southerly winds (S-SW) displaces surface waters through the open ocean, stimulating the upwelling of deep seawater and favoring the stratification and eventual breakage of the thermocline. The concentration of inorganic nutrients and the ratio of marine respect to terrestrial humic-like fluorescence (peak-M/peak-C) increase upwards in the water column because of these processes.
5. Outputs from the PARAFAC modelisation must be interpreted carefully and, as far as possible, contrasted with another data analysis. Single-point measurements (traditional A, C, M and T fluorophores), as well as new statistical approaches (Self-Organising Maps, SOM) can provide useful information in this context.



# Cited Literature





## Literature cited

- Allgaier, M., Riebesell, U., Vogt, M., Thyrraug, R., and Grossart, H.P., 2008. Coupling of heterotrophic bacteria to phytoplankton bloom development at different pCO<sub>2</sub> levels: a mesocosm study. *Biogeosciences*, 5: 1007-1022.
- Alonso-Sáez, L., Vázquez-Domínguez, E., Cardelús, C., Pinhassi, J., Sala, M.M., Lekunberri, I., Balagué, V., Vila-Costa, M., Unrein, F., Massana, R., Simó, R., Gasol, J.M., 2008. Factors controlling the year-round variability in carbon flux through bacteria in a coastal marine system. *Ecosystems* 11, 397–409.
- Aluwihare, L.I., Repeta, D.J., Chen, R.F., 1997. A major biopolymeric component to dissolved organic carbon in surface sea water. *Nature*.
- Aluwihare, L.I., Repeta, D.J., Pantoja, S., Johnson, C.G., 2005. Two Chemically Distinct Pools of Organic Nitrogen Accumulate in the Ocean. *Science*, 308, 1007–1010.
- Álvarez-Salgado, X.A., Nieto-Cid, M., Álvarez, M., Pérez, F.F., Morin, P., Mercier, H., 2013. New insights on the mineralization of dissolved organic matter in central, intermediate, and deep water masses of the northeast North Atlantic. *Limnol. Oceanogr.* 58, 681–696.
- Amon, R.M.W., Benner, R., 1996. Bacterial utilization of different size classes of dissolved organic matter. *Limnol. Oceanogr.* 41, 41–51.
- Andrew, A.A., Del Vecchio, R., Subramaniam, A., Blough, N.V., 2013. Chromophoric dissolved organic matter (CDOM) in the Equatorial Atlantic Ocean: Optical properties and their relation to CDOM structure and source. *Mar. Chem.* 148, 33–43.
- Antoine, D., Morel, A., 1996. Oceanic primary production: 1. Adaptation of a spectral light-photosynthesis model in view of application to satellite chlorophyll observations. *Global Biogeochem. Cycles* 10, 43–55.
- Aparicio, F.L., Nieto-Cid, M., Borrull, E., Romero, E., Stedmon, C.A., Sala, M.M., Gasol, J.M., Rios, A.F., Marrasé, C., 2015. Microbially-Mediated Fluorescent Organic Matter Transformations in the Deep Ocean. Do the Chemical Precursors Matter? *Front. Mar. Sci.* 2, 1–14.
- Aparicio, F.L., Nieto-Cid, M., Borrull, E., Calvo, E., Pelejero, C., Sala, M.M., Pinhassi, J., Gasol, J.M., Marrasé, C., 2016. Eutrophication and acidification: Do they induce changes in the dissolved organic matter dynamics in the coastal Mediterranean Sea? *Sci. Total Environ.* 563-564, 179–189.
- Ariese, F., Van Assema, S., Gooijer, C., Bruccoleri, A.G., Langford, C.H., 2004. Comparison of Laurentian Fulvic Acid luminescence with that of the hydroquinone/quinone model system: Evidence from low temperature fluorescence studies and EPR spectroscopy. *Aquat. Sci.* 66, 86–94.
- Arnosti, C., Grossart, H.P., Muehling, M., Joint, I., Passow, U., 2011. Dynamics of extracellular enzyme activities in seawater under changed atmospheric pCO<sub>2</sub>: a mesocosm investigation. *Aquatic Microbial Ecology*, 64: 285-298.
- Arrieta, J.M., Mayol, E., Hansman, R.L., Herndl, G.J., Dittmar, T., Duarte, C.M., 2015. Dilution limits dissolved organic carbon utilization in the deep ocean. *Scienceexpress* 348, 331–333.
- Azam, F., Hodson, R. E., 1981. Multiphasic kinetics for D-glucose uptake by assemblages of natural marine bacteria. *Mar. Ecol. Prog. Ser.* 6, 213–222.
- Azúa, I., Goiriena, I., Baña, Z., Iriberry, J., and Unanue, M., 2014. Release and consumption of D-amino acids during growth of marine prokaryotes. *Microbiol. Aquat. Syst.* 67, 1–12.
- Badger, M.R., Price, G.D., 2003. CO<sub>2</sub> concentrating mechanisms in cyanobacteria: molecular components, their diversity and evolution. *Journal of Experimental Botany*, 54: 609-622.

- Behrenfeld, M.J., Falkowski, P.G., 1997. Photosynthetic rates derived from satellite-based chlorophyll concentration. *Limnol. Oceanogr.* 42, 1–20.
- Benner, R., 2002. Chemical composition and reactivity of dissolved organic matter, in: Hansell, D.A., Carlson, C.A. (Eds.), *Biogeochemistry of Marine Dissolved Organic Matter*. Elsevier Inc., San Diego, USA, pp. 59–90.
- Berger, W.H., 1989. Global maps of ocean productivity. Pp. 429–455 in *Productivity of Oceans, Past and Present*. W.H. Berger, V.S. Smetacek, G. Wefer, eds, Dahlem Konferenzen, 1989, Life Science Research Report 44, J. Wiley & Sons, New York.
- Béthoux, J.P., Morin, P., Ruiz-Pino, D.P., 2002. Temporal trends in nutrient ratios: chemical evidence of Mediterranean ecosystem changes driven by human activity. *Deep. Res. Part II Top. Stud. Oceanogr.* 49, 2007–2016.
- Bianchi, T. S., 2012. Correction. The role of terrestrially derived organic carbon in the coastal ocean: A changing paradigm and the priming effect. *Proc. Natl. Acad. Sci.* 109, 5134–5134.
- Bianchi, T.S., Thornton, D.C.O., Yvon-Lewis, S.A., King, G.M., Eglinton, T.I., Shields, M.R., Ward, N.D., Curtis, J., 2015. Positive priming of terrestrially derived dissolved organic matter in a freshwater microcosm system. *Geophys. Res. Lett.* 42, 5460–5467.
- Bidle, K.D., Falkowski, P.G., 2004. Cell death in planktonic, photosynthetic microorganisms. *Nat. Rev. Microbiol.* 2, 643–655.
- Bieroza, M., Baker, A., Bridgeman, J., 2009. Exploratory analysis of excitation-emission matrix fluorescence spectra with self-organizing maps as a basis for determination of organic matter removal efficiency at water treatment works. *J. Geophys. Res. Biogeosciences* 114, 1–8.
- Bieroza, M., Baker, A., Bridgeman, J., 2012. Exploratory analysis of excitation-emission matrix fluorescence spectra with self-organizing maps-A tutorial. *Educ. Chem. Eng.* 7, e22–e31.
- Bolaños, R., Jorda, G., Cateura, J., Lopez, J., Puigdefabregas, J., Gomez, J., Espino, M., 2009. The XIOM: 20 years of a regional coastal observatory in the Spanish Catalan coast. *J. Mar. Syst.* 77, 237–260.
- Boyd, T.J., Osburn, C.L., 2004. Changes in CDOM fluorescence from allochthonous and autochthonous sources during tidal mixing and bacterial degradation in two coastal estuaries. *Mar. Chem.* 89, 189–210.
- Braslavsky, S.E., 2007. Glossary of terms used in photochemistry. 3<sup>rd</sup> Edition. *Pure Appl. Chem.* 79, 293 – 465.
- Brereton, R.G., 2012. Self organising maps for visualising and modelling. *Chem. Cent. J.* 6, S1.
- Bricaud, A., Morel, A., Prieur, L., 1981. Absorption by dissolved organic matter of the sea (yellow substance) in the UV and visible domains. *Limnol. Oceanogr.* 26, 43–53.
- Bro, R., 1997. PARAFAC. Tutorial and applications. *Chemom. Intell. Lab. Syst.* 38, 149–171.
- Brussaard, C.P.D. (2004). Viral control of phytoplankton - a review. *J. Eukaryot. Microbiol.* 51, 125–138.
- Brussaard, C.P.D., Noordeloos, A.A.M., Witte, H., Collenteur, M.C.J., Schulz, K.G., Ludwig, A., Riebesell, U. 2013. Arctic microbial community dynamics influenced by elevated CO<sub>2</sub> levels. *Biogeosciences*, 10: 719-731.
- Brussaard, C.P.D., 2004. Viral control of phytoplankton - a review. *J. Eukaryot. Microbiol.* 51, 125–138.

- Brym, A., Paerl, H.W., Montgomery, M.T., Handsel, L.T., Ziervogel, K., Osburn, C.L., 2014. Optical and chemical characterization of base-extracted particulate organic matter in coastal marine environments. *Mar. Chem.* 162, 96–113.
- Bunse, C., Lundin, D., Karlsson, C.M.G., Vila-Costa, M., Palovaara, J., Akram, N., Svensson, L., Holmfeldt, K., González, J.M., Calvo, E., Pelejero, C., Marrasé, C., Dopson, M., Gasol, J.M., Pinhassi, J., 2016. Response of marine bacterioplankton pH homeostasis gene expression to elevated CO<sub>2</sub>. *Nat. Clim. Chang.* 6, 483-487.
- Calbet, A., Sazhin, A.F., Nejtgaard, J.C., Berger, S.A., Tait, Z.S., Olmos, L., Sousoni, D., Isari, S., Martínez, R.A., Bouquet, J.M., Thompson, E.M., Båmsted, U., Jakobsen, H.H., 2014. Future climate scenarios for a coastal productive planktonic food web resulting in microplankton phenology changes and decreased trophic transfer efficiency. *Plos One*, 9, 4.
- Carlson, C.A., Giovannoni, S.J., Hansell, D.A., Goldberg, S.J., Parsons, R., Otero, M.P., Vergin, K., Wheeler, B.R., 2002. The effect of nutrient amendments on bacterioplankton growth, DOC utilization, and community structure in the northwestern Sargasso Sea. *Aquat. Microb. Ecol.* 30, 19–36.
- Carlson, C.A., Hansell, D.A., 2015. DOM Sources, Sinks, Reactivity, and Budgets, in: Hansell, D.A., Carlson, C.A. (Eds.), *Biogeochemistry of Marine Dissolved Organic Matter*. Elsevier Inc., pp. 65–126.
- Carpenter, E.J., Capone, D.G. [Eds.], 1983. *Nitrogen in the marine environment*. Academic Press, New York, pp. 409
- Catalá, T.S., Reche, I., Fuentes-Lema, A., Romera-Castillo, C., Nieto-Cid, M., Ortega-Retuerta, E., Calvo, E., Álvarez, M., Marrasé, C., Stedmon, C.A., Álvarez-Salgado, X.A., 2015. Turnover time of fluorescent dissolved organic matter in the dark global ocean. *Nat. Commun.* 6, 1–8.
- Catalán, N., Kellerman, A.M., Peter, H., Carmona, F., Tranvik, L.J., 2015. Absence of a priming effect on dissolved organic carbon degradation in lake water. *Limnol. Oceanogr.* 60, 159–168.
- Catalán, N., Obrador, B., Felip, M., Pretus, J.L., 2013. Higher reactivity of allochthonous vs. autochthonous DOC sources in a shallow lake. *Aquat. Sci.* 75, 581–593.
- Cauwet G., 2002. DOM in the Coastal Zone, in: Hansell, D.A., Carlson, C.A. (Eds.), *Biogeochemistry of Marine Dissolved Organic Matter*. Elsevier Inc., San Diego, USA, pp. 579–609.
- Cawley, K.M., Ding, Y., Fourqurean, J., Jaffé, R., 2012. Characterising the sources and fate of dissolved organic matter in Shark Bay, Australia: A preliminary study using optical properties and stable carbon isotopes. *Mar. Freshw. Res.* 63, 1098–1107.
- Cawley, K.M., Butler, K.D., Aiken, G.R., Larsen, L.G., Huntington, T.G., McKnight, D.M., 2012. Identifying fluorescent pulp mill effluent in the Gulf of Maine and its watershed. *Mar. Pollut. Bull.* 64, 1678–87.
- Chavez, F.P., Messié, M., Pennington, J.T., 2011. Marine primary production in relation to climate variability and change. *Ann. Rev. Mar. Sci.* 3, 227–260.
- Chen, R.F., Bada, J.L., 1994. The fluorescence of dissolved organic matter in pore waters of marine sediments. *Mar. Chem.* 45, 31–42.
- Chen, R.F., Bissett, P., Coble, P.G., Conmy, R., Gardner, G.B., Moran, M.A., Wang, X.C., Wells, M.L., Whelan, P., Zepp, R.G., 2004. Chromophoric dissolved organic matter (CDOM) source characterization in the Louisiana Bight. *Mar. Chem.* 89, 257–272.
- Clark, L.L., Ingall, E.D., Benner, R., 1998. Marine phosphorus is selectively remineralized. *Nature* 393, 426.

- Claustre, H., Morel, A., Hooker, S.B., Babin, M., Antoine, D., Oubelkheir, K., Bricaud, A., Leblanc, K., Quéguiner, B., Maritorea, S., 2002. Is desert dust making oligotrophic waters greener? *Geophys. Res. Lett.* 29, 10–13.
- Clayton, T.D., Byrne, R.H., 1993. Spectrophotometric seawater pH measurements - total hydrogen-ion concentration scale calibration of m-cresol purple and at-sea results. *Deep-Sea Research Part I-Oceanographic Research Papers*, 40, 2115-2129.
- Coble, P.G., Green, S.A., Blough, N.V., Gagosian, R.B., 1990. Characterization of dissolved organic matter in the Black Sea by fluorescence spectroscopy. *Nature* 348, 432–435.
- Coble, P.G., 1996. Characterization of marine and terrestrial DOM in seawater using excitation-emission matrix spectroscopy. *Mar. Chem.* 51, 325–346.
- Coble, P.G., 2007. Marine optical biogeochemistry: the chemistry of ocean color. *Chem. Rev.* 107, 402–18.
- Coma, R., Ribes, M., Serrano, E., Jiménez, E., Salat, J., Pascual, J., 2009. Global warming-enhanced stratification and mass mortality events in the Mediterranean. *Proc. Natl. Acad. Sci.* 106, 6176–6181.
- Cory, R.M., McKnight, D.M., 2005. Fluorescence spectroscopy reveals ubiquitous presence of oxidized and reduced quinones in dissolved organic matter. *Environ. Sci. Technol.* 39, 8142–8149.
- Cunha, A., Almeida, F.J.R.C., Coelho, N.C. M., Gomes, V., Oliveira, V., Santos, A.L. 2010. Bacterial extracellular enzymatic activity in globally changing aquatic ecosystems. In *Current research, technology and education topics in applied microbiology and microbial biotechnology*. pp. 124-135. Ed. by A. Méndez-Vilas. Formatex Research Center
- Dainard, P.G., Guéguen, C., McDonald, N., Williams, W.J., 2015. Photobleaching of fluorescent dissolved organic matter in Beaufort Sea and North Atlantic Subtropical Gyre. *Mar. Chem.* 177, 630–637.
- Dalzell, B.J., Minor, E.C., Mopper, K.M., 2009. Photodegradation of estuarine dissolved organic matter: a multi-method assessment of DOM transformation. *Org. Geochem.* 40, 243–257.
- De Haan, H., 1977. Effect of benzoate on microbial decomposition of fulvic acids in Tjeukemeer (the Netherlands). *Limnol. Oceanogr.* 22, 38–44.
- De La Fuente, P., Marrasé, C., Canepa, A., Álvarez-Salgado, X.A., 2014. Does a general relationship exist between fluorescent dissolved organic matter and microbial respiration? — The case of the dark equatorial Atlantic Ocean. *Deep Sea Res. Part I Oceanogr. Res. Pap.* 89, 44–55
- Delille, D., 2004. Abundance and function of bacteria in the Southern Ocean. *Cell. Mol. Biol.* 50, 543–551.
- Determann, S., Lobbes, J.M., Reuter, R., Rullkötter, J., 1998. Ultraviolet fluorescence excitation and emission spectroscopy of marine algae and bacteria. *Mar. Chem.* 62, 137–156.
- Dickson, A. G., Sabine, C. L., Christian, J. R. 2007. *Guide to Best Practices for Ocean CO<sub>2</sub> measurements*. North Pacific Marine Science Organization, Sidney, British Columbia. 191 pp.
- Dittmar, T., Koch, B.P., 2006. Thermogenic organic matter dissolved in the abyssal ocean. *Mar. Chem.* 102, 208–217.
- Dittmar, T., Paeng, J., 2009. A heat-induced molecular signature in marine dissolved organic matter. *Nat. Geosci.* 2, 175–179.

Dittmar, T., 2015. Reasons Behind the Long-Term Stability of Dissolved Organic Matter, in: Hansell, D.A., Carlson, C.A. (Eds.), *Biogeochemistry of Marine Dissolved Organic Matter*. Elsevier Inc., pp. 369–388.

Doney, S.C., Balch, W.M., Fabry, V.J., Feely, R.A., 2009. Ocean acidification: a critical emerging problem for the ocean sciences. *Oceanography*, 22, 16-25.

Dryer, D.J., Korshin, G.V., Fabbricino, M., 2008. In situ examination of the protonation behavior of fulvic acids using differential absorbance spectroscopy. *Environ. Sci. Technol.* 42, 6644–6649.

Duarte, C.M., Agustí, S., Gasol, J.M., Vaqué, D., Vázquez-Domínguez, E., 2000. Effect of nutrient supply on the biomass structure of planktonic communities: an experimental test on a Mediterranean coastal community. *Marine Ecology Progress Series*, 206: 87-95.

Durrieu de Madron, X., Guieu, C., Sempéré, R., Conan, P., Cossa, D., D'Ortenzio, F., Estournel, C., Gazeau, F., Rabouille, C., Stemmann, L., Bonnet, S., Diaz, F., Koubbi, P., Radakovitch, O., Babin, M., Baklouti, M., Bancon-Montigny, C., Belviso, S., Bensoussan, N., Bonsang, B., Bouloubassi, I., Brunet, C., Cadiou, J.F., Carlotti, F., Chami, M., Charmasson, S., Charrière, B., Dachs, J., Doxaran, D., Dutay, J.C., Elbaz-Poulichet, F., Eléaume, M., Eyrolles, F., Fernández, C., Fowler, S., Francour, P., Gaertner, J.C., Galzin, R., Gasparini, S., Ghiglione, J.F., Gonzalez, J.L., Goyet, C., Guidi, L., Guizien, K., Heimbürger, L.-E., Jacquet, S.H.M., Jeffrey, W.H., Joux, F., Le Hir, P., Leblanc, K., Lefèvre, D., Lejeusne, C., Lemée, R., Loÿe-Pilot, M.D., Mallet, M., Méjanelle, L., Mélin, F., Mellon, C., Méricot, B., Merle, P.L., Migon, C., Miller, W.L., Mortier, L., Mostajir, B., Mousseau, L., Moutin, T., Para, J., Pérez, T., Petrenko, A., Poggiale, J.C., Prieur, L., Pujo-Pay, M., Raimbault, P., Rees, A.P., Ridame, C., Rontani, J.F., Ruiz Pino, D., Sicre, M.A., Taillandier, V., Tamburini, C., Tanaka, T., Taupier-Letage, I., Tedetti, M., Testor, P., Thébaud, H., Thouvenin, B., Touratier, F., Tronczynski, J., Ulses, C., Van Wambeke, F., Vantrepotte, V., Vaz, S., Verney, R., 2011. Marine ecosystems' responses to climatic and anthropogenic forcings in the Mediterranean. *Prog. Oceanogr.* 91, 97–166.

Eisinger, J., Lamola, A.A., 1971. The Excited States of Nucleic Acids, in: Steiner, R.F. and Weinryb, I. (Ed.), *Excited States of Proteins and Nucleic Acids*. Plenum Press, New York, pp. 107–198.

Ejarque-González, E., Butturini, A., 2014. Self-Organising Maps and correlation analysis as a tool to explore patterns in Excitation-Emission Matrix data sets and to discriminate dissolved organic matter fluorescence components. *PLoS One* 9.

Elderfield, H., 2002. Carbonate Mysteries. *Science*, 296, 1618–1621.

Engel, A., Piontek, J., Grossart, H.P., Riebesell, U., Schulz, K.G., Sperling, M., 2014. Impact of CO<sub>2</sub> enrichment on organic matter dynamics during nutrient induced coastal phytoplankton blooms. *Journal of Plankton Research*, 36: 641-657.

Engel, A., Schulz, K. G., Riebesell, U., Bellerby, R., Delille, B., Schartau, M. 2008. Effects of CO<sub>2</sub> on particle size distribution and phytoplankton abundance during a mesocosm bloom experiment (PeECE II). *Biogeosciences*, 5: 509-521.

Ewald, M., Belin, C., Berger, P., Weber, J.H., 1983. Corrected fluorescence spectra of fulvic acids isolated from soil and water. *Environmental Science and Technology* 17, 501–504.

Feely, R.A., Sabine, C.L., Lee, K., Berelson, W., Kleypas, J., Fabry, V.J., Millero, F.J., 2004. Impact of Anthropogenic CO<sub>2</sub> on the CaCO<sub>3</sub> System in the Oceans. *Science*, 305, 362–366.

Feller, G., Narinx, E., Arpigny, J.L., Aittaleb, M., Baise, E., Genicot, S., Gerday, C., 1996. Enzymes from psychrophilic organisms. *FEMS Microbiol. Rev.* 18, 189–202.

Fellman, J.B., Spencer, R.G., Hernes, P.J., Edwards, R.T., D'Amore, D.V., Hood, E., 2010. The impact of glacier runoff on the biodegradability and biochemical composition of terrigenous dissolved organic matter in near-shore marine ecosystems. *Mar. Chem.* 121, 112–122.

- Ferretto, N., Tedetti, M., Guigue, C., Mounier, S., Redon, R., Goutx, M., 2014. Identification and quantification of known polycyclic aromatic hydrocarbons and pesticides in complex mixtures using fluorescence excitation-emission matrices and parallel factor analysis. *Chemosphere* 107, 344–53.
- Fichot, C.G., Benner, R., 2012. The spectral slope coefficient of chromophoric dissolved organic matter ( $S_{275-295}$ ) as a tracer of terrigenous dissolved organic carbon in river-influenced ocean margins. *Limnol. Oceanogr.* 57, 1453–1466.
- Flamant, C., Pelon, J., Hauser, D., Quentin, C., Drennan, W.M., Gohin, F., Chapron, B., Gourrion, J., 2003. Analysis of surface wind and roughness length evolution with fetch using a combination of airborne lidar and radar measurements. *J. Geophys. Res.* 108, 1–26.
- Fontaine, S., Bardoux, G., Abbadie, L., Mariotti, A., 2004. Carbon input to soil may decrease soil carbon content. *Ecol. Lett.* 7, 314–320.
- Fonte, E.S., Amado, A.M., Meirelles-Pereira, F., Esteves, F.A., Rosado, A.S., Farjalla, V.F., 2013. The combination of different carbon sources enhances bacterial growth efficiency in aquatic ecosystems. *Microb. Ecol.* 66, 871–878.
- Fu, F.-X., Warner, M.E., Zhang, Y., Feng, Y., and Hutchins, D.A., 2007. Effects of increased temperature and CO<sub>2</sub> on photosynthesis, growth, and elemental ratios in marine *Synechococcus* and *Prochlorococcus* (Cyanobacteria). *Journal of Phycology*, 43: 485-496.
- Galloway, J.N., Dentener, F.J., Capone, D.G., Boyer, E.W., Howarth, R.W., Seitzinger, S.P., Asner, G.P., Cleveland, C.C., Green, P.A., Holland, E.A., Karl, D.M., Michaels, A.F., Porter, J.H., Townsend, A.R., Vörösmarty, C.J., 2004. Nitrogen cycles: Past, present, and future, *Biogeochemistry*.
- Gasol, J.M., Del Giorgio, P.A., 2000. Using flow cytometry for counting natural planktonic bacteria and understanding the structure of planktonic bacterial communities. *Scientia Marina*, 64: 197-224.
- Gasol, J.M., Massana, R., Simó, R., Marrasé, C., Acinas, S.G., Pedrós-Alió, C., Sala, M.M., Calvo, E., Vaqué, D., Peters, F., 2012. Blanes Bay (site 55). In ICES Phytoplankton and Microbial Plankton Status Report 2009/2010. ICES Cooperative Research Report No. 313, pp. 138-141. Ed by T. D. O'Brien, W. K. W. Li and X. A. G Morán.
- Gattuso, J.-P., Magnan, A., Bille, R., Cheung, W.W.L., Howes, E.L., Joos, F., Allemand, D., Bopp, L., Cooley, S.R., Eakin, C.M., Hoegh-Guldberg, O., Kelly, R.P., Portner, H.-O., Rogers, A.D., Baxter, J.M., Laffoley, D., Osborn, D., Rankovic, A., Rochette, J., Sumaila, U.R., Treyer, S., Turley, C., 2015. Contrasting futures for ocean and society from different anthropogenic CO<sub>2</sub> emissions scenarios. *Science*. 349, aac4722.
- Giering, S.L.C., Sanders, R., Lampitt, R.S., Anderson, T.R., Tamburini, C., Boutrif, M., Zubkov, M.V., Marsay, C.M., Henson, S.A., Saw, K., Cook, K., Mayor, D.J., 2014. Reconciliation of the carbon budget in the ocean's twilight zone. *Nature*.
- Giering, S.L.C., Sanders, R., Lampitt, R.S., Anderson, T.R., Tamburini, C., Boutrif, M., Zubkov, M.V., Marsay, C.M., Henson, S.A., Saw, K., Cook, K., Mayor, D.J., 2014. Reconciliation of the carbon budget in the ocean's twilight zone. *Nature*.
- Gonsior, M., Peake, B.M., Cooper, W.T., Podgorski, D., D'Andrilli, J., Cooper, W.J., 2009. Photochemically induced changes in dissolved organic matter identified by ultra- high resolution Fourier transform ion cyclotron resonance mass spectrometry. *Environ. Sci. Technol.* 43, 698–703.
- Gontikaki, E., Thornton, B., Huvenne, V.A.I., Witte, U., 2013. Negative priming effect on organic matter mineralisation in NE Atlantic slope sediments. *PLoS One* 8, e67722.

- Goutx, M., Guigue, C., Aritio, D., Ghiglione, J.F., Pujo-Pay, M., Raybaud, V., Duflos, M., Prieur, L., 2009. Short term summer to autumn variability of dissolved lipid classes in the Ligurian sea (NW Mediterranean). *Biogeosciences* 6, 1229–1246.
- Graeber, D., Gelbrecht, J., Pusch, M.T., Anlanger, C., von Schiller, D., 2012. Agriculture has changed the amount and composition of dissolved organic matter in Central European headwater streams. *Sci. Total Environ.* 438, 435–46.
- Gram, L., Grossart, H.P., Schlingloff, A., Kiørboe, T., 2002. Possible Quorum Sensing in Marine Snow Bacteria: Production of Acylated Homoserine Lactones by *Roseobacter* Strains Isolated from Marine Snow. *Appl. Environ. Microbiol.* 68, 4111–4116.
- Green, S.A., Blough, N.V., 1994. Optical absorption and fluorescence properties of chromophoric dissolved organic matter in natural waters. *Limnol. Oceanogr.* 39, 1903–1916.
- Grifoll, M., Aretxabaleta, A.L., Pelegrí, J.L., Espino, M., Warner, J.C., Sánchez-Arcilla, A., 2013. Seasonal circulation over the Catalan inner-shelf (northwest Mediterranean Sea). *J. Geophys. Res. Ocean.* 118, 5844–5857.
- Grossart, H.P., Allgaier, M., Passow, U., Riebesell, U., 2006. Testing the effect of CO<sub>2</sub> concentration on the dynamics of marine heterotrophic bacterioplankton. *Limnology and Oceanography*, 51: 1-11.
- Guadayol, Ò., Peters, F., Marrasé, C., Gasol, J.M., Roldán, C., Berdalet, E., Massana, R., Sabata, A., 2009. Episodic meteorological and nutrient-load events as drivers of coastal planktonic ecosystem dynamics: A time-series analysis. *Mar. Ecol. Prog. Ser.* 381, 139–155.
- Guenet, B., Danger, M., Harrault, L., Allard, B., Jauset-Alcala, M., Bardoux, G., Benest, D., Abbadie, L., Lacroix, G., 2014. Fast mineralization of land-born C in inland waters: first experimental evidences of aquatic priming effect. *Hydrobiologia* 721, 35–44.
- Guerrero-Feijóo, E., Nieto-Cid, M., Álvarez, M., Álvarez-Salgado, X.A., 2014. Dissolved organic matter cycling in the confluence of the Atlantic and Indian oceans south of Africa. *Deep Sea Res. Part I Oceanogr. Res. Pap.* 83, 12–23.
- Hall, G.J., Kenny, J.E., 2007. Estuarine water classification using EEM spectroscopy and PARAFAC-SIMCA. *Anal. Chim. Acta* 581, 118–124.
- Hama, T., Kawashima, S., Shimotori, K., Satoh, Y., Omori, Y., Wada, S., Adachi, T., Hasegawa, S., Midorikawa, T., Ishii, M., Saito, S., Sasano, D., Endo, H., Nakayama, T., Inouye, I., 2012. Effect of ocean acidification on coastal phytoplankton composition and accompanying organic nitrogen production. *Journal of Oceanography*, 68: 183-194.
- Hansell, D.A., Carlson, C.A., Repeta, D.J., Schlitzer, R., 2009. Dissolved Organic Matter in the Ocean. A controversy stimulates new insights. *Oceanography* 22, 202–211.
- Hansell, D.A., 2013. Recalcitrant dissolved organic carbon fractions. *Ann. Rev. Mar. Sci.* 5, 421–45.
- Hansen, H.P., Koroleff, F., 1999. Determination of nutrients. In *Methods of Seawater Analysis*. pp. 159–228. Ed. by K. Grasshoff, K. Kremling and M. Ehrhardt. Wiley-VCH: Weinheim, Germany.
- Hansen, H.P., Grasshoff, K., 1983. Automated chemical analysis. In: Grasshoff K, Ehrhardt M, Kremling K (eds) *Methods of seawater analysis*. Verlag Chemie, Weinheim, pp. 347-395.
- Hargreaves, B.R., 2003. Water column optics and penetration of UVR, in: Helbling, E.W., Zagarese, H. (Eds.), *UV Effects in Aquatic Organisms and Ecosystems*. The Royal Society of Chemistry, Cambridge, UK, pp. 61–99.
- Harshman, R.A., Lundy, M.E., 1994. PARAFAC: Parallel factor analysis. *Comput. Stat. Data Anal.* 18, 39–72.

- Harvey, B.P., Gwynn-Jones, D., Moore, P.J., 2013. Meta-analysis reveals complex marine biological responses to the interactive effects of ocean acidification and warming. *Ecology and Evolution*, 3: 1016-1030.
- Hedges, J.I., Eglinton, G., Hatcher, P.G., Kirchman, D.L., Arnosti, C., Derenne, S., Evershed, R.P., Kögel-Knabner, I., de Leeuw, J.W., Littke, R., Michaelis, W., Rullkotter, J., 2000. The molecularly uncharacterized component of nonliving organic matter in natural environments. *Org. Geochem.* 31, 945–958.
- Helms, J.R., Stubbins, A., Ritchie, J.D., Minor, E.C., Kieber, D.J., Mopper, K.M., 2008. Absorption spectral slopes and slope ratios as indicators of molecular weight, source, and photobleaching of chromophoric dissolved organic matter. *Limnol. Oceanogr.* 53, 955–969.
- Helms, J.R., Stubbins, A., Perdue, E.M., Green, N.W., Chen, H., Mopper, K.M., 2013. Photochemical bleaching of oceanic dissolved organic matter and its effect on absorption spectral slope and fluorescence. *Mar. Chem.* 155, 81–91.
- Henry, W., 1803. Experiments on the Quantity of Gases Absorbed by Water, at Different Temperatures, and under Different Pressures. *Philos. Trans. R. Soc. London* 93, 29–274.
- Hertkorn, N., Benner, R., Frommberger, M., Schmitt-Kopplin, P., Witt, M., Kaiser, K., Kettrup, A., Hedges, J.I., 2006. Characterization of a major refractory component of marine dissolved organic matter. *Geochim. Cosmochim. Acta* 70, 2990–3010.
- Herut, B., Zohary, T., Krom, M.D., Mantoura, R.F.C., Pitta, P., Psarra, S., Rassoulzadegan, F., Tanaka, T., Thingstad, T.F., 2005. Response of East Mediterranean surface water to Saharan dust: On-board microcosm experiment and field observations. *Deep. Res. Part II Top. Stud. Oceanogr.* 52, 3024–3040.
- Ho, T.-Y., Scranton, M.I., Taylor, G.T., Varela, R., Thunell, R.C., and Muller-Karger, F., 2002. Acetate cycling in the water column of the Cariaco Basin: Seasonal and vertical variability and implication for carbon cycling. *Limnol. Oceanogr.* 47, 1119–1128.
- Hönisch, B., Ridgwell, A., Schmidt, D.N., Thomas, E., Gibbs, S.J., Sluijs, A., Zeebe, R.E., Kump, L., Martindale, R.C., Greene, S.E., Kiessling, W., Ries, J., Zachos, J.C., Royer, D.L., Barker, S., Marchitto, T.M., Moyer, R., Pelejero, C., Ziveri, P., Foster, G.L., Williams, B., 2012. The geological record of ocean acidification. *Science* 335, 1058–1063.
- Honjo, S., Eglinton, T.I., Taylor, C.D., Ulmer, K.M., Sievert, S.M., Bracher, A., German, C.R., Edgcomb, V., Francois, R., Iglesias-Rodríguez, M.D., Van Mooy, B.A.S., Repeta, D.J., 2014. Understanding the role of the biological pump in the global carbon cycle. An Imperative for Ocean Science. *Oceanography* 27, 10–16.
- Hood, E., Williams, M.W., Mcknight, D.M., 2005. Sources of dissolved organic matter (DOM) in a Rocky Mountain stream using chemical fractionation and stable isotopes. *Biogeochemistry* 74, 231–255.
- Hopkinson, C.S., Vallino, J.J., Nolin, A., 2002. Decomposition of dissolved organic matter from the continental margin. *Deep. Res. II* 49, 4461–4478.
- Houghton, R.A., 2007. Balancing the Global Carbon Budget. *Annu. Rev. Earth Planet. Sci.* 35, 313–347.
- Howarth, R.W., Marino, R., 2006. Nitrogen as the limiting nutrient for eutrophication in coastal marine ecosystems: Evolving views over three decades. *Limnol. Oceanogr.* 51, 364–376.
- Huguet, A., Vacher, L., Relexans, S., Saubusse, S., Froidefond, J.M., Parlanti, E., 2009. Properties of fluorescent dissolved organic matter in the Gironde Estuary. *Org. Geochem.* 40, 706–719.

Hutchins, D. A., Mulholland, M. R., and Fu, F. X. 2009. Nutrient cycles and marine microbes in a CO<sub>2</sub>-enriched ocean. *Oceanography*, 22: 128-145.

Intergovernmental Panel on Climate Change (IPCC), 2007. *Climate Change 2007: Synthesis Report. Contribution of Working Groups I, II and III to the Fourth Assessment Report of the Intergovernmental Panel on Climate Change.*

Intergovernmental Panel on Climate Change (IPCC), 2013. *Climate Change 2013: The Physical Science Basis. Contribution of Working Group I to the Fifth Assessment Report of the Intergovernmental Panel on Climate Change.*

Ito, Y., Butler, A., 2005. Structure of synechobactins, new siderophores of the marine cyanobacterium *Synechococcus* sp. PCC 7002. *Limnol. Oceanogr.* 50, 1918–1923.

Jaffé, R., McKnight, D., Maie, N., Cory, R., McDowell, W.H., Campbell, J.L., 2008. Spatial and temporal variations in DOM composition in ecosystems: The importance of long-term monitoring of optical properties. *J. Geophys. Res. Biogeosciences* 113, 1–15.

Jiao, N., Herndl, G.J., Hansell, D.A., Benner, R., Kattner, G., Wilhelm, S.W., Kirchman, D.L., Weinbauer, M.G., Luo, T., Chen, F., Azam, F., 2010. Microbial production of recalcitrant dissolved organic matter: long-term carbon storage in the global ocean. *Nat. Rev. Microbiol.* 8, 593–599.

Joos, F., Frölicher, T.L., Steinacher, M., Plattner, G.-K., 2011. Impact of climate change mitigation on ocean acidification projections. pp. 272-290. Ed. by J. P. Gattuso and L. Hanson. Oxford University Press, Oxford.

Jørgensen, L., Stedmon, C.A., Kragh, T., Markager, S., Middelboe, M., Søndergaard, M., 2011. Global trends in the fluorescence characteristics and distribution of marine dissolved organic matter. *Mar. Chem.* 126, 139–148.

Jørgensen, L., Stedmon, C. A., Granskog, M. A., Middelboe, M., 2014a. Tracing the long-term microbial production of recalcitrant fluorescent dissolved organic matter in seawater. *Geophys. Res. Lett.* 41, 2481–2488.

Jørgensen, L., Lechtenfeld, O.J., Benner, R., Middelboe, M., Stedmon, C.A., 2014b. Bacterial production and transformation of dissolved neutral sugars and amino acids in seawater. *Biogeosciences Discuss.* 11, 6151–6184.

Kaiser, K., Benner, R., 2009. Biochemical composition and size distribution of organic matter at the Pacific and Atlantic time-series stations. *Mar. Chem.* 113, 63–77.

Kawasaki, N., Benner, R., 2006. Bacterial release of dissolved organic matter during cell growth and decline: origin and composition. *Limnol. Oceanogr.* 51, 2170–2180.

Kim, J.H., Kim, K.Y., Kang, E.J., Lee, K., Kim, J.M., Park, K.T., Shin, K., Hyun, B., Jeong, H.J., 2013. Enhancement of photosynthetic carbon assimilation efficiency by phytoplankton in the future coastal ocean. *Biogeosciences*, 10: 7525-7535.

Kim, J.M., Lee, K., Shin, K., Yang, E.J., Engel, A., Karl, D.M., Kim, H.-C., 2011. Shifts in biogenic carbon flow from particulate to dissolved forms under high carbon dioxide and warm ocean conditions. *Geophys. Res. Lett.* 38, 1–5.

Kim, S., Kramer, R.W., Hatcher, P.G., 2003. Graphical Method for Analysis of Ultrahigh-Resolution Broadband mass spectra of Natural Organic Matter, the Van Krevelen diagram. *Anal. Chem.* 75, 5336–5344.

Kirchman, D., Knees, E., Hodson, R., 1985. Leucine incorporation and its potential as a measure of protein-synthesis by bacteria in natural aquatic systems. *Applied and Environmental Microbiology*, 49: 599-607.

- Koch, B.P., Witt, M., Engbrodt, R., Dittmar, T., Kattner, G., 2005. Molecular formulae of marine and terrigenous dissolved organic matter detected by electrospray ionization Fourier transform ion cyclotron resonance mass spectrometry. *Geochim. Cosmochim. Acta* 69, 3299–3308.
- Koehler, B., von Wachenfeldt, E., Kothawala, D.N., Tranvik, L.J., 2012. Reactivity continuum of dissolved organic carbon decomposition in lake water. *J. Geophys. Res. Biogeosciences* 117, 1–14.
- Koprivnjak, J.F., Pfromm, P.H., Ingall, E., Vetter, T.A., Schmitt-Kopplin, P., Hertkorn, N., Frommberger, M., Knicker, H., Perdue, E.M., 2009. Chemical and spectroscopic characterization of marine dissolved organic matter isolated using coupled reverse osmosis–electrodialysis. *Geochim. Cosmochim. Acta* 73, 4215–4231.
- Kothawala, D.N., Stedmon, C.A., Müller, R.A., Weyhenmeyer, G.A., Köhler, S.J., Tranvik, L.J., 2014. Controls of dissolved organic matter quality: evidence from a large-scale boreal lake survey. *Glob. Chang. Biol.* 20, 1101–14.
- Kothawala, D.N., von Wachenfeldt, E., Koehler, B., Tranvik, L.J., 2012. Selective loss and preservation of lake water dissolved organic matter fluorescence during long-term dark incubations. *Sci. Total Environ.* 433, 238–246.
- Kowalczyk, P., Tilstone, G.H., Zablocka, M., Röttgers, R., Thomas, R., 2013. Composition of dissolved organic matter along an Atlantic Meridional Transect from fluorescence spectroscopy and Parallel Factor Analysis. *Mar. Chem.* 157, 170–184.
- Krause, E., Wichels, A., Giménez, L., Lunau, M., Schilhabel, M. B., Gerdtts, G., 2012. Small changes in pH have direct effects on marine bacterial community composition: a microcosm approach. *Plos One*, 7.
- Kroeker, K.J., Kordas, R.L., Crim, R.N., Singh, G.G., 2010. Meta-analysis reveals negative yet variable effects of ocean acidification on marine organisms. *Ecology Letters*, 13: 1419–1434.
- Kujawinski, E.B., Longnecker, K., Blough, N.V., Del Vecchio, R., Finlay, L., Kitner, J.B., Giovannoni, S.J., 2009. Identification of possible source markers in marine dissolved organic matter using ultrahigh resolution mass spectrometry. *Geochim. Cosmochim. Acta* 73, 4384–4399.
- Kuzyakov, Y., 2002. Separating microbial respiration of exudates from root respiration in non-sterile soils: A comparison of four methods. *Soil Biol. Biochem.* 34, 1621–1631.
- Laane, R.W.P.M., 1982. Influence of pH on the fluorescence of dissolved organic matter. *Mar. Chem.* 11, 395–401.
- Lakowicz, J.R., 2006. Introduction to fluorescence, in: Lakowicz, J.R. (Ed.), *Principles of Fluorescence Spectroscopy*. Springer Science+Business Media, LLC, Baltimore, Maryland, pp. 1–26.
- Lapierre, J.-F., Del Giorgio, P.A., 2014. Partial coupling and differential regulation of biologically and photo-chemically labile dissolved organic carbon across boreal aquatic networks. *Biogeosciences* 11, 5969–5985.
- Lawaetz, A.J., Stedmon, C.A., 2009. Fluorescence Intensity Calibration Using the Raman Scatter Peak of Water. *Appl. Spectrosc.* 63, 936–940.
- Lawton, J.H., 1995. Ecological experiments with model systems. *Science*, 269: 328–331.
- Le Quéré, C., Moriarty, R., Andrew, R.M., Canadell, J.G., Sitch, S., Korsbakken, J.I., Friedlingstein, P., Peters, G.P., Andres, R.J., Boden, T.A., Houghton, R.A., House, J.I., Keeling, R.F., Tans, P., Arneeth, A., Bakker, D.C.E., Barbero, L., Bopp, L., Chang, J., Chevallier, F., Chini, L.P., Ciais, P., Fader, M., Feely, R.A., Gkritzalis, T., Harris, I., Hauck, J., Ilyina, T., Jain, A.K., Kato, E., Kitidis, V., Klein Goldewijk, K., Koven, C., Landschützer, P., Lauvset, S.K., Lefèvre, N.,

- Lenton, A., Lima, I.D., Metzl, N., Millero, F., Munro, D.R., Murata, A., Nabel, J.E.M.S., Nakaoka, S., Nojiri, Y., O'Brien, K., Olsen, A., Ono, T., Pérez, F.F., Pfeil, B., Pierrot, D., Poulter, B., Rehder, G., Rödenbeck, C., Saito, S., Schuster, U., Schwinger, J., Séférian, R., Steinhoff, T., Stocker, B.D., Sutton, A.J., Takahashi, T., Tilbrook, B., Van Der Laan-Luijkx, I.T., Van Der Werf, G.R., Van Heuven, S., Vandemark, D., Viovy, N., Wiltshire, A., Zaehle, S., Zeng, N., 2015. Global Carbon Budget 2015. *Earth Syst. Sci. Data* 7, 349–396.
- Leahy, J.G., Colwell, R.R., 1990. Microbial degradation of hydrocarbons in the environment. *Microbiol. Rev.* 54, 305–315.
- Legendre, L., Le Fèvre, J., 1991. From individual plankton cells to pelagic marine ecosystems and to global biogeochemical cycles. In *Particle Analysis in Oceanography*. pp. 261-300. Ed. by S. Demers. NATO ASI Series, Springer-Verlag Berlin.
- Legendre, L., Rivkin, R.B., Weinbauer, M.G., Guidi, L., Uitz, J., 2015. The microbial carbon pump concept: potential biogeochemical significance in the globally changing ocean. *Prog. Oceanogr.* 134, 432–450.
- Lekunberri, I., Lefort, T., Romera-Castillo, C., Cardelús, C., Coll-Lladó, M., Ruiz-González, C., Marrasé, C., Gasol, J.M., 2012. Relationship between induced phytoplankton blooms and the structure and dynamics of the free-living heterotrophic bacterial community. *Mar. Ecol. Prog. Ser.* 448, 23–37.
- Lindh, M.V., Riemann, L., Baltar, F., Romero-Oliva, C., Salomon, P.S., Graneli, E., Pinhassi, J., 2013. Consequences of increased temperature and acidification on bacterioplankton community composition during a mesocosm spring bloom in the Baltic Sea. *Environmental Microbiology Reports*, 5: 252-262.
- Liu, J.W., Weinbauer, M.G., Maier, C., Dai, M.H., Gattuso, J.-P., 2010. Effect of ocean acidification on microbial diversity and on microbe-driven biogeochemistry and ecosystem functioning. *Aquatic Microbial Ecology*, 61: 291-305.
- Löhnis, F., 1926. Nitrogen availability of green manures. *Soil Sci.* 22, 253-290.
- Lønborg, C., Álvarez-Salgado, X.A., Davidson, K., Martínez-García, S., Teira, E., 2010. Assessing the microbial bioavailability and degradation rate constants of dissolved organic matter by fluorescence spectroscopy in the coastal upwelling system of the Ría de Vigo. *Mar. Chem.* 119, 121–129.
- Lønborg, C., Álvarez-Salgado, X.A., 2014. Tracing dissolved organic matter cycling in the eastern boundary of the temperate North Atlantic using absorption and fluorescence spectroscopy. *Deep Sea Res. Part I Oceanogr. Res. Pap.* 85, 35–46.
- Maas, E.W., Law, C.S., Hall, J.A., Pickmere, S., Currie, K.I., Chang, F.H., Voyles, K.M., Caird, D., 2013. Effect of ocean acidification on bacterial abundance, activity and diversity in the Ross Sea, Antarctica. *Aquatic Microbial Ecology*, 70: 1-15.
- MacGilchrist, G.A., Shi, T., Tyrrell, T., Richier, S., Moore, C.M., Dumousseaud, C., Achterberg, E.P., 2014. Effect of enhanced pCO<sub>2</sub> levels on the production of dissolved organic carbon and transparent exopolymer particles in short-term bioassay experiments. *Biogeosciences* 11, 3695–3706.
- Maie, N., Yamashita, Y., Cory, R.M., Boyer, J.N., Jaffé, R., 2012. Application of excitation emission matrix fluorescence monitoring in the assessment of spatial and seasonal drivers of dissolved organic matter composition: Sources and physical disturbance controls. *Appl. Geochemistry* 27, 917–929.
- Marañón, E., Cermeño, P., Pérez, V., 2005. Continuity in the photosynthetic production of dissolved organic carbon from eutrophic to oligotrophic waters. *Mar. Ecol. Prog. Ser.* 299, 7–17.

- Marshall, J., Schott, F., 1999. Open-Ocean Convection: Observations, Theory, and Models. *Rev. Geophys.* 37, 1–64.
- Marty, J.C., Chiavérini, J., 2010. Hydrological changes in the Ligurian Sea (NW Mediterranean, DYFAMED site) during 1995-2007 and biogeochemical consequences. *Biogeosciences* 7, 2117–2128.
- Maugendre, L., Gattuso, J.-P., Louis, J., De Kluijver, A., Marro, S., Soetaert, K., Gazeau, F., 2015. Effect of ocean warming and acidification on a plankton community in the NW Mediterranean Sea. *ICES Journal of Marine Science*, 72: 1744-1755.
- Maugendre, L., Gattuso, J.-P., Louis, J., de Kluijver, A., Marro, S., Soetaert, K., Gazeau, F., 2014. Effect of ocean warming and acidification on a plankton community in the NW Mediterranean Sea. *ICES J. Mar. Sci.* 1–12.
- McKnight, D.M., Boyer, E.W., Westerhoff, P.K., Doran, P.T., Kulbe, T., Andersen, D.T., 2001. Spectrofluorometric characterization of dissolved organic matter for indication of precursor organic material and aromaticity. *Limnol. Oceanogr.* 46, 38–48.
- Meakin, N.G., Wyman, M., 2011. Rapid shifts in picoeukaryote community structure in response to ocean acidification. *The ISME Journal*, 5: 1397-1405.
- Millot, C., 1979. Wind induced upwellings in the Gulf of Lions. *Oceanol. Acta* 2, 261–274.
- Millot, C., Taupier-Letage, I., 2005. Circulation in the Mediterranean Sea. *Environ. Chem.* 5, 29–66.
- Mopper, K., Stubbins, A., Ritchie, J.D., Bialk, H.M., Hatcher, P.G., 2007. Advanced instrumental approaches for characterization of marine dissolved organic matter: Extraction techniques, mass spectrometry, and nuclear magnetic resonance spectroscopy. *Chem Rev*, 107: 419–442.
- Moran, M.A., Kujawinski, E.B., Stubbins, A., Fatland, R., Aluwihare, L.I., Buchan, A., Crump, B.C., Dorrestein, P.C., Dyhrman, S.T., Hess, N.J., Howe, B., Longnecker, K., Medeiros, P.M., Niggemann, J., Obernosterer, I., Repeta, D.J., Waldbauer, J.R., 2016. Deciphering ocean carbon in a changing world. *Proc. Natl. Acad. Sci.* 1–9.
- Moran, M.A., Zepp, R.G., 1997. Role of photoreactions in the formation of biologically labile compounds from dissolved organic matter. *Limnol. Oceanogr.* 42, 1307–1316.
- Morán, X.A.G., López-Urrutia, A., Calvo-Díaz, A., Li, W.K.W., 2009. Increasing importance of small phytoplankton in a warmer ocean. *Global Change Biology*, 16: 1137-1144
- Morel, A., Gentili, B., 2009. Yellow substance and the shades of blue in the Mediterranean Sea. *Biogeosciences Discuss.* 6, 8503–8530.
- Motegi, C., Nagata, T., Miki, T., Weinbauer, M.G., Legendre, L., Rassoulzadegan, F., 2009. Viral control of bacterial growth efficiency in marine pelagic environments. *Limnol. Oceanogr.* 54, 1901–1910.
- Motegi, C., Tanaka, T., Piontek, J., Brussaard, C. P. D., Gattuso, J.-P., Weinbauer, M. G., 2013. Effect of CO<sub>2</sub> enrichment on bacterial metabolism in an Arctic fjord. *Biogeosciences*, 10: 3285-3296.
- Murphy, K.R., Ruiz, G.M., Dunsmuir, W.T.M., Waite, T.D., 2006. Optimized parameters for fluorescence-based verification of ballast water exchange by ships. *Environ. Sci. Technol.* 40, 2357–2362.
- Murphy, K.R., Stedmon, C.A., Waite, T.D., Ruiz, G.M., 2008. Distinguishing between terrestrial and autochthonous organic matter sources in marine environments using fluorescence spectroscopy. *Mar. Chem.* 108, 40–58.

- Murphy, K.R., Hambly, A., Singh, S., Henderson, R.K., Baker, A., Stuetz, R., Khan, S.J., 2011. Organic matter fluorescence in municipal water recycling schemes: toward a unified PARAFAC model. *Environ. Sci. Technol.* 45, 2909–2916.
- Murphy, K.R., Stedmon, C.A., Graeber, D., Bro, R., 2013a. Fluorescence spectroscopy and multi-way techniques. *PARAFAC. Anal. Methods* 5, 6557–6566.
- Murphy, K.R., Stedmon, C.A., Graeber, D., Bro, R., 2013b. Appendix A. Decomposition routines for Excitation Emission Matrices 1–29.
- Murphy, K.R., Bro, R., Stedmon, C.A., 2014a. Chemometric Analysis of Organic Matter Fluorescence, in: Coble, P.G., Lead, J., Baker, A., Reynolds, D.M., Spencer, R.G.M. (Eds.), *Aquatic Organic Matter Fluorescence*. Cambridge University Press, New York, pp. 339–375.
- Murphy, K.R., Stedmon, C.A., Wenig, P., Bro, R., 2014b. OpenFluor– an online spectral library of auto-fluorescence by organic compounds in the environment. *Anal. Methods* 6, 658–661.
- Nagata T., 2008. Organic matter–bacteria interactions in seawater. In *Microbial Ecology of the Oceans*, ed. D.L. Kirchman, pp. 207–242. Hoboken, New Jersey: Wiley
- Nagata, T., Kirchman, D.L., 1992. Release of dissolved organic matter by heterotrophic protozoa: implications for microbial food webs. *Arch. fur Hydrobiol. Beih. Ergebn. Limnol.* 35, 99–109.
- Nagata, T., Fukuda, H., Fukuda, R., Koike, I., 2000. Bacterioplankton distribution and production in deep Pacific waters: Large-scale geographic variations and possible coupling with sinking particle fluxes. *Limnol. Oceanogr.* 45, 426–435.
- Newbold, L.K., Oliver, A.E., Booth, T., Tiwari, B., DeSantis, T., Maguire, M., Andersen, G., van der Gast, C.J., Whiteley, A.S., 2012. The response of marine picoplankton to ocean acidification. *Environmental Microbiology*, 14: 2293-2307.
- Nieto-Cid, M., Álvarez-Salgado, X.A., Gago, J., Pérez, F.F., 2005. DOM fluorescence, a tracer for biogeochemical processes in a coastal upwelling system (NW Iberian Peninsula). *Mar. Ecol. Prog. Ser.* 297, 33–50.
- Nieto-Cid, M., Álvarez-Salgado, X.A., Pérez, F.F., 2006. Microbial and photochemical reactivity of fluorescent dissolved organic matter in a coastal upwelling system. *Limnol. Oceanogr.* 51, 1391–1400.
- Obernosterer, I., Sempéré, R., Herndl, G.J., 2001. Ultraviolet radiation induces reversal of the bioavailability of DOM to marine bacterioplankton. *Aquat. Microb. Ecol.* 24, 61–68.
- Opsahl, S., Benner, R., 1997. Distribution and cycling of terrigenous dissolved organic matter in the ocean. *Nature* 386, 480–482.
- Orellana, M.V., Pang, W.L., Durand, P.M., Whitehead, K., Baliga, N.S., 2013. A Role for Programmed Cell Death in the Microbial Loop. *PLoS One* 8.
- Organelli, E., Bricaud, A., Antoine, D., Matsuoka, A., 2014. Seasonal dynamics of light absorption by chromophoric dissolved organic matter (CDOM) in the NW Mediterranean Sea (BOUSSOLE site). *Deep. Res. Part I Oceanogr. Res. Pap.* 91, 72–85.
- Osburn, C.L., Morris, D.P., Thorn, K.A., Moeller, R.E., 2001. Chemical and optical changes in freshwater dissolved organic matter exposed to solar radiation. *Biogeochemistry* 54, 251–278.
- Page, M.G.P., Rosenbusch, J.P., Yamato, I., 1988. The effects of pH on proton sugar symport activity of the lactose permease purified from *Escherichia coli*. *Journal of Biological Chemistry*, 263: 15897-15905.
- Palmiéri, J., Orr, J.C., Dutay, J.-C., Beranger, K., Schneider, A., Beuvier, J., Somot, S. 2014 Simulated anthropogenic CO<sub>2</sub> uptake and acidification of the Mediterranean Sea. *Biogeosciences Discussions*, 11: 6461–6517.

- Para, J., Coble, P.G., Charrière, B., Tedetti, M., Fontana, C., Sempéré, R., 2010. Fluorescence and absorption properties of chromophoric dissolved organic matter (CDOM) in coastal surface waters of the northwestern Mediterranean Sea, influence of the Rhône River. *Biogeosciences* 7, 4083–4103.
- Parlanti, E., Giraudel, J.-L., Roumaillac, A., Banik, A., Huguet, A., Vacher, L., 2006. Fluorescence and principal component analysis and parallel factor (PARAFAC) analysis: new criteria for the characterization of dissolved organic matter in aquatic environments. In: *Proceedings of the 13th Meeting of the International Humic Substances Society, Karlsruhe, Germany*, pp. 369–372.
- Passow, U., Carlson, C.A., 2012. The biological pump in a high CO<sub>2</sub> world. *Mar. Ecol. Prog. Ser.* 470, 249–271.
- Paul, A.J., Bach, L.T., Schulz, K.G., Boxhammer, T., Czerny, J., Achterberg, E.P., Hellemann, D., Trense, Y., Nausch, M., Sswat, M., Riebesell, U., 2015. Effect of elevated CO<sub>2</sub> on organic matter pools and fluxes in a summer Baltic Sea plankton community. *Biogeosciences* 12, 6181–6203.
- Paulino, A.I., Egge, J.K., Larsen, A. 2008. Effects of increased atmospheric CO<sub>2</sub> on small and intermediate sized osmotrophs during a nutrient induced phytoplankton bloom. *Biogeosciences*, 5: 739-748.
- Pelejero, C., Calvo, E., Hoegh-Guldberg, O. 2010. Paleo-perspectives on ocean acidification. *Trends in Ecology & Evolution*, 25: 332-344.
- Pérez, F.F., Ríos, A.F., Rellán, T., Álvarez, M., 2000. Improvements in a fast potentiometric seawater alkalinity determination. *Ciencias Marinas*, 26: 463-478.
- Peters, G.P., Marland, G., Le Quéré, C., Boden, T., Canadell, J.G., Raupach, M.R., 2012. Rapid growth in CO<sub>2</sub> emissions after the 2008-2009 global financial crisis. *Nature Climate Change*, 2: 2-4.
- Pey, J., Pérez, N., Querol, X., Alastuey, A., Cusack, M., Reche, C., 2010. Intense winter atmospheric pollution episodes affecting the Western Mediterranean. *Sci. Total Environ.* 408, 1951–1959.
- Piontek, J., Borchard, C., Sperling, M., Schulz, K. G., Riebesell, U., Engel, A., 2013. Response of bacterioplankton activity in an Arctic fjord system to elevated pCO<sub>2</sub>: results from a mesocosm perturbation study. *Biogeosciences*, 10: 297-314.
- Piontek, J., Lunau, M., Haendel, N., Borchard, C., Wurst, M., and Engel, A. 2010. Acidification increases microbial polysaccharide degradation in the ocean. *Biogeosciences*, 7: 1615-1624.
- Pomeroy, L.R., Shenton, L.R., Jones, R.D.H., Reimold, R.J., 1972. Nutrient flux in estuaries. *Limnol. Oceanogr. Special Symp.* 1: 274–291.
- Pomeroy, L.R., Wiebe, W.J., 2001. Temperature and substrates as interactive limiting factors for marine heterotrophic bacteria. *Aquat. Microb. Ecol.* 23, 187–204.
- Rana, G., Katerji, N., 2000. Measurement and estimation of actual evapotranspiration in the field under Mediterranean climate: a review. *Eur. J. Agron.* 13, 125–153.
- Ray, J.L., Topper, B., An, S., Silyakova, A., Spindelbock, J., Thyraug, R., DuBow, M.S., Thingstad, T.F., Sandaa, R.-A., 2012. Effect of increased pCO<sub>2</sub> on bacterial assemblage shifts in response to glucose addition in Fram Strait seawater mesocosms. *FEMS Microbiology Ecology*, 82: 713-723.
- Reader, H.E., Stedmon, C.A., Nielsen, N.J., Kritzbeg, E.S., 2015. Mass and UV-visible spectral fingerprints of dissolved organic matter: sources and reactivity. *Front. Mar. Sci.* 2, 1–10.
- Repeta, D.J., 2015. Chemical Characterization and Cycling of Dissolved Organic Matter, in: Hansell, D.A., Carlson, C.A. (Eds.), *Biogeochemistry of Marine Dissolved Organic Matter*. Elsevier Inc., San Diego, pp. 21–63.

- Reynolds, D.M., 2014. The Principles of Fluorescence, in: Coble, P.G., Lead, J., Baker, A., Reynolds, D.M., Spencer, R.G.M. (Eds.), *Aquatic Organic Matter Fluorescence*. Cambridge University Press, New York, pp. 3–34.
- Ridgwell, A., Arndt, S., 2015. Why Dissolved Organics Matter, in: Hansell, D.A., Carlson, C.A. (Eds.), *Biogeochemistry of Marine Dissolved Organic Matter*. Elsevier Inc., pp. 1–20.
- Riebesell, U., Schulz, K.G., Bellerby, R.G.J., Botros, M., Fritsche, P., Meyerhöfer, M., Neill, C., Nondal, G., Oschlies, A., Wohlers, J., Zöllner, E., 2007. Enhanced biological carbon consumption in a high CO<sub>2</sub> ocean. *Nature* 450, 545–548.
- Riebesell, U., Fabry, V.J., Hansson, L., Gattuso J.P. (Eds.), 2010. *Guide to best practices for ocean acidification research and data reporting*, 260 pp. Luxembourg: Publications Office of the European Union.
- Riebesell, U., Gattuso, J.P., Thingstad, T.F., Middelburg, J.J., 2013. Arctic ocean acidification: pelagic ecosystem and biogeochemical responses during a mesocosm study. Preface. *Biogeosciences*, 10: 5619-5626.
- Ries, J.B., Cohen, A.L., McCorkle, D.C., 2009. Marine calcifiers exhibit mixed responses to CO<sub>2</sub>-induced ocean acidification. *Geology*, 37: 1131-1134.
- Robinson, R.A., Leslie, W.G., Theocharis, A., Lascaratos, A., 2001. Mediterranean Sea Circulation. *Ocean Curr.* 1–19.
- Rochelle-Newall, E.J., Fisher, T.R., 2002. Production of chromophoric dissolved organic matter fluorescence in marine and estuarine environments: an investigation into the role of phytoplankton. *Mar. Chem.* 77, 7–21.
- Rochelle-Newall, E., Delille, B., Frankignoulle, M., Gattuso, J.P., Jacquet, S., Riebesell, U., Terbruggen, A., Zondervan, I., 2004. Chromophoric dissolved organic matter in experimental mesocosms maintained under different pCO<sub>2</sub> levels. *Marine Ecology Progress Series*, 272: 25-31.
- Romera-Castillo, C., Sarmiento, H., Álvarez-Salgado, X.A., Gasol, J.M., Marrasé, C., 2010. Production of chromophoric dissolved organic matter by marine phytoplankton. *Limnol. Oceanogr.* 55, 446–454.
- Romera-Castillo, C., Sarmiento, H., Álvarez-Salgado, X.A., Gasol, J.M., Marrasé, C., 2011a. Net production and consumption of fluorescent colored dissolved organic matter by natural bacterial assemblages growing on marine phytoplankton exudates. *Appl. Environ. Microbiol.* 77, 7490–8.
- Romera-Castillo, C., Nieto-Cid, M., Castro, C.G., Marrasé, C., Largier, J., Barton, E.D., Álvarez-Salgado, X.A., 2011b. Fluorescence: Absorption coefficient ratio — Tracing photochemical and microbial degradation processes affecting coloured dissolved organic matter in a coastal system. *Mar. Chem.* 125, 26–38.
- Romera-Castillo, C., Álvarez-Salgado, X.A., Galí, M., Gasol, J.M., Marrasé, C., 2013. Combined effect of light exposure and microbial activity on distinct dissolved organic matter pools. A seasonal field study in an oligotrophic coastal system (Blanes Bay, NW Mediterranean). *Mar. Chem.* 148, 44–51.
- Rost, B., Riebesell, U., Burkhardt, S., Sultemeyer, D., 2003. Carbon acquisition of bloom-forming marine phytoplankton. *Limnology and Oceanography*, 48: 55-67.
- Roy, A.S., Gibbons, S.M., Schunck, H., Owens, S., Caporaso, J.G., Sperling, M., Nissimov, J.I., Romac, S., Bittner, L., Mühling, M., Riebesell, U., LaRoche, J., Gilbert, J.A., 2013. Ocean acidification shows negligible impacts on high-latitude bacterial community structure in coastal pelagic mesocosms. *Biogeosciences*, 10: 555-566.

- Sala, M.M., Gude, H., 1999. Role of protozoans on the microbial ectoenzymatic activity during the degradation of macrophytes. *Aquatic Microbial Ecology*, 20: 75-82.
- Sala, M.M., Peters, F., Gasol, J.M., Pedrós-Alió, C., Marrasé, C., Vaqué, D., 2002. Seasonal and spatial variations in the nutrient limitation of bacterioplankton growth in the northwestern Mediterranean. *Aquat. Microb. Ecol.* 27, 47–56.
- Sala, M.M., Güde, H., 2004. Ectoenzymatic activities and heterotrophic bacteria decomposing detritus. *Arch. für Hydrobiol.* 160, 289–303.
- Sala, M.M., Arrieta, J. M., Boras, J.A., Duarte, C.M., Vaqué, D. 2010. The impact of ice melting on bacterioplankton in the Arctic Ocean. *Polar Biology*, 33: 1683-1694.
- Sala, M.M., Aparicio, F.L., Balagué, V., Boras, J.A., Borrull, E., Cardelús, C., Cros, L., Gomes, A., López-Sanz, A., Malits, A., Martínez, R.A., Mestre, M., Movilla, J., Sarmiento, H., Vázquez-Domínguez, E., Vaqué, D., Pinhassi, J., Calbet, A., Calvo, E., Gasol, J.M., Pelejero, C., Marrasé, C., 2016. Contrasting effects of ocean acidification on the microbial food web under different trophic conditions. *ICES J. Mar. Sci.* 73, 670–679.
- Sánchez-Pérez, E.D., 2015. The role of abiotic and biotic mechanisms controlling the dynamics of the dissolved organic matter in pelagic ecosystems (NW Mediterranean). PhD thesis. Université Pierre et Marie Curie.
- Santinelli, C., 2015. DOC in the Mediterranean Sea, in: Hansell, D.A., Carlson, C.A. (Eds.), *Biogeochemistry of Marine Dissolved Organic Matter*. Elsevier Inc., pp. 579–608.
- Sarmiento, H., Romera-Castillo, C., Lindh, M., Pinhassi, J., Sala, M.M., Gasol, J.M., Marrasé, C., Taylor, G.T., 2013. Phytoplankton species-specific release of dissolved free amino acids and their selective consumption by bacteria. *Limnol. Oceanogr.* 58, 1123–1135.
- Schlitzer, R., Monfray, P., Hoepffner, N., 2003. *Global Ocean Productivity and the Fluxes of Carbon and Nutrients: Combining Observations and Models*, JGOFS.
- Schlitzer, R., 2016. Ocean Data View. <http://odv.awi.de>
- Schoo, K.L., Malzahn, A.M., Krause, E., Boersma, M., 2012. Increased carbon dioxide availability alters phytoplankton stoichiometry and affects carbon cycling and growth of a marine planktonic herbivore. *Marine Biology*, 160: 2145-2155.
- Schroeder, K., Josey, S.A., Herrmann, M., Grignon, L., Gasparini, G.P., Bryden, H.L., 2010. Abrupt warming and salting of the Western Mediterranean Deep Water after 2005: Atmospheric forcings and lateral advection. *J. Geophys. Res. Ocean.* 115, 1–18.
- Schulz, K. G., Bellerby, R. G. J., Brussaard, C. P. D., Budenbender, J., Czerny, J., Engel, A., Fischer, M., Koch-Klavnsen, S., Krug, S.A., Lischka, S., Ludwig, A., Meyerhöfer, M., Nondal, G., Silyakova, A., Stühr, A., Riebesell, U., 2013. Temporal biomass dynamics of an Arctic plankton bloom in response to increasing levels of atmospheric carbon dioxide. *Biogeosciences*, 10: 161-180.
- Shimp, R.J., Pfaender, F.K., 1985. Influence of easily degradable naturally occurring carbon substrates on biodegradation of monosubstituted phenols by aquatic bacteria. *Appl. Environ. Microbiol.* 49, 394–401.
- Smith, D.C., Azam, F., 1992. A simple, economical method for measuring bacterial protein synthesis rates in seawater using 3H-leucine. *Marine Microbial Food Webs*, 6: 107-114.
- Søndergaard, M., Stedmon, C.A., Borch, N.H., 2003. Fate of terrigenous dissolved organic matter (DOM) in estuaries: Aggregation and bioavailability. *Ophelia* 57, 161–176.
- Statham, P.J., 2012. Nutrients in estuaries-An overview and the potential impacts of climate change. *Sci. Total Environ.* 434, 213–27.

- Stedmon, C.A., Markager, S., Bro, R., 2003. Tracing dissolved organic matter in aquatic environments using a new approach to fluorescence spectroscopy. *Mar. Chem.* 82, 239–254.
- Stedmon, C.A., Markager, S., 2005. Tracing the production and degradation of autochthonous fractions of dissolved organic matter using fluorescence analysis. *Limnol. Oceanogr.* 50, 1415–1426.
- Stedmon, C.A., Thomas, D.N., Granskog, M.A., Kaartokallio, H., Papadimitriou, S., Kuosa, H., 2007. Characteristics of Dissolved Organic Matter in Baltic Coastal Sea Ice: Allochthonous or Autochthonous Origins? *Environ. Sci. Technol.* 41, 7273–7279.
- Stedmon, C.A., Bro, R., 2008. Characterizing dissolved organic matter fluorescence with parallel factor analysis: a tutorial. *Limnol. Oceanogr. Methods* 6, 572–579.
- Stedmon, C.A., Álvarez-Salgado, X.A., 2011. Shedding light on a black box: UV–Visible spectroscopic characterization of marine dissolved organic matter., in: Jiao, N., Azam, F., Sanders, S. (Eds.), *Microbial Carbon Pump in the Ocean*. Science/AAAS, Washington, DC, pp. 62–63.
- Stubbins, A., Spencer, R.G.M., Chen, H., Hatcher, P.G., Mopper, K.M., Hernes, P.J., Mwamba, V.L., Mangangu, A.M., Wabakanghanzi, J.N., Six, J., 2010. Illuminated darkness: Molecular signatures of Congo River dissolved organic matter and its photochemical alteration as revealed by ultrahigh precision mass spectrometry. *Limnol. Oceanogr.* 55, 1467–1477.
- Stubbins, A., Lapierre, J.F., Berggren, M., Prairie, Y.T., Dittmar, T., Del Giorgio, P.A., 2014. What's in an EEM? Molecular Signatures Associated with Dissolved Organic Fluorescence in Boreal Canada. *Environ. Sci. Technol.* 48, 10598–10606.
- Taylor, L.L., Quirk, J., Thorley, R.M.S., Kharecha, P.A., Hansen, J., Ridgwell, A., Lomas, M.R., Banwart, S.A., Beerling, D.J., 2016. Enhanced weathering strategies for stabilizing climate and averting ocean acidification. *Nat. Clim. Chang.* 6, 402–406.
- Tedetti, M., Longhitano, B.R., García, A.N., Guigue, A.C., 2012. Fluorescence properties of dissolved organic matter in coastal Mediterranean waters influenced by a municipal sewage effluent (Bay of Marseilles, France). *Environ. Chem.* 9, 438–449.
- Teeling, H., Fuchs, B.M., Becher, D., Klockow, C., Gardebrecht, A., Bennke, C.M., Kassabgy, M., Huang, S., Mann, A.J., Waldmann, J., Weber, M., Klindworth, A., Otto, A., Lange, J., Bernhardt, J., Reinsch, C., Hecker, M., Peplies, J., Bockelmann, F.D., Callies, U., Gerdts, G., Wichels, A., Wiltshire, K.H., Glöckner, F.O., Schweder, T., Amann, R., 2012. Substrate-controlled succession of marine bacterioplankton populations induced by a phytoplankton bloom. *Science* 336, 608–611.
- Teira, E., Fernández, A., Álvarez-Salgado, X.A., García-Martín, E., Serret, P., Sobrino, C., 2012. Response of two marine bacterial isolates to high CO<sub>2</sub> concentration. *Marine Ecology Progress Series*, 453: 27–36.
- The Globe Carbon Cycle Project. University of New Hampshire <http://globecarboncycle.unh.edu/>
- Thingstad, T.F., Hagström, A., Rassoulzadegan, F., 1997. Accumulation of degradable DOC in surface waters: Is it caused by a malfunctioning microbial loop? *Limnol. Oceanogr.* 42, 398–404.
- Thingstad, T.F., Havskum, H., Zweifel, U.L., Berdalet, E., Sala, M.M., Peters, F., Alcaraz, M., Scharek, R., Pérez, M., Jacquet, S., Flaten, G.A.F., Dolan, J.R., Marrasé, C., Rassoulzadegan, F., Hagström, Å., Vaulot, D., 2007. Ability of a “minimum” microbial food web model to reproduce response patterns observed in mesocosms manipulated with N and P, glucose, and Si. *J. Mar. Syst.* 64, 15–34.
- Turner, J.T., 2015. Zooplankton fecal pellets, marine snow, phytodetritus and the ocean's biological pump. *Prog. Oceanogr.* 130, 205–248.

- Vacher, L., 2004. Étude par fluorescence des propriétés de la matière organique dissoute dans les systèmes estuariens. Cas des estuaires de la Gironde et de la Seine. PhD thesis. Université Bordeaux 1, pp. 255.
- Vázquez-Domínguez, E., Vaqué, D., Gasol, J.M., 2007. Ocean warming enhances respiration and carbon demand of coastal microbial plankton. *Glob. Chang. Biol.* 13, 1327–1334.
- Vila-Reixach, G., Gasol, J.M., Cardelús, C., Vidal, M., 2012. Seasonal dynamics and net production of dissolved organic carbon in an oligotrophic coastal environment. *Mar. Ecol. Prog. Ser.* 456, 7–19.
- Volk, T., Hoffert, M.I., 1985. Ocean Carbon pumps: Analysis of relative strengths and efficiencies in ocean-driven atmospheric CO<sub>2</sub> changes, in: Sundquist, E.T., Broecker, W.S. (Eds.), *The Carbon Cycle and Atmospheric CO<sub>2</sub>: Natural Variations Archean to Present*. AGU Monograph 32. American Geophysical Union, Washington, DC, pp. 99–110.
- Walker, S A., Amon, R.M.W., Stedmon, C.A., Duan, S., Louchouart, P., 2009. The use of PARAFAC modeling to trace terrestrial dissolved organic matter and fingerprint water masses in coastal Canadian Arctic surface waters. *J. Geophys. Res.* 114, G00F06.
- Walker, S.A., Amon, R.M.W., Stedmon, C.A., 2013. Variations in high-latitude riverine fluorescent dissolved organic matter: A comparison of large Arctic rivers. *J. Geophys. Res. Biogeosciences* 118, 1689–1702.
- Weber, G., 1961. Enumeration of components in complex systems by fluorescence spectrophotometry. *Nature* 90, 27-29.
- Weinbauer, M.G., Bonilla-Findji, O., Chan, A.M., Dolan, J.R., Short, S.M., Imek, K., Wilhelm, S.W., Suttle, C.A., 2011. *Synechococcus* growth in the ocean may depend on the lysis of heterotrophic bacteria. *J. Plankton Res.* 33, 1465–1476.
- Weishaar, J.L., Aiken, G.R., Bergamaschi, B.A., Fram, M.S., Fujii, R., Mopper, K.M., 2003. Evaluation of specific ultraviolet absorbance as an indicator of the chemical composition and reactivity of dissolved organic carbon. *Environ. Sci. Technol.* 37, 4702–4708.
- Welschmeyer, N.A., 1994. Fluorometric analysis of chlorophyll a in presence of chlorophyll b and pheopigments. *Limnol. Oceanogr. Methods* 39, 1985–1992.
- White, A., 1959. Effect of pH on fluorescence of tyrosine, tryptophan and related compounds. *Biochem. J.* 71, 217–220.
- Wichard, T., Poulet, S.A., Boulesteix, A.L., Ledoux, J.B., Lebreton, B., Marchetti, J., Pohnert, G., 2008. Influence of diatoms on copepod reproduction. II. Uncorrelated effects of diatom-derived alfa, beta, gamma, delta-unsaturated aldehydes and polyunsaturated fatty acids on *Calanus helgolandicus* in the field. *Prog. Oceanogr.* 77, 30–44.
- Wilson, H.F., Xenopoulos, M.A., 2009. Effects of agricultural land use on the composition of fluvial dissolved organic matter. *Nat. Geosci.* 2, 37–41.
- Yamada, N., Tsurushima, N., Suzumura, M., 2013. Effects of CO<sub>2</sub>-induced seawater acidification on microbial processes involving dissolved organic matter. *Energy Procedia* 37, 5962–5969.
- Yamashita, Y., Tanoue, E., 2003. Chemical characterization of protein-like fluorophores in DOM in relation to aromatic amino acids. *Mar. Chem.* 82, 255–271.
- Yamashita, Y., Tanoue, E., 2008. Production of bio-refractory fluorescent dissolved organic matter in the ocean interior. *Nat. Geosci.* 1, 579–582.
- Yamashita, Y., Maie, N., Briceño, H., Jaffé, R., 2010a. Optical characterization of dissolved organic matter in tropical rivers of the Guayana Shield, Venezuela. *J. Geophys. Res.* 115, 1–15.

- Yamashita, Y., Scinto, L.J., Maie, N., Jaffé, R., 2010b. Dissolved Organic Matter Characteristics Across a Subtropical Wetland's Landscape: Application of Optical Properties in the Assessment of Environmental Dynamics. *Ecosystems* 13, 1006–1019.
- Yamashita, Y., Panton, A., Mahaffey, C., Jaffé, R., 2011. Assessing the spatial and temporal variability of dissolved organic matter in Liverpool Bay using excitation-emission matrix fluorescence and parallel factor analysis. *Ocean Dyn.* 61, 569–579.
- Yan, M., Fu, Q., Li, D., Gao, G., Wang, D., 2013. Study of the pH influence on the optical properties of dissolved organic matter using fluorescence excitation–emission matrix and parallel factor analysis. *J. Lumin.* 142, 103–109.
- Yao, X., Zhang, Y., Zhu, G., Qin, B., Feng, L., Cai, L., Gao, G., 2011. Resolving the variability of CDOM fluorescence to differentiate the sources and fate of DOM in Lake Taihu and its tributaries. *Chemosphere* 82, 145–55.
- Yentsch, C.S., Menzel, D.W., 1963. A method for the determination of phytoplankton chlorophyll and phaeophytin by fluorescence. *Deep Sea Res.* 10, 221–231.
- Yoshimura, T., Nishioka, J., Suzuki, K., Hattori, H., Kiyosawa, H., Watanabe, Y.W., 2010. Impacts of elevated CO<sub>2</sub> on organic carbon dynamics in nutrient depleted Okhotsk Sea surface waters. *J. Exp. Mar. Bio. Ecol.* 395, 191–198.
- Yoshimura, T., Suzuki, K., Kiyosawa, H., Ono, T., Hattori, H., Kuma, K., Nishioka, J., 2013. Impacts of elevated CO<sub>2</sub> on particulate and dissolved organic matter production: Microcosm experiments using iron-deficient plankton communities in open subarctic waters. *J. Oceanogr.* 69, 601–618.
- Yu, G.H., He, P.J., Shao, L.M., 2010. Novel insights into sludge dewaterability by fluorescence excitation-emission matrix combined with parallel factor analysis. *Water Res.* 44, 797–806.
- Yuan, X., Zhou, W., Huang, H., Yuan, T., Li, X., Yue, W., Gao, Y., Liu, S., Pan, G., Liu, H., Yin, K., Harrison, P.J., 2016. Bacterial influence on chromophoric dissolved organic matter in coastal waters of the northern South China Sea. *Aquat. Microb. Ecol.* 76, 207–217.
- Zark, M., Riebesell, U., Dittmar, T., 2015. Effects of ocean acidification on marine dissolved organic matter are not detectable over the succession of phytoplankton blooms. *Sci. Adv.* 1, 1–7.
- Zeebe, R.E., 2012. History of Seawater Carbonate Chemistry, Atmospheric CO<sub>2</sub>, and Ocean Acidification. *Annu. Rev. Earth Planet. Sci.* 40, 141–165.
- Zeri, C., Beşiktepe, Ş., Giannakourou, A., Krasakopoulou, E., Tzortziou, M., Tsoliakos, D., Pavlidou, A., Mousdis, G., Pitta, E., Scoullou, M., Papanthanassiou, E., 2014. Chemical properties and fluorescence of DOM in relation to biodegradation in the interconnected Marmara–North Aegean Seas during August 2008. *J. Mar. Syst.* 135, 124–136.
- Ziolkowski, L.A., Druffel, E.R.M., 2010. Aged black carbon identified in marine dissolved organic carbon. *Geophys. Res. Lett.* 37, 4–7.
- Zsolnay, A., 2003. Dissolved organic matter: Artefacts, definitions, and functions. *Geoderma* 113, 187–209.